Identification and characterisation of new genes important for p53- dependent, stress-induced apoptosis.

Thesis

UNRESTRICTED

IDENTIFICATION AND CHARACTERISATION OF NEW GENES IMPORTANT FOR P53-DEPENDENT, STRESS-INDUCED APOPTOSIS

Thesis submitted for the degree of Doctor of Philosophy at the Open University

Discipline of Life Sciences

By

Federica Polato, Degree in Biotechnology

Mario Negri Institute for Pharmacological Research, Milan, Italy

September 2005

DATE OF SUBMISSION 29 SEPTEMBER 2005

DATE OF AWARD 15 APRIL 2006

ProQuest LLC.
789 East Eisenhower Parkway
P.O. Box 1346
Ann Arbor, MI 48106 – 1346

ACKNOWLEDGMENTS

I would like to thank my boss Dr. Massimo Broggini, head of the Molecular Pharmacology Laboratory, Department of Oncology at the "Mario Negri" Institute for his suggestions, scientific support and encouragments which have been fundamental for the completation of this program. I would like to thank my English supervisor Professor John Lunec (University of Newcastle) for his support, constructive criticisim and help during this period. I am also grateful to Dr. Maurizio D'Incalci, head of the Oncology Department at the "Mario Negri" Institute, who supervised my work. I would like to thank the friends and collegues of the laboratory for sharing with me their expertises, particularly to Drs. Stefano Zangrossi, Sergio Marchini, Annamaria Codegoni, Faina Vikhanskaya, Mirko Marabese, Maria Antonietta Sabatino, Giovanna Damia, Eugenio Erba. I would like to thank Stefania Filippeschi for kindly helping me with the generation of the bibliography.

CONTENTS PAGE

LIST OF FIGURES

Figure **Page**

LIST OF TABLES

Table **Page**

SUMMARY

The present thesis is aimed at the characterisation of an unknown gene named DRAGO (DRugs Activated Gene Overexpressed), isolated in the Laboratory of Molecular Pharmacology at the Mario Negri Institute as a p53-inducible gene by differential expression analysis in cells following genotoxic insults. The structure of the human DRAGO has been molecularly characterised. The coding region contains exons 2, 3, 4, 5 and the first 26 bases of exon 6. The remaining bases of this exon (4 Kb) constitute the 3' untranslated region (3'UTR). Interestingly, the gene presents two large (45–50 Kb) introns. Both the presence of such introns, and of the large 3'UTR suggest a strong gene regulation at transcriptional and post–transcriptional levels. This observation is also supported by the presence of several AU and CU rich regions, which are known to be involved in degradation/stability of mRNA. A fragment upstream the 5' of the coding region of DRAGO was isolated and demonstrated to have promoter activity. In transfection experiments the promoter activity of the isolated region was two-fold increased by human p53. An even stronger promoter activity in response to p73 and its isoforms was observed. Moreover, DNp73 was able to induce DRAGO expression co–operating with p73 and its isoforms.

The presence of DNA mutations in the gene has been investigated by using single strand conformation polymorphism (SSCP) analysis and DNA

sequencing. For these studies, 12 human cancer cell lines of different origin and four cell sublines made resistant to anticancer drugs were analysed but no mutations were detected. The investigation was also extended to human tumor biopsies and again no mutations could be detected. The functional role of the DRAGO gene has been studied by ectopically overexpressing it in eukaryotic cells. An inhibitory effect on cell growth and the formation of a large number of vacuoles leading to the disruption of the plasmatic membrane could be observed upon its overexpression. The phenotypic changes induced by DRAGO overexpression were therefore evaluated using specific deletion mutants and it was demonstrated that cells can tolerate the expression of DRAGO mutant with deletion of a few aminoacids in the C–terminus. The computational analysis of the protein revealed that DRAGO protein is likely a transmembrane protein. The theoretical prediction was supported by immunofluorescence experiments using deletion mutants transiently expressed in cells and by the analysis of GFP (green fluorescent protein) –derived deletion mutants clones, showing that the fluorescence was localised in the membrane. DRAGO–null mice have been generated: they are viable and do not present any macroscopical alterations. Mouse embryo fibroblasts (MEF) were isolated from homozygously deleted mice. DRAGO –/– MEFs were more resistant to drug treatment than wild–type MEF due to the inability of the cells to activate apoptosis. This newly isolated gene can be therefore considered as a novel potential target for the development of new therapeutic anticancer agents.

CHAPTER 1

INTRODUCTION

1.1 Cancer and cancer genes

Cancer is a term covering a plethora of conditions characterised by uncontrolled cellular proliferation.

As the average age rises in many countries and consequently cancer-related deaths, cancer will be one of the most common causes of death in the 21st century. Cancer is a complex disease in which somatic cells evade normal restrictions to clonal expansion and autonomy. Normal somatic cells are, in fact, totally dependent for their proliferation upon extracellulary received mitogenic signals (1). The unregulated proliferation of transformed cells kills and invades normal tissues giving rise to a bewildering array of clinical outcomes. For these reasons cures for cancer must be as diverse as the diseases themselves making difficult to design effective treatments.

Although cancers are extremely diverse and heterogeneous, their development and progression are driven by a defined number of critical events whose convergence is required for cancer inception and evolution. These pivotal steps comprise aberrations in the regulations of a restricted number of key pathways that control cell proliferation and cell survival leading to the establishment of all tumors. Mutations have been generally found in genes governing growth control (2).

Those genes, defined "cancer-genes", whose alterations enhance net cell growth, could be generally grouped into three types of genes: oncogenes, tumor-suppressor genes and stability genes.

In genetic diseases, mutations in one gene can cause disease; conversely, in most human malignancies mutations in cancer genes contribute to the development of cancer since only when several genes are defective cancer invasion arises (3).

Under normal conditions, proto-oncogenes (oncogenes with regular functions) are the genes whose expression stimulates appropriate cell growth of somatic cells especially those required for the continued renewal and turnover of some tissues.

A mutation in a critical position in a proto-oncogene causes uncontrolled cell growth by activating persistent growth stimulatory signal transduction pathways even when cells are receiving no mitogenic signals. The oldest and best studied oncogene is c-Src (4). In normal cells, c-Src is a kinase involved in proliferation, maintenance of normal intercellular contacts and cell motility. Even though its role in tumor development and progression is not fully understood, it is known that whenever overactivated and overexpressed through mutations or stimulation by growth factors, c-src can induce increased proliferation, invasion and motility (5).

Tumor-suppressor genes normally keep cell numbers down, either by halting the cell cycle and thereby preventing cellular division or by promoting programmed cell death. When these genes are rendered non-functional through mutation, the cell becomes malignant. Among tumor suppressors the prototypic genes are the RB and p53 genes. At the top of the list is p53, being implicated in more than 50% of human cancers (6) and p53-related topics will be further discussed in this work.

The first tumor suppressor to be cloned was the retinoblastoma (RB) gene (7-10). It was identified as the gene carrying the mutations responsible for the onset of retinal tumors.

In familial cases of retinoblastoma, mutation in the RB gene is inherited through the germ line, and affected children develop disease early in life that frequently affect both eyes (11). RB was subsequently found to be mutated in other human cancers, such as small-cell lung carcinoma and osteosarcoma. The retinoblastoma protein has been implicated in many cellular processes, such as control of cell cycle, DNA-damage responses, DNA repair, DNA replication, apoptosis and differentiation, all of which could contribute to its function as tumor suppressor (12-16).

Defective proto-oncogenes and tumor-suppressor genes act similarly at a physiologic level: they promote the inception of cancer by increasing tumor cell number through the stimulation of cell birth or the inhibition of cell death or cell cycle arrest.

A third class of cancer genes, called stability or repair genes, do not control cell birth or death directly. They drive the neoplastic process in different way when they are mutated. They control the rate of mutation of all genes keeping genetic alterations at a minimum. When stability genes are inactivated, cells acquire mutations in other genes at an accelerated rate. All genes are potentially affected by genetic alterations. Only mutations in proto-oncogenes and tumor-suppressor genes or in general in critical genes affect net cell growth conferring a selective growth advantage to mutant cells driving thereby the initiation of tumors. The

class of stability genes includes genes associated with mismatch repair (MMR), nucleotide-excision repair (NER) and base-excision repair (BER) which are responsible for repairing subtle mistakes made during normal DNA replication or induced by exposure to mutagens. Other stability genes control processes involving large portions of chromosomes such as those responsible for mitotic recombination and mitotic chromosomal segregation.

1.2 DNA damage and cancer

As it has been underlined, cancer is a disease of our genes. DNA accumulates changes conferring either a gain of function by activating proto-oncogenes or a loss of function by inactivating tumor-suppressor genes (17). In this manner, cancer development can be viewed as an evolutionary process whenever somatic mutations in cellular genes, which are usually detrimental to the cell, produce cells that can escape the normal constraints of proliferation and death (18).

The causes of cancer are many and varied and include genetic predisposition, environmental influences, infectious agents and ageing. These events transform normal cells into cancerous ones by altering the cellular networks of molecular pathways responsible for the control of cellular proliferation.

Oxidizing and alkylating agents, ultra violet (UV) and ionizing radiations (IR) are just few representative examples of damaging agents. The

damage induced by these agents is responsible for determining biological consequences like mutations and cell death.

DNA repair activities are extremely important for the cell because unrepaired DNA damage has the potential to be mutagenic, cytotoxic and carcinogenic. Maintenance of genomic integrity is therefore the major challenge for a cell, which is continuously exposed to genotoxic stresses (19). Cells have thus evolved complex surveillance networks in order to safeguard the genome against the possible detrimental effects of mutations by detecting DNA breaks, replication arrest, or defects in mitotic spindle assembly. These networks comprise DNA repair and DNA-damage checkpoint pathways which are responsible for the recovery of the cellular damage through the mobilisation of DNA repair factor and the activation of pathways which slow down or arrest the progression through the cell cycle to provide time for the repair, thus preventing mutations from being propagated (20). The cell cycle is characterised by different phases during which the genetic information is accurately transmitted from one cell to its daughters. Such faithful transmission required an accurate replication of DNA (the "S" phase) during which chromosomes are duplicated. After DNA synthesis, DNA and cellular components are equally and precisely distributed between two identical daughter cells ("M" phase). Between the S and M phases two gap periods occur, G1 and G2 respectively, which are intermediate phases and during which cell prepares itself for DNA synthesis (G1) and mitosis (G2). The term "cell cycle checkpoints" characterises monitored points of the cell cycle at

transitions between the different phases (21), and it refers to mechanisms by which the cell actively halts progression through different phases until it can ensure that an earlier process, such as DNA replication or mitosis has been completed properly. These cell-cycle checkpoints are believed to prevent the replication of damaged DNA (G1/S and intra-S checkpoints) or segregation of damaged chromosomes (G2/M checkpoints) (22, 23).

1.3 DNA damage response

The cellular response to DNA damage can be considered as a complex network of interacting signal transduction pathways consisting of sensors, transducers, and effectors (20) (Fig. 1.1).

The "stimulus" (DNA damage) is detected by "sensor proteins" that recognise the DNA lesion itself or eventual chromatin alterations that follow DNA breakage. Then the "transducers", a system composed of upstream and downstream protein kinases together with adaptor proteins, are brought into action: they transmit the damage signal to a series of downstream "effector molecules" through a transduction cascade that amplifies the initial DNA-damage signal and triggers the mechanisms necessary for the repair.

DNA can be damaged in a variety of ways. Energy released by free oxygen radicals, generated by normal metabolic process or by exposure to IR, can break the phosphodiester bonds in the backbone of the DNA helix involving either a single strand or both strands. The latter damage, defined as double-strand breaks (DSB) is probably the most dangerous form

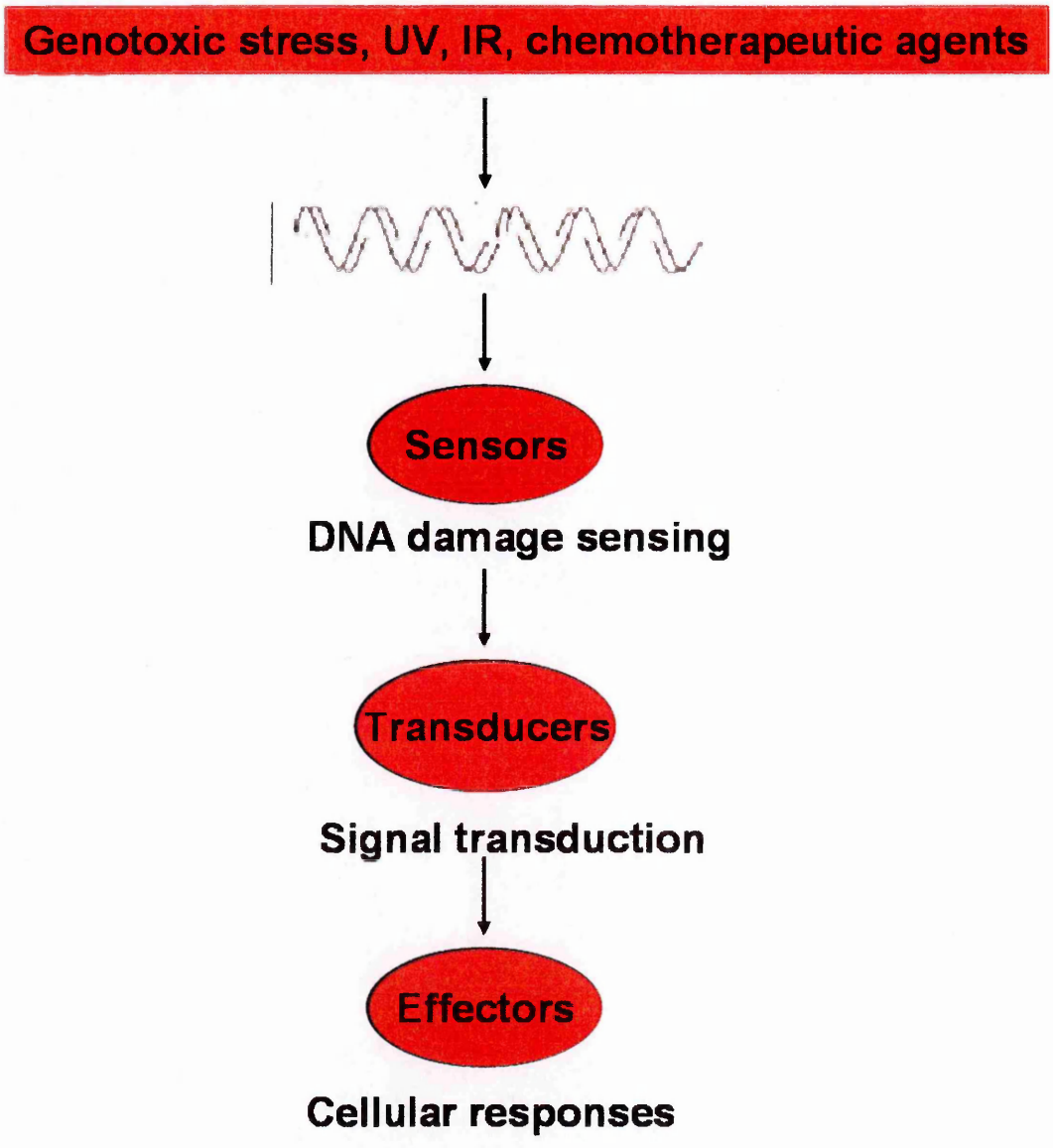

Figure 1.1

Schematic view of the general DNA damage response signal-transduction pathway.

among the many types of damages that exist within the cell (24). Other damages can be inflicted by alkylating chemicals that can modify bases or cause inter- or intra-strand crosslinks. Furthermore, inhibitors of DNA topoisomerases can lead to enhanced single or DSB (25).

Even though cells can adapt to low levels of unreparable damages (26), one DNA DSB is sufficient to kill a cell if it is located in an essential gene (27). DNA DSBs are considered to be particularly biologically important because their repair is more difficult than that of other types of DNA damage. Incorrect repair of chromosomal breakage may cause gross chromosomal loss, amplification or rearrangement that can lead to cancer.

Each type of DNA lesion requires specific cellular responses depending on the specific nature of the damage. Although cells use different signalling pathways, there are commonalities in the various networks that cells use to deal with DNA damage.

As mentioned above, the message (damage signal) is transmitted via a standard signalling mode of protein phosphorylation: a central role is played by two well characterised and highly conserved protein kinases, ATM (ataxia–telangectasia mutated gene) and ATR (ATM–related gene).

1.3.1 The PI3K and PIKK families

ATM and ATR belong to a conserved family of proteins most of which possess a serine/threonine kinase activity.

All the members contain a domain with motifs that are typical of the phosphatidylinositol 3–kinases (PI3Ks), which constitute a lipid kinase

family characterized by its ability to phosphorylate inositol ring 3'-OH group in inositol phospholipids, generating second messengers that regulate fundamental cellular processes such as cell growth, survival and motility. In human cancer, this pathway is frequently constitutively activated by genomic aberrations such as mutation, amplification, deletion and re-arrangement (28).

The PI3K family is divided into three classes. Class 1A of PI3Ks is composed of heterodimer, the catalytic subunit p110 and its associated regulatory subunit p85. In quiescent cells, p85 binds to p110 inactivating its kinase activity. Upon growth factor stimulation, p85 binds to the phosphorylated tyrosine in receptor tyrosine kinases or in their substrate adaptor proteins. The binding relieves the inhibition of p110 which in turn can phosphorylate the phosphatidylinositol 4,5-bisphosphate (PIP_2) to produce phosphatidylinositol 3,4,5-triphosphate (PIP_3), a second messenger that binds to proteins containing a pleckstrin homology domain recruiting them to cellular membranes (29). Among these, the serine-threonine kinase AKT, once recruited by PIP_3, is the predominant and essential mediator for the regulation of both growth and proliferation by PI3K. In cancer, the deregulation of the PI3K/AKT pathway, which causes its constitutive activation is involved in tumorigenesis by inducing cell survival thus inhibiting apoptosis (30, 31). The phosphorylation of PIP_2 to generate PIP_3 is reversed by the PTEN phosphatase. PTEN is a negative regulator of the PI3K signalling and functions as a tumor suppressor.

Genetic inactivation of PTEN occurs in numerous human tumors and results in a constitutive upregulation of PI3K signals (32, 33).

There are three known isoforms of Class 1A p110 (p110α/β/δ) and seven known p85 subunits generated by alternative splicing. Only p110α and p85α have been found to be mutated in tumors. Class I B PI3Ks consists of only one member, p110γ, which associates with the p101 regulatory subunit and is directly activated by G-protein-coupled receptors and indirectly by other receptors. The single isoform of the class-III PI 3-kinase and the three isoforms of the class-II PI 3-kinase (PI3K-C2α, PI3K-C2β, PI3K-C2γ) are all capable of using phosphatdylinositol (PI) as a substrate to produce PIP_3.

On the basis of their structural relation to the PI3K, the kinase family to which ATM and ATR belong to is named PI3K-like protein kinases (PIKKs) that also include other three members: ATX/SMG-1, mTOR/FRAP and DNA-PK (DNA–dependent protein kinase).

mTOR/FRAP is the only kinase of the family that is not directly involved in the response to damage.

Whereas ATM and DNA-PK respond primarily to DSBs (above all those induced by IR and radiomimetic drugs), ATR and SMG1 respond to both UV light damage and DSBs. ATM and ATR are the prototype actors in the DNA-damage signalling pathways (34).

1.3.2 Sensors of damage

In undamaged cells ATM kinase activity is low or minimal but it is rapidly engaged whenever cells have to deal with stress affecting DNA or chromatin structures. In unstressed cells ATM molecules reside predominantly in the nucleus and are held together as homodimers with the kinase domain of each molecule blocked and thus inactivated by the tight binding to an internal domain of the protein surrounding ser 1981.

The introduction of DNA breaks, and in particular DSB, causes specific chromatin alteration leading to the activation of ATM by conformational changes in the molecule. This stimulates the kinase to autophosphorylate the ser 1981, causing the dissociation of the homodimer (35). ATM can "sense" chromatin structure changes without binding DNA at the sites of damage. A possible role in sensing DNA breaks might be held by the MNR (Mre11, Rad50 and Nbs1) complex (36-39) which binds DNA at breaks, unwinds the ends and recruits ATM thus activating it (40).

By contrast, induction of the DNA-damage signalling pathway following UV-light irradiation seems to be triggered by blockage of either transcription or replication. The ATR kinase has been implicated as a sensor of replication blockage and might have a similar role in sensing blocked transcription complexes (41). Hence, whereas ATM seems to become engaged in signalling pathways primarily following the introduction of DNA breaks, ATR has a critical role in virtually all cellular stress responses that share inhibition of replication-fork progression as a

common mechanism. ATR has been reported to be engaged also in cellular responses to DNA breaks.

SMG1 which is a recently discovered member of the PIKK family, might respond to both DNA damage and truncated mRNA species that arise as a result of blocked transcription (42).

DNA-PK, which is activated by DSBs, is a heterodimer containing a large catalytic subunit and two smaller accessory proteins that seem to function as sensor of DSB consequently recruiting the catalytic subunit. DNA-PK-dependent phosphorylation has been reported for two proteins, the WRN (Werner syndrome protein) DNA helicase and Artemis. Phosphorylation affects WRN's helicase activity which might act in DSB repair (43, 44), whereas Artemis which normally possesses a single stranded 5'-3' exonuclease activity, after phosphorylation becomes capable of opening hairpin structures that are typically formed at the ends of DSBs (45).

1.3.3 Tranducer phase

ATM and ATR cooperate closely with two other classes of proteins. These are the checkpoints mediators, also known as adaptors, and the transducer kinases CHK1 and CHK2.

The mediators are those proteins that are initially recruited to the sites of DNA damage and/or replication blockade.

The ATM-related mediators include MDC1 (mediator of DNA damage checkpoint 1), 53BP1 (p53 binding protein 1), BRCA1 (breast cancer 1), NBS1 (Nijmegen breakage syndrome-1), H2AX (Histone-2A family,

member X) and SMC1 (structural maintenance of chromosomes 1). These proteins are phosphorylated by ATM and seem to facilitate ATM signalling and processing/repair of the lesions (38).

ATR exists in a complex with the ATR-interacting protein (ATRIP) both before and after exposure to stress such as UV irradiation. In vitro experiments showed that replication protein A (RPA) a single-strand DNA (ssDNA) binding protein involved in DNA replication would bind ATRIP (46-48). The accumulation of the RPA on the ssDNA would lead to the recruitment of ATRIP and hence of its partner ATR. ATR localisation at the site of DNA damage or the arrested replication fork are thought to be important (47). ATR also needs the recruitment of other protein complexes to the ssDNA sites to carry out its cellular functions.

Among these proteins, there are RAD17-containing complex, 9-1-1 (RAD9-RAD1-HUS1) complex, claspin, BLM (Bloom syndrome protein) and H2AX which are phosphorylated in an ATR/CHK1-dependent manner (49-51). The 9-1-1 and RAD17-containing complexes, and the RPA protein have also been implicated as possible sensors of replication stresses and other type of damages (23, 41, 52, 53). The checkpoint transducer kinases, triggered by phosphorylation of ATM and ATR, are CHK2 and CHK1 respectively (53).

1.3.4 Effector phase

Once phosphorylated, CHK1 and CHK2, in turn can phosphorylate a plethora of downstream effector proteins comprising cell cycle regulators,

such as CDC25 phosphatases, various DNA repair proteins, transcription factors such as p53 or E2F1, chromatin components and regulators such as histone H2AX and Tousled kinases (Tlk). Those effectors are responsible for cell cycle control, activation of DNA repair activities, apoptosis and senescence (20, 34, 53, 54). Among those effectors the tumor suppressor protein p53, which is phosphorylated at different, yet specific, residues by ATM, ATR, CHK1 and CHK2, has an important role in mediating part of the response of mammalian cells to DNA damage and other types of cellular stress thus determining the fate of the cells.
In the following chapters an overview over its functions and role in the cellular response to damage is presented.

1.4 P53 protein

The p53 gene product is a key player in the cellular response to stresses and DNA damage and for this reason p53 probably represents one of the major obstacles to tumor development and inception. It plays a pivotal role in regulating cell growth and death. It was one of the first tumor suppressor genes to be identified, even though it was initially considered an oncogene (55-57). Genetic and functional data collected afterwards showed it is a tumor suppressor (58, 59). Germline mutations of p53 gene result in Li-Fraumeni syndrome, which predispose individuals to a variety of cancer types (60). P53 null mice, generated by homologous targeting, are susceptible to spontaneous development of tumors at a young age (61). Additionally, the function of p53 as a tumor suppressor is further

supported by the fact that the p53 protein does not function correctly in most tumor. In approximately 50% of human cancers p53 is directly inactivated as a result of mutations in p53 gene (62, 63). In the majority of the remaining cancer cases, p53 activity is compromised by alternative mechanisms. It can be inactivated through the binding to viral proteins, such as the E6 protein of human papillomavirus (HPV) after viral infections or by amplification or overexpression of MDM2 (mouse double minute 2), the negative regulator of p53 protein or as a result of silencing of key p53 co-activators like $p14^{ARF}$ through deletion of the gene (64).

1.4.1 Structure of p53

The human p53 gene was shown to span about 20 Kb of DNA and to be localised to the short arm of chromosome 17 (17p13). The p53 gene comprises 11 exons with the translation start site located in exon 2 for a cDNA encoding a protein of 393 aminoacids with an apparent molecular weight of 53 kDa. P53 has several functional domains (Fig. 1.2). The N-terminal region contains the transactivation domain (TA) which is divided into 2 subdomains, named activator domains (AD). AD1 spans from residue 1 to 42 and provides the generic transactivation functions: it interacts with the basal transcription machinery by contacting TATA box-binding protein (TBP)-associated factor (TAF) components of TFIID (TFII70 and TFII37) (65, 66) whereas the activator domain 2 (AD2) which is located within residues 43 to 63, is required for p53-dependent apoptosis (67-70). The first domain also contains the binding sites for

MDM2 (19-26), the main regulator of p53 stability. These two domains are followed by a proline-rich region (PRD, 64-92) that contains five copies of the sequence PXXP and is necessary for the induction of apoptosis and contributes to growth suppression (70-75). The central core domain of the protein is required for sequence-specific DNA binding. This region, also known as the sequence-specific DNA binding domain (DBD), comprises residues 102-292 and is crucial for the key role of p53 as a transcription factor (76-78). The tetramerisation domain (TD), within residues 324-355 is necessary for formation of the p53 tetramer (79) which is the functional form of the p53 transcription factor (80-82). Upstream to the TD, within residues 316 and 325, there is the nuclear localisation signal (NLS) for p53 intracellular localisation. In addition, the C-terminus (residues 364-393) is involved in the regulation of the DNA-binding activity. Moreover, C-terminus itself possesses a nonspecific DNA-binding activity, which seems to be implicated in p53-mediated repair of damaged DNA and in DNA and RNA reannealing (83). The mechanism by which the C-terminus could regulate the specific DNA-binding of p53 is controversial. The C-terminus has been reported to exert repressive effects on DNA-binding activity through the control of p53 conformation (84). On the other hand, the C-terminus can mediate aspecific interactions with DNA and may interfere with sequence-specific DNA-binding through the central DBD (85, 86). Recent NMR analyses of p53 protein has suggested an overall conformational effect by the C-terminus (87). However the exact role of C-terminus in regulating p53 function is still poorly understood (88).

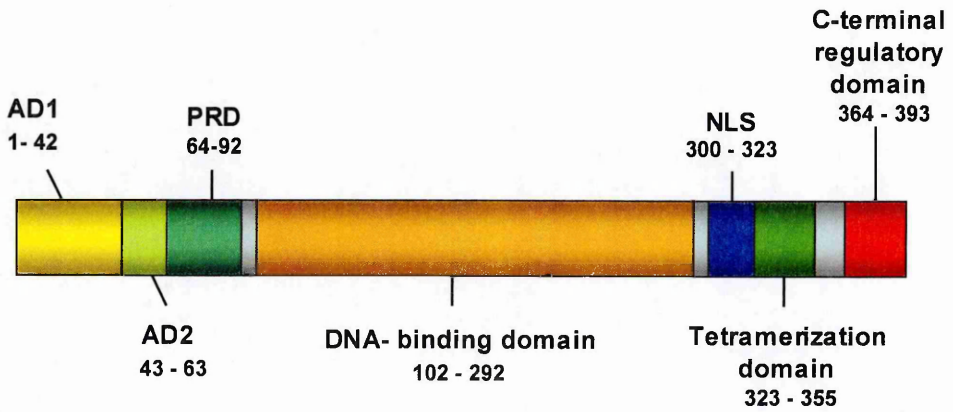

Figure 1.2

Structure and domains of the p53 protein. The N–terminal domain contains the transactivation (TA) domain, which is divided in AD1 and 2, and the proline rich domain (PRD).

1.4.2 Activation and regulation of p53

The p53 network is normally "off". It is activated following stress such as IR, UV radiation, hypoxia, heat and cold shock, growth factor withdrawal, oncogene activation, ribonucleotides depletion, telomerase erosion, inflammation (and its associated nitric oxide signalling) and the treatment with cytotoxic drugs (89) (Fig. 1.3). The induction of p53 involves the stabilisation of the protein itself for many hours at a high intracellular concentration, the transformation of the protein from a latent to an active form (through a covalent modification of the protein) and the localisation of the protein to the nucleus, allowing p53 to carry out its major function as transcription factor. It binds to a particular DNA sequence thus activating adjacent genes (90). These genes directly or indirectly lead to DNA repair or to the inhibition of the cell cycle or to cell death.

The p53 tumor suppressor protein negatively regulates cell growth through the induction of cell cycle arrest or apoptosis (6). Thus, in dividing tissue, there are mechanisms acting to downregulate the function of p53. The principal mechanisms that govern p53 activity are exerted at the protein level. These include regulation of p53 stability, control of the subcellular localisation of the p53 protein, posttranslational modifications, and conformational changes that allow activation of the binding activity of p53. One of the central component of the regulation of p53 is the p53-interacting protein MDM2 E3 ubiquitin ligase (91). MDM2 binds tightly to p53 and renders it inactive. This inactivation is achieved through at least

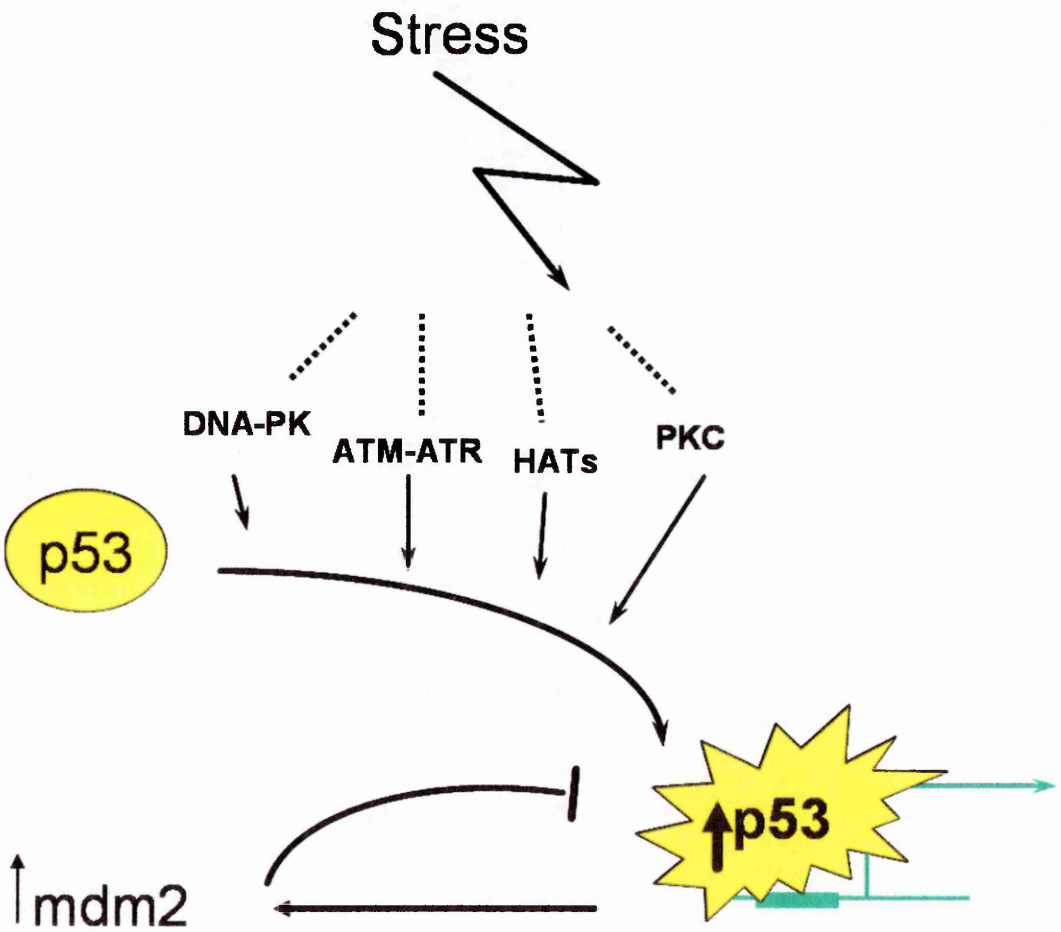

Figure 1.3

Schematic representation of activation of p53 network following stress.

two distinct molecular mechanisms: on the one hand, MDM2 interferes with the transcriptional activity of p53, by virtue of its binding to the N-terminal transactivation domain of p53; this blocks critical interactions with other protein necessary for p53-dependent regulation of gene expression. On the other hand, MDM2 plays a critical role in the degradation of p53. In normal proliferating cells the p53 protein is kept at a very low level due to a very short protein half-life (6-20 minutes), which is controlled in large part by the constant removal of newly synthesised p53 by mechanisms involving proteasome-mediated degradation. Through a cascade of enzymatic reactions several copies of ubiquitin are attached to the C-terminus of p53. The final ubiquitylation enables p53 to be detected by the protein degradation machinery. MDM2 is the enzyme involved in targeting p53 to this machinery. The process is regulated by a feedback loop since p53 itself binds to the regulatory region of the gene encoding MDM2 thus driving the expression of its own negative regulator (92). MDM2 binds to the N-terminus of p53 activating the addition of ubiquitin group to p53 which is then degraded. This lowers the concentration of p53 and, in turn, reduces the transcription of the MDM2 gene, so closing the feedback loop and allowing p53 levels to rise again (93). While MDM2 is the prominent E3 ligase of p53, it is important to note that other E3 ligases have been shown to promote p53 degradation, including Pirh2 and COP1 (94, 95).

The levels of p53 within the cell increase dramatically (3-20 fold) following stress or damage induction. This increase in protein level is attributed mainly to an increase in p53 stability and can be achieved through

conformational changes in the protein resulting from chemical and covalent modification, such as the addition or the removal of phosphate, acetyl, glycosyl, ribose, ubiquitin or sumo chemical groups (summarised in figure 1.4). Recently, it has been found that p53 can be also methylated (96) and neddylated (97). Phosphorylation sites in p53 are clustered within the N- and C- termini. Phosphorylation of the N-terminus does not affect its DNA-binding ability but interferes with its affinity for MDM2 and hence for its subsequent degradation. Many stress signals, including some DNA-damaging agents, are able to activate kinases responsible for the phosphorylation of numerous sites within or near the N-terminal MDM-2 – binding region of p53 (98) hence increasing p53 stability.

The p53-MDM2 loop is, in fact, the focal point of many different types of stresses that activate the p53 pathway (99).

For instance, DNA strand breaks initiate a series of phosphorylation events through several stress-response kinases such as ATM, ATR, Chk1 and Chk2 which have been shown to phosphorylate p53. Particularly, the ATM kinase has been implicated as the prime candidate for phosphorylating p53 at Ser15 in response to IR whereas ATR phosphorylates p53 on serine 15 and 37 after cellular exposure to UV light. ATM and ATR also activates Chk2 and Chk1, respectively, which phosphorylate p53 at ser20 (and possibly at other residues). Furthermore, ser15 phosphorylation triggers a series of subsequent post-translational modifications (phosphorylation or acetylation) on p53 that contribute to both its stabilisation and biochemical activation. These findings might add

complexity in the regulation of p53 stability (100). Other kinases that have been shown to phosphorylate the N-terminus of p53 are casein kinase (CK) 1 and 2 , JNK (Jun N-terminal kinase) and DNA-PK, p38, CAK (CDK-activating kinase), protein casein C (PKC) (89, 101, 102). Nevertheless, DNA damage can also induce changes in MDM2 phosphorylation and this is thought to contribute to blocking the degradation of p53 (103). Stabilisation of p53 can be also achieved through the phosphorylation of residues at the C-terminus. Whereas phosphorylation of ser315 by Aurora kinase (AUR K) increases p53 stability (104), phosphorylation at Thr55 by TAF1 promotes p53 for degradation (105). The N-terminus of p53 is thought to contain a nuclear export sequence (aminoacids 11-27). DNA-damage induced phosphorylation of ser15 and ser20 may also block export of p53 mediated by nuclear exportation signal (NES) thereby maintaining p53 within the nucleus (106). Coupled with the stabilisation of p53, phosphorylation of ser15, thr18 and ser20 also stimulates recruitment of transcription factors including p300, CBP (both transcriptional co-activators and histone acetyl-transferases HATs) P/CAF (a p300/CBP-associated HAT). These factors stimulate transcription from p53-responsive promoters and also promote acetylation of a cluster of C-terminal lysine residues (320, 372, 373, 382 and 381) in p53 that are normally targets for ubiquitylation (107) thus contributing to p53 stabilisation.

Several studies have shown that negative regulation of the DNA binding activity of p53 depends on the C-terminus and this inhibitory activity can

be relieved by a number of modifications within this region of p53. The C-terminus of p53 normally folds back and thus inhibits the DNA-binding domain located in the central part of the p53 protein. The N-terminus of p53 has also been shown to play a role in regulating dissociation from DNA, and it is likely that modifications at both ends of p53 are important in controlling the DNA binding function.

Acetylation of lysine residues is not the only modification that occurs to activate p53 function. Other modifications which are involved in switching on the activity of p53 include sumoylation (108-110), phosphorylation, glycosylation, of lysine residues or phosphorylation of serine residues near to the C-terminus: these modifications can favour the DNA binding of p53, presumably by interfering with the C-terminus folding.

Lysine modifications are complicated since, beside those forehead mentioned, they could be even subject to ubiquitination, neddylation and hydroxylation (111). Lysine methylation leads to addition of up to 3 methyl groups to the ε-amino group and different methylation states have distinct functional consequences (112). For istance, methylation of p53 at Lys372 by Set9 methyltransferase stabilises p53 and retains it in the nucleus, thereby increasing its transcriptional activity (96). A forehead mentioned modification of p53, neddylation, has been recently identified. Unlike methylation, modification of lysine residues of p53 by NEDD8 inhibits its transcriptional activity (97). Further studies will increase the knowledge about how other posttranslational modifications regulate the stability and activity of p53.

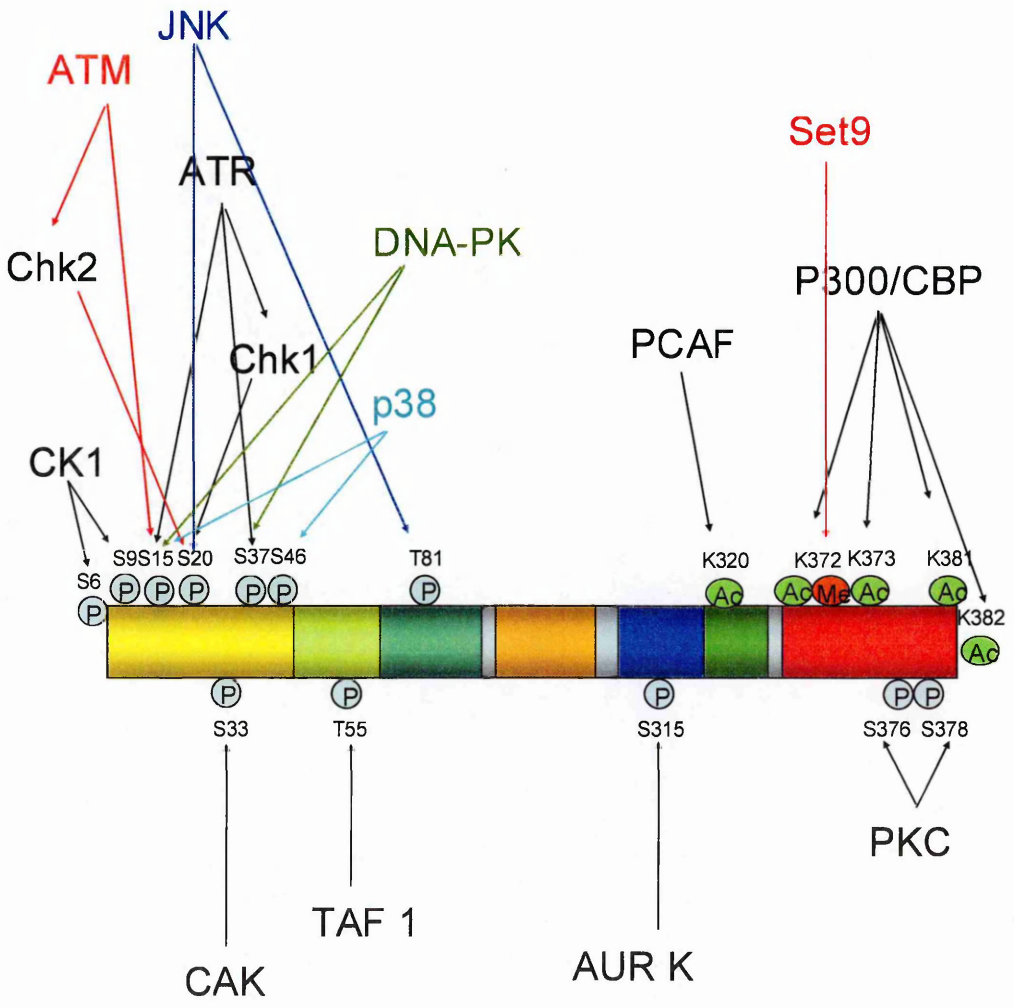

Figure 1.4

Schematic representation of some post-translational modifications of p53. Phosphorylation of serine (S) and threonine (T) residues are represented as P. Acetylation (Ac) and methylation (Me) of lysines (K) are also indicated.

1.4.3 Regulation of MDM2

Besides those events that lead to the posttranslational modification and the following stabilisation of p53, other stress such as hypoxia, high doses of UV and some cytotoxic drugs efficiently reduce MDM2 mRNA and protein levels (99, 113-116). Hyper-proliferation, induced by dominant oncogenes, can operate by inducing expression of $p14^{ARF}$, which binds to MDM2 and blocks its ability to mediate the degradation of p53. Nevertheless, the transcription factors YY1 (Yi Yang 1) negatively regulates p53 by enhancing the MDM2-dependent proteasomal degradation (117, 118) whereas the de-ubiquitination enzyme HAUSP (herpesvirus associated ubiquitin-specific protease), also known as USP7, has been recently discovered to bind to p53 in cells and to deubiquitinate p53 both in vitro and in vivo (119). Conversely, it has subsequently demonstrated that HAUSP deubiquitinates MDM2 rather than p53, thus leading to the stabilisation of MDM2 which then destabilises p53 (120). Other proteins, such as Rb and L11, which is a ribosomal protein, bind to the acidic domain of MDM2 and prevent it from targeting p53 for degradation (121-124). 14-3-3 sigma increases p53 stability by binding its C-terminus and blocking MDM2-mediated ubiquitination (125)). Conversely, PML (promyelocytic leukaemia) protein can bind MDM2 and sequester it to the nucleolus (126).

1.5 The p53 response: functions of p53

The p53 protein has been denoted "the guardian of genome" (127) for its role in preventing the accumulation of genetic alterations. This task is achieved through the induction of cell cycle arrest or senescence to prevent the replication of damaged DNA and playing a direct role in the repair of DNA through NER and BER. P53 is also called the "cellular gatekeeper" (6) being a critical player in the suppression of tumor development for its well-documented activity in apoptosis and contributing to the inhibition of angiogenesis (Fig. 1.5).

The best understood function of p53 is the ability to inhibit growth of aberrant or stressed cells. Inhibition of cell growth is thus associated with cell cycle arrest, differentiation, senescence or apoptosis. The ability to prevent growth of potential tumor cells is critical for its ability to function as a tumor suppressor.

1.5.1 P53 is a transcription factor

The growth and tumor suppressing activities of p53 are strictly related to its main function as a transcription factor (128-130) that binds as a tetramer to DNA in a sequence specific manner activating or repressing transcription of an increasing number of genes (131-134). Acting as a transcription factor, p53 activates vital damage-containment procedures to restrict aberrant cell growth in response to UV and IR, oncogene activation, hypoxia, heat shock, growth factor withdrawal, the loss of normal cell contact and the application of cytotoxic drugs (64, 89, 135).

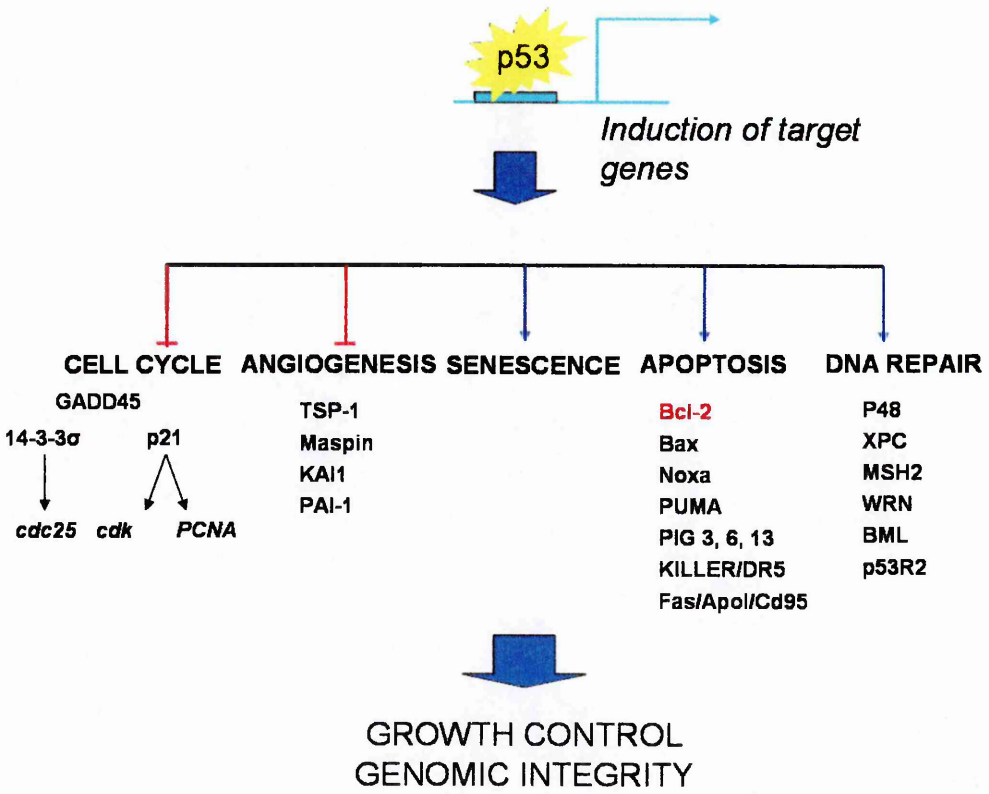

Figure 1.5

Summary of p53 functions.

The criteria that influence p53 to stimulate cell cycle arrest or apoptosis are only partially understood and are under intensive study. General factors influencing the final choice between life and death of p53 include p53 expression level, the type of stress signal, the cell type and the cellular context at the time of cellular exposure to stress (136).

The idea that the function of a transcription factor is critical for the role of p53 as a tumor suppressor is supported by the observation that almost all naturally occurring mutations in the p53 gene are mostly localised in the DBD thus compromising its ability to bind cognate recognition sequences (64).

The active p53 in the tetrameric form binds to four palindromic copies of its consensus sequence which is a pentamer and has been precisely defined (5'-RRRCW-3'). The canonical consensus binding site for p53 (p53BS), also defined as responsive element (p53RE), is defined as two decamers 5'- RRRCWWGYYY-3' separated by 0-21 nucleotides (nt). In the motif, R is G or A, W is T or A, Y is C or T (90, 137). The two pentamers in each decamer are arranged head-to-head (HH). The $p21^{Waf1/CIP1}$ (p21) gene promoter is the paradigm of this kind of base arrangement (90). These p53BS have been found both 5' to a gene and in the first or second introns of a gene (138, 139). Nevertheless, p53 is also able to repress the transcription from various promoters and emerging evidence indicates that transcriptional repression by p53 is important for its ability to promote apoptosis (140-142). Transcriptional repression by p53 is mediated through several mechanisms. P53 can interfere with the functions of DNA-

binding transcriptional activators such as SP1 and E2F (143, 144). P53 may interfere with transcriptional activator not by preventing the binding to DNA, but by disrupting its interactions with other components of the transcriptional machinery (145, 146). The second mechanism involves interference with the basal transcriptional machinery by p53. P53 may interact with the basal transcriptional machinery, such as TBPs and certain TAF, at the gene promoter or in solution (66, 147-150). This may disrupt transcriptional processes such as pre-initiation complex assembly. Another mechanism of transcriptional repression could be that p53 recruits chromatin-modifying factors such as histone deacetylase (HDAC). Alterations in chromatin structure may reduce promoter accessibility to the transcriptional machinery or activator proteins (151-153). It is also possible that differences within the p53-binding site itself could have pivotal effects on the action of p53. A peculiar example is given by the gene MDR1. In this case, the p53BS harboured by the MDR1 promoter presents a particular orientation, with head-to-tail (HT) pentamer arrangement (154). The authors proposed that this conformation could affect p53 protein conformation leading to an inactive p53.

Recently an intriguing promoter arrangement of a p53-dependent gene, $BTG2^{TIS21/PC3}$ has been reported. BTG2 function may play a role in cell cycle control, cell growth, differentiation and cellular response to DNA damage (155, 156). For this gene, the pentamer organisation of p53BS is again different from those reported for the canonical p53BS (HH) or MDR1 promoter (HT). In fact, the arrangement of the pentamer has a tail-to-tail

(TT) configuration. This specific arrangement could account for the particular response of the BTG2 promoter to the DNp73α protein (see ahead chapter 1.5.3) in a p53 dependent manner in neuroblastoma cells in contrast with other p53 target genes such as p21, which was completely repressed by DNp73 (157). P73 (see ahead chapter 1.5.1) shares structural and functional homology with p53. It is a transcriptional factor and can bind the canonical p53BS in the promoter of p53 target genes and thus transactivate them. This topic will be further discussed in depth. DNp73α is a p73 isoform lacking the transactivation domain. The authors proposed two models in order to explain the particular pentamer arrangement of BTG2 p53BS. On one hand they suggest that DNp73 and p53 form heterotetramers which are transcriptionally inactive on the canonical p53BS, but, through a conformational change, active on the BTG2 promoter. This is not according to previously published data (158) which demonstrated a weak interaction between p53 and p73. On the other hand, p73α being unable to bind BTG2 non canonical p53BS could suggest that DNp73α would not be able to compete with p53 in binding to its responsive element.

Furthermore recently collected observations could suggest an additional mechanism of transcriptional regulation of p53-induced genes. It has in fact been discovered that p53 can also activate target genes through a non-canonical sequence. The first such example is the p53-induced gene 3 (PIG3), which has been implicated in the accumulation of reactive oxygen species and apoptosis induction (159). PIG3 can be induced by

p53 through a microsatellite sequence, the pentanucleotide motif TGYCC repeated 10, 13 or 15 times within its translated region (160). Another recently described example is the gene encoding the pro-apoptotic phosphatase PAC1, which is induced through binding p53 to a novel palindromic binding site (161). It is a 12-base pair (bp) palindromic consensus sequence (5'-CCCCACGTGAGG-3') mapping from -202 to -191 bp in the PAC1 promoter.

Several p53 responsive genes have been identified but intensive studies have so far established direct roles for only a small group as mediators of the p53 response.

In the following paragraphs p53 functions will be specifically discussed.

1.5.2 Cell cycle arrest

Among the target genes stimulated by p53 to halt the cell cycle, p21 is probably the most critical and well studied (162, 163). It is an inhibitor of cyclin-dependent kinases (CDKs). CDKs are key regulator of the cell cycle, working together with their partners, the cyclin proteins, to ensure the correct progression through different phases of the cell cycle. By inhibiting several CDKs, p21 can block both G1–to–S and the G2–to–mitosis transitions (164-166).

Another target of p53 that contributes to the p53-induced G2 arrest is 14-3-3 sigma. The 14-3-3 family proteins play a role in signal transduction and cell cycle control. 14-3-3 sigma binds to CDC25C and keeps it in the cell cytoplasm. CDC25C is a phosphatases that acts upon cyclin B-CDC2,

a kinase essential for the G-2 to M-phase transition. Keeping CDC25C in the cytoplasm prevents it from activating cyclin B-CDC2 in the nucleus and these cells are blocked in the G-2 phase of the cell cycle. Further potential mediators of the G2 arrest include GADD45 (167) and Reprimo (168).

1.5.3 Apoptosis

P53 is implicated in the induction of the apoptotic signalling pathways, known as the extrinsic and the intrinsic pathways, that lead to the activation of the caspases, a group of cysteine proteases which, upon activation, destroy cellular machinery and lead to eventual cell death (169). The extrinsic pathway is mediated by particular "death" receptors (DR), that belong to the tumor necrosis factor receptor (TNF-R) family which form the death-inducing-signalling-complex (DISC) (170) thus leading to the activation of caspase dependent cell death. The intrinsic pathway is triggered by the release of apoptogenic factors from depolarised mitochondrial membrane, including cytochrome c and Smac/DIABLO (Smac, second mitochondria-derived activator of caspases; DIABLO, direct IAP-binding protein with low pI), Omi/HtrA2 (Htr2A, high temperature requirement A2), apoptosis inducing factor (AIF) and endonucleases G (EndoG), which lead to the eventual cell death through caspase-dependent and caspase-independent mechanisms.

Released cytochrome c allows the formation of the apoptosome complex which consists of apoptotic protease-activating factor 1 (APAF-1) and procaspase-9, which is actived after being recruited into the apoptosome.

Active caspase-9 finally promotes the activation of caspase cascade by cleaving the effector caspases, caspase-3, -6 and -7, which execute the death program (171). Smac/DIABLO and Omi/HtrA2 bind to a group of apoptosis inhibitors called inhibitors of apoptosis proteins (IAPs), such as XIAP (x-linked inhibitor of apoptosis protein) and cIAP1 (cellular inhibitor of apoptosis protein 1), thus relieving their inhibition on caspases (172-174). On the other hand, AIF and EndoG appear to promote DNA degradation through a caspase independent pathway (175, 176).

The release of mitochondrial apoptogenic factors is regulated by the pro- and anti-apoptotic Bcl-2 family proteins, which either induce or prevent the permeabilisation of the outer mitochondrial membrane. Several genes of the Bcl-2 family proteins are transcriptionally regulated by p53 thus encoding potential mediators of p53-induced apoptosis. The prototype of this class of mediators is the bax gene, a pro-apoptotic member, which governs the release of cytochrome c from the mitochondria (177-179). The Bcl-2 family members are classified on the basis of structural similarity to the Bcl-2 homology (BH) domains (BH1, BH2, BH3 and BH4) and to a transmembrane domain. The BH3 domain, which is present in all members and is essential for heterodimerisation among members, is the minimum domain required for the pro-apoptotic function (180, 181). The Bcl-2 family is subdivided into 3 classes: prosurvival proteins, structurally similar to Bcl-2 such as Bcl-X_L; pro-apoptotic proteins, Bax and Bak and the pro-apoptotic BH3-only proteins (182). Among the latter, a key subset

of the Bcl-2 family genes are p53 targets, including Noxa, (183) PUMA (p53 up-regulated modulator of apoptosis) (181, 184) BID (185) and Bad. Some of this BH3 domain-only proteins function upstream of BAX/BAK to induce apoptosis in response to a different set of conditions in a tissue and cell type-specific manner (186). For instance, PUMA and Noxa are activated in a p53-dependent apoptosis after DNA damage. PUMA can also mediate apoptosis induced by p53, hypoxia, DNA damaging agents and endoplasmatic reticulum (ER) stress in human colorectal cancer cells (187, 188). Bad has been shown to regulate apoptosis induced by growth factors and nutrient deprivation (189). Bid mediates apoptosis transmitting apoptotic signal mediated by death receptors to Bax/Bak in hepatocytes (190) whereas Bim is required for apoptosis induced by cytokines in hematopoietic cells (191). These BH3-only protein receive the death signals transmitting them to Bcl-2 family members containing multiple BH domains (192, 193). Bax and Bak can be either directly activated by BH3-only proteins or indirectly through inhibition of Bcl-2 or Bcl-XL proteins (194, 195).

These proteins, as well as another p53 induced gene product, namely p53AIP1 (196), localise to the mitochondria promoting mitochondrial membrane potential perturbation with the consequent activation of the intrinsic apoptotic pathway. The mitochondrial membrane potential could be perturbed by other p53 target genes coding for redox-controlling enzymes and named PIGs, such as PIG3, POX2/PIG6 and ferredoxin reductase (159, 197, 198). The reactive oxygen species (ROS) produced

by these PIGs cause damages to the mitochondria thus initiating the apoptotic pathway. p53 has been demonstrated to localise to the mitochondria following DNA damage or hypoxia, where p53 can interact with antiapoptotic proteins such as Bcl-2 and Bcl-X_L. The binding of p53 to Bcl-2 and Bcl-X_L liberates Bak and Bax thereby allowing them to induce changes in the mitochondrial membrane leading to activation of the caspase cascade resulting in cell death. Since in this case p53-induced apoptosis does not involve its transcriptional ability, this represents the transcription-independent way of mediating apoptosis (199).

P53 has also been implicated in the membrane death receptor-induced pathway of apoptosis also known as the extrinsic pathway.

P53, in fact, upregulates the expression of at least three of the death receptors, FAS (APO1/Cd95), DR5/KILLER, DR4, PERP (p53 apoptosis effector related to PMP–22) and PIDD (p53-induced protein with a death domain) and one of the death receptor ligands FASL.

The cell-surface receptor FAS belongs to the TNF-R receptor family and is a key component of the extrinsic death pathway (200). Fas is activated by binding of its ligand, FASL, expressed mainly by T-cell (201), which induces the oligomerisation of the receptor with subsequent activation of the caspase cascade in the apoptotic pathway. Fas transcription is induced by p53 in response to gamma irradiation and in a tissue-specific manner (202). In addition to stimulating Fas transcription, overexpressed p53 may enhance cell surface expression of Fas by promoting the trafficking of the receptor from the Golgi to the membrane (203).

Other members of this receptor family that are induced by p53 are DR5/KILLER and DR4, which are bound by the TNF-related apoptosis-inducing ligand (TRAIL). Both receptors contain a conserved death domain (DD) motif (an intracellular globular protein interaction domain) and signal apoptosis. Ligation of TRAIL to its receptors results in trimerisation of the receptors and clustering of the receptors's intracellular DD, leading to the formation of the DISC and thus inducing apoptosis. PIDD, was initially identified as a prime target gene in an erythroleukemia cell line that undergoes G1 phase arrest and subsequent apoptosis after p53 expression (204). PIDD can form a complex with caspase 2, called PIDDosome and seems to involved in caspase 2 activation, in response to genotoxic agents (205). Another pro-apoptotic gene, PERP, is a putative tetraspan transmembrane protein that represents a new member of the PMP-22/gas3 family of proteins implicated in cell growth regulation. The presence of a p53-responsive element in the promoter and of higher levels of PERP mRNA in cells undergoing apoptosis than in arresting cells support the hypothesis that PERP contributes to p53-mediated apoptosis, even though details have to be defined (206).

1.5.4 P53 "choice" between life and death

Different type of cells often show different biological responses to a given stress (207). For example, thymocytes and splenocytes undergo p53-dependent apoptosis after IR, whereas fibroblasts arrest cell cycle after DNA damage but can undergo apoptosis following different stimuli. In

most cases, cells can respond to DNA damage by activating either growth arrest or apoptosis. The ability of cells to execute a choice between life and death suggests that p53 pathway is able to sense whether or not recovery from DNA damage has been successful thus permitting the p53 response to be attenuated or promote an irreversible and fatal outcome. The currently accepted model for the explanation of cellular choice involves a complex number of factors, not yet complete, that should direct p53 to differentially transactivate promoters of growth arrest or apoptosis genes.

Originally, intracellular levels of p53 were correlated with the outcome of p53 activation, since p53 has been shown to bind with higher affinity to the promoter consensus sequence of cell cycle arrest genes (e.g. p21, GADD45, MDM2). Whereas, death would be induced when high levels of p53 are present in the cell because promoters of apoptotic genes contain low affinity p53 binding sites (208). This model could suggest that increased level or activity of p53, after strong damages, can lead to the induction of the apoptotic pathway rather than growth arrest. Stronger damage induces more p53 and the persistence of damage would keep p53 active thus determining and leading to the induction of those genes whose promoters have low affinity for p53 (209). Furthermore, p53 mutants with marginally altered conformations retain sufficient activity to induce arrest but not apoptosis (68, 210, 211).

Further studies have demonstrated exceptions to the proposed relationship between promoter binding and the induction of apoptosis

(212, 213). It is now accepted that there are factors that are likely to play an essential role in determining the final cellular decision between cell cycle and apoptosis. Different post-translational modifications of p53 have been found to drive the p53 toward the activation of specific pro-apoptotic genes (AIP). In addition, there are cellular factors able to induce p53-dependent apoptosis such as JMY (214), ASPP (apoptosis stimulating protein of p53) 1 and 2 (215) and recently also p53 family members, p73 and p63 which were also shown to be required for p53-induced apoptosis (216).

1.5.5 Senescence

Cellular senescence has been defined by Hayflick (217) as the irreversible loss of replicative potential occurring in primary somatic cell culture. Normal cells grown *in vitro* do not divide indefinitely but cell growth is arrested after a fairly reproducible number of cell divisions and this process has been defined as replicative senescence. Among mechanisms that have been suggested as putatively responsible for blocking cellular divisions, the erosion and eventual dysfunction of telomeres is the best established and investigated (218). During successive cellular divisions the telomeres in normal cells shorten progressively (219, 220). This erosion of telomeres length has been attributed to the inability of the DNA replication machinery to completely replicate the ends of chromosomes (221). Thus, proliferating cells experience progressive telomere shortening until the telomeres become critically short and dysfunctional. Dysfunctional

telomeres signal normal cells to cease proliferation provoking a senescent phenotype (222, 223). Senescent cells remain metabolically active and undergo to characteristic changes in cell morphology, physiology and gene expression (224). They are unable to express genes required for proliferation in contrast with quiescent cells which are in a non-proliferative state promptly reversed if they are exposed to mitogens (225).

Mammalian telomeres consist of a long stretch of TTAGGG repeats followed by single-strand termini consisting of 10 to 300 bases (222) that end in a lariat-like structure called T-loop (226). Various telomere-specific proteins bind to the single- and double-strand regions. The T-loop and telomere-associated proteins form a protective cap that stabilises the ends of linear chromosomes preventing their degradation, recombination and end-joining reactions (227). When telomeric DNA sequence or structure is altered, cells undergo chromosome end associations and fusions leading to growth arrest or death.

Immortal cells which proliferate indefinitely are able to maintain telomeres at a stable length because they can express the enzyme telomerase, which can add the telomeric sequences to chromosomes ends *de novo*. Most human normal cells do not express the telomerase (222, 223, 228). Replicative senescence is an example of a more general process named as cellular senescence, which is a signal transduction program activated by normal cells in response to various stress and leading to irreversible growth arrest. These include telomere uncapping, DNA damage, oxidative stress, certain oncogene activity, specifically Ras and its downstream

effectors and others (229-231). These stimuli are not independent of one another or mutually exclusive. Oxidative stress can cause DNA damage and also accelerate telomere shortening rates (232-234).

P53 together with Rb, another paradigmatic tumor suppressor protein, plays a critical role in the induction of senescence. Both proteins are in fact activated during senescence and in human fibroblasts the inactivation of both p53 and Rb is required to prevent the onset of senescence, whereas the inactivation of only one protein delay the entry into senescence (235). In MEF, p53 loss is sufficient to overcome senescence, whereas Rb has to be inactivated together with the related p107 and p130 components of the Rb family to prevent senescence.

In the context of senescence, p53 seems to be controlled by two major pathways. One is the DNA damage-response pathway, mediated by the ATM/ATR and Chk1/Chk2 proteins, which cause the post-translational stabilisation of p53 through phosphorylation. The other pathway acts through the $p14^{ARF}$ or ARF ($p19^{ARF}$ in mouse). As already described, the ARF product activates p53 by sequestering MDM2 in the nucleolus thereby preventing the MDM2-mediated targeting of p53 to proteolytic degradation.

Recent evidence from cell culture models clearly demonstrates that telomere shortening provides a DNA damage signal similar to that induced by DSBs. Human fibroblasts undergoing replicative senescence display nuclear foci containing phosphorylated H2AX and 53BP1 and the activation of checkpoint kinases CHK1 and CHK2, all hallmarks of DSBs

(236, 237). P53 in its stabilised state (through post-translational modifications or prevented MDM2 targeting), increases the expression of p21, an inhibitor of cyclin E/cdk2 complexes thus causing cell cycle arrest (as discussed previously in the chapter 1.4.3.1). P21 expression levels rise in both growth arrested (for example quiescent) cells and senescent cells: however, p21 increases to its highest levels in senescent cells for a relatively long interval. Several weeks after human fibroblast cultures reach senescence, p21 levels gradually fall as $p16^{INK4a}$ (p16) levels rise. P16 is an inhibitor of cyclin D/Cdk4,6 complexes and is induced upon various situation of stress and is highly expressed in senescent cells. It is encoded by the INK4a/ARF locus, which encode as alternative transcript, the tumor suppressor $p14^{ARF}$ which share 2 exons but has a separate promoter and the first exon is translated in a different reading frame. Both p16 and $p14^{ARF}$ are induced in situations of stress (238, 239).

1.5.6 Genetic stability

As a tumor suppressor, p53 has also an important role in DNA repair and recombination. As recently described, during apoptosis, p53 can also have a transactivation-independent role in maintenance of genetic stability. In eukaryotic cells, the main DNA-repair processes are NER, BER, MMR, Non-Homologous End-Joining (NHEJ) and Homologous recombination (HR) (19).

NER is the process by which the cell recognises and repairs damaged bases and disrupted base pairings caused by UV light or oxidative

damage. P53 can affect NER in vivo both in a transactivation–dependent and independent manner. In fact, it can upregulate the expression of p48 and xeroderma pigmentosum complementation group C (XPC) which are key components of the NER machinery (240, 241). P48 is one of the components of UV-damage DNA-binding proteins (UV-DDB) induced after UV damage. P48, whose expression is regulated by p53, may in turn directly affect p53 protein levels, which implies a mutual regulatory interaction between the two proteins (242). XPC together with RAD23B form a complex that is involved in identifying disrupted base pairings (243). P53 can also affect NER in a transactivation-independent manner. An example is the possible function of p53 as a chromatin-accessibility factor in NER. After recognition of UV-associated lesions, p53 seems to recruit the histone acetylase p300 to the NER site to acetylate histone H3, thereby relaxing chromatin and enhancing the detection of the lesion in the entire genome (244).

DNA base damage generated by IR, alkylating and methylating agents, as well as endogenous hydrolytic and oxidative processes is corrected by the BER pathway. Thus, BER is critically important for regulating spontaneous mutations (245). A recently published work (246) reported that BER intermediates could induce p53-independent cytotoxic and genotoxic responses, hence implying that p53 might not be involved in the process. However, Zhou *et. al.* (247) demonstrated that BER is stimulated by recombinant wild-type p53 in an in vitro reconstituted system, where p53 might directly interact with some of the components of BER pathway. A

direct interaction of the tumor suppressor with some of the proteins belonging to the BER machinery could suggest a transactivation-independent function of p53. P53 can in turn affect BER in a transcription-dependent fashion. An example is the effect of p53 on 3-methyladenine (3-MeAde) DNA-glycosylase gene (MPG) transcription. After exposure to nitric oxide (NO), p53 can repress the expression of MPG (gene belonging to the BER pathway) thus preventing the onset of a mutator phenotype resulting from the increased accumulation of point mutation after NO-induced DNA damage (248).

MMR is the DNA-repair process that removes mispaired nucleotides and insertion or deletion loops.

P53 affects MMR activating the expression of a MMR's protein, MutS homologue-2 (MSH2), in a transcription-dependent manner by binding to the p53RE present in the MSH2 promoter. It has been reported that p53 can synergise with the transcription factor Jun in the regulation of human MSH2 in response to UV exposure (249). This is one the several examples of the cooperation of p53 and MMR in DNA damage response.

NHEJ is the mechanism by which most chromosomal DSB are repaired in somatic cells. It is error prone since it leads to the joining of the breaks without a template. As regards the regulation of NHEJ by p53 there are contradictory results. For instance, it has been reported that wild–type p53 protein is able to rejoin DNA with DSBs, indicating a transactivation-independent role of p53 in NHEJ (250, 251). Conversely, it has been also

shown, that DSB rejoining increases with loss of wild-type p53 (252) and also wild–type p53 was reported to inhibit NHEJ (253-256).

HR is a fundamental and error-free process, conserved in all organisms (257) and involved in genomic stability, chromosome segregation during meiosis and DNA repair (258). In mammalian cells, HR is strongly stimulated by DSB (259). During HR, the sequence lost in one ds-DNA molecule is replaced by exchanges with an intact homologous DNA partner (19), which can be found on the sister chromatid, leading to sister chromatid exchange (SCE) in the homologous chromosomes or on ripetitive sequences that are dispersed through the genome (260). The most documented model is the DSB repair model which accounts for DSB repair after genotoxic stress, during meiotic recombination or gene targeting. RAD51 is perhaps the most essential component of the pathway because it catalyses the strand exchange reaction (261). RAD51 binds to ssDNA and after having polymerised, upon RAD52 stimulation, searches the homology on sister chromatid with the help of the helicase rad54 (262). Once the homology search is successful, the homologous duplex is captured and the ssDNA filament bound to RAD51 aligns and invades it to form heteroduplex structure allowing the exchange between the aligned chromatids (263). This step form cruciform junctions, known as Holliday junctions (HJ) which can migrate along the chromosomal branch leading to the elongation of the heteroduplex molecule. DNA polymerases use the intact copy to re-synthesise the deleted DNA sequences, DNA ligase join the newly synthesised fragments and the HJ are resolved by specific

endonucleases that are known as resolvases (264). P53 seems to physically interact with proteins involved in the HR machinery, heteroduplex structures or holliday junctions together with helicases. Wild–type p53 alone might check the fidelity of HR events by either specific mismatch recognition in the heteroduplex intermediates correcting them exonucleolytically or by halting DNA exchange between imperfectly homologous sequences (265). The mechanism through which p53 influences the HR process seems to be transactivation-independent. It interacts with RAD51 thus likely affecting RAD51 activity. P53, in fact seems to abrogate the polymerisation of RAD51, thus limiting its activity (266). It is necessary to finely control the HR machinery to allow the process to proceed at optimum efficiency thus preventing hyper-recombination. Uncontrolled hyper-recombination, in fact, leads to genomic instability, including chromosomal deletions, translocations and gene amplifications. It is not known whether p53 loss alone can lead to hyper-recombination or whether p53 mutation lead to an increase in HR. However, it has been shown that the abrogation of wild-type p53 results in an increase of chromosomal aberration and frequency in spontaneous mutations (267-269). Furthermore, p53 can also interact with helicases, such as WRN and BLM belonging to the RecQ helicase family. This family is highly conserved in evolution and is required for genomic stability maintenance. Mutations in three of the RecQ-helicase genes in humans, BLM, WRN and RecQ4, lead to cancer predisposition disorders, Bloom syndrome (BS), Werner syndrome (WS) and Rothmund-Thomson

syndrome (RTS) respectively (270). There are several example of inter-regulation between p53 and the RecQ helicases. (271). For istance, p53 can form a complex with Sp1 thus preventing Sp1 to bind to the promoter of WRN helicase, which is transcriptionally regulated by Sp1. Another example is given by the interaction between p53 and BLM helicase. p53 and BLM cooperate affecting HR and sister chromatid exchanges. BLM and p53 co-localise and physically associate with each other and RAD51. In particular, BLM is required for efficient p53 accumulation and association with RAD51 during HR response to damage (272).

Further evidence for a role of p53 in DNA repair comes from the induction of a new ribonucleotide reductase gene, designated p53R2, by p53 after damage. Ribonucleotide reductase is a rate limiting step enzyme for DNA synthesis as it catalyses the conversion of ribonucleoside diphosphates to their corresponding deoxyribonucleotides. P53R2 gene is inducible by DNA damage suggesting that this enzyme has a crucial role in supplying precursors for DNA repair. P53, once activated by ATM in response to DNA damage, directly induces p53R2, suggesting that p53 could participate in DNA repair activity also by direct induction of p53R2 following to DNA damage (273).

1.5.7 Inhibition of blood-vessel formation

During the progression from normal to malignant phenotype, the cells have to recruit new blood vessels to ensure sufficient nutrient-bringing blood for tumor growth. To prevent neovascularisation, p53 can stimulate

the expression of the thrombospondin-1 (TSP-1), a potent inhibitor of angiogenesis. In cultured fibroblasts from patients with Li-fraumeni syndrome the loss of the wild–type allele for p53 can also result in the reduced expression of TSP-1 (274). In various neoplastic cell lines, the levels of TSP-1 expression show an inverse correlation with malignant progression (275-278). A p53-inducible gene, named BAI–1 (brain-specific angiogenesis inhibitor 1) encodes a product that contains 5 thrombospondin type 1 repeats and is specifically expressed in the brain (279): this gene has been shown to inhibit in vivo the neovascularisation induced by bFGF (basic fibroblast growth factor) in rat cornea, thus suggesting that this gene can play a significant role as a mediator of p53 inhibition of angiogenesis. Other genes involved in suppression of tumor metastasis have been identified. Among them KAI–1 (280), maspin (mammary serine protease inhibitor) (281) and PAI–1 (plasminogen activator inhibitor 1) (282) have been found to be up-regulated by p53 thus emphasizing the role of p53 in the negative regulation of cell invasion and metastasis.

1.6 P53 and its family members

1.6.1 Structure of p53 family member gene and their products

Even though p53 discovery has been in 1979, two novel proteins belonging to the p53 family of transcription factors were identified only 20

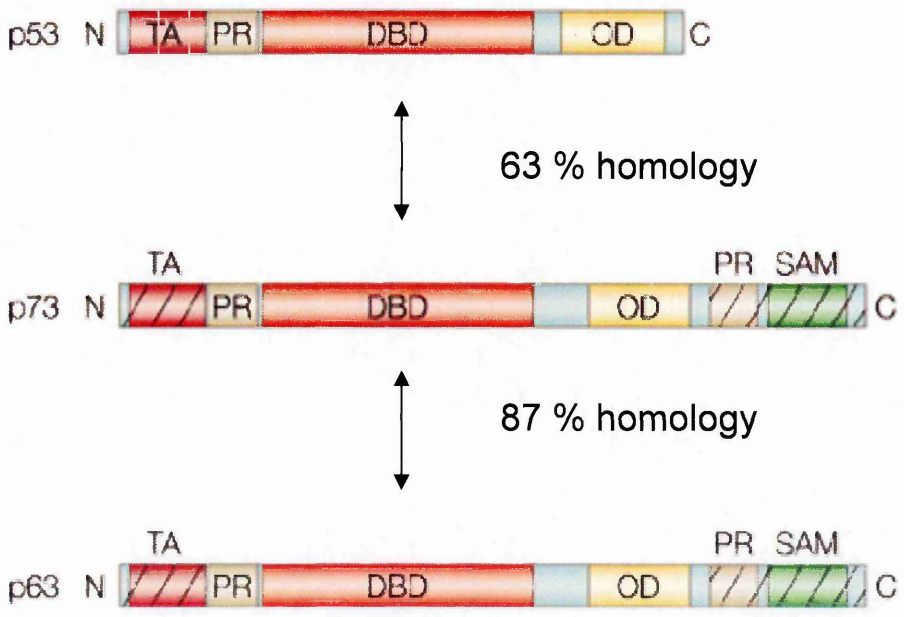

Figure 1.6

Structure and homology between p53, p63 and p73.

years afterwards. The first homologue to be discovered was p73 (283) and then the other homolog, p63 (also named KET, p51, p40, p73L) appeared (284-288). P53, p73 and p63 share a remarkable structural similarity. The three most conserved domains in all three genes are the NH_2-terminal TA, the central DBD and the oligomerisation domain (OD) in the COOH-terminal. The highest level of homology is reached in the DBD (63% between p53 and p73 and 60% identity between p53 and p63) suggesting that the three genes can transactivate the same target promoters (Fig. 1.6). The high conservation of the OD suggests that these family members can form hetero-oligomers as well as homo-oligomers, although published data show that homo-oligomers are favoured (158, 283, 289, 290). Both p63 and p73 contain in their long C-terminus a protein-protein interaction domain known as "sterile alpha motive" (SAM). Up to now, TP53 has a single promoter encoding both the full length p53 and the alternative splice variant of 40 KDa called DNp53. This splicing occurs at the 5' end of p53 RNA thus affecting the N-terminus of the protein. This N-terminally truncated form has been described in literature and termed p53/p47 and DNp53 (291, 292). DNp53 retains the intron 2 by alternative splicing and its translation starts at codon 40 (291). DNp53 oligomerises with full-length p53 ad interferes with its transcriptional and apoptotic functions. DNp53 does not respond to DNA damage.

For TP63 and TP73, two promoters have been identified: P1 in the 5' untranslated region upstream to the non coding exon 1 and P2 within the 23 kb spanning intron 3. P1 and P2 promoters produce two distinct

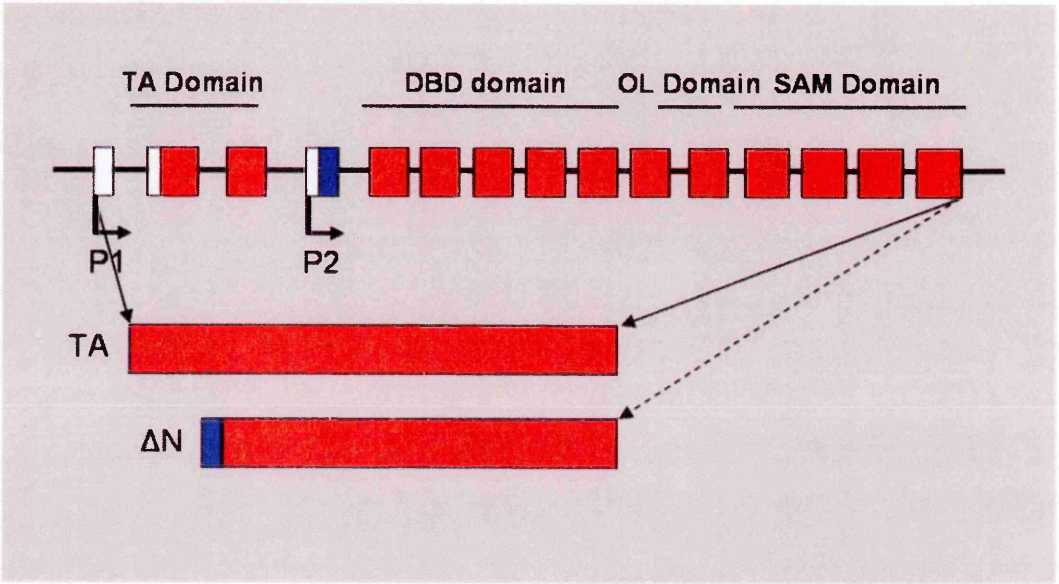

Figure 1.7

Structure of TA and of DN isoforms of p73 and p63.

classes of proteins: those containing the TA (TAp73 and TAp63) and those lacking it (DNp73 and DNp63) (Fig. 1.7). In addition, alternative exon splicing of the P1 transcripts of TP63 and TP73 gives rise to other isoforms lacking the transactivation domain (DN'p73, Ex2Delp73, and Ex2/3Delp73 ad DNp63) (283, 293, 294). Alternative splicing generates additional complexity at the C-terminus: TP73 and TP63 undergo multiple C-terminal splicing generating nine transcripts for TP73 (α, β, γ, δ, ε, ζ, η, η_1 and $\phi-\alpha$ being the full-length) (Fig. 1.8) (283, 295, 296) and three for TP63 (α, β, γ) (284).

1.6.2 Function of p63 and p73 and role in cancer development

Only a small percentage of human tumors have been shown to harbor p63 and p73 mutations (297), in contrast to p53 whose functional loss through mutation is a pre-eminent finding in most human cancers. TA proteins resemble p53 functions transactivating many p53 target genes. Therefore, these proteins can regulate cell cycle and apoptosis after DNA damage. Despite their functional and structural similarity with p53, p63 and p73 play important and unique roles in human and mouse development and differentiation. P63 and p73 knock-out mice exhibit severe developmental abnormalities (298-300) and this is in contrast to p53-null mice, which are highly tumor prone but lack a development-defective phenotype. The literature on p63 and p73 is complex and controversial, and their role in tumor suppression has been much debated. Irwin and Kaelin (297) have been reported that only in a small percentage of human tumors p63 and

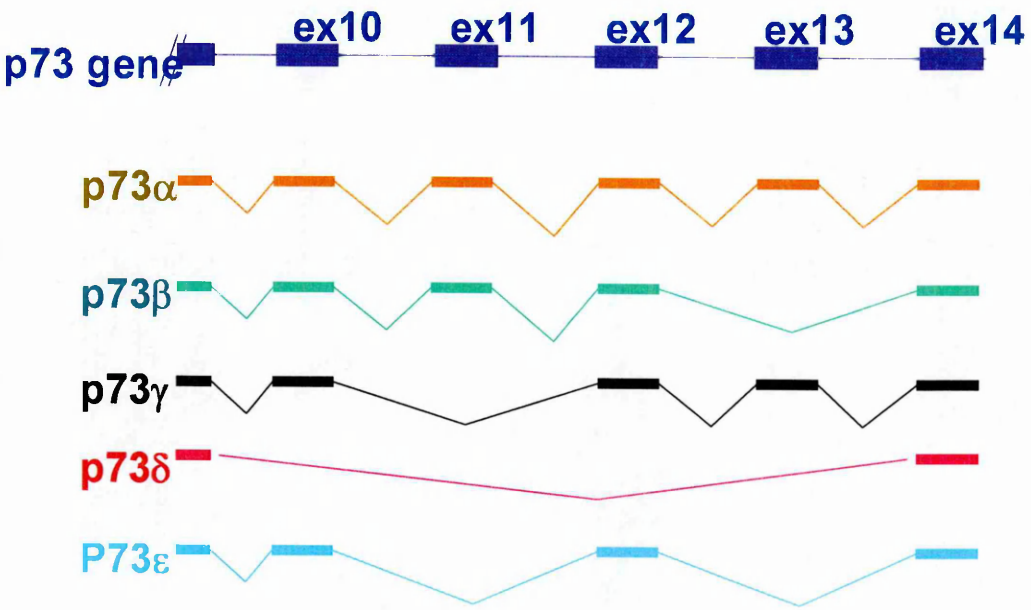

Figure 1.8

C-terminal splicing variants of p73.

p73 were mutated. However, recent studies have shown that some isoforms of p63 and p73 are overexpressed in human tumors (301, 302) whereas certain tumors exhibit loss or reduced expression of p63 and/or p73 (303-308). Recently, heterozygous knock–out mice for either p63 or p73 ($p63^{+/-}$ and $p73^{+/-}$) showed shorter life span than wild-type mice and develop spontaneous malignant lesions. All these data seem to demonstrate that these genes could act as tumor suppressors (309).

1.6.3 Function of DN isoforms

DN isoform proteins, lacking of the transactivation domain should not induce the transcription of target genes. Several studies have demonstrated that DN isoforms (in particular those manuscripts dealing with DNp73) act as dominant negative inhibitors of the TA proteins and of the other family members in cell culture (293, 296, 310). Acting as a dominant negative inhibitor, DNp73 can interfere with the p53 binding to its downstream responsive elements and can inhibit the transcription of the TA isoforms (TAp73 and TAp63). This effect can be mediated either by competition through its DNA binding domain, as for p53-responsive elements, and/or by protein-protein interaction through its oligomerisation domain. Recent data show that upon strong DNA damage DNp73 is rapidly degraded, releasing the block exerted on p73 and p53, thus allowing cell cycle arrest and apoptosis to proceed. Therefore the relative accumulation of DNp73 in human tumors could be an important determinant of cellular response to treatment. In several manuscripts it

has been reported that the level of DNp73 is higher in those patients with a poorer prognosis. However the levels of TAp73 in those tumors were still in excess (311-313). Nevertheless, in a recent paper, using a tet inducible expression of DNp73 in cells, it has been found that although the DNp73 levels were well above those of TAp73 and wild–type p53 there was no effect on the malignant phenotype. Furthermore, DNp73α does not induce a higher resistance to drug treatment in vitro or a more aggressive tumor in vivo (314).

Recently DNp73 has been strikingly shown, despite the lack of the TA domain, to be able to transactivate gene expression (315). Other studies have reported that both DNp73α and TAp73α were able to induce the accumulation of the endogenous wild–type p53 in various cell lines (316, 317). Recently, as reported in chapter 1.4.3, DNp73α was shown to induce the p53-dependent activation of $BTG2^{TIS21/PC3}$ expression at the promoter level in a neuroblastoma cell line. These findings together would strongly suggest that DN isoforms can have other functions, distinct from a simple antagonism on the TA isoforms and on p53.

1.7 Identification of a new p53-dependent gene

Despite being discovered 25 years ago, the tumour suppressor p53 continues to be highly studied, receiving most of the attention in the field of cancer research. Since its discovery in 1979, the number of publications centred on p53 are even more than 35,000 and it is considered the

common denominator in human cancer. P53 is, in fact, the most induced gene in response to cellular stress signals.

As a transcription factor, p53 can transactivate and transrepress many target genes; more than 100 have been identified through gene array analysis. Bioinformatic studies also predict more than 4,000 human gene containing putative p53 binding sites although the presence of a p53 binding site does not necessary mean that the gene containing this binding site is efficiently transactivated by p53. Moreover, p53 can repress the expression of many genes without these binding sites (318).

For this reasons and considering that p53 is highly mutated in cancers, it can serve as "nodal" point for the integration of a large number of different signals (64). This could suggest that there have to be numerous downstream genes acting as mediators of the different p53-dependent functions. Despite many of those functions of p53 have been elucidated, there are yet functions not completely explainable through the available p53 network. Either the search of other genes activated by p53, and therefore acting downstream to p53, or of genes having a complementary but p53 independent activity, is one important area of research which could help in better understanding the "behaviour" of cancer cells and possibly in future better rationalise the therapy for patients suffering from cancer.

Starting from this consideration, a program aimed at discovering new p53 dependent genes activated following damage started in the Laboratory of Molecular Pharmacology at the Mario Negri Institute. By using the

differential-display technique, a cDNA fragment expression was increased after treatment the cells with a synthetic derivative of distamycin A able to interact with the DNA minor groove. In figure 1.9 a representative differential display experiment is reported showing the cDNA fragment overexpressed 24 hours after treatment of the wild-type p53 expressing ovarian cancer cell line A2780.

This fragment has been cloned and sequenced and was found to match to a sequence (named KIAA0247) deposited in gene bank together with 80 new cDNAs (KIAA0201 to KIAA0280) deduced by analysis of cDNA clones from a cDNA library (319). The referenced publication does not contain any information regarding either the structure or the function of those genes whose cDNA sequence has been deposited. However, the authors reported the expression profiles for each cDNAs. In particular, the KIAA0247 cDNA has been found to be ubiquitously expressed at low levels in all human tissues tested. The isolated cDNA has been named DRAGO (DRug Activated Gene Overexpressed).

In order to isolate the complete cDNA containing the isolated fragment corresponding to the DRAGO gene, a cDNA library, prepared from human fibroblasts using λgt10 vector was hybridised with the isolated fragment as a probe in order to isolate the clone containing the full length cDNA of DRAGO. The positive clones were isolated and sequenced. In the meantime, during the sequencing of the isolated clones, the full-length cDNA (5,338 bp) subcloned in a pBluescript–SKII+ (pBS) vector was

kindly given by Nagase from Kazusa (Japan). The complete cDNA has 5,338 base pair and putatively codes for a protein of 303 amino acids.

To verify whether the increase was mediated by p53, the effects of antitumour drugs were evaluated in isogenic model-systems differing for p53 expression. For this purpose, the HCT-116 colon carcinoma cell line with wild–type p53 (clone 40.16, p53 +/+) or disrupted by targeted homologous recombination (clone 379.2, p53 –/–) have been used. An increased transcription of the isolated cDNA could not be observed by either RT-PCR or real time PCR in cells where the p53 gene had been inactivated (clone 379.2), suggesting that the activity of the gene under investigation is regulated by p53.

1.7.1 DRAGO induction by anticancer agents

The mRNA induction of DRAGO was further investigated by real-time PCR experiments after the cellular treatments with several cytotoxic compounds differing from distamycin A by their mechanism of action, such as cisplatin, taxol, doxorubicin and fluorouracil, obtaining in each case an increased production of the same fragment. However, after UV and topotecan treatments, no increase in the expression of DRAGO was measured (Fig. 1.10 and table 1.1).

Drugs were selected among conventional anticancer agents in order to use at least one compound from each group into which they are classified and that are known to induce the expression of p53.

Conventional chemotherapy included a number of families defined by both their chemical structure and mechanism of action: alkylating agents, antibiotics, antimetabolites, topoisomerase I and II inhibitors, mitosis inhibitors and others. These conventional treatments have basically evolved over the DNA molecule as its main molecular target (320).

Alkylating agents were the first compounds identified to be useful in cancer. These drugs add methyl or other alkyl groups onto target molecules. The most common site of alkylation is the N-7 position of guanine, but it varies depending on the family of drugs. The alkylating agents can act by attaching alkyl groups to DNA bases. This alteration results in the DNA being fragmented by repair enzymes in their attempts to replace the alkylated bases. Another mechanism by which alkylating agents cause DNA damage is the formation of cross-links, bonds between atoms in the DNA. In this process, two bases are linked together by an alkylating agent that has two DNA binding sites. Cross-linking prevents DNA strands from being separated for synthesis or transcription. Finally the action of alkylating agents causes the mispairing of the nucleotides leading to mutations.

Alkylators belong to one of several families: nitrogen mustards, nitrosoureas, triazenes, platinum compounds and antibiotics. These compounds can also be classified into either minor or major groove alkylating agents (320).

The platinum compounds such as Carboplatin and Cisplatin (cDDP) are alkylating agents of the DNA major groove. These related drugs covalently

bind to DNA with preferential binding to the N-7 position of guanine. They are able to bind to two different sites on DNA producing cross-links, either intrastrand or interstrand resulting in inhibition of DNA synthesis and transcription (320).

Brostallicin (PNU-166196) is a novel compound which is able to alkylate mostly N3–position of adenine on the DNA minor groove. These agents, which belong to the generally classified minor groove binders (MGB) have been shown to be highly effective in *in vitro* and *in vivo* preclinical tumour models unresponsive to other antineoplastic agents (321). The main representatives of this class, which reached the clinical trials, are the Brostallicin ad the antitumour agents derived from CC-1065, that is, Adozelesin, Carzelesin, and Bizelesin (322).

A number of antibiotics such as anthracyclines, dactinomycin, bleomycin, adriamycin, mithramycin, bind to DNA and inactivate it. Thus the synthesis of RNA is prevented. General properties of these drugs include: interaction with DNA in a variety of different ways including intercalation (squeezing between the base pairs), DNA strand breakage and inhibition with the enzyme topoisomerase II (320).

Most of these compounds have been isolated from natural sources and antibiotics. However, they lack the specificity of the antimicrobial antibiotics and thus produce significant toxicity.

The anthracyclines (doxorubicin and their analogs epirubicin and idarubicin) inhibit topoisomerase II and form free radicals.

The main epipodophillotoxin, etoposide (VP-16), also inhibits topoisomerase II.

Topoisomerase I transiently breaks a single strand of DNA during DNA replication, thereby reducing torsional strain. Inhibitors of this enzyme derive from camptothecin, such as topotecan and irinotecan (323).

The antimetabolites interfere with enzymes that contribute to DNA synthesis. In this group there are antifolates, fluoropyrimidines, raltitrexed, cytarabine, gemcitabine, and adenosine analogs (fludarabine, pentostatin, cladribine). 5-Fluorouracil (5-FU; Adrucil®, Fluorouracil, Efudex®, Fluoroplex®) is an effective pyrimidine antimetabolite. Fluorouracil is synthesized into the nucleotide, 5-fluoro-2-deoxyuridine. This product acts as an antimetabolite by inhibiting the synthesis of 2-deoxythymidine because the carbon - fluorine bond is extremely stable and prevents the addition of a methyl group in the 5-position. The failure to synthesize the thymidine nucleotide results in little or no production of DNA (324).

Mitotic spindles are essential when a cell starts to divide itself into two new cells. These spindles are very important because they help to split the newly copied DNA such that a copy goes to each of the two new cells during cell division. Spindles are microtubular fibers formed with the help of the protein "tubulin". The antimitotic drugs disrupt the formation of these spindles and therefore interrupt cell division. Among them, Vincristine is a mitotic disrupter since it binds to tubulin, thus preventing the formation of spindles and cell division. In contrast to other microtubule antagonists, taxol disrupts the equilibrium between free tubulin and mircrotubules by

shifting them in the direction of assembly, rather than disassembly. As a result, taxol treatment causes both the stabilization of microtubules and the formation of abnormal bundles of microtubules. The net effect is still the disruption of mitosis (325).

1.7.2 Mouse DRAGO expression

Analogously to human, a mouse cDNA library has been screened using the same human cDNA fragment of DRAGO gene as a probe for the isolation of the murine cDNA coding the murine homologue of human DRAGO gene product.

The full length murine cDNA analog consists of 5,338 bp coding for a putative protein of 302 aminoacids. The comparison between the human and murine sequences revealed a striking 80% similarity both at nucleotide and aminoacid level.

The mRNA induction of DRAGO was further investigated in isogenic murine systems differing for p53 status by semi-quantitative RT PCR experiments. MEF expressing a wild–type p53 or lacking it was treated with several cytotoxic compounds and total RNA was extracted from treated and untreated cells. Semi quantitative RT-PCR experiments confirmed that the murine homologue to human DRAGO gene is induced upon cytotoxic treatments in a p53-dependent manner.

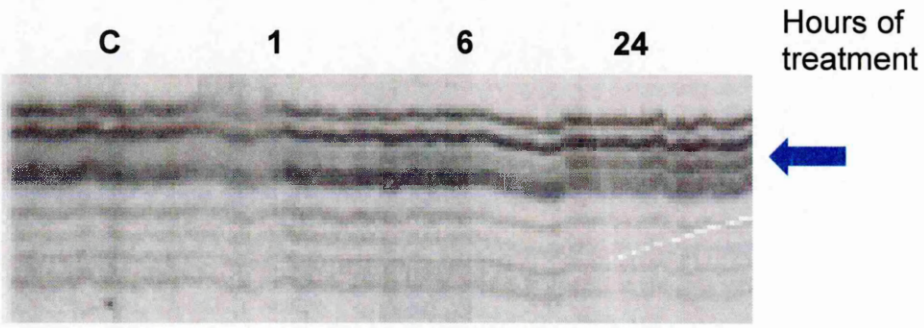

Figure 1.9

Representative differential display experiment showing the induction of a cDNA fragment 24 hours after treatment in A2780 cell lines.

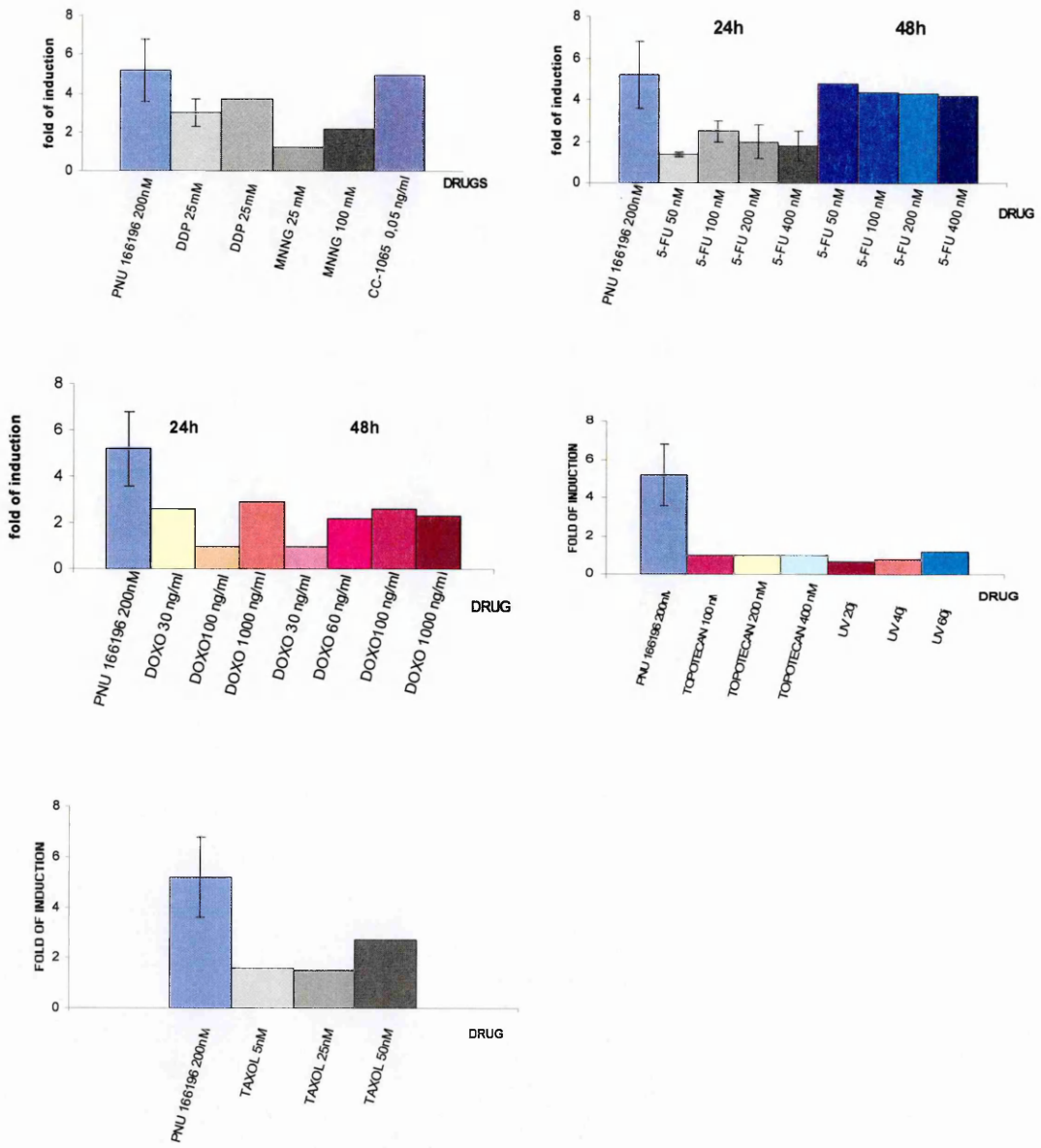

Figure 1.10

Expression of DRAGO induced after cytotoxic compounds and UV treatments.

DRUGS	DRAGO
PNU 166196 (200nM x24h)	++
DDP (25 mM x1h R=24) *	+
DDP (25 mM x1h R=6)	-
MNNG (25 mM x2h R=24) *	-
MNNG (100 mM x2h R=24)	+'/'-'
TAXOL (5 nM x24h) *	-
TAXOL (25 nM x24h)	-
TAXOL (50 nM x24h)	+++
UV 20j *	-
UV 40j	-
UV 60j	-
5-FU (50 nM x24h) *	-
5-FU (100 nM x24h)	+
5-FU (200 nM x24h)	-
5-FU (400 nM x24h)	-
5-FU (50 nM x 48h)	++
5-FU (100 nM x 48h)	++
5-FU (200 nM x 48h)	++
5-FU (400 nM x 48h)	++++
DOXO 30 ng/ml (24h) *	+
DOXO 60 ng/ml (24h)	
DOXO100 ng/ml (24h)	-
DOXO 1000 ng/ml (24h)	+
DOXO 30 ng/ml (48 h)	-
DOXO 60 ng/ml (48h)	+
DOXO100 ng/ml (48h)	+
DOXO 1000 ng/ml (48h)	+
CC-1065 (0,05 ng/ml x1h R=24h)	++

Table 1.1

Summary of level of DRAGO mRNA induction upon treatments at indicated doses

1.8 AIMS

Tumorigenesis can be viewed as an evolutionary process that allows somatic cells that evade normal controls of cell proliferation and cell death to promote their unlimited clonal expansion.

As outlined in chapters 1.1 and 1.2, cancer evolution can be fueled by genomic instability caused by faulty cell division or defective DNA repair. However, cells are efficiently protected from tumorigenesis by several failsafe mechanisms and checkpoints. One of the most important components of the systems that keep us relatively safe from cancer is p53 which is arguably the most well-known tumor suppressor gene (see chapter 1.4). Despite the considerable amount of knowledge that has been accumulated on p53, the p53 network is not yet fully understood. Furthermore, the available sequences of the human genome have allowed the identification of genes that are theoretically transcriptionally activated by p53. The main outcome of p53 activity in controlling tumor growth is cell cycle arrest and apoptosis. Among these functions, much less is known about the mechanisms by which p53 induces apoptosis. For this reason, an ongoing program in the Molecular Pharmacology Laboratory at the Mario Negri Institute is aimed at identifying new gene downstream of p53 with particular emphasis on those involved in apoptosis. By using the differential display technique DRAGO, a new gene, has been isolated, the expression of which is induced following cellular damage. Preliminary data suggest that DRAGO is a new gene activated following induction of DNA

damage in a p53-dependent way (see chapter 1.7.1). The present studies have been undertaken with the overall aim to provide a preliminary characterisation of the DRAGO gene. The work described here had the following specific objectives:

i. The initial aim was to characterise the structure of the gene at a molecular level. Thus, the full length cDNA has been compared with the available sequences of human genome.

ii. As DRAGO is a p53 downstream gene, a genomic fragment comprising a region upstream the first exon has been isolated with the aim to characterise the promoter region putatively containing the p53 canonical responsive elements. The promoter activity of genomic fragments isolated and the responsiveness to p53 induction have been examined using the luciferase reporter gene assay in transient transfection experiments in the absence or presence of p53. Given that p53 belongs to a family of genes including p63 and p73, the hypothesis has been tested that these functionally homologous family members might induce the expression of DRAGO in analogy to p53. The effect of DNp73α on p73 isoforms transactivation of DRAGO gene expression was also evaluated.

iii. Many human genes with tumor suppressor activity, like p53, have been found to be mutated or altered in human tumors. So another aim of the present study has been the search for any mutations of the DRAGO gene at a nucleotide level. To this end, on the basis of the molecular structure SSCP analysis, followed by DNA sequencing, have been

performed in human cell lines, cells with acquired resistance against cytotoxic drugs and human tumor sample.

iv. In order to understand the putative secondary structure of the protein, a computational analysis of the sequence of protein, derived on the basis of the cDNA, have been performed.

v. To understand the evolutionary conservation of DRAGO, the human sequence has been compared with cDNA sequences from different organisms for which the genome was available from the public gene bank.

vi. Another important objective of the study was the characterisation of the function of the gene under investigation. To that end, the effects of the overexpression of the gene were evaluated in stable and transient transfections experiments. The full length cDNA, the coding region of the gene and different deletion fragments have been subcloned in an expression plasmid under a strong promoter ensuing the constitutive expression of the gene in an *in vitro* model. Furthermore, the function of the DRAGO gene was explored by investigating and characterizing mice in which the gene was knocked out (KO). KO fibroblasts have been isolated from mouse embryos and used for *in vitro* experiments to evaluate of the response to DNA damage.

CHAPTER 2

MATERIALS AND METHODS

2.1 Cell culture

2.1.1 Culture condition

All the cell culture procedures were carried out aseptically in laminar flow hoods. Cells were maintained in a humidified incubator at 37 °C with 5% CO_2.

The human cancer cell lines used in these studies were: the human ovarian carcinoma cell lines A2780, SW626, COS-7, IGROV-1 and SKOV-3, the human colocarcinoma cell lines HCT-116 and SW620, the human acute lymphoblastic leukaemia (ALL) cell lines ALL-PO, Reh, Tom-1, the human osteosarcoma cell lines U2OS and Saos-2, the metastatic prostate carcinoma cell line DU145, the human lymphoblastoids cell line CEM, the human promyelocytic cell line HL-60 and the murine fibroblast cell line Swiss 3T3. Drug-resistant cell lines were: A2780/cp70, an A2780 cellular clone resistant to DDP (326); 1A9PTX22 resistant to paclitaxel, were generated from 1A9 (327) and kindly given by NCI; CEM-VM1 (328), generated from their drug–sensitive parental CEM cells, were selected for their resistance to VM26; LoVo/DX were selected from LoVo cells for their resistance to doxorubicin (329) and also to other chemotherapeutic agents, such as etoposide and vincristine (330).

All the ovarian cancer cell lines (except COS–7), the ALL cell lines, SW620 and U2OS cells were grown in RPMI 1640 supplemented with 10% (v/v) fetal calf serum (FCS) and 2 mM of L-Glutamine.

DU145, CEM and HL-60 were grown in RPMI 1640 supplemented with 10% (v/v) heat-inactivated FCS and 2 mM of L-Glutamine.

Saos-2, Swiss 3T3 and COS–7 cells were maintained in DMEM supplemented with 10% of FCS and 2 mM of L-Glutamine. To the culture medium of Swiss 3T3 and COS–7 cells, 1 mM Na-pyruvate (Mascia Brunelli, Milan-Italy), 1% non-essential amino acid (Mascia Brunelli) were added. COS–7 medium also required 20 mM Hepes Buffer solution (Mascia Brunelli). LoVo/DX were grown in Ham's F12 medium supplemented with 10% of FCS and 2 mM of L-Glutamine. The different media were purchased from Sigma (Milan–Italy) and contained all the minerals and supplements necessary for the growth of the cells except for the serum (Sigma) and the L-glutamine (Sigma), which were added when needed.

Cells were passaged routinely to maintain them in the growth logarithmic phase. The cells were renewed every four-five months of culture.

Passage procedures for leukemia cell lines provided for seeding cells at a suitable density after counting the cell at the cell culture counter (Coulter Channelyser® 256, Beckman Coulter, Milan-Italy). The other cell lines were washed twice with warm sterile phosphate buffer saline (PBS, Bio-Whittaker, Milan-Italy) and detached with a solution of 1x trypsin/EDTA (Bio-Whittaker). The trypsin activity was stopped by adding calf serum-containing medium. After centrifugation at 1,200 rpm for 10 minutes, cells were resuspended in the appropriate medium, counted and seeded at the desired concentration.

2.1.2 Long term storage of cultured cells

To cryopreserve batches of cells, exponentially growing epithelial cells were washed twice with PBS, detached and centrifuged at 1,200 rpm for 10 minutes at room temperature. Cells growing in suspension were only centrifuged as reported above. The cell pellet was resuspended in culture medium containing 50% of cryoprotective medium (Bio-Whittaker) and 20% of calf serum to a density of 5 x 10^6 cells/ml. Aliquots of 1 ml were cooled slowly on ice 30 minutes, pre-frozen in nitrogen liquid stream for 3 hours and then immersed in liquid nitrogen. To recover from the cell bank, each vial of cells was thawed rapidly to 37 °C in a water bath, transferred in fresh medium and centrifuged at 1,200 rpm for 10 minutes. Pellets were then resuspended in the appropriate culture medium and moved to a tissue culture flask. The day after cells were washed and new, fresh medium was added.

2.2 Generation of cellular clones

2.2.1 Subcloning of the full length cDNA

To transfer the gene of interest in the genome of host cells, the DNA was excised from the plasmid of origin by restriction endonuclease digestion and subcloned in the appropriate expression vector. The expression vector used was the $pCDNA_3$ (Invitrogen, Milan, Italy). The principal features of this plasmid are: the presence of a strong viral promoter (cytomegalo virus, CMV) driving the transcription, a polylinker sequence

(also known as multiple cloning site – MCS) the DNA recognition sequence for many restriction enzymes to facilitate the subcloning of the gene of interest, a bacterial resistance gene (ampicillin) for selection of recombinants and an eukaryotic resistance gene (neomycin) for selection of cells containing the plasmid. To subclone the gene of interest, the general molecular biology techniques reported in Sambrook and Russel (331) were followed. Briefly, the gene of interest was excised from the plasmid of origin by digestion with the appropriate restriction enzymes for 1 hour at 37 °C in a buffer supplied with the enzyme. The entire reaction was loaded on 1% agarose gel (see section 2.7.1). The appropriate band containing the cDNA was excised from the gel and the DNA extracted from the agarose (section 2.7.2). The cDNA thus obtained was stored at –20 °C. The $pCDNA_3$ plasmid was digested with the same restriction enzymes used to excise the cDNA from the original plasmid, loaded on agarose gel and purified from it. The linearised $pCDNA_3$ plasmid was ligated with the excised cDNA insert in a 1:3–1:5 proportion in 10 µl of a solution containing 3 U of T4 DNA ligase (Promega, Milan–Italy) and 1x Rapid Ligation Buffer (30 mM Tris-HCl, pH 7.8, 10 mM $MgCl_2$, 10 mM DTT and 1 mM ATP, supplied with the ligase) for 4 hours at room temperature. Five µl of this solution were then used to transform competent bacteria.

2.2.2 Subcloning of the coding sequence

The coding region (nucleotides 269-1180) of DRAGO was obtained by PCR (see section 2.4) amplification using as a template the construct pBS-DRAGO. The coding region was subcloned in three vectors $pCDNA_3HA$ (see Results chapter 6.2), pEGFP–C1 (BD Bioscience Clontech, Milan–Italy) and pGEX–3X (Amersham Biosciences, Milan–Italy). Briefly, the pEGFP–C1 vector has the same features of the $pCDNA_3$ vector described above except for the bacteria selection which is a kanamycin resistance. The main characteristic is the presence of the cDNA encoding the GFP with the MCS at the 3' end of the GFP cDNA. Therefore the genes cloned into the MCS are expressed as fusions to the C–terminus of the GFP protein as they are in the same frame as GFP and there are no intervening stop codons. The pGEX–3X vector is designed for inducible, high–level intracellular expression of genes or gene fragments as fusions with *Schistosoma japoncum* Glutathione S–transferase (GST). This vector has a *tac* promoter for chemically inducible (using the lactose analogue isopropyl β–D–thiogalactoside, IPTG), high level expression of exogenous protein in *E. coli* hosts. The MCS is located at the 3' end of the cDNA encoding the GST protein. Therefore, genes therein cloned are expressed as fusions to the C–terminus in frame with the GST protein. The factor Xa protease recognition site for cleaving the desired protein from the fusion product is between the GST coding sequence and the MCS. Bacterial cells carrying the pGEX–3X vector are selected for ampicillin resistance.

Forward and reverse primers were designed to contain the restriction enzyme specific sequence at their 5' termini in order to further allow sub-cloning in the vectors. The sequences of the forward and reverse primers are listed in figure 2.1 for each construct. Underlined are the recognition sites for restriction enzymes in the forward and reverse primers, which are *Xho*I and *Xba*I, *BamH*I and *EcoR*I, *Kpn*I and *Hind*III for subcloning in the pCDNA$_3$HA, pGEX–3X and pEGFP–C1 vectors, respectively. PCR amplification conditions were as follows: 95 °C for 40 seconds; annealing for 30 seconds; 72 °C for 1 minute and 30 seconds, for a total of 30 cycles, followed by an additional step at 72 °C for 7 minutes. The annealing temperature (AT), specific for each set of primers is indicated in figure 2.1. The PCR products were analysed through 1% agarose gel. The size of the PCR amplified fragments was compared with the marker's run. The DNA band of the expected size were extracted from the gel, subcloned in the pGEM–T easy vector for TA cloning (see section 2.2.4), excised by restrictrion endonuclease digestion with appropriate enzymes to be subcloned in the suitable vector. The procedure with respect to the restrictions and to the vectors was followed as described in section 2.2.1.

2.2.3 Subcloning of the deleted mutants

N– and C–terminus deleted mutants of DRAGO coding region were generated by PCR and subcloned in the pCDNA$_3$HA, pGEX–3X and pEGFP–C1 vectors. The entire coding region subcloned in the same

pCDNA$_3$HA

Forward	>XHOI 5'–CTCGAGTGCCATGGCAGGATAGCACC–3'
Reverse	>XBAI 5'–TCTAGATCATGCTTCTTTCAACAGTG–3'
AT	60 °C

pGEX–3X

Forward	Gex S 5'–GGATCCCCTGCCATGGCAGGATAGCACCA–3'
Reverse	Gex A 5'–GAATTCTGCTTCTTTCAACAGTGGAAT–3'
AT	60 °C

pEGFP–C1

Forward	KIA1 5'–AAGCTTGCCATGGCAGGATAGCCACCAAA–3'
Reverse	KIA2 5'–GGTACCTCATGCTTCTTTCAACAGTG–3'
AT	60 °C

Figure 2.1

Primers for subcloning the coding sequence of DRAGO in the vectors here reported. The sites specific for restriction enzymes were underlined.

vector was used as template. Primers were designed to contain the restriction enzyme specific sequence at their 5' termini in order to further allow sub-cloning in the vectors. For N–terminus deleted mutants, the reverse primer was the same (XBAI and GexA respectively for $pCDNA_3HA$ and pGEX–3X constructs, see figure 2.1) as that used for the entire PCR amplified coding region. Similarly, for the C–terminus deleted mutants, the forward primer was the same as for the entire coding region (XHOI, GexS and KIA1 for $pCDNA_3HA$, pGEX–3X and pEGFP–C1 constructs). The sequences of the primers and the corresponding annealing temperatures are listed in figure 2.2 for each construct. PCR conditions for amplification and the subcloning procedure were the same as described in 2.2.2.

2.2.4 TA cloning

This technique provides a one step cloning strategy for a direct insertion of PCR product into a vector (T–vector), taking advantage of the Taq enzyme non-template dependent activity of adding an adenenine (A) to the 3' ends of PCR products. The T–vector contains in its MCS complementary an unpaired 3' thymidine (T). PCR products were ligated at a ratio 1:5, 1:10 in the pGEM-T easy vector from the cloning kit (pGEM–T easy vector systems) purchased from Promega and following the manufacture's instructions.

pCDNA$_3$HA–deletion mutants

Forward	**XHOI** 5'–CTCGAGTGCCATGGCAGGATAGCACC–3'	
Reverse	**HA–C1** 5'–TCTAGATCATGACGTGAGGGATAAAAGGCTTTG–3'	62 °C
	HA–C2 5'–TCTAGATCATGCAGTTTCTTTGTGTGC–3'	60 °C
	HA–C3 5'–TCTAGATCACCAGGAAGAGGTGGTTGC–3'	60 °C
	HA–C4 5'–TCTAGATCAGGCAGAGCCCCAGGCTTCACATAG–3'	62 °C
	HA–C5 5'–TCTAGATCAATCTTCTCCACCTGCAGAGGA–3'	60 °C
	HA–C6 5'–TCTAGATCATTGCTCCCTTGGCACGCTCCT–3'	62 °C
Forward	**HA–N1** 5'–CTCGAGTCAGTGTTTGCCGTGGCCTCC–3'	58 °C
	HA–N2 5'–CTCGAGGTGTTCCTTCCGCTAGTG–3'	58 °C
	HA–N3 5'–CTCGAGGGAGACGGACTTGCTTCC–3'	58 °C
	HA–N4 5'–CTCGAGGAGAATGGTGGCTACATCTGCCACCCC–3'	58 °C
	HA–N5 5'–CTCGAGTGCAGAGACCCCCTGACAGCAGGC–3'	58 °C
	HA–N6 5'–CTCGAGTGTGCTGAAGGCTACATGTTGAAG–3'	58 °C
Reverse	**XBAI** 5'–TCTAGATCATGCTTCTTTCAACAGTG–3'	

pGEX–3X deletion mutants

Forward	**GEX S** 5'–GGATCCCCTGCCATGGCAGGATAGCACCA–3'	
Reverse	**GEX–C1** 5'–GAATTCTCATGACGTGAGGGATAAAAGGCTTTG–3'	61 °C
	GEX–C2 5'–GAATTCTCATGCAGTTTCTTTGTGTGC–3'	59 °C
	GEX–C3 5'–GAATTCTCACCAGGAAGAGGTGGTTGC–3'	61 °C
	GEX–C4 5'–GAATTCTCAGGCAGAGCCCCAGGCTTCACATAG–3'	62 °C
	GEX–C5 5'–GAATTCTCAATCTTCTCCACCTGCAGAGGA–3'	61 °C
	GEX–C6 5'–GAATTCTCATTGCTCCCTTGGCACGCTCCT–3'	62 °C
Forward	**GEX–N1** 5'–GGATCCCCTCAGTGTTTGCCGTGGCCTCCG–3'	59 °C
	GEX–N2 5'–GGATCCCCGTGTTCCTTCCGCTAGTG–3'	53 °C
	GEX–N3 5'–GGATCCCCGGAGACGGACTTGCTTCC–3'	59 °C
	GEX–N4 5'–GGATCCCCGAGAATGGTGGCTACATCTGCCACCCC–3'	59 °C
	GEX–N5 5'–GGATCCCCTGCAGAGACCCCCTGACAGCAGGC–3'	57 °C
	GEX–N6 5'–GGATCCCCTGTGCTGAAGGCTACATGTTGAAG–3'	59 °C
Reverse	**GEX A** 5'–GAATTCTGCTTCTTTCAACAGTGGAAT–3'	

pEGFP–C1 deletion mutant

Forward	**KIA1** 5'–AAGCTTGCCATGGCAGGATAGCCACCAAA–3'	
Reverse	**HA–C2** 5'–TCTAGATCATGCAGTTTCTTTGTGTGC–3'	61 °C

Figure 2.2

PCR condition (primers sequences and AT) for the amplification of N– and C–terminus deletion mutants of DRAGO coding region.

2.2.5 Preparation of competent bacterial cells for transformation

Bacterial strains in the experiments reported in this thesis were XL1Blue (Stratagene) and JM110 (Stratagene). The latter, an *E. coli* strain which lacks both *dam* (DNA adenine methylation) and *dcm* (DNA cytosine methylation) gene was used for pCDNA$_3$HA constructs, being the *Xba*I restriction enzyme site, used for cloning, methylation sensitive (see section 2.2.3). The methylation avoids the cleavage by means of the enzymes.

From a sterile bacterial cellular suspension, 10 µl of suspension were spread to an agar plate containing LB (Luria–Bertani) agar and incubated overnight at 37 °C.

Complete LB agar (Sigma) (which is constitute by LB broth and agar–1.5% w/v) and LB broth (Sigma) where purchased as lyophilised powder to be reconstituted in a suitable volume of deionised water per grams of powder as indicated by the manufacturer. The solution was then autoclaved at 120 °C for 10 minutes and poured on 90-mm dish (Corning-Costar, Milan-Italy) and allow to dry under sterile hood.

Whenever required to the medium the antibiotic of selection (for pCDNA$_3$ and pGEX–3X derived plasmids, ampicillin at the final concentration of 50 µg/ml; for pEGFP–C1 derived plasmids, kanamycin at the final concentration of 10 µg/ml was added after autoclaving once it had cooled to 55 °C).

A single colony was picked-up with a sterile disposable loop, and resuspended in a sterile 50 ml conical tube, with 10 ml of sterile LB

medium and allowed to grow in a 37 °C heated shaking incubator (Folabo, Milan–Italy) at 225 rpm overnight. One ml of such liquid bacterial culture was then transferred into 100 ml of sterile LB medium and placed into the 37 °C heated shaking incubator at 225 rpm.

To harvest bacterial cells in logarithmic growth phase, 2 hours later, 1 ml of liquid culture was transferred, under a laminar flow in a disposable cuvette and the absorbance at 600 nm wave-length was read on the spectrophotometer. *E. coli* concentration in the liquid culture was calculated by considering that 1 A_{600} nm unit corresponds to about 10^9 bacterial cells/ml. When the 600 nm absorbance reached A 0.3 units (corresponding to roughly 2.4 x 10^8 cells/ml;) the bacterial suspension was transferred in two ice-cold sterile 50 ml conical tubes and the cell growth was stopped by placing the tubes on ice for 15 minutes. *E. coli* cells were pelleted by centrifugation at 3,000 rpm for 10 minutes at 4 °C and, after removing the LB medium, cell pellets were pooled in the same tube by gentle resuspension in 10 ml of ice-cold sterile 0.1 M $CaCl_2$ solution (*obtained by dilution of a 2 M $CaCl_2$ solution, prepared by dissolving 14.7 g of $CaCl_2$ in 100 ml H_2O and filtering the solution with a syringe equipped with a 0.2 μm filter*). After addition of 40 ml of ice-cold sterile 0.1 M $CaCl_2$ solution, bacterial suspension was incubated on ice for 30 minutes and subsequently centrifuged at 3,000 rpm for 10 minutes at 4 °C. The supernatant was then removed and the cell pellet was carefully resuspended in 5 ml of an ice-cold sterile 0.1 M $CaCl_2$ containing 15% (v/v) glycerol (Sigma). This bacterial suspension was dispensed in 1.5 ml

Eppendorf tubes (Eppendorf, Milan–Italy) (400-500 µl aliquots for each tube) and kept at 4 °C for 24 hours after which the tubes were quickly frozen in liquid nitrogen and stored at –80 °C. The cells maintained their competence for transfection for 1-2 months when kept at –80 °C.

Fifty µl of freshly prepared competent cells were transformed with 50 ng of a DNA vector able to confer ampicillin resistance and 1/100,000 (dilution factor, 10^5) of the bacterial suspension was plated as described in agar plates. Transformation efficiency, calculated on the basis of the formula (NUMBER OF COLONIES) x (10^3) X (DILUTION FACTOR) / 50 ng, was expressed as the number of colony forming units (CFU) per µg of plasmid DNA. Generally, 10^6-10^8 CFU per µg of plasmid DNA were indicative of a good preparation of competent bacterial cells.

2.2.6 Transformation of bacteria

In an ice-cold 10 ml Falcon 2059 tube (Falcon, Becton Dickinson), 50 µl of competent bacterial cells were diluted to a final volume of 100 µl with 0.1 M $CaCl_2$ and either 50 ng of purified plasmid or half of the volume of the ligation reaction. The mixture was gently mixed and the tube was chilled on ice for 30-40 minutes, incubated for 2 minutes at 42 °C in a water bath and for 2 minutes again on ice. After a 5 minute incubation at room temperature, 900 µl of LB medium were added and tube was placed into a 37 °C heated shaking incubator at 225 rpm for 1 hour. The tube was then centrifuged at 3,000 rpm for 5 minutes at room temperature, most of the supernatant LB removed and the bacterial cell pellet resuspended in the

remaining fluid and spreaded into 90-mm dish, containing LB agar medium plus the antibiotic of selection and incubated overnight at 37 °C without agitation.

2.2.7 Identification of recombinant clones and purification of DNA from bacteria

Each colony, representing antibiotic-resistant/transformed growing bacterial cells, was picked-up with a sterile disposable loop and dissolved in a 15 ml falcon tube containing 3 ml of liquid LB medium supplemented with antibiotic and allowed to grow overnight at 37 °C with shaking at 225 rpm.

Plasmidic DNA was purified from bacterial suspension using the Quiagen mini-prep kit (Quiagen, Milan–Italy). The procedure, starting from 1.5 ml of bacterial suspension was exactly as described by the manufacturer. The recovered DNA, in 50 µl of water, was subjected to restriction digestion with appropriate restriction enzymes to verify that the insert was indeed present in the colony isolated. After digestion and separation on agarose gel, the fragments of DNA were visualised by using an UV transilluminator. The positive colonies containing the right insert were stored at –80 °C after the addition of 0.5 ml of 50% sterile ultra pure glycerol (Sigma) to 0.5 ml of the bacterial suspension used for the enzyme digestion. When necessary, the remaining DNA was used for confirmation by DNA sequencing, which was performed through custom sequencing services (through a core facility available at Mario Negri Bergamo, Bergamo, Italy). Once verified that the plasmid contained the right insert and sequenced, if necessary, a

large scale preparation of DNA was performed, using the Qiagen Plasmid Midi Kit (Qiagen) following the procedures reported in the instruction manual.

The DNA recovered from the midi preparation was quantified at the spectrophotometer by reading the absorbance at 260 nm and 280 nm. The quality of the DNA prepared was determined by the ratio between 260 nm and 280 nm absorbances, which should be 1.8.

For quantification the extinction coefficient was used. The amount of DNA was calculated considering that a solution of 50 µg of DNA/ml would give a reading of 1 at 260 nm.

2.2.8 DNA-Transfection

DNA was transfected in different cell lines by using the calcium phosphate precipitate method. Sterile water–dissolved DNA was mixed with a 0.25 M $CaCl_2$ solution (obtained solution from a stock solution 2 M $CaCl_2$, see 3.2.5) in a volume of 250 µl. In a 4 ml transparent tube (Falcon), 250 µl of a 2X HEPES-Buffered Saline (HEBS 2X) were placed:

HEBS 2x	*final concentration*
1.6g NaCl	*280 mM*
0.074g KCl	*10 mM*
0.027g $Na_2HPO_4 \cdot H_2O$	*1.5 mM*
0.02g Dextrose	*12 mM*
1g HEPES	*50 mM*

The salts are dissolved in 50-70 ml of distilled water and the pH of the solution is then adjusted to 7.2 with 0.5 N NaOH and then brought to 100 ml with sterile water.

With the use of a 1 ml sterile pipette fixed to an automatic pipettor placed in the tube containing the HEBS solution, the air was forced inside the tube. To the bubbling solution, the DNA-$CaCl_2$ mixture is added dropwise, then, vortexed for 20 seconds and kept in a tube holder for 30 minutes. The solution is then added dropwise to the cells seeded in a 25 cm^2 flask and incubated 16 hours at 37 °C. The day after, cells are visualised under the microscope to verify the presence of small precipitates of $CaPO_4$ on the cell surface. The cells are then extensively washed with sterile PBS at least three times and resuspended in complete culture medium.

2.2.9 Isolation of cell clones stably expressing the gene of interest

Forty–eight hours after the end of transfection, the cells were detached with trypsin/EDTA solution. After counting, the cells were seeded in 9 mm plates at a density of 5,000 cells/ml in medium containing the selection antibiotic (500 µg/ml of G418 for neomycin resistance gene containing plasmids). At these antibiotic concentrations parental cells were killed and the only cells growing were likely to be those which have integrated in their DNA the transfected plasmid. The plates were then incubated at 37 °C and the medium renewed every two-three days. Once the colonies were formed as visualised under the microscope, they were isolated from the other by using plastic rings which were stuck to the plate by using

vaseline. Twenty µl of a trypsin/EDTA solution were added to the single colony isolated to detach the cells which were then placed in a 24–wells plates containing 1 ml of medium plus selection antibiotic. The different clones picked up from the original plates were grown and passed in duplicate in 6 well plates. One plate was used to maintain the cell clone for further studies and for long term storage. The other was used to verify the overexpression of the mRNA of the gene of interest by screening the clones thus obtained by Northern blotting. The clones selected were then expanded and stored in different aliquots in liquid nitrogen.

2.3 Luciferase reporter assay

These experiments were performed to evaluate the promoter activity of DNA fragments subcloned in the promoterless plasmid pGL2–Enhancer vector (Promega), carrying a non mammalian gene luciferase followed by a viral enhancer and a multiple cloning site at its 5'. The genomic fragments to be analysed for promoter activity are subcloned in the multiple cloning sites of pGL2 vector using restriction enzymes–based ligations. In same cases fragments were excised from the DNA region in which it was contained by restriction enzymes reaction. Otherwise fragments were PCR amplified to introduce the sequence site for cleavage of suitable restriction enzymes for subsequent cloning in the pGL2–enhancer vector. Primers are listed in figure 2.3 and underlined is the restriction enzyme sequence introduced by PCR. Once verified the exact insertion and orientation of the fragment using the procedures reported in

964 bp

Forward **KpnI** 5'–CCCGGGAGGTACCTGGCCCGGCCGGCGGCGCGT–3'

Reverse **XhoI–rev** 5'–GTTTTTGAGATTAAAGAGCACTCGAGGCGCGGG–3'

AT: 62 °C

2.5–Kb

Forward **XhoI-fwd** 5'–GAAAAGTTACCCTCGAGGAATTTAGGAGC–3'

Reverse **HindIII** 5'-TTGAGCGAACACCCTCTAACAAGCTTTC–3'

AT: 58 °C

Figure 2.3

PCR conditions (sequence primers and AT) for amplification of promoter fragments 964–bp and 2.5–Kb. The sequence for the restriction enzymes is underlined.

2.2.5, the plasmids are transfected in mammalian cells growing in culture. The luciferase activity was evaluated in transient transfection (following the procedure described in 2.2.8). The transient expression of this plasmid in mammalian cells results in a very low level of luciferase (due to the absence of a promoter), which was detected in cell lysates using a commercially available kit (Dual luciferase system, Promega). Forty–eight-72 hours following transfection, the medium was removed and the cell processed as reported in the manual of instruction of the kit. The luciferase levels were measured in a luminometer and the values corrected for the expression of a control plasmid co-transfected with the plasmid under examination, which encoded a renilla luciferase distinguishable from the fire-fly luciferase utilised in these experiments.

2.4 PCR

The polymerase chain reaction (PCR) follows the principles in which a pair of primers (forward and reverse) defines the region to be amplified. After denaturation (generally at 95 °C), primers are allowed to anneal to their complementary strand by lowering the temperature to their optimal annealing temperature which is specific for each set of primers and is linked to the oligonucleotides sequence. AT can be calculated on the basis of the following formula: AT=Tm–t, where Tm = 4x (G+C) +2x (A+T) is the melting temperature and 3 °C>t>5 °C. An elongation step allows the Taq DNA polymerase to start the polymerisation reaction downstream of the 3' ends of the primers (generally at a temperature of 72 °C). These three

steps are then repeated for "n" (usually 30) cycles to allow exponential amplification of the target sequence. A final step, at 72 °C for 7–10 minutes allows the Taq polymerase to conclude the polymerisation step.

Amplification is measured by resolving products through agarose gel electrophoresis. Whenever necessary, PCR products were then purified from gel.

PCR reaction mix was made using as a Taq purchased from Takara (Gennevilliers, France) with which all the components necessary for the reaction (except for the primers and DNA template) are provided. PCR reaction mix was made following manufacturer's instructions. Generally, nucleotides (dNTPs) are used to a final concentration of 0.2 mM, $MgCl_2$ to a final concentration of 1.5 mM, and 0.5 U of Taq. Forward and reverse primers were added to a final concentration of 500 nM. Primers were designed on the basis of the sequence reported in the Genbank database. The "GeneFisher" software free available online (web address: http://bibiserv.techfak.uni-bielefeld.de/genefisher/) was used to design the best set of primers to be used for each gene. Synthesis of oligonucleotides used as primers was performed by Sigma.

To the reaction mix, DMSO (dimethyl sulfoxide) was also added to a final concentration of 5%. To the final reaction mixture, a quantity of DNA template was added, (20 ng of plasmidial DNA, 100 ng of genomic DNA) then quickly spinned in a microfuge to recover all the fluids at the bottom of the tube and placed in PTC–200 thermal cycler (MJ research, Watertown, MA). Amplification conditions and cycle numbers were

selected each time according to the AT of the pair of primers and the length of the PCR product to be amplified.

2.5 SSCP analysis

This analytical method was developed for detecting a single point mutation in a DNA sequence.

The SSCP technique comprises amplification of DNA by PCR, denaturation and electrophoresis in a neutral polyacrylamide gel.

2.5.1 Sample preparation

Exons 1–5 of human DRAGO gene were amplified by PCR (see 2.4) using as a template, genomic DNA extracted from either human cancer cell lines or human tumors using the Wizard genomic DNA purification kit (Promega) following the instruction manual provided by the manufacturer. Tumor tissues were obtained at first laparotomy before any chemotherapy, freed of necrotic, hemorrhagic and connective tissue and immediately put in liquid nitrogen, then stored at –80 °C until processed. Ovarian tumors were kindly given by Prof. Costantino Mangioni (Ospedale San Gerardo, Monza, Italy). DNA samples from other tumor types were kindly given by Prof. Cappella (Ospedale di Circolo, Varese). PCR procedure was performed as described in section 2.4, except for the reaction mix, which was the PCR master mix purchased from Promega following the manufacturer's instruction. The primers are listed in figure 2.4 and the AT is indicated. The final volume of each reaction was 50 µl: 10 µl of the

Forward **Exon 1** 5'–TACAGCTGGGTCAGTGACGCGG–3'
Reverse **Exon 1** 5'–ACTCACCCGGGAGCCGGC–3'
AT: 60 °C

Forward **Exon 2** 5'–AGCCACTTCTGTGCTTGCCTCT–3'
Reverse **Exon 2** 5'–CTCCAGGTGACTCATTAGAC–3'
AT: 52 °C

Forward **Exon 3** 5'–AATGGACGATACATTAGAGA–3'
Reverse **Exon 3** 5'–TTCCTGTAGAGGCCTTCAGA–3'
AT: 52 °C

Forward **Exon 4** 5'–AGTAATGCTTGCACCTGCCT–3'
Reverse **Exon 4** 5'–ATGTCTGTATTGCACCATTC–3'
AT: 52 °C

Forward **Exon 5** 5'–AGCAAGGACCCTAAGCAGCTA–3'
Reverse **Exon 5** 5'–GAATCCAGCATGATAAGGTG–3'
AT: 52 °C

Figure 2.4

PCR conditions (primers sequences and AT) for amplification of human exons of DRAGO gene.

amplification product were loaded on 1% agarose gel to be checked as specifically amplified. Ten µl were destined for sequencing, 20 µl were mixed with 40 µl of denaturing buffer (see receipt below) and heat denatured at 95 °C for 5 minutes and then chilled on ice for 2 minutes.

Denaturing buffer	*Final concentration*
9,5 ml deionised formamide 100%	*95%*
20 µl NaOH 5M	*10 mM*
250 µl Xylene cyanol 10%	*0.25% (w/v)*
250 µl Bromophenol blue 10%	*0.25% (w/v)*

to a final volume of 10 ml.

2.5.2 Gel preparation and electrophoresis

A 16x20 cm gel electrophoresis apparatus with 0.8 cm thick spacers was used. SSCP analysis was performed loading the denatured PCR fragment on 0.7x polyacrylamide gel prepared as follows:

	Final concentration
11.27 ml MDE gel solution 2x	*0.75x*
3 ml TBE 10x	*1x*
300 µl APS 10%	*1%*
30 µl TEMED	*0.1%*

to a final volume of 30 ml with deionised water.

The MDE (FMC BioProduct, Vallensbaek Strand, Denmark) gel solution is a polyacrylamide like matrix highly sensitive to DNA conformational differences.

Gel electrophoresis was carried out at 150V at room temperature for at least 12 hours.

2.5.3 Gel staining

The gels were stained with silver. Before staining, they were immersed in a fix solution and kept in horizontal rotation for 6 minutes. The gels were then washed twice in deionised water for 2 minutes.

Fix solution was prepared diluting a stock solution of Nitric acid 10% in deionised water. Nitric acid 10% was prepared as a dilution in deionised water of starting nitric acid 65% solution.

The gels were stained in a staining solution for 30 minutes in rotation and at the end of the incubation they were washed rapidly in deionised water.

Staining solution	*final concentration*
1 g $AgNO_3$	*0.2% (w/v)*
500 µl Formaldehyde 37%	*0.037% (v/v)*

to a final volume of 500 ml with deionised water. This solution was prepared just prior to be used.

After staining, the gels were immersed in a developing solution for 5–10 minutes in agitation, until the electrophoresis pattern was detectable (visible).

Developing solution	*final concentration*
12.5 g Na_2CO_3	*2.5% (w/v)*
500 µl Formaldehyde 37%	*0.037% (v/v)*
4 mg Na Thiosulphate	*0.002%(w/v)*

to a final volume of 500 ml with deionised water. To this solution, formaldehyde and Na Thiosulphate were added just before use.

After developing, a Stop solution, Glacial Acetic acid 10%, was added to the developing solution, agitated for 3 minutes and then washed in deionised water for 2 minutes.

2.6 RNA analysis

2.6.1 Isolation of total RNA

To isolate total RNA, the SV total RNA isolation Systems (Promega) was used. RNA was then prepared following exactly the manufacture's instructions except for the final elution volume containing the purified RNA which is smaller (generally 50 µl) than that suggested by the manufacture's instructions. An aliquot of this solution was then used to determine the RNA concentration, as described above. Samples were stored at –80 °C until use.

2.6.2 Northern blotting analysis

Northern blotting is electrophoresis and transfer of RNA to a membrane followed by hybridisation to a specific probe. It provides the quantification of the levels of RNA species within a cell.

2.6.2.1 Sample preparation and gel analysis

During gel electrophoresis a denaturing agent, formaldehyde, completely unfolded RNA molecules by reacting with amine groups preventing the formation of G-C and A-T base pairs. A formaldehyde agarose gel was prepared in MOPS (Sigma) buffer as reported here:

Formaldehyde Agarose Gel	*final concentration*
0.8 g ultra pure agarose	*1%*
8 ml MOPS buffer 10x	*1x*
14.4 ml formaldehyde 37%	*6.66%*
57.6 ml water	

The agarose is dissolved in water by boiling. The other reagents are added when the gel reached approximately 60 °C.

MOPS Buffer (10x)	*final concentration*
93 g MOPS	*0.2 M*
20.51 g NaAc	*0.5 M*
1.86 g EDTA	*10 mM*

to 500 ml with deionised water. The pH was adjusted to 7 with NaOH and the solution autoclaved.

The gel was poured in a chemical hood and let until solidified.

Equal amounts of RNA (generally 10 µg) were mixed with 3 volumes of a RNA denaturing solution prepared just prior to use as follows:

RNA Denaturing Solution	*final concentration*
2.5 ml deionised formamide	*50%*
0.5 ml MOPS 10x	*1x*

806 µl formaldehyde 37% *6%*

to a final volume of 5 ml with sterile water.

Formamide is deionised to remove ionic contaminants which could hydrolyse RNA. To do this commercially available Formamide was added to mixed-bed resin (BioRad) (5 g resin/100 ml formamide) and stirred for at least 1 hour in the dark. Formamide was filtered from the resin with whatmann paper, aliquoted and stored at -20 °C.

RNA samples were denatured at 65 °C for 15 minutes and quickly chilled on ice. Then 1/6th of the volume of loading buffer was added to the mixture immediately before loading.

RNA loading buffer	*final concentration*
500 µl glycerol	*50%*
25 µl bromophenol blue 10%	*0.25%*
475 µl of water	

1 µl of ethidium bromide (10 mg/ml) is added to 29 µl of this solution. The solution is aliquoted and stored at –20 °C.

The gel run was carried out in MOPS buffer (1x) at constant voltage of 80 V, for 2-3 hours. At the end of the run of the gel, two distinct, abundant, ribosomal bands (18S and 28S) were visualised under UV-light as indication of a good separation and absence of degradation. The RNA was then blotted onto a membrane.

2.6.2.2 Blotting procedure

A capillary blot was set up using a solution of 20x SSC (175.3 g NaCl, 88.2 g sodium citrate in 1 l of water) as transfer buffer.

The wick was made up of 2 pieces of 3MM paper with each end dipping into the transfer solution. The gel was placed on the wick with wells facing down, and air bubbles were gently removed. A nylon membrane (GeneScreen Plus, PerkinElmer, Boston, MA) of exactly the same size of the gel was soaked in 20x SSC for at least 10 minutes and carefully placed on top of the gel and gently squeezed to remove air bubbles. Three sheets of 3MM paper where then added over the membrane followed by Kleenex towels. The blot system was left for 16-24 hours after which the membrane was removed, washed by immersion in deionised water, left to dry at room temperature for approximately 30 minutes and examined under UV light to mark the position of the RNA 18S and 28S fragments. The membrane was then baked at 80 °C for 2 hours to remove any residual formaldehyde from the RNA, as this could affect the efficiency of the hybridisation. The blot was stored at 4 °C until ready for hybridisation.

2.6.2.3 Preparation of probes for Northern blot analysis

Radioactive probes suitable for determining the level of the mRNA of the gene of interest were prepared by using PCR amplified fragments and a klenow fragment of polymerase I – based method. In particular, a commercially available kit (Rediprime, Amersham Biosciences) was used to label 50 ng of DNA following all the steps described in the manual. The

radioactive nucleotide was the ^{32}P-labeled dCTP (Amersham Biosciences, 3,000 Ci/mmole). Purification of the probe from unlabelled nucleotide was performed using Sephadex G50 columns (Roche Diagnostics, Milan–Italy) exactly following the manufacturer instructions. The incorporated radioactivity was detected by cherenkov counts and the probe was diluted to a final concentration of 500,000 cpm/ml in the hybridisation solution.

2.6.2.4 Hybridisation

Before hybridisation with a probe, the membrane was pre-hybridised for at least 4 hours at 42 °C in a glass bottle with 10-15 ml of hybridisation solution:

Hybridisation solution	*final concentration*
2 ml NaCl 5M	*2 M*
5 ml deionised formamide 100%	*50%*
2 ml dextran sulphate 50%	*10% (w/v)*
250 µl Salmon sperm DNA 10 mg/ml	*100 µg /ml*

The salmon sperm DNA was prepared by boiling the solution for 10 minutes, chilling on ice and storing in aliquots at –20 °C.

The radiolabeled probe was denatured by boiling for 5 minutes and quickly chilling on ice for 5 minutes again. The denatured probe was added directly to the hybridisation solution without touching the membrane and the mixture was gently mixed. The blot hybridisation was performed by overnight incubation at 42 °C. The membrane was washed twice at room temperature for 10 minutes with 2x SSC, followed by two 2 washes of 15

minutes each at 65 °C with 2x SSC + 1% SDS and a final wash in 2x SSC for 10 minutes. The blot was kept humid by wrapping it in Saran wrap and either exposed to film overnight at -80 °C or exposed to a phosphorimager screen (Amersham Biosciences, formerly Molecular Dynamics) for at least 5 hours at room temperature.

When necessary, the probe was stripped from the membrane by boiling the blot for 10 minutes in 0.5% (w/v) SDS solution. The blot was again kept humid, checked for radioactivity and either stored at 4 °C or hybridised with another probe.

2.7 Agarose Gel

2.7.1 Gel preparation and gel electrophoresis

Agarose gel of different percentages (w/v = grams of powdered agarose per 100 ml of TAE running buffer) was prepared by dissolving desired grams of ULTRA pure agarose (Sigma) in a suitable volume (ml) of 1x TAE buffer:

TAE Buffer (50x)	*final concentration*
242 g Tris base	*2 M*
100 ml EDTA 0.5M, pH 8	*50 mM*
57.1 ml glacial acid acetic	

to 1 l with deionised water. The solution was stored at room temperature.

The solution was heated in a microwave and boiled until all the agarose was dissolved. The solution was then cooled to approximately 50 °C before pouring in a casting tray.

To be loaded on the gel, DNA/RNA were mixed with 1/6th of the volume of loading buffer 6x.

Loading Buffer 6x	*final concentration*
1 ml EDTA 0.5 M	*0.1 M*
2.5 g sucrose	*50% (w/v)*
100 µl bromophenol blue 10%	*0.25% (w/v)*
100 µl xylene cyanol 10%	*0.25% (w/v)*

to a final volume of 5 ml of deionised water. Ten µl of ethidium bromide (10 mg/ml) were then added and the solution was stored at 4 °C.

Samples were electrophoresed at 100 V for approximately 30 minutes in TAE 1X buffer. DNA bands were visualised under UV light with UV transilluminator. The assessment of the expected DNA fragment length was possible thanks to the available molecular weight markers solutions (Fermentas, Burlington, Ontario–Canada) which were loaded in a lane parallel to that of the samples and electrophoresed together with the samples.

2.7.2 DNA extraction from agarose gel

PCR products or bands of desired length obtained after restriction enzymes reaction were removed from the gel under the trans-illuminator.

The DNA was then extracted from the agarose slice using the "MiniElute" gel extraction kit (Qiagen) exactly following the manufacturer's instruction.

2.8 Screening of genomic libraries

Both human and mouse genomic clones containing the genomic DRAGO sequences were isolated by screening either a human or a mouse genomic library spotted on filters obtained through the UK Human Genome Mapping Project Resource Centre (UK-HGMP-RC).

The human PAC library RPCI1 has been constructed in the vector, pCYPAC2N. The source is a normal male blood donor, and the insert size is about 110 kb. The mouse PAC library RPCI21 is subcloned in pPAC4 vector. The source is a female 129/SvevTACfBr mouse spleen genomic DNA. Both libraries consist of approximately 120,000 clones spotted on 22.2 x 22.2 cm Hybond N nylon membranes (Amersham Biosciences). Each clone has been spotted twice to give 36,864 (18,432 x 2) spots on each membrane. 7 filters cover the whole library. The 7 filters were prehybridised at 65 °C in 25 ml of a solution containing 6x SSC, 100 µg/ml of salmon sperm, 0.5% SDS and 5x Denhardt's solution (a 50x Denhardt's solution is prepared by dissolving 1 g of Ficoll 400, 1 g of polyvinylpyrrolidone and 1 g of BSA (bovine serum albumin) fraction V in 100 ml of water; the solution is then filtered and stored at –20 °C) with gentle, continuous agitation. To this solution, radiolabeled human DRAGO–derived cDNA probes (prepared as reported in 2.6.2.3) was added and the incubation continued for further 16 hours at 65 °C. The

filters were then washed twice at room temperature in 2x SSC, followed by two 2 washes of 15 minutes each at 65 °C with 2x SSC + 1% SDS and a final wash in 2x SSC for 10 minutes and exposed to autoradiographic films. Once developed, the films were oriented with the grid supplied with the filters and the positive clones identified. This procedure was facilitated by the double spotting of each clone. The identified, positive clones, where requested to the UK-HGMP-RC and obtained as *E. coli* colonies carrying the clone of interest streaked on LB agar containing kanamycin (25 µg/ml). Each clone was restreaked onto the same agar type and incubated overnight at 37 °C to obtained single colonies. One of those per each clone was then picked up and inoculated into LB broth containing kanamycin and let grow overnight at 37 °C. From the bacterial culture, the PAC clones were isolated using the Qiagen midi preparation kit. To isolate shorter genomic fragments containing the DRAGO gene, an aliquot of the genomic DNA isolated was digested with different restriction enzymes in their appropriate buffer, supplied together with the enzyme, for 16 hours at 37 °C and the entire reaction loaded on 0.8% agarose gels. After 16 hours running at 30 V, the gel was visualised under UV and a picture collected for subsequent identification for the positive bands. The restriction fragments of genomic DNA thus separated by agarose gel run were blotted as regards the Southern blotting procedure to a nylon membrane. The transfer of the DNA to a membrane was carried out as described for Northern blotting in section 2.6.2.2 and hybridised with a radiolabeled human DRAGO–derived cDNA probe (the radiolabelling conditions were

the same as described in section 2.6.2.3). For human genomic DNA, a 160bp–PCR fragment corresponding to the 5' region of the DRAGO cDNA was used. PCR conditions were those described previously (section 2.4). The forward primer was 5'–CCGAAGCCGGCGACCGCCCC–3' and the reverse primer was 5'–GGCGCTCACAGCTTCCACGC–3', and the AT was 60 °C. For the mouse genomic DNA human exon 1, 3 and 5 were used and obtained by PCR as described in 2.5.2. Hybridisation and washing conditions were the same used for the screening of the genomic filters. The autoradiograph was compared to the ethidium bromide picture and the bands which hybridised with the probe identified. A second digestion was performed on the remaining genomic DNA maintaining exactly the same conditions previously used. Once separated on gel, the bands corresponding to the previously selected positive bands were excised and isolated as described in section 2.7.2. The band containing the fragment from human genome was ligated in the MCS of pGL2 vector using the same restriction enzyme used for the digestion of the human genomic clone and sequenced using the primers available from the manufacturer. The positive clones were further amplified and the DNA isolated from them was used in transient transfection experiments for the determination of luciferase activity. The fragment from mouse genome isolated from gel agarose as described in 2.7.2 was subcloned in the MCS of pBS vector using the same enzymes used for digestion of the mouse genomic clone. The construct was verified by sequencing using the T7 primer.

2.9 Induction of GST–fusions in bacteria and purification

To recover GST fusion proteins produced in *E. coli* cells containing a recombinant pGEX–3X plasmid (see sections 2.2) the GST Gene Fusion System, purchased from Pharmacia Biotech, was used, following the procedure suggested by the manufacturer's instruction manual.

From a glycerol stock stored at –80 °C, each *E. coli* pGEX–3X recombinant was streaked onto a LB medium agar plate in sterility and incubated overnight at 37 °C.

One colony was picked up and inoculated into 5 ml of LB medium containing the antibiotic of selection (see 2.2.5) then incubated for 12–15 hours at 37 °C with vigorous shaking. The grown culture was then diluted 1:100 into fresh pre–warmed LB medium with the antibiotic and let grow at 37 °C with shaking. Then the steps followed were exactly the same described in the instruction manual provided with the purification system previously mentioned. Briefly, the bacterial culture was grown until the A_{600} reached 0.5–2, then by the addiction of 0.1 mM IPTG the culture induced to produced fusion proteins with a 2–6 hour–incubation. The bacterial culture was centrifuged to sediment the cells and the pellet resuspended in a final volume of ice–cold PBS corresponding to 1/20 of volume of the starting bacterial culture. The cells were disrupted with a sonicator on ice and fusion proteins were solubilised by addition of 1% Triton X–100 to the sonicated cells and gently rotation for 30 minutes. Then the solution was centrifuged and to the supernatant was loaded on the Glutathione Sepharose 4B. This agarose matrix carried glutathione molecules which

bound the fusion proteins through the GST–tag. After washes to remove non specifically bound proteins, the fusion proteins were eluted with 10 mM of GSH from the matrix. The eluates were monitored for GST–fusions protein by either SDS–PAGE or Western blotting (see section 2.10). Moreover, to identify the fraction in which the fusion protein was located, aliquots of supernatants after solubilisation cell debris pellet were saved after solubilisation. Aliquot of supernatant after the addition of the sepharose matrix was saved.

2.10 Western blotting

Western blot analysis involves separating proteins using sodium dodecyl sulphate polyacrylamide gel electrophoresis (SDS–PAGE), transferring them to nitro-cellulose electrophoretically and then using specific antibodies to detect the protein of interest.

2.10.1 Calibration curve preparation

Solutions of BSA (ranging between 1 and 20 µg/200 µl) were prepared from a stock solution of BSA obtained by dissolving powdered BSA (Sigma) in water. In a 1.5 ml tube, 200 µl of each BSA solution were mixed with 600 µl of distilled water and 200 µl of BioRad protein assay dye (BioRad). In the blank sample, 800 µl of distilled water was mixed with 200 µl of BioRad Protein assay dye. Samples were rapidly transferred into disposable cuvettes (PBI International, Milan-Italy) and the absorbance at

595 nm was measured in the spectrophotometer. The absorbance value corresponding to the blank sample was subtracted from the values obtained in the BSA-containing samples. Each calibration sample was run in triplicate. The calibration curve obtained in such a way, allows extrapolation of the exact absorbance value corresponding to 1 μg of proteins present in the solution.

Protein concentration in the total cellular extract was determined according to Bradford protocol.

The concentration of proteins in the samples was determined by mixing in a 1.5 ml tube 10 μl of protein samples (see section 2.9) with 200 μl of BioRad protein assay dye and distilled water in a final volume of 1 ml. Samples were processed as for the calibration curve and the amount of proteins calculated from the absorbance value corresponding to 1 μg of proteins (obtained from the calibration curve).

2.10.2 SDS-PAGE

An equal amount of protein of each sample was mixed with the same amount of 2x SDS loading buffer and was boiled for 5 minutes :

SDS Loading Buffer (2x)	*final concentration*
200 μl Tris 1 M, pH 8.8	*100 mM*
400 μl DTT 1 M	*200 mM*
800 μl SDS 10%	*4%*
400 μl glycerol	*20%*

40 µl bromophenol blue 10% *0.2%*

to a final volume of 2 ml with sterile water

Samples were loaded onto 5% stacking gel and 12% separating gel:

Stacking Gel	*final concentration*
1.25 ml Tris-HCl 0.5 M, pH 6.8	*125 mM*
0.1 ml SDS 10% (w/v)	*0.1% (w/v)*
1.25 ml 40% acrylamide/bis 29.1:0.9	*5% (w/v)*
To a final volume of 10 ml with deionised water.	
50 µl ammonium persulphate 10% (w/v)	*0.05% (w/v)*
5 µl TEMED	

Separating Gel	*final concentration*
2.5 ml Tris-HCl 1.5 M, pH 8.8	*750 mM*
0.2 ml SDS 10% (w/v)	*0.1% (w/v)*
3 ml 40% acrylamide/bis 29.1:0.9	*12% (w/v)*
To a final volume of 10 ml with deionised water.	
100 µl ammonium persulphate 10% (w/v)	*0.05% (w/v)*
7.5 µl TEMED	

Stacking and separating gels were prepared shortly before pouring. Ammonium persulphate catalyses polymerisation and TEMED accelerates the reaction and so these two reagents were added last.

Proteins were resolved on a minigel apparatus (BioRad) and run for 2 hours at 50 V in 1x TGE buffer:

Running Buffer (TGE 5x)	*final concentration*
15.15 g Tris base	*25 mM*

72 g glycine	*192 mM*
5 g SDS	*0.1% (w/v)*

to a final volume of 5 l with deionised water. The buffer was stored at room temperature.

Electrophoresis progress was followed using pre-stained molecular weight markers prepared following the manufacturer's instructions (Fermentas).

2.10.2.1 Coomassie Blue staining

Coomassie Blue R250 (*0.25 g Coomassie Blue, 45 ml methanol, 45 ml glacial acetic acid, to a final volume of 100 ml with deionised water. Filter the solution through paper*) was used to colour the polyacryilamide gels after SDS–PAGE by incubating the gel immersed in the coomassie solution for 60 minutes and washing it overnight in a de–staining solution (*30 ml methanol, 5 ml glacial acetic acid, to a final volume of 50 ml with deionised water*).

2.10.3 Protein transfer and detection

The separated proteins were transferred onto nitro-cellulose (at 60 V for 3 hours) using BioRad Mini transfer blot equipment in 1x transfer buffer:

Transfer Buffer 1x	*final concentration*
24.2 g Tris Base	*50 mM*
28.5 g glycine	*100 mM*
4 ml SDS 10%	*0.01%*

800 ml methanol *20%*

to a final volume of 4 l with deionised water. The solution was stored at room temperature.

Filters were stained with Ponceau red solution (Sigma) to check sample loading. Blots were placed in TBS-T 0.1% with 10% non-fat dried milk:

TBS-T 0. 1%	*final concentration*
2.42 g Tris base	*20 mM*
8 g NaCl	*137 mM*
1 g Tween 20%	*0.1% (w/v)*

to a final volume of 1 l with deionised water. The pH was adjusted to 7.6 with concentrated HCl and stored at 4 °C.

and shaken overnight at 4 °C to block non-specific binding. All following procedures were carried out at room temperature on a shaker. Blots were exposed for 1 hour at room temperature to the desired antibodies diluted to the optimal working solution in TBS-T 0.1%. After incubation, the blots were washed twice with TBS-T 0.1% and incubated with the appropriate horseradish-peroxidase linked anti-mouse IgG secondary antibody (Amersham) for 1 hour using 1:3,000 dilution. Blots were washed as previously described, and detection was performed with enhanced chemiluminescent detection system (ECL, Amersham-Life Science). Briefly, the horseradish peroxidase acts as a catalyst for the oxidation of a luminol substrate, which subsequently emits small but sustained quantities of light. This chemiluminescence is specifically enhanced allowing an

image to be recorded on photosensitive film. Blots were exposed to film for different time ranging from 15 seconds to 3 minutes and developed using X-o graph compact x-2 developer with Kodak GBX developer and fixer.

2.11 In vitro synthesis of proteins

To synthesise a polypeptide in vitro, the TNT T7 Quick Coupled Transcription/Translation system (Promega) was used following the manufacturer's instructions. This system provides a convenient single–tube, coupled transcription/translation reaction for in vitro translation of eukaryotic genes subcloned downstream from the T7 RNA polymerase promoters. One µg of circular expression vector carrying the coding sequence of the protein of interest and a T7 primer sequence was used as cDNA template.

The polypeptide in vitro synthesised was then analysed by SDS–PAGE.

2.12 Immunofluorescence

Cells were seeded and grown for 24 hour or to confluency on glass coverslip. They were washed once with PBS and fixed with 4% paraformaldehyde overnight at 4 °C. During three PBS washes at room temperature, residual paraformaldehyde cross–linking activity was quenched by adding a drop of 1 M glycine, pH 8.5, to the second and third PBS washes and leaving it 5 and 10 minutes respectively. The samples were permeabilised with 0.5% Triton X–100 in Hepes buffer (20 mM

Hepes, 300 mM sucrose, 50 mM sodium chloride, 3 mM magnesium chloride) 4 minutes at 4 °C, then washed twice with PBS and twice with PBS–0.1% BSA. Primary monoclonal antibody anti–DRAGO (dilution 1:100 from cellular surnatant) was then added in PBS–1% BSA for 30 minutes at 37 °C. Coverslips were washed in PBS and Alexa–Fluor 488 antibody anti–mouse (Invitrogen) (1:500 dilution) for 30 minutes at 37 °C. After further washes with PBS, glass coverslips were mounted in Mowiol 4–88 (Hoechst, Frankfurt/Main, Germany) and observed in a Zeiss Axiophot photomicroscopy equipped for epifluorescence (Carl Zeiss, Oberkochen, Germany).

2.13 Animal procedure

Procedures involving animals and their care are conducted in conformity with the institutional guidelines that are in compliance with national (D.L. n.116,G.U., suppl.40, 18 Febbraio 1992, Circolare No. 8, G.U., 14 Luglio 1994) and international laws and policies (EEC Council Directive 86/609, OJ L 358,1, Dec 12, 1987; Guide for the use of Laboratory Animals, United States National Research Council, 1996).

2.14 Isolation and handling of primary mouse embryonic fibroblasts (MEF)

Primary MEFs were isolated from wild–type and DRAGO –/– embryos at embryonic day 12–15. Timed pregnant female at 12 to 15 days gestation

were sacrificed and individual fetuses were removed and washed repeatedly with sterile PBS. After removing the head and red organs (liver, heart and kidney) each embryo was broken (cut) into small pieces and then incubated with trypsin/EDTA at 37 °C for 15 minutes. After removing the trypsin by centrifugation at 1,200 rpm for 10 minutes, the tissue homogenate was resuspended in MEFs culture medium, DMEM supplemented with fetal bovine serum (Hyclone, Logan, UT) and 2 mM of L–Glutamine and placed in 100 mm culture plates (one plate for each embryo sacrificed). The plates were incubated at 37 °C overnight. The day after, the fibroblasts were visualised under the microscope. The medium was removed and replaced with fresh culture medium. These cells were considered passage 0. When the cells on the passage 0 plates became confluent, they were detached as described in chapter 2.1.1 except that 1x trypsin diluted in PBS (without EDTA) was used (from a stock 10x purchased from Bio–Whittaker). The cells were then counted and seeded at a density of 6 x 10^4/ml (9 x 10^5 in a tissue culture T75 flask). Cells were passaged at the same density as standard 3T3 protocol (332). To determine the cellular growth rate of DRAGO –/– MEF culture relatively to the growth rate of wild–type (WT) MEFs, in a 6–wells plates both genotypes were seeded in triplicate at a density of 1.5 x 10^4/ml. One plates a day was then used to harvest the cellular growth of MEFs in order to determine the cell number in each culture every day.

2.15 MEF treatments

2.15.1 Preparation of drug solutions

The drugs used in the experiments were cisplatinum (DDP, Sigma), taxol (obtained through the NCI), doxorubicin (DX, Nerviano Medical Centre, Milan–Italy), campthotecin (CPT, Sigma) 5-Fluorouracil (5-FU, Sigma), PS341 (CTI, Milan, Italy), VP-16 (Sigma).

DDP was prepared fresh for any experiment by preparing a solution of 0.5 mg/ml in medium and allowing this solution to equilibrate with proteins present in the serum at 37 °C for 30 minutes before treatments. Taxol, CTP, 5–FU, VP–16 and PS341 were prepared in DMSO as respectively 2 mM, 20 mM, 5 mM (both 5–FU and VP–16) and 10 mM stock solutions and subsequently diluted in fresh medium the day of treatment. The stock solution was maintained at –20 °C. DX was prepared as a 5 mM solution in water and stored at –20 °C in the dark. After treatment, the medium containing the drugs and the remaining solutions were properly discarded.

2.15.2 Cell growth inhibition

To investigate the effects on cell growth of either drug or UV and X rays treatment, both MEFs WT and MEFs DRAGO –/– were seeded at a density of 1 x 10^4 cells/ml in either 24–wells plates whether treated with drugs or 6–wells plates whether exposed to UV or X rays. When treated with drugs, 48 hours after seeding a concentration range of drug was added into 2 replicate wells. Treatment was performed for 24 hours and

after 72 hours cells were washed with sterile PBS and stained with crystal violet. Control untreated cells were stained in the same manner. Otherwise, 6–wells plates of MEFs were entirely exposed to a range of UV or X rays and after 72 hours washed with PBS and stained with crystal violet. The degree of growth inhibition induced by UV and X rays was evaluated comparing the absorbance of treated cells stained with crystal violet with that of untreated ones (control cells). Basically, the stained cells were resuspended with 500 µl of a solution of 0.1 N HCl in isopropyl alcohol. The absorbance of each well was then read using a Titertek equipped with a filter for 550 nm.

2.15.3 DAPI/sulphorhodamine staining

Cells were seeded on glass coverslips and after 24 hours, they were treated with anticancer drugs. Forty–eight hours after treatment, cells were washed with PBS and fixed with 95% Ethanol for 1–2 hours. Cells were washed with PBS twice and in de–ionised water. Cells were incubated with a DAPI/sulphorhodamine solution for 15–30 minutes in the dark (*3.5 mg DAPI was dissolved in 100 ml in deionised water; to 0.5 ml of DAPI solution diluted in 100 ml of, 3 mg of sulphorhodamine was added. The volume was brought to 300 ml by adding the Na–Tris HCl pH8 solution:*

Tris base *12 g*

NaCl *6g*

HCl 1 M *54 ml*

H_2O to a final volume of 1 L.

After futher washes with deionised water glass coverslips were mounted in Entellan (Merck, Milan–Italy) and observed in a Zeiss Axiophot photomicroscopy equipped for epifluorescence (Carl Zeiss, Oberkochen, Germany).

2.16 Genotypic screening of heterozygous mice breeding

For routine genotyping of the litters from breeding of heterozygous (HE) KO mice, two PCR reactions were built up using three primers. One set of primers (GW723 5'–TTCCTGCTAGTCAGACACGCCTGTG–3', GW722 5'–TACACAGGTGGCAGTTAGGCATCC–3' AT: 61 °C) was designed by Genoway laboratory for screening test to detect the excision of the targeted region. The forward and the reverse primers of this set were designed at the 5' and the 3' end respectively of the targeted region which comprised the genomic fragment between exon 3 and 5. Therefore the PCR reaction might expect the amplification of either 10–Kb fragment for WT mice or a 3.6–Kb band for HO KO mice. For HE mice both bands of 10 Kb and 3.6 Kb were expected. However, among those bands, only the smaller one was detected, being the 3.6–Kb band more efficiently amplified. Therefore, in order to discriminate HE and KO mice, a second set of primers, formed by the same forward primer (GW723) of the previous set and a reverse primer (KO725 5'–GCCTTCTGCACACAGGTACTCG–3' AT: 63 °C) mapping a region in the exon 3 which is deleted in the HO KO mice was designed. In this manner a 1.3–Kb band was expected with HE KO and WT mice, conversely no band amplification was expected with HO KO mice.

RESULTS

CHAPTER 3

MOLECULAR CHARACTERISATION OF DRAGO GENE

3.1 Introduction

As reported in the Introduction (Chapter 1.7), DRAGO is a new gene which has been isolated as a cDNA fragment overexpressed in cell lines after treatment with several cytotoxic agents. The cDNA fragment, once isolated and sequenced, perfectly matched to the sequence KIAA0247 already present in gene bank. Beside the nucleotide sequence referred to the cDNA of this isolated gene, no functional and structural information has been reported. To start with the characterisation of this challenging gene, the determination of molecular structure has been posed as the initial steps to undertake.

3.2 Molecular characterisation

The description of the exon-intron organisation of the gene is a necessary prerequisite for most of the subsequent investigations and characterisations carried out in the present work. Using the information available with the full-length cDNA, the structure of the human DRAGO gene was molecularly characterised. The entire cDNA sequence (5,338bp) was compared with the sequences of human genome available from the public gene bank by using the BLASTN program at the NCBI database. The comparison led to the identification of two human genomic clones (BAC R-1046B16 clone of library RPCI-11 and BAC C-2216L1 clone of library CalTech-D) from chromosome 14 which together comprise

the full length cDNA. These results allow to build the genomic structure of the gene, which is composed of 6 exons, with canonical exon-intron junctions (GT..AG). The first exon (188 bp) spans nucleotide 1-188 comprising most of the 5' untranslated region (5'UTR) which overlaps part of the second exon. The coding region starts from the base 269, located in the second exon (189-389). Exons 2, 3 (390-587), 4 (588-726) and 5 (727-1,154) (201, 198, 140 and 427 bp respectively) correspond to the coding region which contains the first 26 bases (1,155–1,180) of exon 6 (4,184 bp). Therefore the coding region results to be comprised between nucleotides 269 and 1,177 (1,180 including the stop codon "tga"), whereas the remaining 4,158 nucleotides form 3'UTR which is entirely located in the last sixth exon. Interestingly, the gene presents two large introns (45-50 kb) between exons 1-2 and 2-3, respectively (Fig. 3.1).

3.3 Isolation of DRAGO genomic sequences

To confirm the sequence of the genomic DNA regions of DRAGO and to isolate the region containing the gene, a human genomic library spotted in duplicate in seven different filters, obtained through the UK-HGMP-RC was used. These filters contain genomic DNA clones and can be hybridised with different probes derived from the human DRAGO cDNA to isolate the genomic sequence of interest. For the purpose of this study, a 160 bp–fragment obtained by PCR (see chapter 2.4) and corresponding to

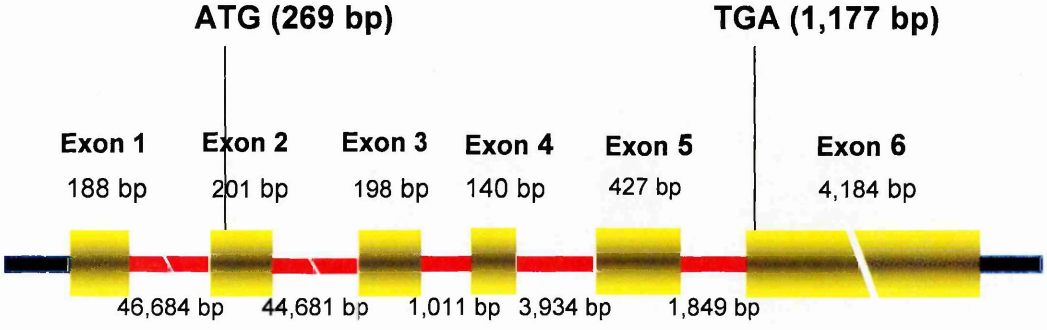

Figure 3.1

DRAGO gene structure. The length of exons and introns is indicated together with the position of the start (ATG) and the stop (TGA) codons.

the 5' region of the human DRAGO cDNA was used as a probe.

Figure 3.2 shows an example of an autoradiograph indicating the presence of two positive spots. On the whole set of seven filters, the use of this cDNA probe led to the identification of two positive clones which could be univocally identified through the coordinates of the filters and requested to the UK-HGMP-RC. The two positive clones (67A24 and 92D20 from the RPCI human PAC library 1) thus obtained were grown in LB media and the DNA was isolated from the overnight culture using procedures described in the materials and methods chapter (chapter 2.8). Since each of these clones contained approximately 100 Kb of DNA, it was necessary to pinpoint smaller DNA fragments containing the DRAGO gene for further characterisation. To do this, DNA was digested with different appropriate restriction enzymes and half of it loaded on 0.8% agarose gels to separate the fragments of different length. At the end of the run, the gel was stained with ethidium bromide and the bands visualised under UV light. Figure 3.3A shows fragments of the two clones digested with the restriction enzymes *BamH*I, *EcoR*I and *Hind*III. The gel was blotted overnight to a nylon filter and hybridised with the same probe used for the screening of the genomic PAC library and corresponding to the 5' region of the cDNA DRAGO sequence to identify the fragments inside the genomic sequence present in the clone which contains the DRAGO gene. The results of the hybridisation are shown in figure 3.3B, from which one can deduce that few digested fragments gave positive hybridisation and hence contained the sequence of DRAGO used to

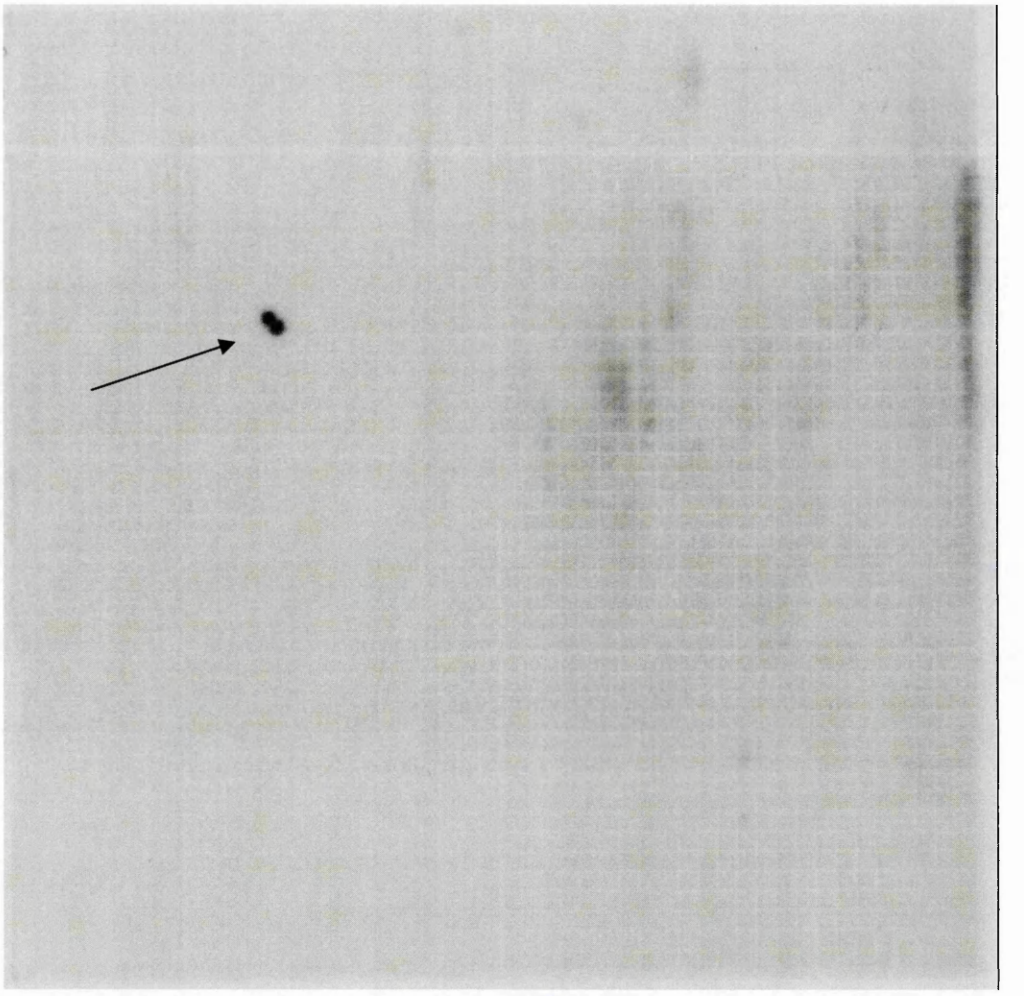

Figure 3.2

Screening of the RPCI human genomic PAC library 1.

The figure shows a representative autoradiography obtained from a filter containing the genomic DNA that was probed with a ^{32}P–labelled DRAGO cDNA fragment. Each clone is spotted in double on the filter. The arrow points the DRAGO positive clone (67A24) which has been selected based on screening.

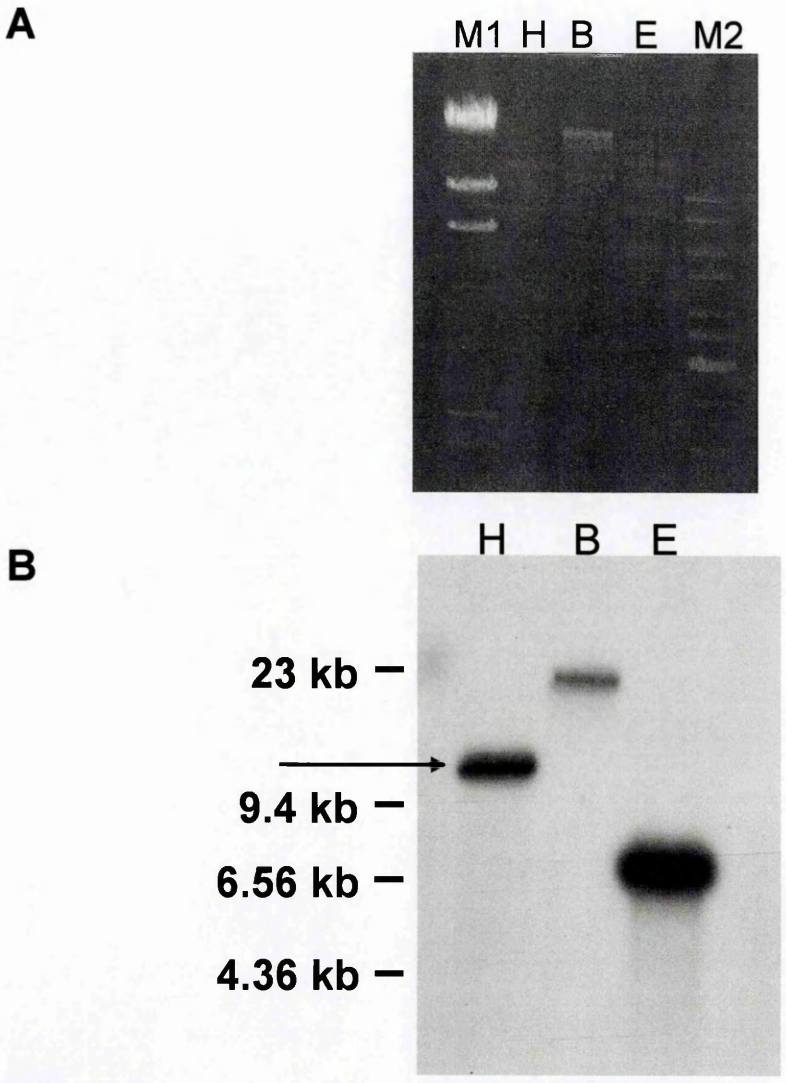

Figure 3.3

Southern Blot of digested genomic 67A24 clone obtained from the RPCI human PAC library 1.

Panel A. Ethidium bromide staining of the gel. DNA isolated from the clone was digested with *Hind*III (H), *BamH*I (B) and *EcoR*I (E) and resolved on agarose gel. M1 is the λ DNA/*Hind*III marker 2, M2 is the 1 Kb DNA molecular weight marker.

Panel B. Autoradiography of the gel transferred to a nylon membrane and hybridized with ^{32}P–labelled DRAGO probe. Numbers on the left are derived from M1 molecular weight markers. The arrow point to the 10 Kb fragment of the DRAGO clone digested with *Hind*III isolated for further study.

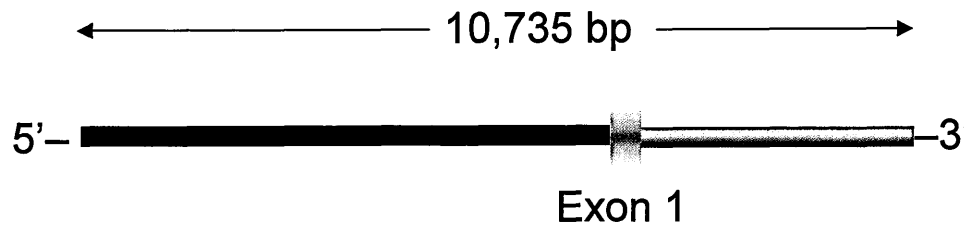

Figure 3.4

Schematic representation of the *Hind*III 10,735–bp fragment isolated from agarose gel (see figure 3.3). The sequence of the fragment compared with genomic sequences present in the NCBI gene bank database resulted to match with a genomic sequence containing a large portion of about 7 Kb genome located upstream to the first exon of DRAGO gene, the first exon and about 3 Kb region mapping the first intron of the gene.

hybridise. From these experiments a DNA fragment of approximately 10 Kb (10,735 bp), obtained from the 67A24 clone after digestion with the restriction enzyme *Hind*III was isolated for further characterisation.

This DNA fragment was subsequently subcloned in the *Hind*III site contained in the multiple cloning site of the pBluescript SKII plasmid. This recombinant plasmid was used to sequence the DNA inserted. The sequences were obtained using the sequences contained in the plasmid as primers. The obtained sequence was compared with the human genomic sequences present in the NCBI gene bank database which resulted to completely match with the genomic sequence from the BAC R-1046B16 clone of library RPCI-11 and to overlap the first exon. This sequence, in fact, starts about 7 kp upstream to the 5' end of DRAGO cDNA sequence (Fig. 4.4), contains the exon 1 and about 3 kb downstream the same exon, thus located in the first intron.

3.4 Discussion

One of the aims of this thesis has been to molecularly characterise the newly identified DRAGO gene. Previous experiments performed in the laboratory of Molecular Pharmacology at the Mario Negri Institute where the present thesis has been realised, showed that the sequence of full length cDNA of the newly isolated DRAGO gene corresponded to the cDNA of the deposited gene KIAA0247 (accession number D87434). The comparison between the cDNA sequence with the human genomic sequences present in the NCBI gene bank database allows the description

of the molecular organisation which reveals the presence of six exons, two long introns of respectively 46,684 and 44,681 bp, and a large 3'UTR (4,153 bp). All these large portions of non-coding regions suggest a strong gene regulation both at transcriptional and post-transcriptional level. In fact, the analysis of the 3'UTR sequence revealed the presence of AU- and CU-rich regions, which are known to be motives recognised by factors acting on the mRNA stability of genes like those coding for proto-oncogenes, transcription factors, cytokines, lymphokines, growth factors and their receptors (333). Nevertheless, two introns of about 50 Kb could contain the binding sites for transcriptional factors involved in the transcriptional regulation of the gene expression or cryptic ATGs as start codons for hypothetic DRAGO isoforms. Anyway, those aspects regarding the regulation of DRAGO gene will be studied in the future but it will not be the object of this thesis. The alignment of the cDNA of DRAGO with the human genomic sequences from NCBI databases led to the identification of two clones from chromosome 14 which comprise the intronic and exonic sequences of DRAGO gene. These findings have been confirmed by the isolation of the genomic clone containing the gene of interest from a genome library. The isolation of this clone allows the following investigations regarding the promoter isolation of DRAGO which will be discussed further in this chapter.

CHAPTER 4

CHARACTERISATION OF THE PROMOTER REGION

4.1 Introduction

As outlined in the introduction chapter (1.7), the activity of DRAGO gene is regulated by p53 as suggested by either the semi-quantitative RT-PCR or the real time PCR experiments. On the basis of these observations, two questions have been addressed. The first set of experiments described in this chapter was aimed at the identification of the promoter region possibly containing the p53 consensus sequence. Secondly the focus was on the evaluation of the possible role of the different p73 isoforms in determining the transcriptional activation of DRAGO. This question is particularly pertinent considering that the p73 gene shares relatively high sequence homology with p53 in the central DNA binding domain, thus enabling it to bind and activate the same downstream genes which are activated by p53 (see introduction chapter 1.6.1-1.6.2). The investigation has been also addressed at elucidating the role of DNp73 which, lacking the transactivation domain, has been mostly considered to antagonise the TA isoforms of p73 and p53. As discussed in the Introduction chapter recent findings suggest that DNp73 can have other functions. Starting from these evidences, the effect of DNp73 has been also evaluated in the experiments reported here.

4.2 Promoter activity of the 10,735 bp-HindIII DRAGO genomic region

Once it had been verified that the *Hind*III–digested 10,735 bp cloned sequence was indeed a sequence corresponding to the genomic region around the exon 1, containing the initial non coding cDNA of the DRAGO gene and a genomic region immediately 5' to this non coding part, the isolated DNA region was then investigated for the putative promoter activity. The full length fragment of 10,735 bp was entirely subcloned in the *Hind*III site of the multiple cloning site of the promoter-less pGL2–enhancer vector. This vector contains the luciferase cDNA and a multiple cloning site at 5' to the cDNA (without promoter) and is generally used to determine the efficiency of putative genomic promoter regions to drive the transcription of the luciferase gene. Using the method reported in chapter 2.2.7, recombinant clones were selected and the DNA partially sequenced to further verify the presence of the right insert and to determine the orientation. One of the clones tested containing the sense orientation inserted fragment has been chosen.

In p53-defective cells, the 10,735 bp-genomic region did not reveal any transcriptional promoter functionality. Nevertheless, it has been tested if p53 could induce this putative promoter region by co-transfecting an expression vector containing the human p53 cDNA with the construct containing the luciferase gene under the control of the human DRAGO fragment of 10,735 bp as described in chapter 2.3. However p53 did not induce the transcriptional activation of the 10,735–bp fragment.

4.3 Isolation of p53 responsive region

Since the entire 10,735–bp region did not respond to p53 induction, a smaller DNA fragment was then isolated from the 10,735 bp genomic region by using the *Kpn*I restriction site located 214 bp upstream to the first exon of the genomic region and in the multiple cloning site of the pGL2 vector, in which the same region is subcloned. The digestion with the *Kpn*I restriction enzymes of the 10,735-pGL2 construct resulted in the deletion of a DNA fragment of about 7,000 bp from the 10,735–bp genomic region. The 3'–end of remaining 3,761–bp fragment (which will be referred as the 3.8–kb fragment) was still functionally linked to the reporter gene luciferase and thus the 5'–end has been re–ligated to the vector to have a new construct. The 3.8–kb fragment (Fig. 4.1A) which consists of the initial non coding part of the DRAGO gene (exon 1), a genomic intronic region 3' to this non coding part and a sequence stretch contiguous to exon–1 5'–end, has been subjected to investigation for its transcription promoter activity. In p53–defective cells, the transcription of the reporter gene could not be detected. However, in cells where p53 functionality had been restored (as described in the previous section) the promoter activity of the 3.8–kb fragment was two–fold higher than in its absence (Fig. 4.1B) which is consistent with the results of the experiments carried out in isogenic models differing for p53 expression (see Introduction chapter 1.7). The observed p53 regulation has been compared to the transcriptional activation induced by p53 on another promoter fragment isolated from the human p21 gene and known to be

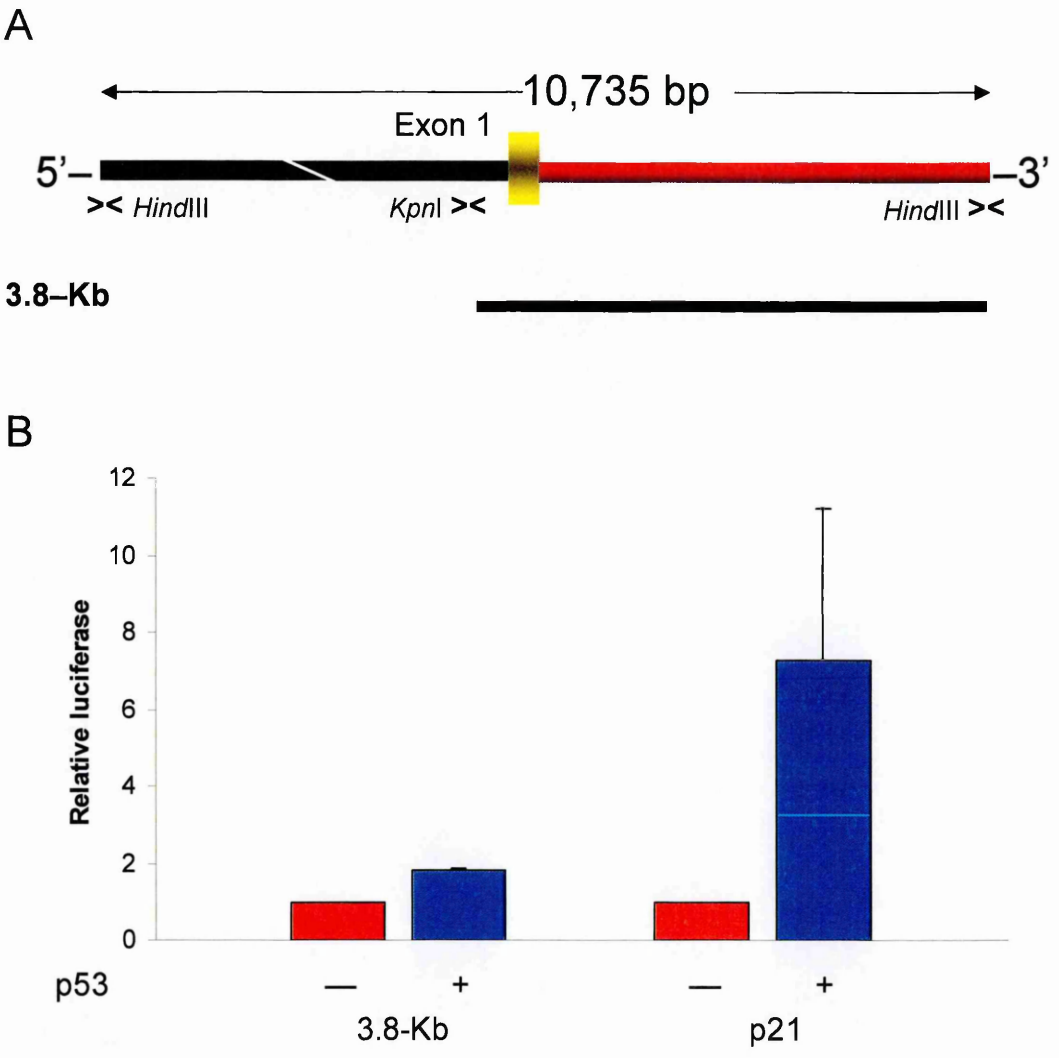

Figure 4.1

Panel A. Schematic representation of the 3.8–Kb fragment obtained by digesting the construct pGL2–10,735–bp with *Kpn*I restriction enzyme. One of the sites of cleavage is contained in the 10,735–bp fragment and upstream the exon 1. The other was contained in the pGL–2 MCS. The symbol **><** indicates the position of the restriction site.

Panel B. Levels of luciferase expression upon the 3.8-Kb fragment induction either in the presence (blue column) or in the absence (red column) of p53 in p53-defective Saos-2 cells (see chapter 2.3). Whenever p53 functionality had been restored, the promoter activity of 3.8–Kb was increased by 2 fold. As a positive control, the level of induction of the p21 promoter by p53 was considered.

activated by p53, which was obtained from Dr. Carol Prives, Columbia. University, NY.

4.4 Analysis of putative p53 responsive elements

The 3.8–kb fragment revealed to putatively contain p53 responsive elements, even though the transcriptional activation induced by p53 was lower than that observed with a well known p53–responsive promoter gene like p21. Furthermore, the luciferase assay showed that in the absence of p53, the 3.8–kb fragment exhibited no promoter functionality. The fragment was then investigated for the presence of a promoter region predictable by bioinformatics. For this purpose, the PromoterInspector program from Genomatix Software GmbH was used which find a good match with a theoretical promoter region comprised between base 1 and 792 of the 3.8–kb.

On the basis of these indications, a region starting from base 1 of the 3.8–kb and base 964 bp was further isolated by PCR amplification using a set of primers designed in order to introduce a *Xho*I restriction enzyme site of cleavage (as reported in chapter 2.3–2.4) at the 3'–end of the fragment amplified. The 964–bp fragment, obtained by PCR amplification using the 10,735–bp region as template DNA, showed a *Kpn*I restriction site at the 5'–end (which was the same used to isolate the 3.8–kb fragment and present in the sequence itself) and a *Xho*I restriction site, introduced by PCR. The fragment was then subcloned in the multiple cloning site of the pGL2 vector after digestion of both the plasmid and the PCR fragment with

*Kpn*I and *Xho*I restriction enzymes. After checking the right insertion by sequencing, the 964–bp–pGL2 construct was analysed for the promoter activity.

In p53-defective cells, it showed by itself a promoter activity but, when p53 functionality was restored, the 964–bp fragment revealed no increase in the promoter activity (Fig 4.2).

Considering that the 3.8–kb fragment resulted to be responsive to p53, the analysis was then focussed on the remaining 2.5 kb. The fragment was isolated by PCR amplification using a set of primers designed to introduce a *Xho*I restriction site at the 5'–end whereas a *Hind*III restriction site at the 3' end was indeed present in the sequence itself. Once amplified and digested, the PCR fragment was then subcloned in the pGL2 vector for gene-reporter assays. The 2.5–kb fragment showed a promoter activity similar to that observed with the 3.8–Kb fragment in the absence of p53 (Fig 4.3).

The 3.8–kb was then analysed for the presence of the canonical consensus DNA-binding sequence, RRRCWWGYYY, recognised by p53. The search has been performed with the PROMOTION program that has been developed by Dr. Riccardo Bonomi from the Molecular Pharmacology Laboratory of Mario Negri Institute. Considering that the variability and degeneracy of the p53 binding motif complicates their identification, the search for consensus sequences has been focused on the core sequence, CWWG. The score of the alignment between the nucleotide stretch and the promoter region under investigation has been

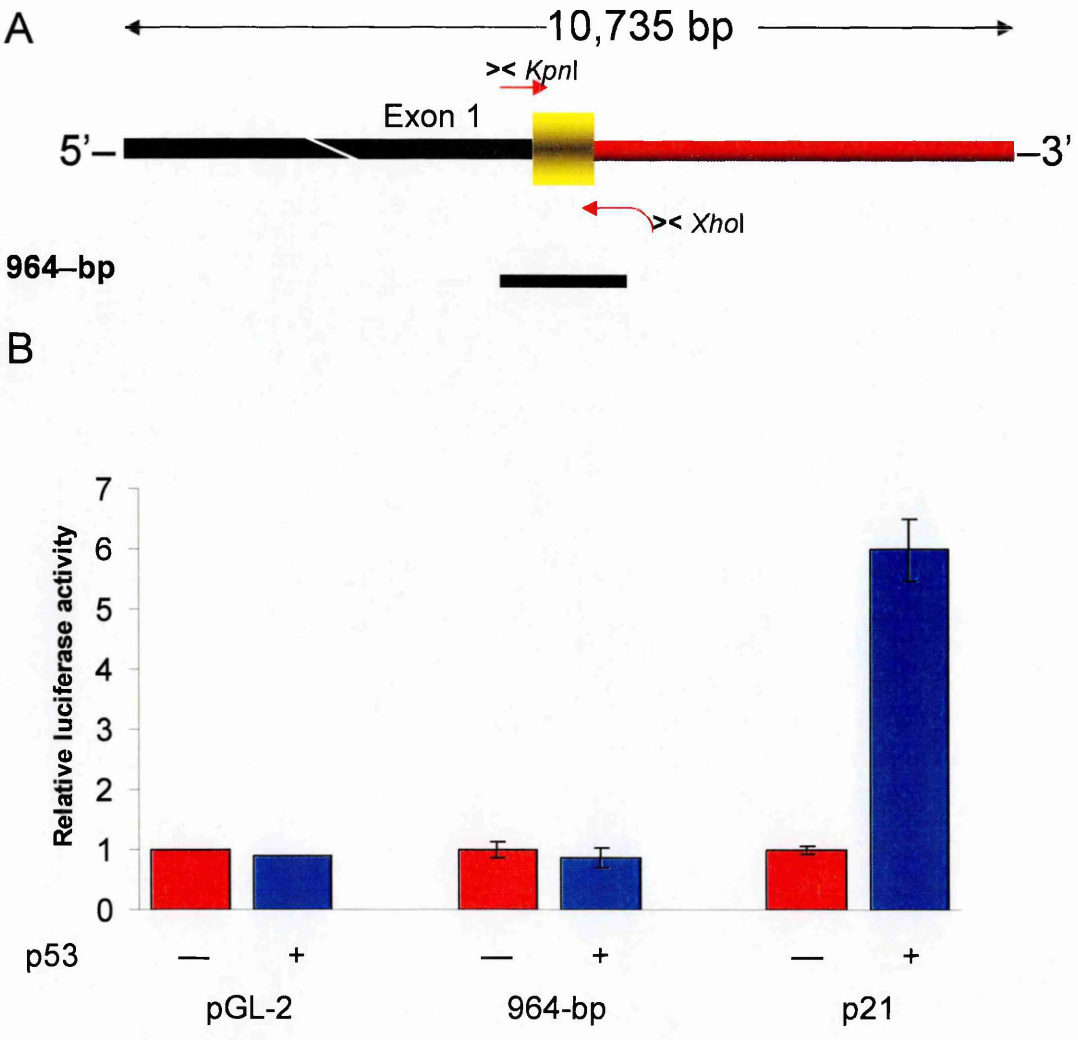

Figure 4.2

Panel A. schematic representation of the 964–bp fragment, obtained by PCR amplification followed by restriction with *Kpn*I and *Xho*I enzymes (the *Xho*I restriction site was introduced by PCR). The primers are represented as red arrows. The *Xho*I restriction site which is carried by the downstream primers is indicated.

Panel B. Levels of induction of the 964–bp promoter by p53 was evaluated in Saos–2 cells. In the presence of p53, the promoter activity did not increase as compared to the luciferase activity of the empty vector (pGL2) in the presence of p53.

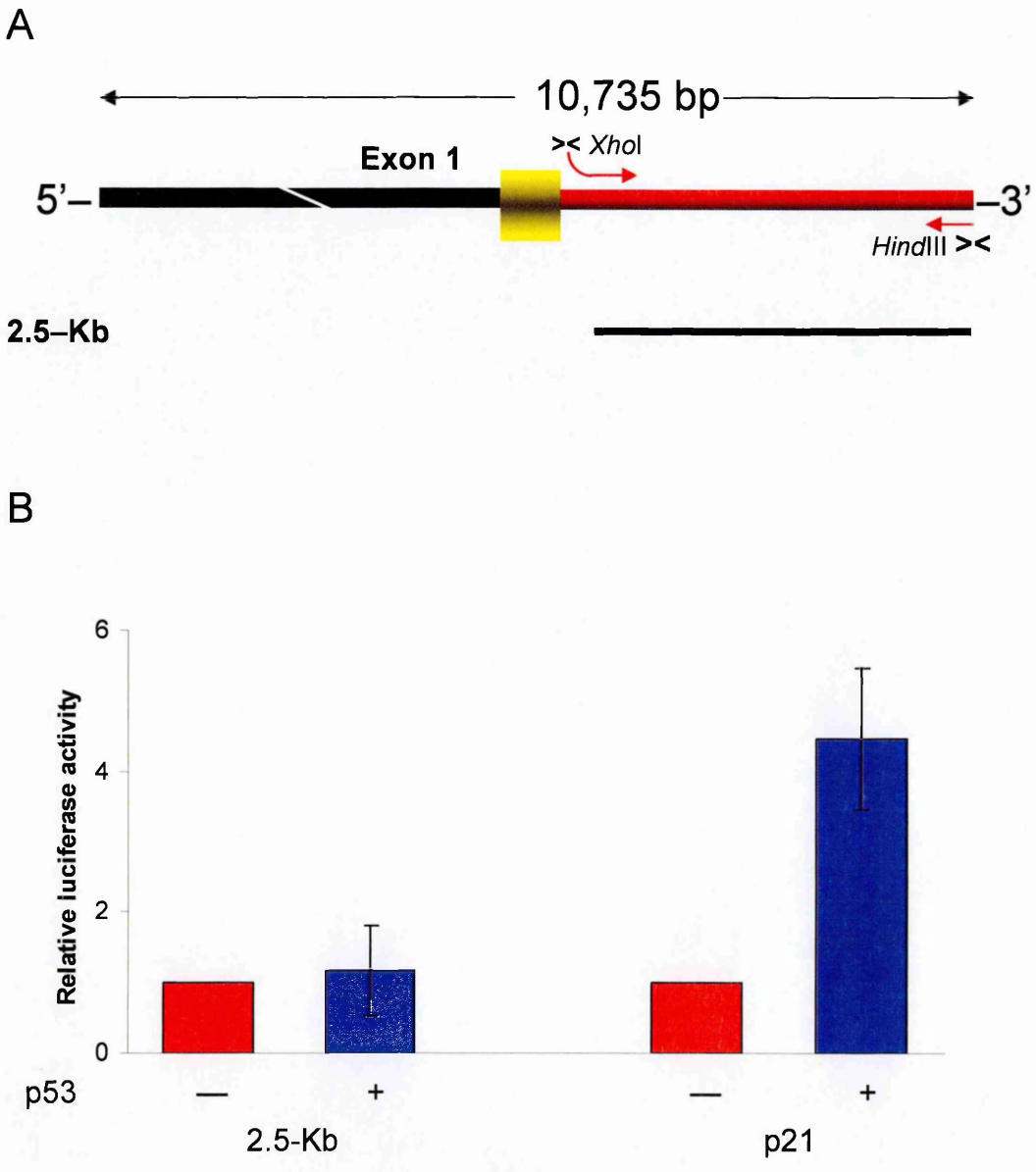

Figure 4.3

Panel A. Schematic representation of the 2.5–Kb fragment which was obtained by PCR amplification followed by restriction with *Xho*I and *Hind*III enzymes (the *Xho*I site was introduced by the upstream primer).

Panel B. The promoter activity of the 2.5–Kb fragment was evaluated in Saos–2 cells in the presence or in the absence of p53. The level of induction of the luciferase expression by p53 was similar to that measured with the 3.8–Kb promoter.

set equal to 100, which means that only the exact matches between the consensus motif CWWG and the promoter sequence have been taken into consideration. As discussed in the introduction chapter, the binding motif RRRCWWGYYY is commonly repeated in two pairs, with a spacer region between the two sequences that consists of a number of nucleotides that can vary from 0 to approximately 20 bp. The matches were screened on the basis of their relative distance from each other and considered only whenever they fit with the above mentioned criterion. In figure 4.4 the putative binding sites recognised by p53 are highlighted showing that, although the binding pattern can deviate from the consensus RRRCWWGYYY, the number of sites can be reiterated into clusters. In figure 4.5, a diagram showing DRAGO putative p53 BS and those of some known p53 target genes has been reported, revealing no evident similarities with DRAGO p53 BS and those present in the genes reported. In particular, p53 responsive elements of the BTG2 gene have also been reported, since this gene shares with DRAGO the feature of being inducible by DNp73α (see Chapter 1.5.1).

4.5 Role of p73 in gene transcription

Considering that p73 can bind to the motives originally identified as p53-binding site within the promoter and the first intronic sequence of its downstream genes and that the regions isolated responded to p53 less than expected, the same regions were analysed for their ability to transcriptionally activate DRAGO in the presence of p73. The experiments

GGTACCTGGC CCGGCCGGCG GCGCGTGCGT GCAGGGCCTC CCGGCGGGGC GGTCGCGGCG GCGCGACGCC
GGCGCCGTTG CGTGCGCGCC TGGCCCTGCC CCTTTCCCGC CCCTTCCCCG CCCCCTCCCC TCCGCGGGGC
CTCCCCCGCC CGCGCGGTAC AGCTGGGTCA GTGACGCGGG CGCTGCAGCC GTCGCTACCG CCGCGTTCTA
TTCTCCGAAG CCGGCGACCG CCCCACCTCC TCCCTCCCTC CCGCCCGCTT CCTCTGCCCA CAGCGCCGGC
CAGAGCGAGC TAGACAAGGG CACGCGGGGC CTCGCCTAGA CCCGAGAAGA CTGCGGGCGC GCGCAAGCGG
CGGCGTGGAA GCTGTGAGCG CCCCCATCCC GGAGGTCTCC GCCGGCTCCC GGGTGAGTTG TCACCGCGGC
CCGGGGGCGG CGGGGCCGGC ATTGTGCCAT CGACGCGCTC GGCCGGCTGT CAGGGGCGCG GGACCAGCGC
GCACCGCCCA GGAGTGACGC TGGCCGGAGC CCGGGCCGGC TTCGGCGGCT CCCCGCGCTT CTCTGCGCCG
GCCCGCTGTC ACCCGGCCGC GAGCCGCGCC GCTGGGAGCC CCGCGCTGGC GTGGCGCGGC CAGCCGGCCA
GCAGTGGGGG CTGCGCGGCC GGGGGGACCG GCGGCTGGTT TGCGGCCGGG AACTTGGTGA CCCGCGGTCC
GGGGCGCGCC GTCCCGCGTC GCTGCCCGGG CAGCACCGGA AGAGCCAGAC GCCGTGCCGA TGGGTGCAGA
GGAGGTAGGC AGAGGCCCTC TGTGCCACTG TCATTACTGC CCTCAGCCCA GCAAAGCTGC GGGGCTTGCG
CTGGGGCAGG GCTGGCTTAG AGAAGGTGGA TTTCCTGAGG AAATCTCAGA GCCCGCCTGT GCGCACCGCG
GCATTCGGGA GCCCCCGCGC CTCGGCTGCT CTTTAATCTC AAAAACTTCT CTTATTAACC AGGCTAAACT
CCCCGAAACC AGCTATTTTC TTTCAAAAAG TAGGCACGTA CATACAGACT TTCCTTTTTT CGCTTGGTTT
TGAGACCCCA GCTATGAGTG TGGATCTGAC TCTCCCTCAT GGGAGTCGTG GCTGGGGAGC TGCTGAAGTG
GAGAAAAGTT ACCCTGGACG AATTTAGGAG CAGGAGGGGG AGGTGGTTAT GGGGACAGCA AGACCCAGGA
GCAAAGAGGC GTCAAAATAA AGTCTTGGGC TGGTTAAAGG GAAGTTGGCG TCTGGGCAAG GAGGCCTAAA
GCTGTTGTTC CCACAGAATT TTCTTTCAGT GGCAGGCGAC ATGCTGGGCT TTGTTGCTCT CGCTAACTGG
GCTCCTGTGT GCTCTTCCAG AGGTGCAGTA AGATTACTCA GTTCAATTAG GCCTAGGGAT TTACTCCCTT
TTTTGATCTA CAGAGATGGG AAGTATGTCT TTCCTTCACA GTAGTTAATT CATTTCTTGC TGTTTTCGTT
CCTCTGGTGT AAAAACATAC ATAGGAGTTA CGCACACACA CCTTTTCTGT TTTGGGAATT CCACACCCAA
ACTGTCACCA TCTAGTGGAG GCTAGTAGAG ACATGTGCTT GGCACTGACT TCTGAGTTCT CTGGGTTTTG
TGTTTTTAGC TAGAAGCATA TTCAACCAGA AATTAAAATT TTCCTGGAGT TGGGGGAGGT ATGTCTACAT
CTCAGGAAAG AAGGTATTTA AGCAGCAATA ATATGGAAAG GTTCTTGAGG ACTTACTGAG TACCAACCTT
TGTGCTAAGG GCTTTACTTT TTTGAACTCA TTTAATAACA GACTTTTGAT GTAGATATTA TTATCCCCAT
TCTTCTAGTT GAGACCCAAA CCAAACAAGT TAAATAACTC GCCCATGTCA CATAGGTATC TCATGGTGGA
GCCCACAGTC TGAACTACTA GATTATACTG CTAGTTTCTG GTTTGTTTAC CTTTTGATAA AATTGAACCT
GGAGTCTTTC TAAAACCTTC TGAAAGCACT GCTGCTTCAG GCTGTTTCTC AGATCATGAG CATTCTAAAC
TCTTTCTCCT GGGTACACAC TTACGGTATG TTTGCATAAG ATTCATTTGT TCATTCTTTC ATTCAGTACT
CCCAAGTAGT TATGTGATAC CGAATGTATG CCAGGCACTG TGCTAGGTAT TGCAGGTACT GCATTGAATA
AGTCAGAATC CAGCTCTCAT GGACTCACAG CCTTTAAGTC CATTTGTTTT GGTTTATGTT GTTAGCTTTC
ATTGCTGGCC ATTTGCTGCT GAAGGAACTT CTGCCCAGCG AGTTAAACAG AGGACAGTAT TGGTATGAGT
CCTGATAGAT AGGACTTCCT GTCTGCAGAG TAATTTTTTG GATACTGTAG TAGAAATGGC ATATGAAACA
AATCCTCACT TACACCTAGA TAGAGACAGG TGCCAGGGTG CTCAGTGTTT AAACCCTGAG AGCAAACCCA
CTGTCAAATG GGCAAGTTTG ACTTCTTTCG CTGAAGCCTG CCTTCTGAAA GCCCAGAATT TGGTGAGATA
GAAGAGAAAG AAGGGTAGAA TGAGGTGTTA CAGATACAGG CTGGCAGATA AAGAGACCTC AGCACTTTGT
CTGTTTTCCT GGTCAGTCTC TGAGGTGTGG TGATTGAACT TGTGTTCTTT TTTATTTTTT ATTTTTTTTG
AGATGGAGTC TCGCTCTGTC ACCCGGGCTG GAGTGCAGTG GCACGATCTC GGCTCACTGC AACCTTCACC
TCCCAGGTTC AAACGATTCT CTGCCTCAGC CTCCTGAGCA GCTGGGACTA CAGGTGCGTG TCATCACGCC
TGGCTAATTT TTGTATTTTT AGTAGAGACT TGGTTTTACC ATGTTGGCTA GGCTGGTCTC GAACGCCTGA
CCTCAGGTGA TCTGCCCGTC TTGGCCTCCC AAAGTGTTGG GATTACGGGC GTGAGCCACC GTGCCCGGCC
TGAACTTGTG TTCTTATGTA ATGTTGCATC TCTCAGTAGG GGATGTCCTC CTTTGCTCTT TTGGTGGGGC
AGCAATTCCT GCAGCAGCCT TCCCTCTACA TGCACACACA CACCCCTTCC AAAAGGTAAT AATTCACCTG
GTTTCTTTAA AGTTAGAACT TCTTTCAAGT TTATTGCTAC TAAGCATTGT TTCACTCCCT CCACACTTGT
CCATTTCCCA CATAAAAACT TGGCTTTTGC TTCAAATATT TTCTTCTGCC CTTTTTTCAT ATCCTTAGCT
CTTCTGACAA CCAAGTTACT ACTGGTATCA TTTGTAGGCT GGGAGAAATA CAGCATCTTT AAAAAAAAAT
AGTGAGGTAC ATACTCTTCC TCATTTCAGT ACCAAACAAG TGAACTGTGG AGAATGAAGC AGAACCACTT
GCCAGCAGAG AGGGAAGGCC AGAGGGCACA CGTGGTTGTC TTTCCCCTCT AGTTCCCCAT TTATTAAGAG
ACAATTCACA CTTGCAGGCC CGAATGTCAG CAGATCCATT GGGCCCAGGT TGTGTAATTG CCATACATGA
AGTGAGTTAT TAAGCTCCTG AAATGACATG CTATCTCCTA GTTGAAGCTG ACAAGCAGGA TTTATTTTCC
CTCTTCTTTC TGTCTGGACA CTATGGAAGT CTTGTTAGAG GGTGTTCGCT CAAGCAGTGG GAGAAAGATC
AGAAGGAGCC AATAGAGGAG GGAGCCCCAT GTCTTGTCTT CTTTTCAACT TTGAGAGCAA ACATTGCTTT
GTTGCAGACT TGAATGTTGA GGATTAGGAC ATTTGGTTAA ATGTAAGCTT

Figure 4.4

Sequence of the 3.8–Kb fragment. Putative binding sites of p53 are highlighted.

Binding site	*RRRCW* →	*WGYYY* ←		*RRRCW* →	*WGYYY* ←
Bax	tcACA	AGTTa	G	AGACA	TGTCC
p21 5' site	GAACA	TGTCC		CAACA	TGTTg
p21 3' site	GAAgA	AGaCT		GGGCA	TGTCT
mdm2	gGtCA	AGTTg		GGACA	cGTCC
Noxa	AGGCT	TGTCC		CGGCA	AGTTg
BTG2 BS1	AGACA	TaCCC	AG	GAAgA	TGTTC
BTG2 BS2	AcGCA	TGTTC		AGGCA	TGCaT
BTG2 BS3	AGGCg	AGgCC	G	GGGCc	TGCCC
BTG2 BS5	GGcCc	TGCCT		GGACA	TGCCa
Scotin BS1	tAACg	AGTaC	TCCTGGGCA	GtGCA	AGTTC
Scotin BS2	GGcCT	TGTTa	G	GAACTt	TGTCC
Scotin BS3	cAGCc	TGTgT	GTACCCTAG	GAGC	TGTTa
Scotin BS4	GAGCc	AGggT		GAGCA	GTTa
Scotin BS5	GAGCA	GTTa	CCTGGAGGT	GGtCT	TGgTC
PUMA BS1	ctcCT	TGCCT	T	GGGCT	AGgCC
PUMA BS2	ctGCA	AGTCC		TGaCT	TGTCC
DRAGO BS1	AGACA	AGggC	ACGCGGGGCCT	cGcGT	AGaCC
DRAGO BS2	GGGCT	TGCgC	TGGGGCA	GGGCT	gGCTT
DRAGO BS3	cAtCT	AGTgg		AGGCT	AGTag
DRAGO BS4	cttCT	AGTTg	AGACCCAAACC	AAACA	AGTTa
DRAGO BS5	GccCA	TGTCa	CATAGGTA	tctCA	TGgTg
DRAGO BS6	ctACT	AGaTT	ATA	ctGCT	AGTTT
DRAGO BS7	AGACT	TGgTT	T	tAcCA	TGTTg
DRAGO BS8	AcACT	TGTCC	ATTTCCCACATAA	AAACT	TGgCT
DRAGO BS9	AAACA	AGTga	ACTGTGGAGAATGAAGCAGAAGCAGAA	ccACT	TGCCa
DRAGO BS10	ATACA	TGaag	TGAGTTATTAAGCTCCTGAAA	tGACA	TGCTa
DRAGO BS11	ctcCT	AGTTg	AAGC	tGACA	AGCag
DRAGO BS12	AGtCT	TGTTa	GAGGGTGTTC	GctCA	AGCag
Binding site	*WGYYY* ←	*RRRCW* →		*WGYYY* ←	*RRRCW* →
BTG2 BS4	cTGaa	AAAcg	C	TGCCC	GGGgA
BTG2 BS4'	AGTCC	GGGCA	G	AGCCC	GAGCA
BTG2 BS6	AGTTT	tcACT	C	ccCTT	AGGCA
BTG2 BS6'	TGCATa	AGGaA	GG	TtCTC	cGACT

Figure 4.5

Diagram showing p53 canonical binding sites (HH orientation) of some p53 target genes and DRAGO responsive elements. In the lower raws, BTG2 binding sites in the TT orientation have been reported. The alignment does not reveal any evident similarities between DRAGO putative p53 binding sites with those of other p53 target genes here reported.

were performed as those described when p53 promoter activation has been studied. The first region to be analysed has been the 3.8–kb which showed a slightly stronger promoter activity in the presence of p73 compared to the induction level driven by p53. Similarly, the evaluation of the role of p73 has been extended to the 2.5–kb region which contains more putative consensus binding sequences than the 964-bp promoter. The 2.5–kb region showed a slight increase of transcriptional activation in response to p73 compared to p53.

As mentioned in the introduction chapter (1.6.1) different isoforms of p73 are generated by alternative splicing of p73 gene. The full length protein, which has been used in the experiments carried out with the 3.8–kb fragment, is defined as alpha p73 (p73α), and, at least, 4 C–terminal isoforms (beta-p73β, gamma-p73γ, delta-p73δ and epsilon-p73ε) have been described so far. Since these isoforms can have different transcriptional activation potency (289, 334), the fragment of 2.5 Kb was used to test the specific activity of the different p73 isoforms. A typical experiment is reported in figure 4.6 showing the ability of different p73 isoforms to activate the promoter region and revealing that p73 is a stronger activator of the promoter fragment than p53. Among different p73 isoforms, beta and gamma isoforms are the strongest, being able to induce an increase of about 5–6 fold. In parallel, experiments have been performed with the p21 promoter in the same conditions as those used for the 2.5–Kb fragment. The smallest 964 bp fragment did not respond to any of the p73 isoforms as observed previously for p53.

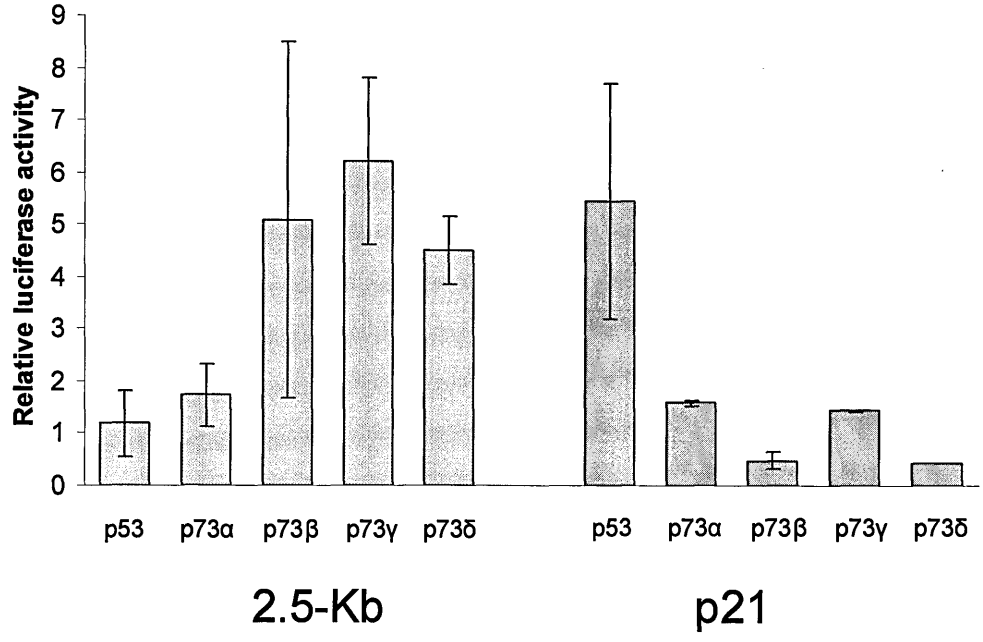

Figure 4.6

Activity of the 2.5–Kb fragment linked to the luciferase gene evaluated in Saos-2 cells cotransfected with different isoforms of p73 and p53. The level of the activation of the 2.5–Kb fragment was compared with that of the p21 promoter fragment.

4.6 Fragments retaining promoter activity

The localisation of the putative p53 binding site has given the possibility to create a series of constructs derived from the 2.5–Kb fragment-pGL2, in order to better investigate the promoter activity of the region in presence of p53 and p73.

Five constructs have been generated by restriction with several enzymes the cleavage site of which were present in the constructs. The constructs obtained were SmaI, PstI, PH3, HP4 and SP5 (Fig. 4.7A). The SmaI and PstI, constructs have been obtained by digesting with either *Sma*I or *Pst*I restriction enzymes respectively. The cleavage of the 2.5–Kb fragment-pGL2 by *Sma*I restriction enzymes resulted in the deletion of about 1.6 Kb from the construct. The remaining 6.8–Kb fragment has been purified from the agarose gel, on which the restriction reaction was loaded, and re-ligated. Similarly, the restriction reaction of the same promoter construct with the *Pst*I enzyme generated two fragments of 680 bp and 7.8 Kb, the last of which, purified from the agarose gel, was re-ligated. The remaining constructs, PH3, HP4 and SP5, were obtained after restriction with *Pst*I and *Hind*III (PH3), *Hind*III and *Pvu*II (HP4) and *Sma*I and *Pst*I (SP5), respectively. The double reaction with *Pst*I and *Hind*III enzymes, generated three different fragments of 7 Kb, 730 bp and 680 bp respectively. The *Pvu*II and *Hind*III enzymes cleaved the promoter construct into 2 fragments of 7.5 kb and 990 bp. The digestion with *Sma*I and *Pst*I restriction enzymes generated two fragments of 6.5 Kb, 3.3 Kb

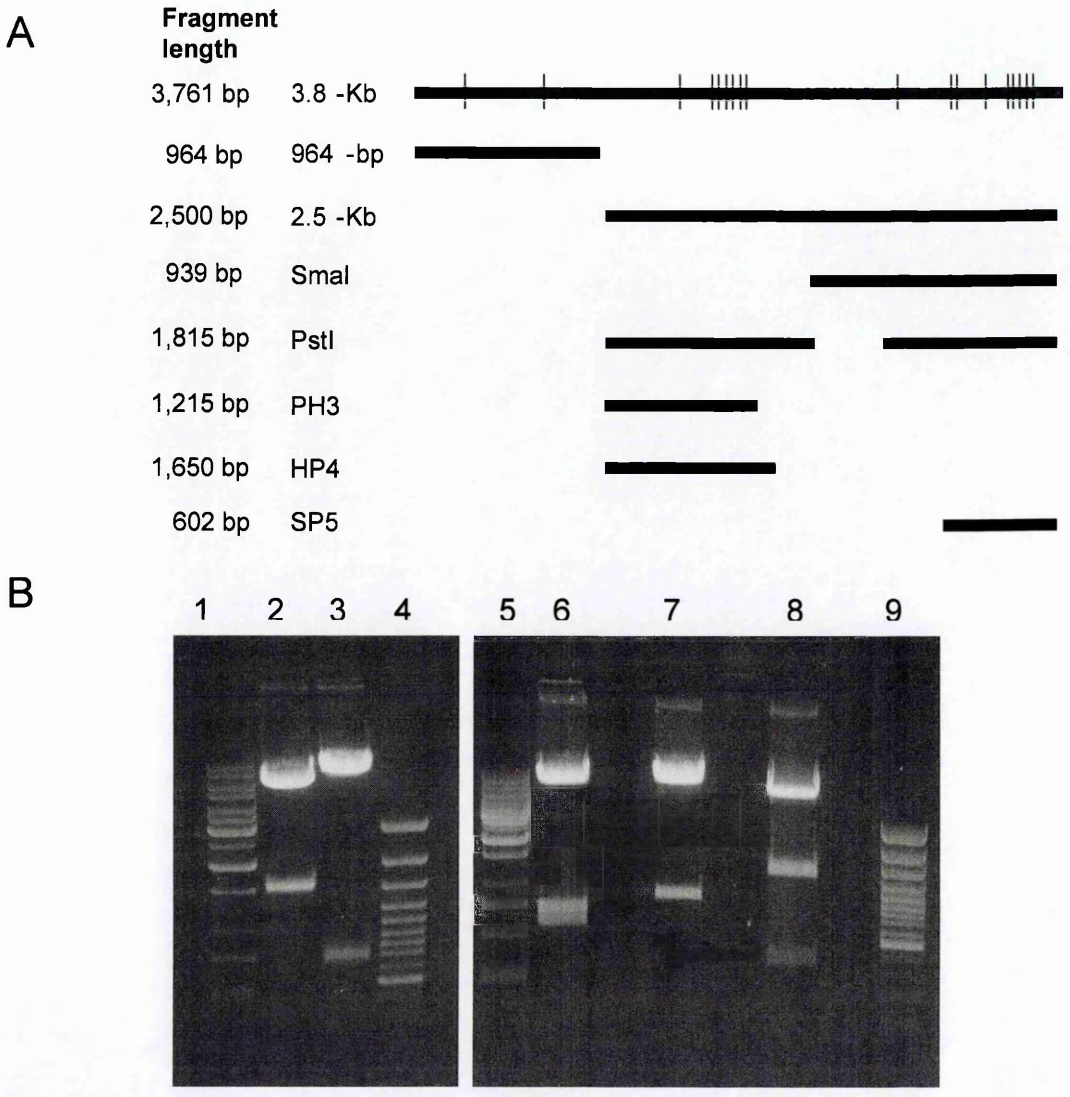

Figure 4.7

Panel A. Schematic representation of the SmaI, PstI, PH3, HP4 and SP5 fragments generated by restriction of the 2.5–Kb promoter. 3.8–Kb and 964–bp promoter fragments are represented. The position of the putative p53 binding motives is also represented on 3.8–Kb fragment–bar as vertical segments.

Panel B. Agarose gel electrophoresis of the restriction reactions of the pGL2–2.5–kb construct. Lanes 1 and 5: 1 Kb DNA molecular marker; lane 4 and 6: 100–bp plus DNA molecular marker; lane 2: pGL2–2.5–kb construct digested by *Sma*I enzyme; lane 3: restriction with *Pst*I enzyme; lane 6: *Pst*I and *Hind*III double digestion; lane 7: *Hind*III and *Pvu*II; lane 8: *Sma*I and *Pst*I.

and 1.2 Kb. In all the cases described the reactions were loaded on an agarose gel to allow the separation of the different fragments (Fig. 4.7B) and the purification of the desired ones. Particularly, the longest fragments were purified to be re-ligated. Since the extremities of each fragment were sticky and not compatible, being digested by enzymes recognising different consensus sequences, they were refilled to make them blunt to allow subsequent re-ligation of the generated fragments. Each promoter construct obtained have been verified by sequencing.

Those deletions of the 2.5-Kb sequence retained a promoter activity responsive to p73, particularly to the beta and gamma isoforms, while the p53-dependent luciferase activity was almost abolished (Fig. 4.8). The SP5 fragment (577 base pairs) was particularly responsive to p73 gamma as reported in figure 4.8. In figure 4.9 a schema of the degree of responsiveness to p53 and p73 isoforms are illustrated.

4.7 Role of DNp73

To further study the role of p73 in DRAGO transactivation, the ability of the transactivation domain deficient isoform DN-p73 to block p73 promoter activation has been evaluated. The 2.5-Kb promoter-luciferase construct has been co–transfected with the p73 and DNp73 expression plasmids. The p21-luciferase construct has been used as a control. As expected, transactivation of p21 promoter by p73 tended to decrease in the presence of DNp73, whereas the transactivation of the 2.5–Kb fragment-pGL2

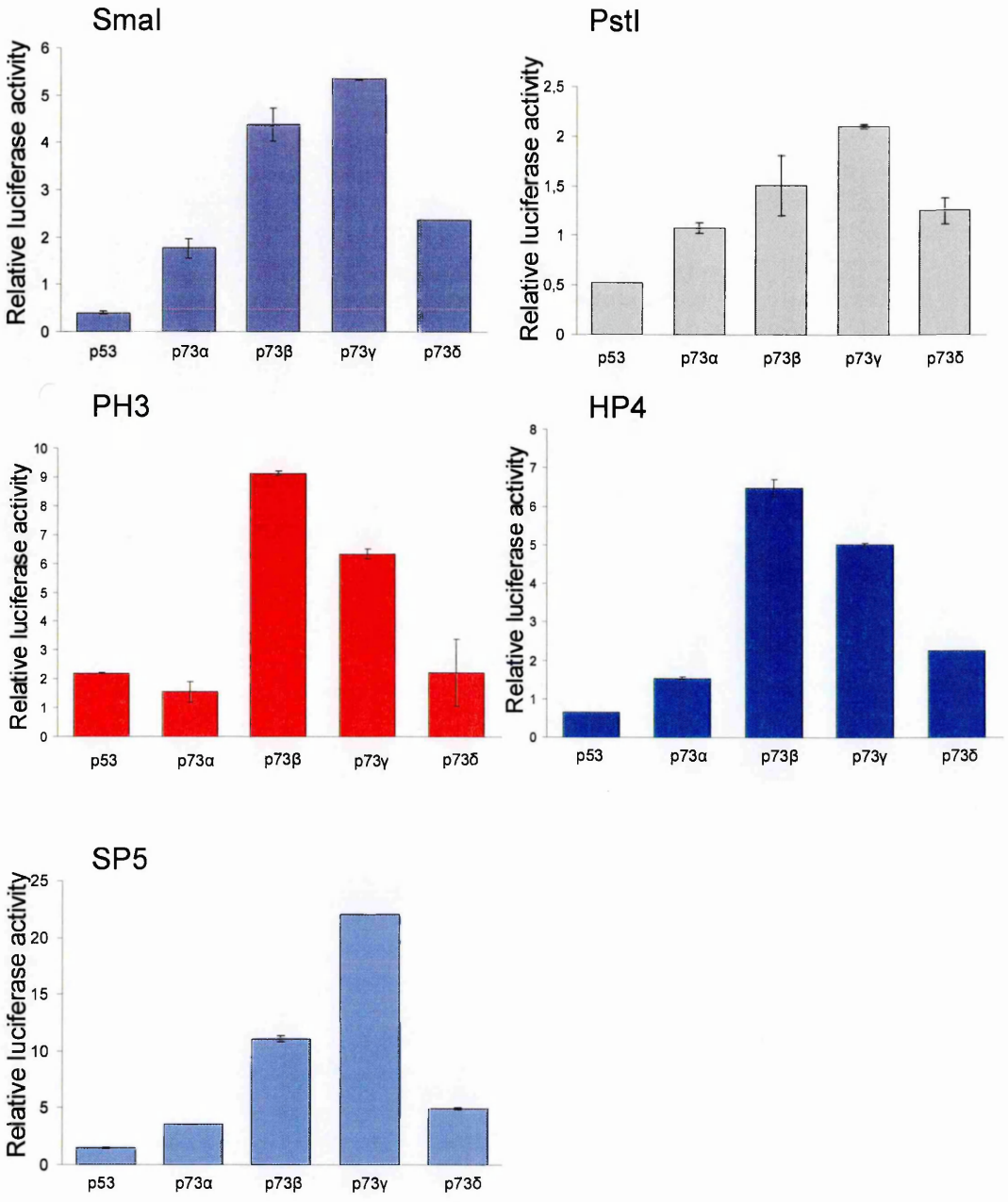

Figure 4.8

Luciferase activity of the 2.5–kb derived fragments in Saos–2 cells cotransfected with p53 and with different isoforms of p73.

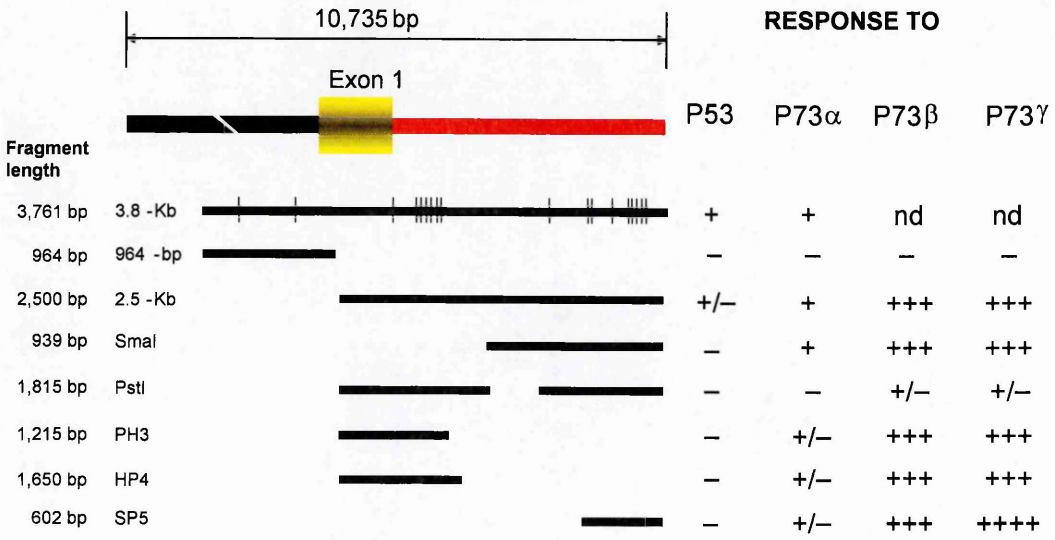

Figure 4.9

Summary of the response of the 3.8–Kb fragment and of the deleted mutants derived from it, to p53, p73α, p73β and p73γ. On the 3.8–Kb promoter bar, p53 binding motives are represented as vertical segments

construct, by means of the different p73 isoforms increased with the presence DNp73 as reported in figure 4.10. Nevertheless, the increase of DNp73 amounts determined a concentration-dependent increase in luciferase activity, which suggests a cooperation between p73 and DNp73 in transactivating the 2.5–Kb construct (Fig. 4.11). Conversely, the same effect was not observed with the p21 promoter which was indeed downregulated as the DNp73 amounts increased (Fig. 4.12). DNp73 per se is also able to transactivate 2.5–Kb fragment-luciferase construct when transfected in the absence of p53 or p73. This effect was not observed when the p21 promoter sequence was used.

4.8 Discussion

The results presented in this chapter confirm that there is a strict relationship between p53 and DRAGO, having isolated a region which is likely to be bound by p53 which in turn would induce the expression of the gene. Moreover, the present experiments clearly indicate that the DRAGO might be more efficiently transactivated by p73 than by p53. In general, p53 is a stronger transactivator than p73. There are examples in the literature, however, showing that certain genes respond better to p73 than to p53 (i.e p57, ADA) (335, 336).

The different TA p73 isoforms showed a different transactivation efficiency in inducing DRAGO. Particularly, the beta and gamma isoforms seem to be the strongest activators of the gene in the experiments carried out with the different fragments derived from the 3.8–Kb promoter fragment, even

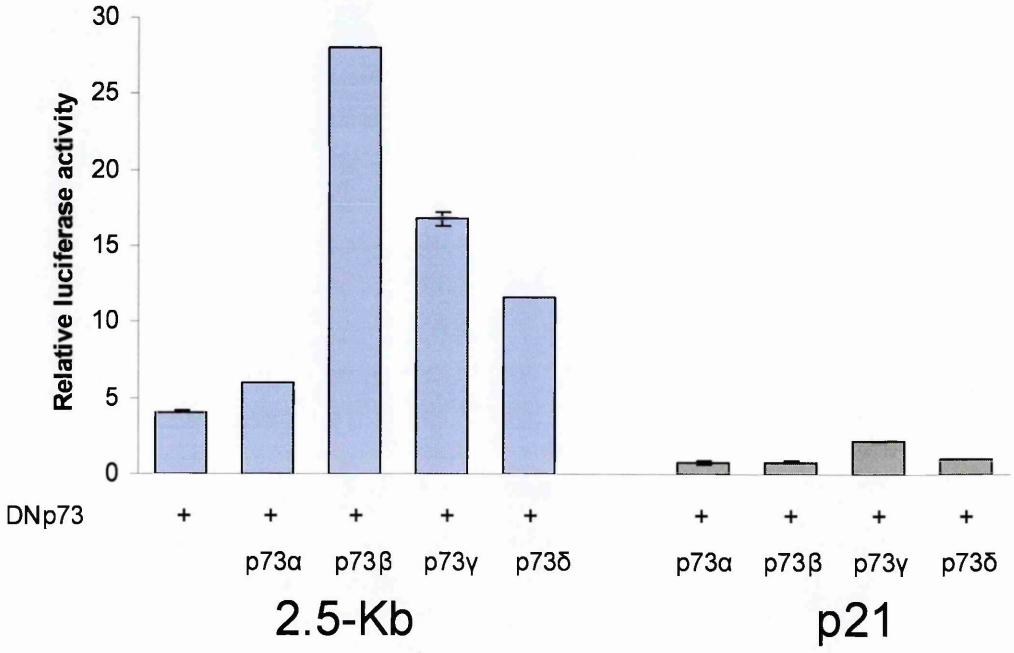

Figure 4.10

Effect of DNp73 contransfected with different p73 isoforms on the activity of the 2.5–Kb promoter and p21 promoter.

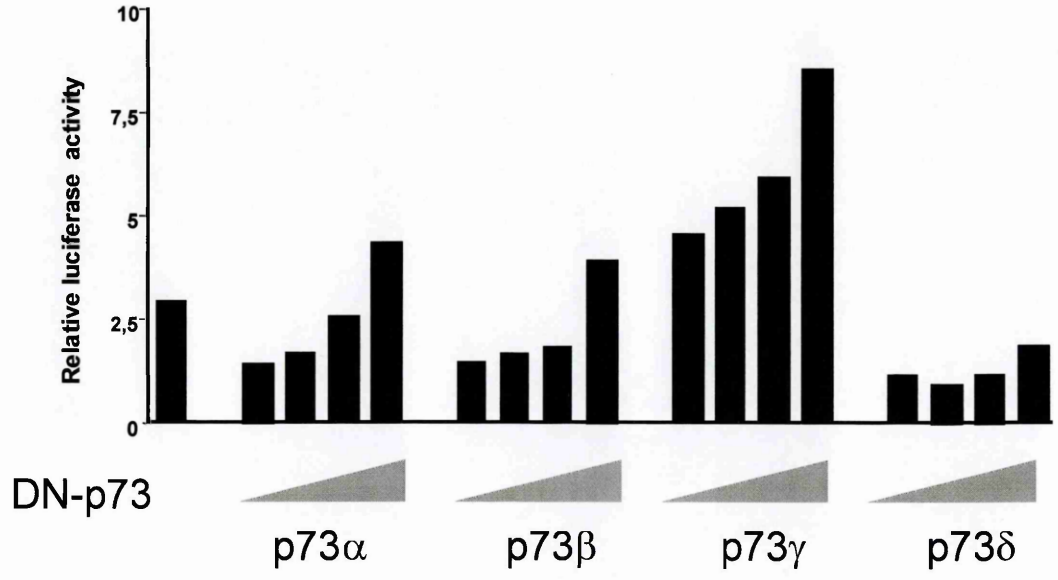

Figure 4.11

DN-p73 cooperation with p73α, p73β, p73γ, p73δ in transactivation of 2.5–Kb fragment-luciferase construct. Increasing concentrations of DN-p73 was cotransfected with a fixed amount of p73 isoforms. The first column shows induction of 2.5 Kb fragment by DN-p73 alone.

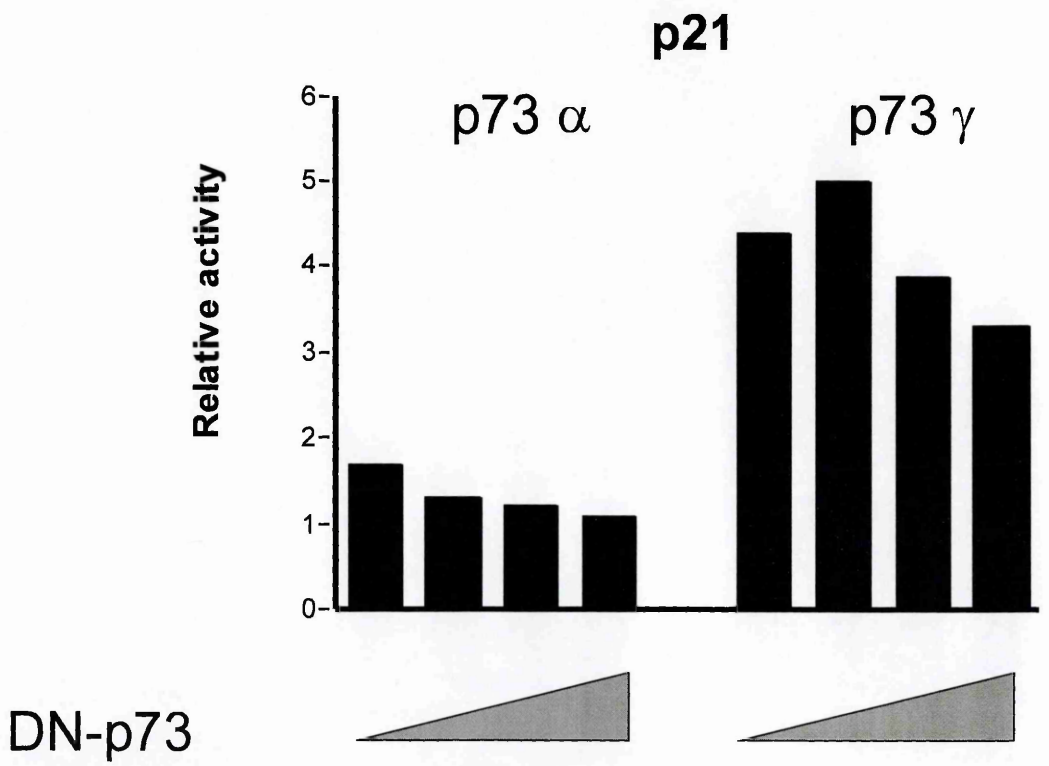

Figure 4.12

DN-p73 repression of transcription activity of p73α and p73γ on p21-luciferase promoter. Increasing concentration of DN-p73 were used in co-transfection experiments with p73α and p73γ.

when the p53 activity was completely abolished. Moreover, these experimental analyses support the hypothesis that the role of DNp73 is not merely to antagonise the p73 isoforms or p53 transcriptional activation of their target genes. As discussed in the introduction chapter, several evidences reported in the literature support the idea that DNP73 act on p53 or p73 isoforms either as a dominant negative, thus exerting an antagonising effect or as a co-operator, therefore acting in a synergistic manner with the same transcriptional factor.

These observations gain more interests when the sequence of those fragments retaining the promoter activity is considered. The 2.5–Kb fragments is in fact characterised by the presence of numerous putative p53 consensus binding sequences. Those sequences present several mismatches in respect to the canonical RRRCWWGYYY sequence, which are consistent with the degenerate nature of the p53 binding site, that are critical for regulatory control since it allows diversity and flexibility in timing and levels in response to cellular signals. However, those binding sequences are reiterated into clusters, which should stabilise binding and mediate expression likewise in the MDM2 and p21 genes.

However, these encouraging results need to be confirmed by other experimental approaches to better verify that these sequences are really functionally bound by p53 and p73 isoforms. Experiments such as either the EMSA (electrophoretic mobility shift assay) or ChIP (chromatin immunoprecipitation) have been planned to be carried out in the future. Another simple and efficient approach could be the introduction of site-

specific mutations in DNA sequences that are considered to be the consensus binding elements for p53 and p73 different isoforms.

The sequences showing stronger activity in response to p53 and especially to p73 are mostly located in the first intron, similarly to what observed for several other p53/p73 target genes (i.e MDM2, KILLER/DR5, DR4, CD95 (Fas/APO–1) receptor) (138, 139, 337-339). As previously mentioned, the molecular structure of DRAGO gene revealed the presence of two introns of considerable length implying a probable involvement of these sequences in the regulation of the gene expression. This could also suggest the presence of binding motives for other transcription factors but most likely of other binding motives for p53 and its family members. These points will be studied in the future by using bioinformatics tools together with the experimental tests on longer genomic sequences.

CHAPTER 5

MUTATIONAL ANALYSIS

5.1 Introduction

As discussed in introduction chapters, cancer development takes advantage from mutations or, in general, alterations in genes especially those responsible for cellular growth control. P53 is a paradigmatic example. As "cancer gene" it has been found to be mutated in almost half of the tumors (see chapter 1.4). On the basis of this consideration, possible mutations in DRAGO gene exons have been searched by performing the SSCP analysis and DNA sequencing.

5.2 SSCP analysis

SSCP analysis permits to evidentiate even a point mutation occurring on a single strand of a gene of interest. Mutations in a gene are in fact responsible to a different electrophoresis profile if compared to that of a non mutated one. The presence of DNA mutations in the gene has been investigated in exons 1, 2, 3, 4 and 5 which were amplified by PCR from genomic DNA extracted from 12 human cancer cell lines of different origin and used for SSCP analysis. In figure 5.1 a representative SSCP gel of not mutated fragments has been reported. Fragments with a suspected mutation (see figure 5.2 as an example) were subjected to direct DNA sequencing. In figure 5.3 (panel A) the sequence of the exon 1 of SKOV–3 cells has been reported. The perfect alignment between the sequence of interest (indicated as query and corresponding to exon 1 from SKOV–3

cells) and the DRAGO cDNA has also been showed in panel B of figure 5.3. As reported in chapter 3.2, the first exon of DRAGO cDNA spans nucleotides 1–188. In the table 5.1, the 12 human cancer cell lines investigated have been reported. The PCR fragments with suspect mutations which have been sequenced are indicated. Nevertheless, for each exon, even if putatively not mutated on the basis of the SSCP analysis, random PCR fragments have been chosen for sequencing. In any cases, the alignment of either the suspected mutated or the putative not mutated exons with the genebank DNA sequence of DRAGO revealed no DNA mutations among the cell lines tested.

As DRAGO gene resulted to be not mutated in the panel of human cell lines which represent an in vitro model, then the search for mutations have been address to clinical samples. Genomic DNA was therefore purified from human tumor biopsies and investigated to verify if some mutations could be found. The analysed samples included ovarian cancer, colon cancer, endometrial cancer and leukemia. Among the tumor samples investigated, no mutations could be detected on the basis of the SSCP analysis (Fig. 5.4) and no more tumor samples have been studied. Since the overexpression of DRAGO upon drug treatment induces the arrest of cellular growth as it will be discussed further in the result chapter, it has been investigated if the gene is mutated in cell lines resistant to drugs acting by different mechanisms. For this purpose DRAGO has been examined for mutations by direct sequencing of the exons 1–5 obtained by PCR amplification of the genomic DNA isolated from human cancer cell

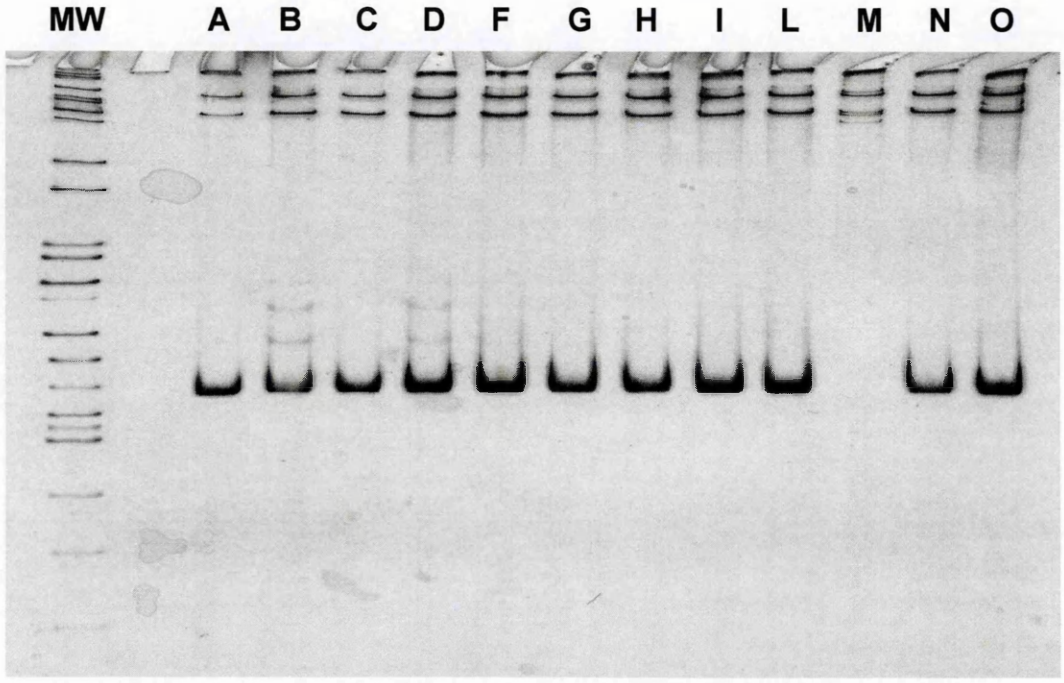

Figure 5.1

Representative SSCP gel (see 2.5) PCR fragments corresponding to the exon 5 in the 12 cell lines tested (cell lines are indicated with a letter: see table 5.1 to identify cell lines and the corresponding origin). Fragments did not show altered migration suggesting that they were not mutated.

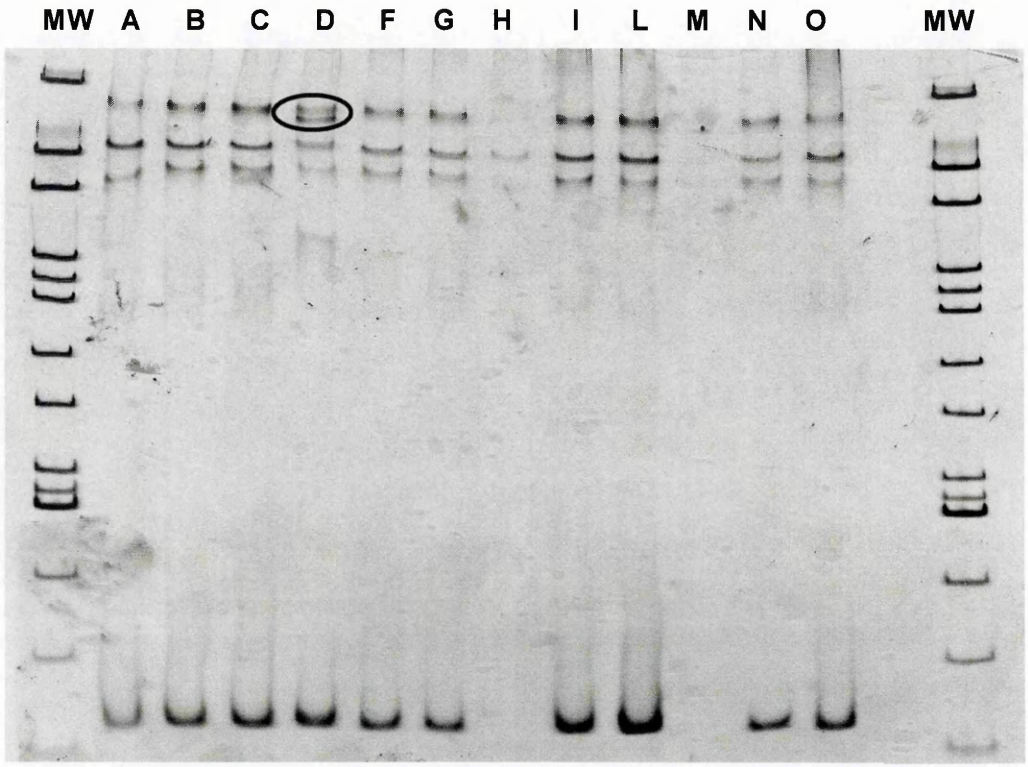

Figure 5.2

Representative SSCP gel (see 2.5) of PCR fragments corresponding to the exon 1 in 12 cell lines tested (cell lines are indicated with a letter: see table 5.1 to identify cell lines and the corresponding origin). The fragment with suspect mutation has been highlighted.

A

>Exon1_SKOV–3

CGCTGCAGCCGTCGCTACCGCCGCGTTCTATTCTCCGAAGCCGGCG
ACCGCCCCACCTCCTCCCTCCCTCCCGCCCGCTTCCTCTGCCCACA
GCGCCGGCCAGAGCGAGCTAGACAAGGGCACGCGGGGCCTCGCC
TAGACCCGAGAAGACTGCGGGCGCGCGCAAGCGGCGGCGTGGAA
GCTGTGAGCGCCCCCATCCCGGAGGTCTCCGCCGGCTCCCGGGTG
AGTANNNNN

B

Query= exon1_SKOV-3

Subject= *Homo sapiens* mRNA for KIAA0247 gene

```
> gi|1665762|dbj|D87434.1|     Homo sapiens mRNA for KIAA0247 gene, partial cds
          Length=5338

 Score =  381 bits (192),  Expect = 6e-103
 Identities = 192/192 (100%), Gaps = 0/192 (0%)
 Strand=Plus/Plus

Query  35   CCGAAGCCGGCGACCGCCCCACCTCCTCCCTCCCTCCCGCCCGCTTCCTCTGCCCACAGC  94
            ||||||||||||||||||||||||||||||||||||||||||||||||||||||||||||
Sbjct  1    CCGAAGCCGGCGACCGCCCCACCTCCTCCCTCCCTCCCGCCCGCTTCCTCTGCCCACAGC  60

Query  95   GCCGGCCAGAGCGAGCTAGACAAGGGCACGCGGGGCCTCGCCTAGACCCGAGAAGACTGC  154
            ||||||||||||||||||||||||||||||||||||||||||||||||||||||||||||
Sbjct  61   GCCGGCCAGAGCGAGCTAGACAAGGGCACGCGGGGCCTCGCCTAGACCCGAGAAGACTGC  120

Query  155  GGGCGCGCGCAAGCGGCGGCGTGGAAGCTGTGAGCGCCCCCATCCCGGAGGTCTCCGCCG  214
            ||||||||||||||||||||||||||||||||||||||||||||||||||||||||||||
Sbjct  121  GGGCGCGCGCAAGCGGCGGCGTGGAAGCTGTGAGCGCCCCCATCCCGGAGGTCTCCGCCG  180

Query  215  GCTCCCGG  222
            ||||||||
Sbjct  181  GCTCCCGG  188
```

Figure 5.3

Panel A: Sequence of PCR fragment amplified from genomic DNA extracted from SKOV–3 cells and corresponding to exon 1 of DRAGO cDNA.

Panel B: Blast result between the sequence of exon 1 (panel A) and nucleotide sequence of DRAGO cDNA (gi: 1665762) deposited in genebank has been reported. Exon 1 from SKOV–3 cells which seemed to be mutated on the basis of SSCP analysis, perfectly matched with DRAGO cDNA.

Cell line	Origin	Exon 1	Exon 2	Exon 3	Exon 4	Exon 5
A: SW620	Colon	normal	normal	**sequenced**	normal	normal
B: SW626	Ovary	normal	**sequenced**	normal	normal	normal
C: IGROV	Ovary	normal	normal	normal	normal	**sequenced**
D: SKOV-3	Ovary	**? sequenced**	normal	normal	**? sequenced**	normal
F: DU145	Prostate	normal	normal	normal	normal	normal
G: REH	ALL	normal	normal	normal	normal	normal
H: ALLOPO	ALL	normal	normal	normal	normal	normal
I: TOM	ALL	normal	normal	normal	normal	normal
L: U2OS	Osteosarcoma	normal	normal	normal	normal	normal
M: SAOS	Osteosarcoma	normal	normal	normal	normal	normal
N: CEM	T–Leukemia	normal	normal	normal	normal	normal
O: HL60	T–Leukemia	normal	normal	normal	normal	normal

Table 5.1

Summary of SSCP analysis.

The first two columns report the 12 cell lines used in this study and their origin, respectively. Exons 1–5 were PCR amplified and analysed. Fragments with suspect mutations (indicated with a question mark ?) were sequenced as reported in the table. Additional PCR fragments with normal electrophoresis pattern were selected and sequenced in order to verify they were not mutated.

lines of different origin resistant to cisplatin (A2780/cp70), taxol (1A9PTX22), etoposide (CEM-VM1) or doxorubicin (LoVo/DX). However, each of the fragments analysed perfectly matched with the genebank DNA sequence of DRAGO. Examples of some sequences of exons derived from drug resistant cell line DNA are reported in figure 5.5.

5.3 Discussion

Altogether these results strongly support the idea that DRAGO seems to be not mutated in human cancer cell lines sensitive or resistant to cytotoxic treatments. The same observations has been confirmed in clinical samples of human tumors where mutations have not been found among the limited number of the analysed samples. Considering that the human cell lines are more frequently mutated than the corresponding clinical cancers, it is unlikely that human tumors could be mutated in genes that are not altered in the nucleotide sequence in cell lines. For these reasons the analysis for searching mutations in DRAGO gene has not been extended to other clinical samples of human tumors. These data, therefore suggest that DRAGO is not frequently mutated and are in line with what observed for other p53 downstream genes, like p21 (340), which has not been found mutated in human tumor samples. On the other hand, as p53 is frequently mutated in human tumors, it is not strictly necessary that its downstream effector genes are non-functional being its inactivation enough to de-regulate cellular growth or death thus leading to cancer inception, as widely discussed in the Introduction chapter.

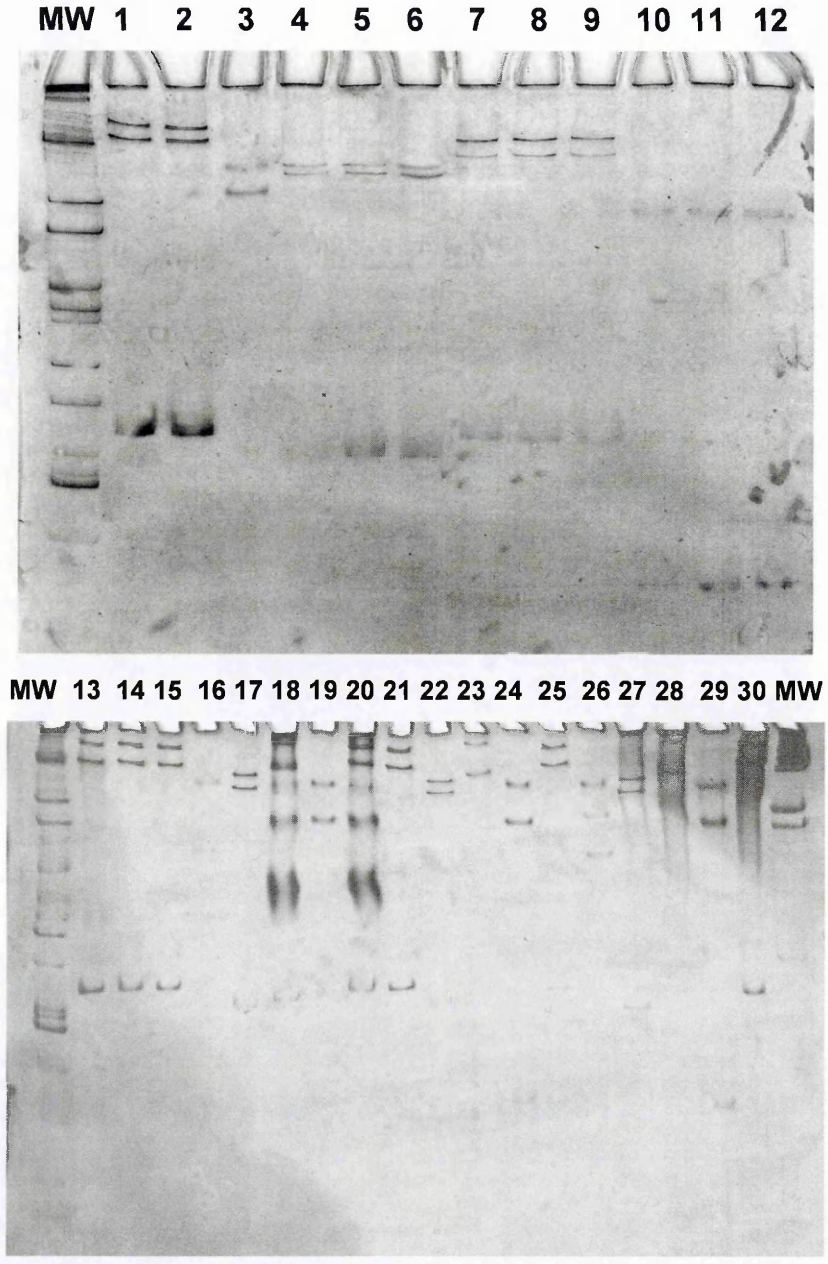

Figure 5.4

SSCP analysis on DNA samples derived from ovarian (3 cases, indicated as I, II, III), colon, endometrial cancers and leukaemia. Lane 1–3, exon 1 of I, II, III ovarian cancers respectively; lane 4–6, exon 2 of I, II, III ovarian cancers; lane 7–9, exon 3 of I, II, III ovarian cancers; lane 10–12, exon 4 of I, II, III ovarian cancers; lane 13–15, exon 5 of I, II, III ovarian cancers; lane 16–20, exons 1–5 of colon cancer; lane 21–25, exons 1–5 endometrial cancer; lane 26–30, exons 1–5 leukemia. Among human cancers analysed no mutations were detected.

Query exon 1 of CEM–VM1 cell lines

```
>gi|1665762|dbj|D87434.1| Homo sapiens mRNA for KIAA0247 gene, partial cds
Length = 5338

Query: 21  CCGAAGCCGGCGACCGCCCCACCTCCTCCCTCCCTCCCGCCCGCTTCCTCTGCCCACAGC 80
           ||||||||||||||||||||||||||||||||||||||||||||||||||||||||||||
Sbjct: 1   CCGAAGCCGGCGACCGCCCCACCTCCTCCCTCCCTCCCGCCCGCTTCCTCTGCCCACAGC 60

Query: 81  GCCGGCCAGAGCGAGCTAGACAAGGGCACGCGGGGCCTCGCCTAGACCCGAGAAGACTGC 140
           ||||||||||||||||||||||||||||||||||||||||||||||||||||||||||||
Sbjct: 61  GCCGGCCAGAGCGAGCTAGACAAGGGCACGCGGGGCCTCGCCTAGACCCGAGAAGACTGC 120

Query: 141 GGGCGCGCGCAAGCGGCGGCGTGGAAGCTGTGAGCGCCCCCATCCCGGAGGTCTCCGCCG 200
           ||||||||||||||||||||||||||||||||||||||||||||||||||||||||||||
Sbjct: 121 GGGCGCGCGCAAGCGGCGGCGTGGAAGCTGTGAGCGCCCCCATCCCGGAGGTCTCCGCCG 180

Query: 201 GCTCCCGG 208
           ||||||||
Sbjct: 181 GCTCCCGG 188
```

Query Exon 3 of A2780/cp70 cell line

```
gi|1665762|dbj|D87434.1| Homo sapiens mRNA for KIAA0247 gene, partial cds
Length=5338

Query  1    TGTGCCCCCTACCACCGGAGCCAGAGAATGGTGGCTACATCTGCCACCCCCGGCCCTGCA  60
            ||||||||||||||||||||||||||||||||||||||||||||||||||||||||||||
Sbjct  390  TGTGCCCCCTACCACCGGAGCCAGAGAATGGTGGCTACATCTGCCACCCCCGGCCCTGCA  449

Query  61   GAGACCCCCTGACAGCAGGCAGTGTCATCGAATACCTGTGTGCTGAAGGCTACATGTTGA  120
            ||||||||||||||||||||||||||||||||||||||||||||||||||||||||||||
Sbjct  450  GAGACCCCCTGACAGCAGGCAGTGTCATCGAATACCTGTGTGCTGAAGGCTACATGTTGA  509

Query  121  AGGGCGATTACAAATACCTGACGTGTAAGAATGGCGAGTGGAAACCAGCCATGGAGATTA  180
            ||||||||||||||||||||||||||||||||||||||||||||||||||||||||||||
Sbjct  510  AGGGCGATTACAAATACCTGACGTGTAAGAATGGCGAGTGGAAACCAGCCATGGAGATTA  569

Query  181  GCTGCCGTCTCAACGAGG  198
            ||||||||||||||||||
Sbjct  570  GCTGCCGTCTCAACGAGG  587
```

Query: exon 4 of Lovo/DX cell line (reverse sequence)

```
gi|1665762|dbj|D87434.1| Homo sapiens mRNA for KIAA0247 gene, partial cds
          Length=5338

Query  6    CTGCTATGATGGAAAGACTTCAGCTTTGGCTGCAGCAGCACAAACAGCACCACGAGGAGG  65
            ||||||||||||||||||||||||||||||||||||||||||||||||||||||||||||
Sbjct  726  CTGCTATGATGGAAAGACTTCAGCTTTGGCTGCAGCAGCACAAACAGCACCACGAGGAGG  667

Query  66   AGAATGAGCGCCACGGAGCTGGCAGTAGAAGCCACTATAGACAGCGTGGGGACCCCAAGT  125
            ||||||||||||||||||||||||||||||||||||||||||||||||||||||||||||
Sbjct  666  AGAATGAGCGCCACGGAGCTGGCAGTAGAAGCCACTATAGACAGCGTGGGGACCCCAAGT  607

Query  126  GATGTGTGGGTGTCTTTAT  146
            ||||||||||||||||||
Sbjct  606  GATGTGTGGGTGTCTTTAC  588
```

Figure 5.5

Representative PCR amplified exons sequences from drug resistant cell lines. The exon 4 sequence is in the reverse sense. The reported sequences show perfect match with the cDNA sequence (gi: 1665762) deposited in the genbank.

CHAPTER 6

CHARACTERISATION OF THE FUNCTION OF THE DRAGO GENE

6.1 Introduction

As outlined in the previous chapter, the analysis of either the cDNA sequence or the primary aminoacid sequence did not reveal any similarity to known domains that could help to hypothesise any functional role of the protein or its subcellular localisation. Moreover, as reported in the introduction chapter, DRAGO mRNA has been found ubiquitously expressed at very low level. The strategy that has been undertaken was to study any biochemical and morphological modifications induced by DRAGO overexpression in both eukaryotic and prokaryotic (bacterial) cells in either transient or stable transfections. Another effort here reported regarded the functional analysis of domains at either the NH2– or COOH–terminus of the protein coded by DRAGO.

6.2 Effects of gene overexpression in eukaryotic cells

The effects of gene overexpression were evaluated in cells carrying constructs in which the isolated cDNA was functionally linked to a strong viral promoter. The complete cDNA (5,338 bp) and the coding region (nucleotides 269-1,180) were used for vector assembly. The full length cDNA sequence was excised from pBS plasmid (see 1.7) by restriction with *Hind*III and *Kpn*I enzymes and inserted into $pCDNA_3$ digested with the same enzymes. The coding region was indeed inserted into the $pCDNA_3HA$ expression vectors which was prepared from $pCDNA_3$ by

insertion of the HA tag coding sequence. The latter was excised from a vector available in the laboratory by restriction with the *Kpn*I and *Xho*I enzymes used to digest the $pCDNA_3$ vector as well. Whereas the coding portion of DRAGO cDNA was amplified by PCR using a set of primers designed to introduce the sequences for *Xho*I and *Xba*I restriction sites at the 5' and 3', respectively. After digestion with the above mentioned enzymes, the coding region was then sub-cloned in frame with the HA sequence, after restriction of the $pCDNA_3HA$ with the same enzymes. Each construct was automatically sequenced to verify its correct assembly and transfected into A2780 ovarian cancer cell lines. Fifteen days later, the colonies were stained with crystal violet, washed and photographed. Figure 6.1 shows the photographs of a plate in which A2780 cells were transfected with the full-length cDNA (B) or with vector $pCDNA_3$ alone (A) and flasks were the A2780 cells were transfected with the coding sequence subcloned in the $pCDNA_3HA$ vector (D) or with the vector alone (C). In both cases, no colonies were detected in DRAGO transfected cells (B and D), whereas a large number of colonies was present in the culture transfected with vectors alone (A and C). The overexpression of the complete cDNA (5,338 bp) or its 1,180 bp fragment (coding region) prevented therefore colony formation. This effect was observed not only in A2780 cells (ovary carcinoma), but also in SaoS2 and U2OS lines (human osteosarcoma) cell lines and in murine fibroblasts Swiss 3T3 cells. Failure to isolate stable clones was probably due to the strong growth-suppressing effect following gene-overexpression.

A2780

A pCDNA$_3$/control **B pCDNA$_3$/DRAGO**

SKOV–3

C pCDNA$_3$–HA/control **D pCDNA$_3$–HA/DRAGO**

Figure 6.1

Effect of the overexpression of DRAGO on A2780 and SKOV-3 cells stably transfected with the full length DRAGO cDNA (B) or the coding region (D). A and C are respectively the A2780 and SKOV–3 cells transfected with the vector alone

6.3 Morphologic modification in contrast phase microscopy

Morphologic changes following gene overexpression were evaluated in fibroblast 3T3 cells transiently transfected with the construct $pCDNA_3HA$-DRAGO, used for the stable transfection experiments. The morphological effects have been analysed within a short time (24 and 48 hours) from transfection by contrast phase microscopy. The overexpression of DRAGO caused a series of dramatic morphological changes in the transfected cells which were characterised by the presence of several cytoplasmic vacuoles. In some cases the cell membranes appeared disrupted and the vacuole content was extra-cellularly released (Fig. 6.2). Transfection with the vectors alone was not associated with any evident morphologic alteration.

6.4 Analysis of functional domains: deletion mutants

The results reported in the chapter 6.2 explain why it is impossible to study the gene-induced changes in phenotype in stable transfected clones because of the intrinsic growth inhibition ability of the gene itself. Therefore, the phenotypic changes induced by the cDNA overexpression were evaluated using specific deletion mutants. The aim of these studies was to identify regions of the protein encoded by the gene which could be responsible for the growth suppressive activity.

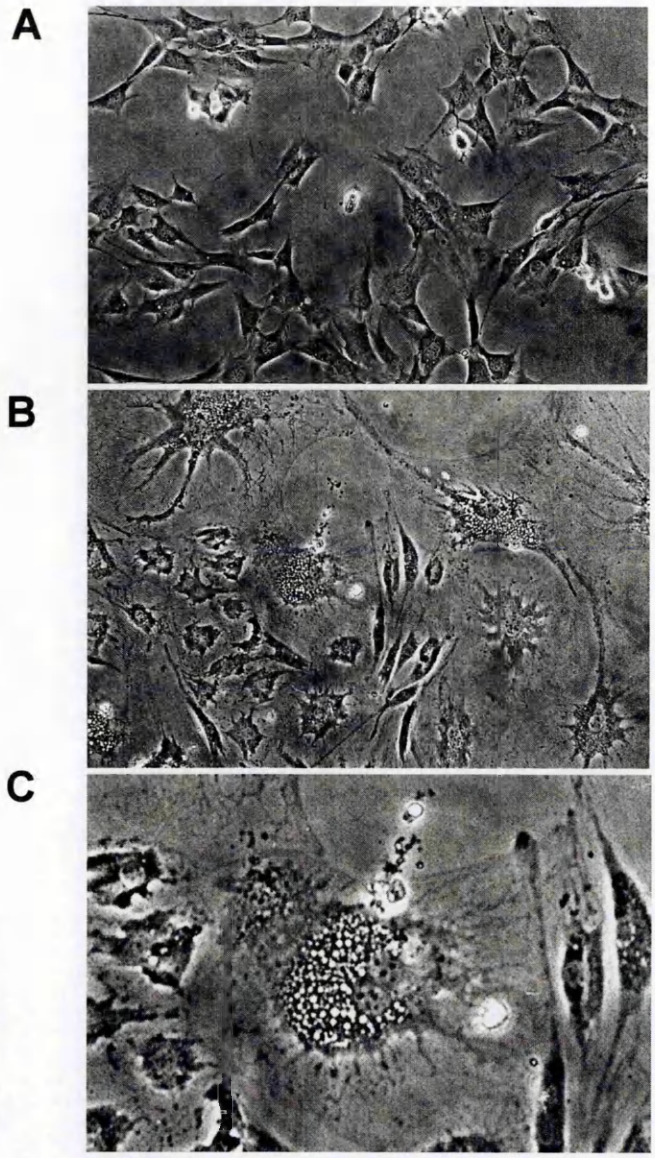

Figure 6.2

Evaluation of morphological effects by contrast phase microscopy in fibroblast 3T3 cells transiently transfected with DRAGO.

Panel A: 3T3 fibroblasts transfected with the vector ($pCDNA_3HA$) as control.

Panel B: 3T3 fibroblasts transfected with the coding region of DRAGO ($pCDNA_3HA$–DRAGO)

Panel C: an enlargement of the photograph in panel B showing the presence of several vacuoles inside the cell and the release of cytosolic material outside the broken plasmatic membrane.

6.4.1 Analysis of deletion mutants in prokaryotic cells

The entire coding region of the DRAGO was subcloned in the pGEX–3X vector used for the expression of the protein in bacteria, in particular in the *E. coli* strain. With this vector, the coding sequence for the protein of interest is subcloned in frame with the GST tag. The resulting GST-fused proteins can be easily isolated and purified from bacteria. At the 3' of the cDNA coding the GST enzyme there is a protease–specific recognition site which can be cleaved by appropriate protease (the factor Xa protease) to release the desired protein from the fusion product for subsequent studies (sequence identification, cristallography etc). The full length coding region has been PCR amplified using the pBS-DRAGO construct as a template and primers designed to introduce the cleavage site for *BamH*I and *EcoR*I at the 5' and 3' end of the PCR fragment respectively. The PCR fragment was subcloned in the pGEM-T plasmid for the TA cloning and verified by DNA sequencing. Then the construct has been digested with the *BamH*I and *EcoR*I restriction enzymes to get a fragment with the suitable extremities to be subcloned in the pGEX–3X vector. The first methionine used to synthetise the protein is the one present in the GST tag. The gene methionine has been removed so that all the constructs start from aminoacid 2.

Starting from the entire 303 aminoacid sequence, progressive deletions were designed either at N– or C–terminus (Fig. 6.3). similarly as the full length coding region, the deletion mutants were generated by PCR using

as a template the coding sequence subcloned in the pGEX–3X vector and primers spanning the desired region, containing sequences recognised by the same restriction enzymes used for the full length coding region subcloning in the pGEX–3X vector (*BamH*I and *EcoR*I). Different N-terminus deletion mutants produced were:

N1: 12-303 aa cDNA construct: 893 bp 11 aminoacids deleted

N2: 23-303 aa cDNA construct: 860 bp 22 aminoacids deleted

N3: 35-303 aa cDNA construct: 824 bp 34 aminoacids deleted

N4: 49-303 aa cDNA construct: 782 bp 48 aminoacids deleted

N5: 60-303 aa cDNA construct: 749 bp 59 aminoacids deleted

N6: 74-303 aa cDNA construct: 707 bp 73 aminoacids deleted

Similarly, different C-terminus deletion mutants have been generated:

C 1: 2-290 aa cDNA construct: 884 bp 13 aminoacids deleted

C 2: 2-275 aa cDNA construct: 839 bp 28 aminoacids deleted

C 3: 2-260 aa cDNA construct: 794 bp 43 aminoacids deleted

C 4: 2-245 aa cDNA construct: 749 bp 58 aminoacids deleted

C 5: 2-230 aa cDNA construct: 704 bp 73 aminoacids deleted

C 6: 2-215 aa cDNA construct: 659 bp 88 aminoacids deleted

The PCR products (Fig. 6.4) were then processed similarly as the full length coding region has been subcloned in the pGEX–3X vector (with the same procedure to subclone in the pGEX–3X vector the full length coding region. In summary they were subcloned in the pGEM-T to be digested with the *BamH*I and *EcoR*I restriction enzymes to get the deleted fragments with the suitable extremities to be subcloned in the pGEX–3X

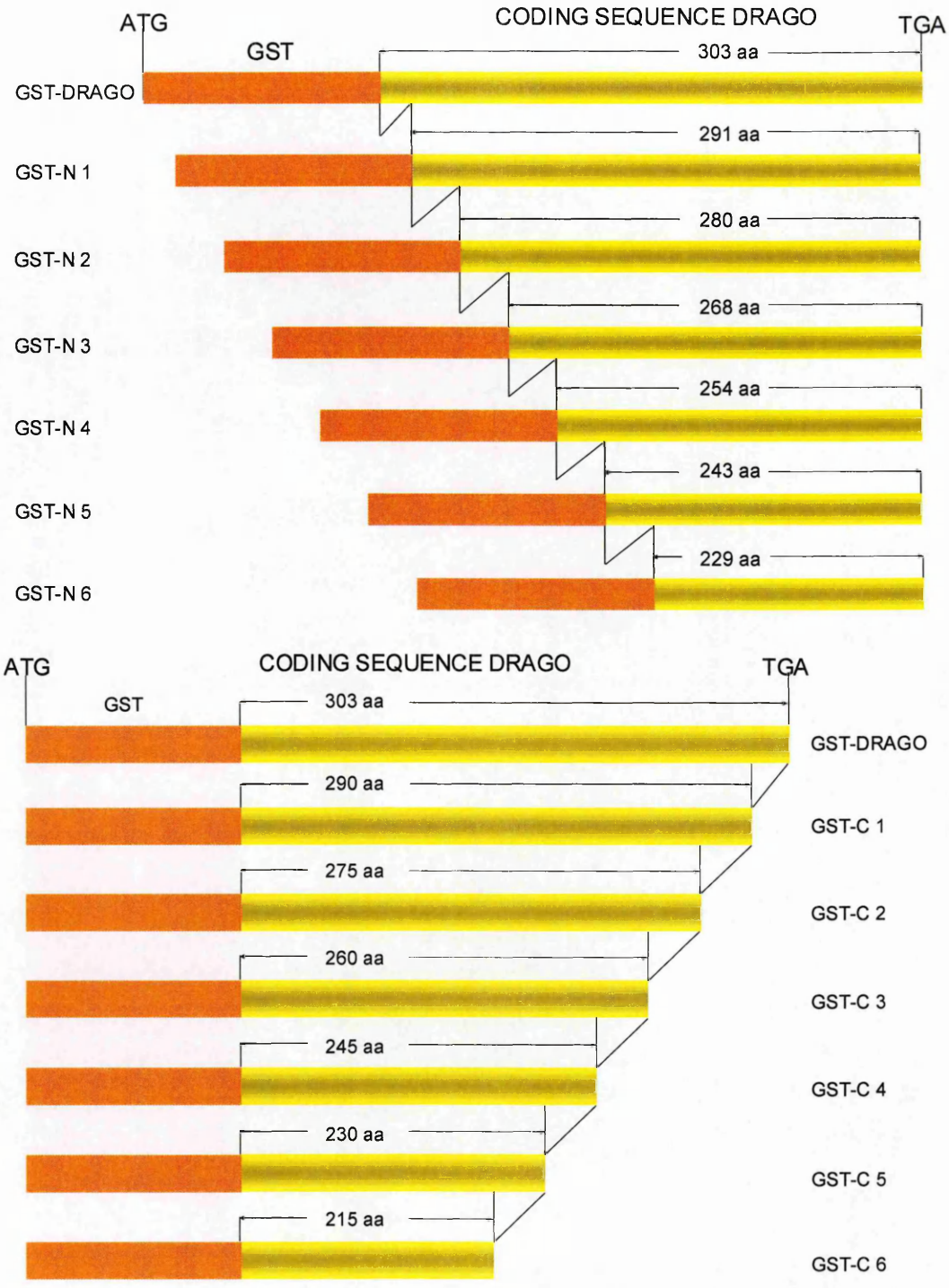

Figure 6.3

Progressive deletions at N– and C–terminus of the coding region of DRAGO generated deletion mutants which were subcloned in frame with the GST–tag in the pGEX–3X vector to be expressed in bacteria

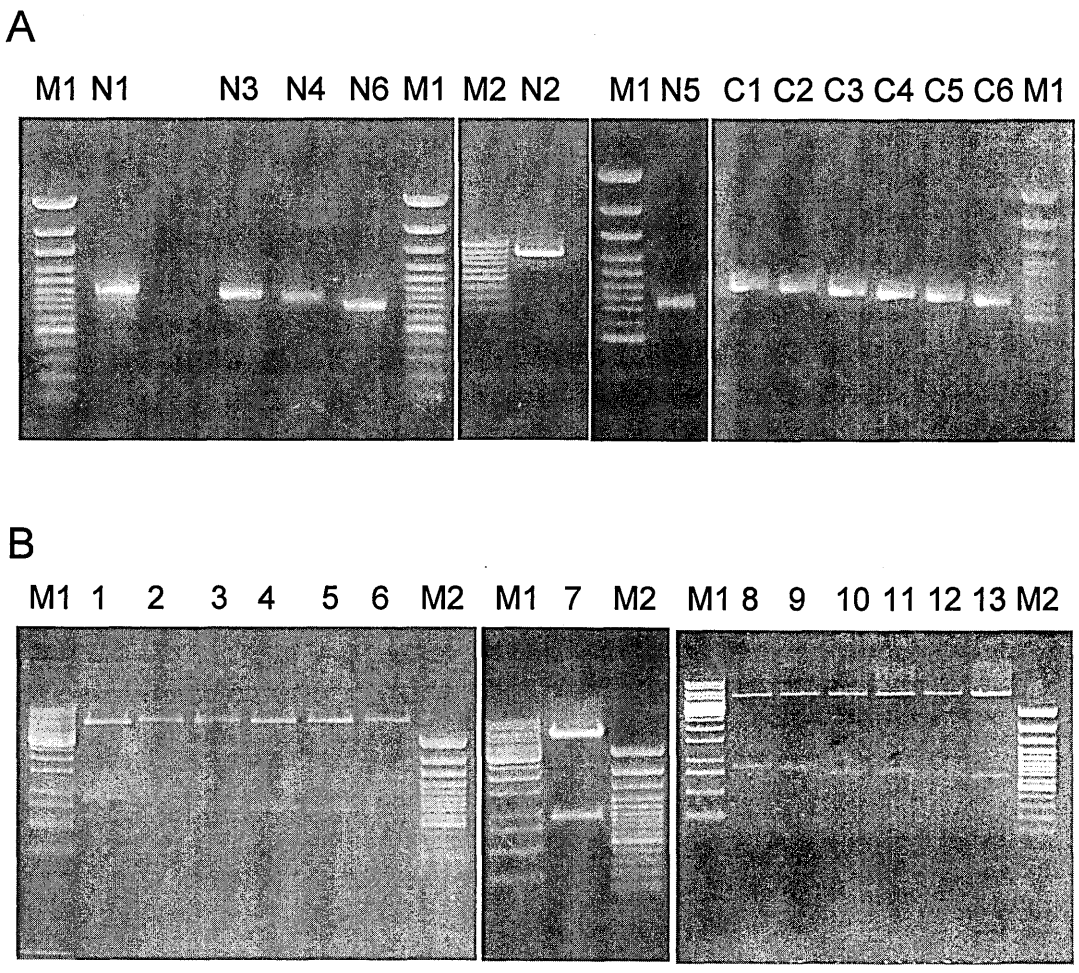

Figure 6.4

Panel A: PCR fragments corresponding to the N– and C–terminus deleted DRAGO cDNAs. Correspondence with the expected molecular weight was verified with the molecular weight marker (M1 and M2) ladder in each gel. Panel B: pGEX–3X constructs were verified by restriction with *EcoR*I and *BamH*I enzymes which caused the excision of the deleted cDNA from the plasmid vector. Lane 1: pGEX–N1, lane 2: pGEX–N3; lane 3: pGEX–N4, lane 4: pGEX–N5; lane 5: pGEX–N6; lane 6: pGEX–DRAGO; lane 7: pGEX–N2; from lane 8 to13: pGEX–C1 to pGEX–C6; M1: 1 KB DNA ladder molecular marker; M2: 100 bp DNA ladder plus molecular marker.

vector. The first methionine used to synthesise the protein is the one present in the GST tag as for the pGEX-DRAGO.

The GST constructs, after confirmation by sequencing, have been used to transform XL1-blue bacteria and their presence verified by standard molecular biology technique. The bacteria expressing the different constructs were induced with IPTG to stimulate the production of the peptides encoded by the DNA sequence inserted in the vector. After 4-6 hours following induction, the bacteria were harvested, lysed and the proteins loaded onto SDS polyacryilamide gels. These evidentiated the exogenous proteins, present in relatively higher amounts, which, starting from the first deletion for the C-terminus (Fig. 6.5A) and form the third for the N-terminus, show a progressive reduction in molecular weight. This result was also confirmed by Western blotting (Fig. 6.5B), using monoclonal antibody against DRAGO (see next section). It is interesting to underline that even bacteria did not produce the full length protein coded by DRAGO cDNA fused to the GST tag (Fig 6.5).

Taking advantage of the GST tag, the purification of the N- and C-terminal deleted proteins produced by bacteria has been carried out by using a glutathione–bound matrix to sequester the GST-fusion proteins. The structure of glutathione is in fact complementary to the Glutathione–S–Transferase–binding site. Therefore, fusion proteins binding to the matrix are retained by the matrix and then isolated from the other proteins present in the lysates. Unfortunately, no GST-fused protein has been recovered from the bacteria. The exogenous GST-fusion proteins were

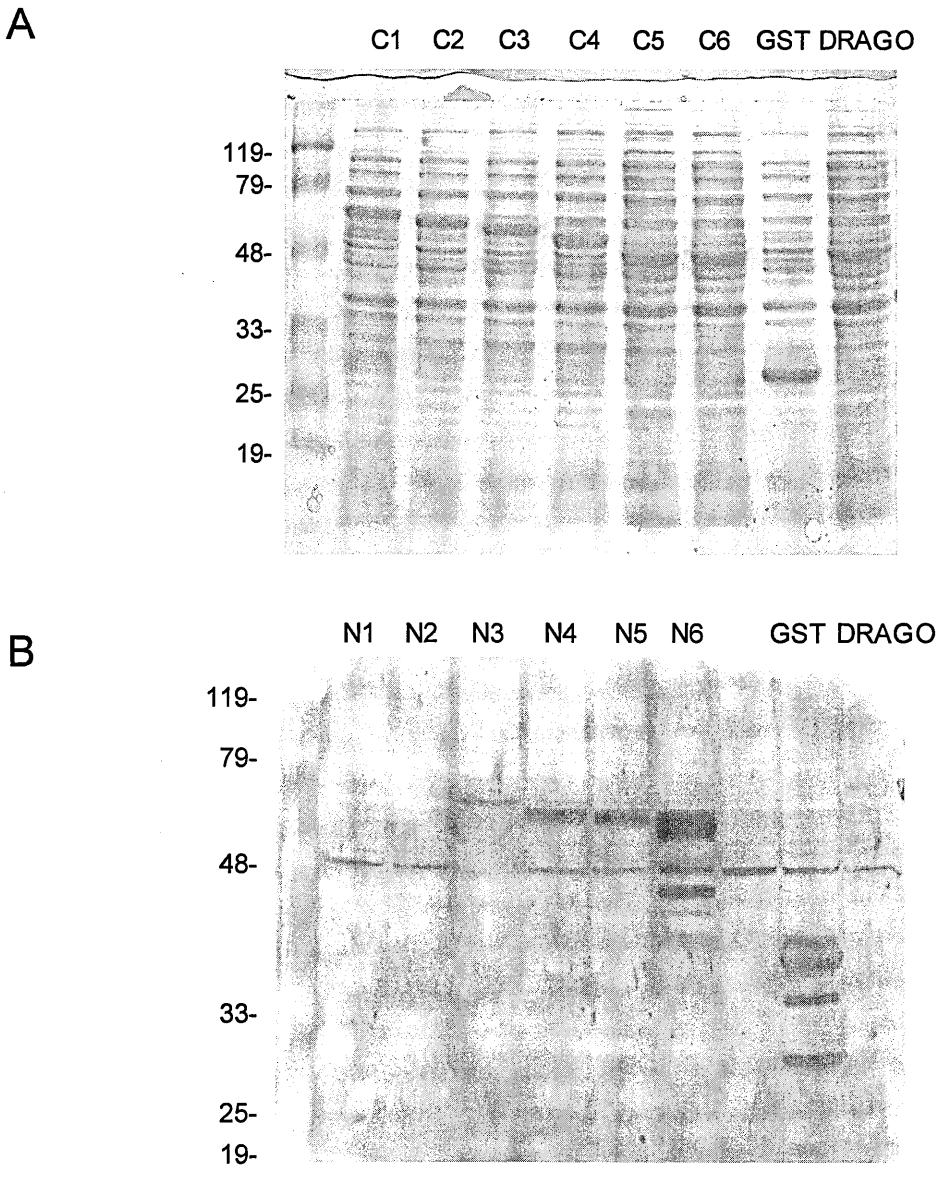

Figure 6.5

N– and C– terminal deletion mutants expressed by bacteria upon induction.

Panel A: SDS–PAGE of cellular lysates obtained from bacteria expressing C–terminal deleted proteins. Exogenous proteins were present in relatively higher amounts as revealed after Coomassie blue staining of the gel (see section 2.10.1).

Panel B: N–terminal deleted proteins from bacterial extracts were detected by Western Blotting, using monoclonal antibody against DRAGO.

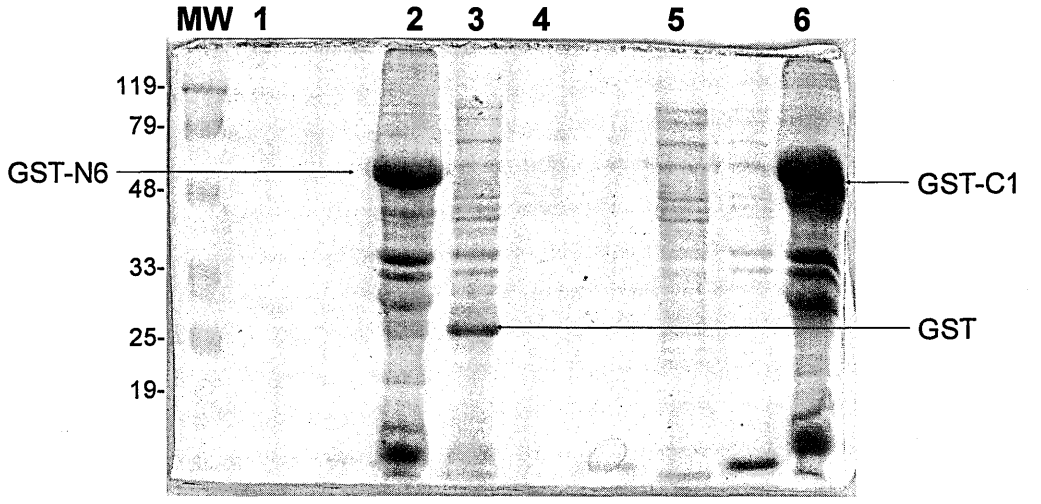

Figure 6.6

SDS–PAGE of different eluates and aliquots of supernatant and bacterial pellet saved during the purification of GST–fusion proteins exogenously expressed by bacteria, as reported in chapter 3.9. Lane 1: eluate corresponding to GST–N6 fusion protein purified from bacterial cells which were induced to produce it. Lane 2: aliquot of bacterial cell pellet from GST–N6 bacterial culture. Lane 3: aliquot of the eluate corresponding to purification of GST from pGEX–3X transformed bacterial cells. Lane 4: aliquot of first wash of the GSH–bound matrix after binding to GST–carrying proteins. Lane 5: aliquots of supernatant flowed through the GSH–bound matrix. Lane 6: aliquot of bacterial cell pellet from GST–C1 bacterial culture.

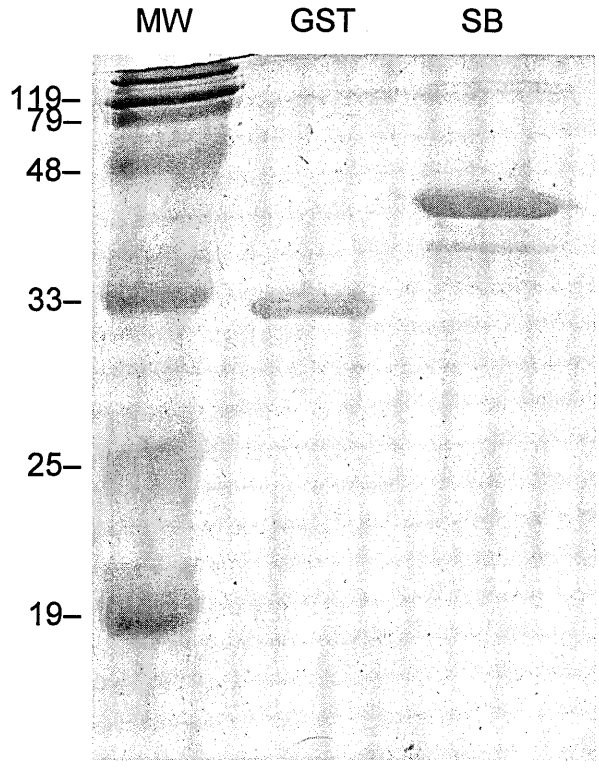

Figure 6.7

SDS–PAGE of purified GST and GST–SB after Coomassie Blue staining. Numbers on the left refers to the molecular weight marker (MW).

retained in the insoluble material after bacterial lysis, as observed when bacteria debris have been loaded on SDS polyacrylamide gels (Fig. 6.6). These proteins tended to accumulate in the inclusion bodies, thus making their purification and subsequent cleavage from the GST tag for sequencing difficult.

6.4.1.1 Production of monoclonal antibodies

Monoclonal antibodies against DRAGO have been generated in collaboration with ARETA INTERNATIONAL biotech (Gerenzano, Varese–Italy). Since the purification of all the deleted mutants, fused to the GST protein produced by bacteria, was not successful, as antigen a smaller peptide (SB) corresponding to the last 82 aminoacids at the C-terminus of DRAGO has been produced and purified. The nucleotide fragment coding the 82 aminoacids has been PCR amplified using the pGEX-DRAGO construct as a template. The upstream primer was designed to introduce the sequence recognised by *BamH*I restriction enzyme. The downstream primer was the primer with the *EcoR*I site designed for the PCR amplification of the full length coding sequence. The PCR fragment obtained was then loaded on an agarose gel, purified and subcloned on the pGEM-T vector. It was then digested with the appropriate enzymes and subcloned in the pGEX–3X vector. The construct has been confirmed by sequencing and transferred into bacteria. The bacteria were then induced to produce the GST-SB peptide similarly as done with the N-terminus and C-terminus deleted mutants. The purification of the peptide

has been carried out using the GSH-matrix. The elution has been checked on a SDS polyacrylamide gel, confirming the presence of the SB eluate (Fig. 6.7). The purified SB-GST peptide has been then used as antigen for the production of monoclonal antibodies.

6.4.2 Analysis of deletion mutants in eukaryotic cells

In parallel analogous PCR products have been subcloned in the $pCDNA_3$-HA expression plasmid which was previously generated by inserting the HA tag sequence in the commercially available $pCDNA_3$ plasmid. The HA tag is a short aminoacid sequence which can be recognised in cell by specific antibodies. The advantage of this tag is that the short sequence is unlikely to interfere with the structure and function of the protein to be studied. The deletion mutants generated by PCR had *Xho*I and *Xba*I sequences inserted at the 5' and 3' by *ad hoc* designed primers and necessary for the subcloning in the $pCDNA_3HA$ vector. The PCR amplified fragments (Fig. 6.8) were processed similarly to those inserted in the pGEX–3X vector, therefore, after having been inserted in the pGEM-T easy vector, they were digested with the appropriate restriction enzymes and subcloned in the $pCDNA_3HA$ vector. The HA tags constructs (Fig. 6.9) were verified by sequencing and transfected in eukaryotic cells. Taking advantage of a neomycin resistance gene present in the same plasmid used for subcloning, clones growing in neomycin were isolated and further characterised. In particular, so far two clones have been obtained in SKOV-3 ovarian cancer cells, i.e. the C2 and the C6 deletion mutants.

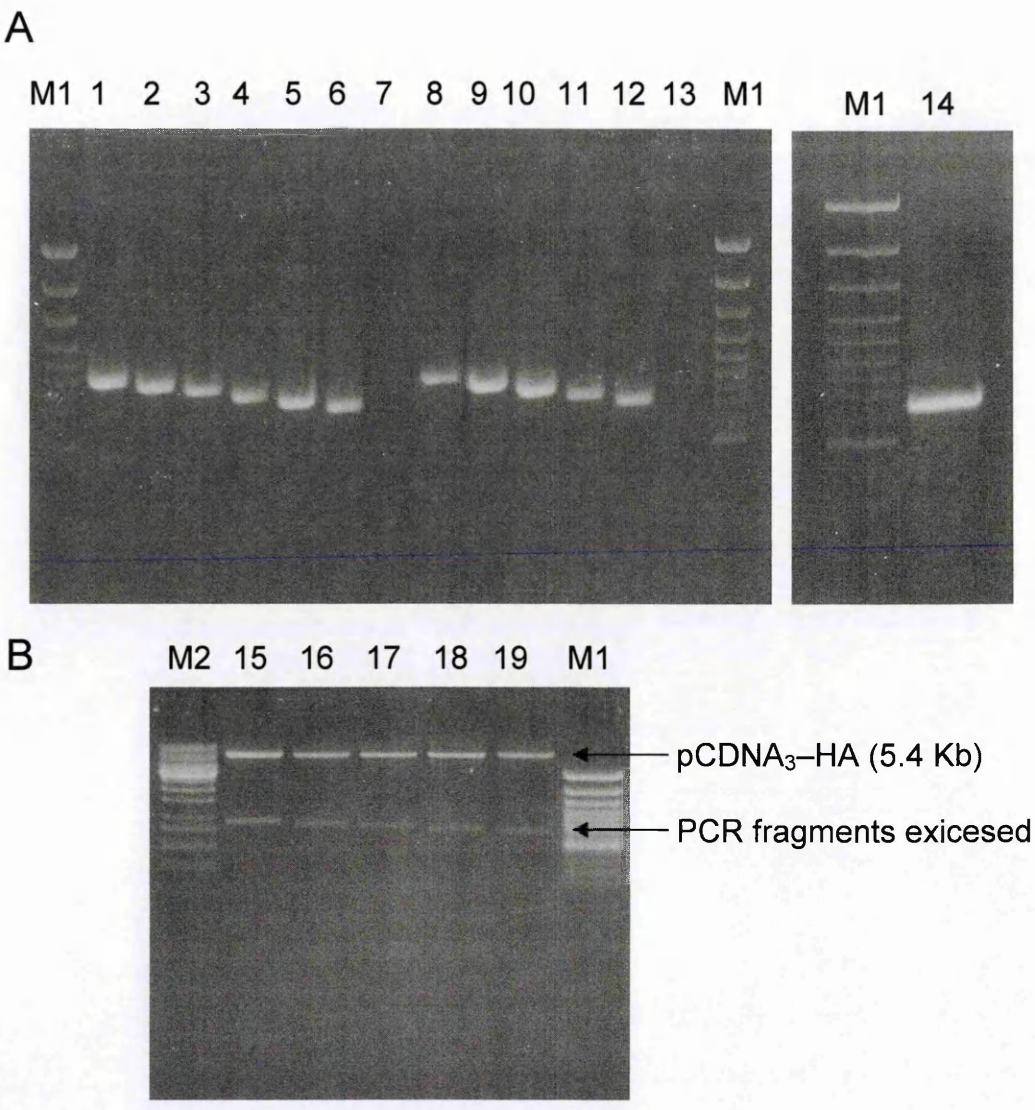

Figure 6.8

Panel A. PCR fragments corresponding to N– and C– terminal deleted cDNAs fragments of DRAGO. M1: 100–bp DNA ladder plus. Lane 1–6: N1–N6 PCR fragments, lanes 7 and 13 correspond to the blank PCR reactions (reaction without template to verify that the amplification was specific). Lanes 8–12 and 14: C1–C6 PCR fragments.

Panel B. HA constructs were verified by double restriction with *Xho*I and *Xba*I enzymes. The empty vector ($pCDNA_3HA$, 5.4 kb about) and the cDNA deleted fragments are pointed with arrows.

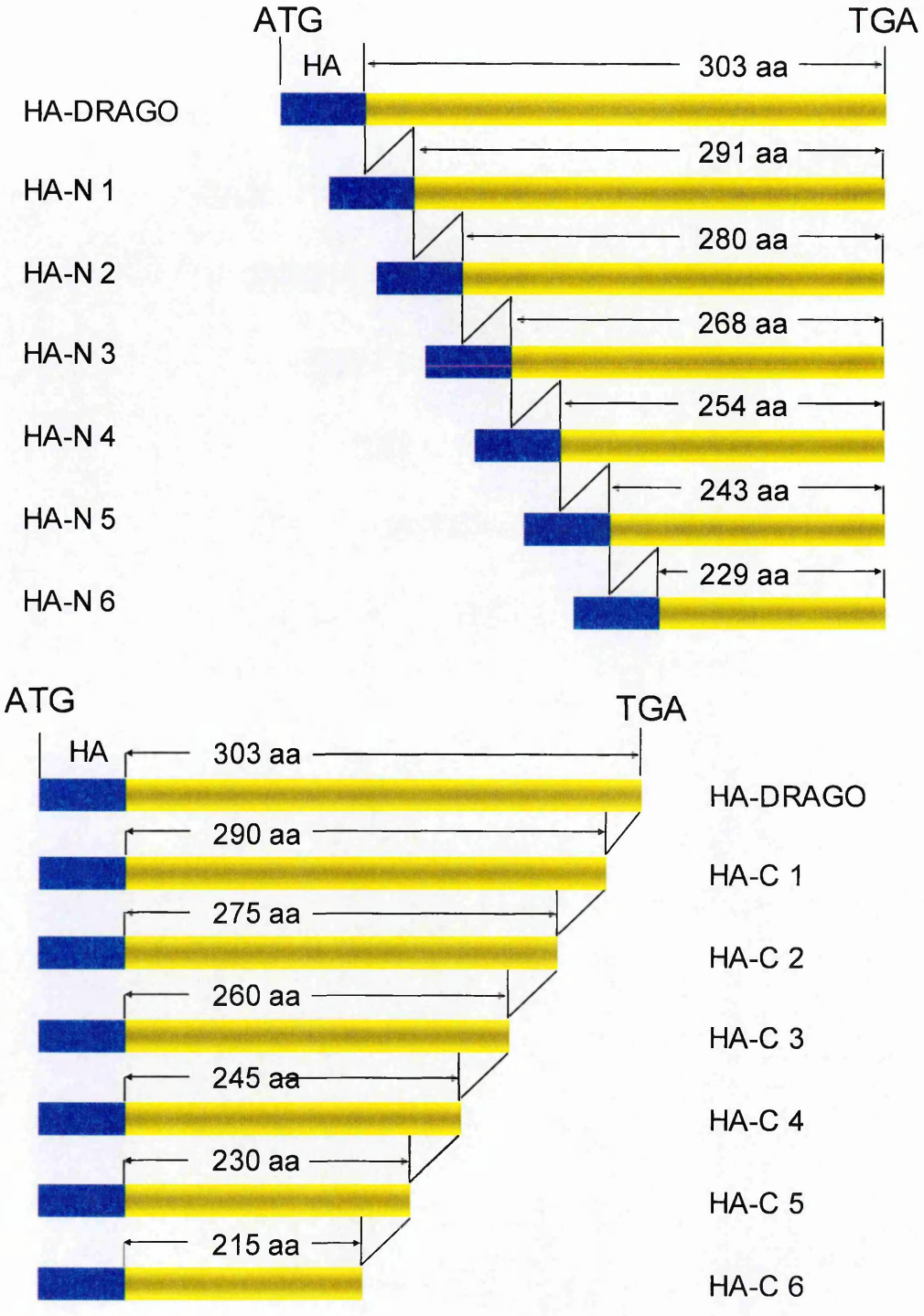

Figure 6.9

Progressive deletions at N– and C– terminus of the coding region of DRAGO generating deletion mutants which were subcloned in frame with the HA tag in the $pCDNA_3$ vector to be expressed in eukaryotic systems.

The growth of these clones were followed for different *in vitro* passages. At each passage total RNA was extracted and after several passages all the RNAs collected loaded on agarose gel, blotted and hybridised with a ^{32}P-labeled probe generated from a gene fragment (C6). The results showed that both C2 and C6 deletion mutants could be evidentiated at RNA level. After 8 passages in vitro both clones retained the expression of C2 and C6 (Fig 6.10). Among the clones able to grow in neomycin, those stably transfected with the empty vector and the pCDNA$_3$HA-DRAGO constructs were also isolated. However, as reported in the Northern blot, clones carrying the pCDNA$_3$-DRAGO construct did not express the gene at RNA level. This is consistent with the results previously discussed in the chapter 6.2, where the overexpression of the full length DRAGO prevented colony formation.

In parallel, three SKOV-3 clones transiently expressing the N-terminus deletion mutants N3, N4, N6, were investigated. The analysis was addressed to those deleted mutants selected on the basis of the results obtained when bacteria were induced to express the N-terminal deletion mutants. N3-construct transiently transfected cells expressed the deleted gene at RNA level after few passages following transfection, as confirmed by Northern blotting using the exon 3 as a probe (Fig 6.11A). However, stably expressing clones isolated for their resistance to the antibiotic neomycin did not retain any detectable expression at RNA level (Fig. 6.11B).

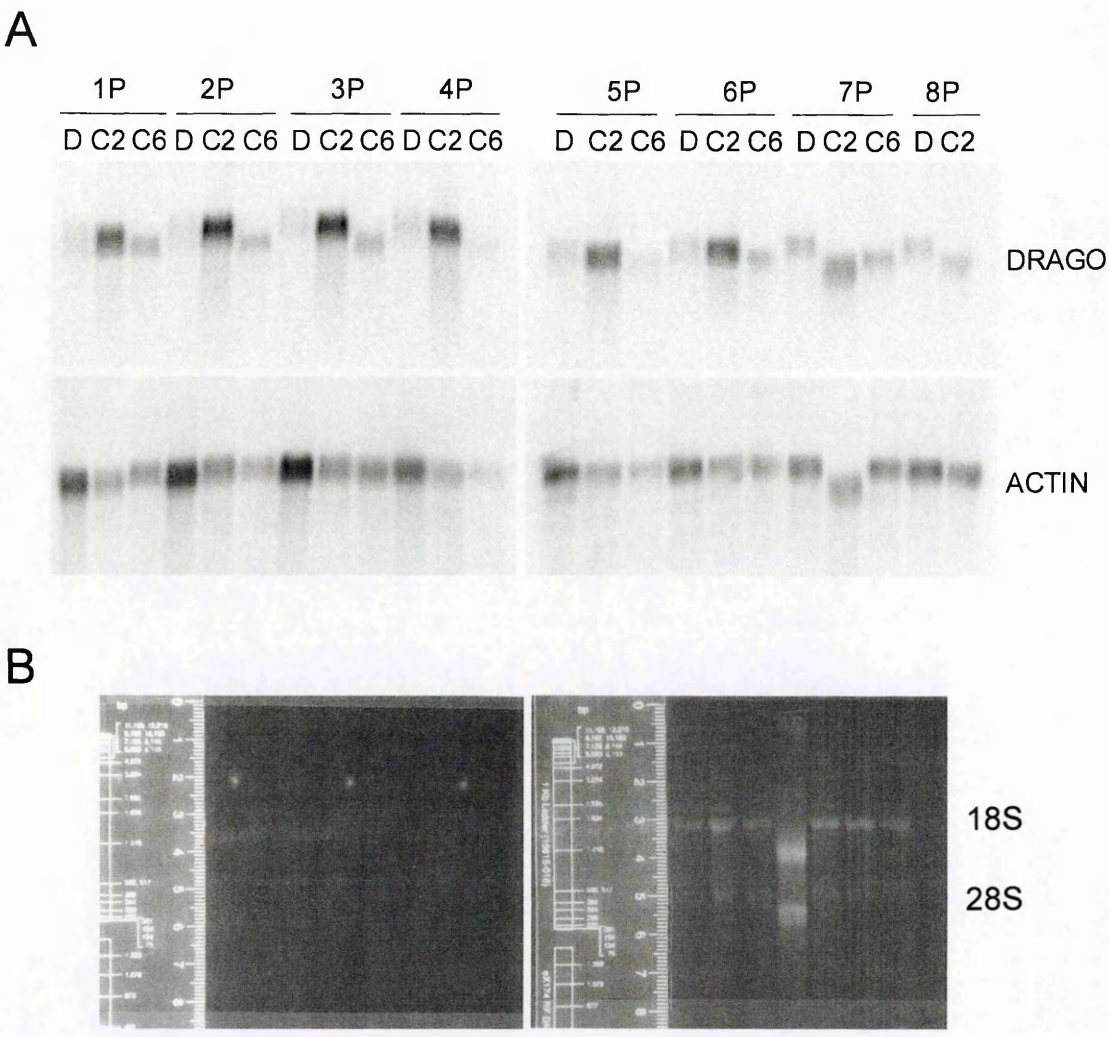

Figure 6.10

Panel A: Northern blot showing the expression of DRAGO deletion mutants in clones derived from SKOV–3 cells which were retained after 8 passages. Total RNA was extracted from C2 and C6 cellular clones and from cellular clones derived from cells transfected with $pCDNA_3HA$–DRAGO (D) which grew in the presence of neomycin. Total RNA was then separated on agarose gel (panel B) and transferred to a nylon filter. The blot was hybridised with a DRAGO cDNA probe.

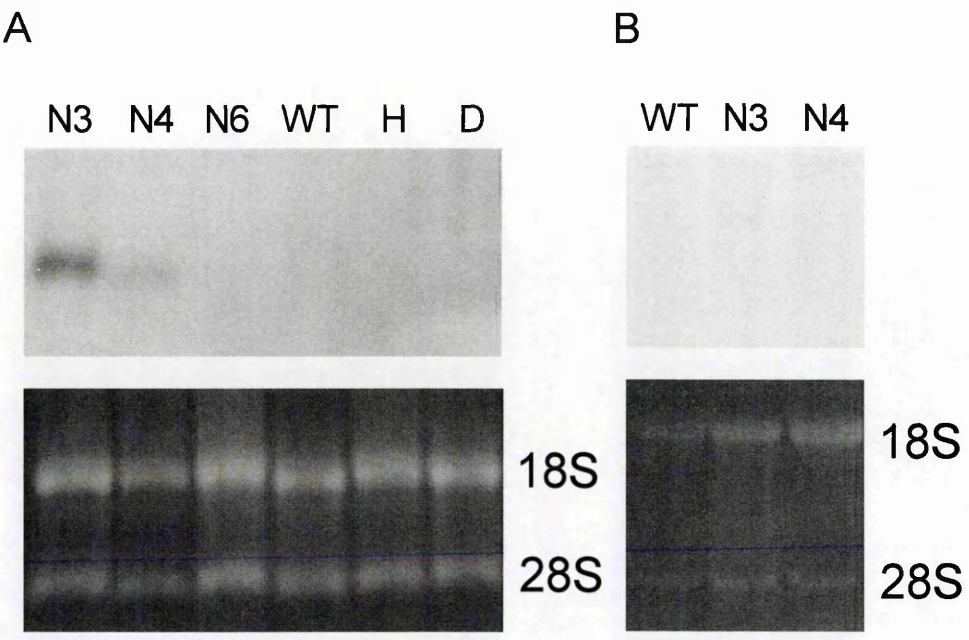

Figure 6.11

Northern blot to detect the expression of N–terminus deletion mutants (N3, N4 and N6) in either transiently (panel A) or stably (panel B) expressing SKOV–3 clones.

Panel A. Total RNA was extracted from SKOV–3 cells transiently transfected with $pCDNA_3HA$–N3 (N3), $pCDNA_3HA$–N4 (N4), $pCDNA_3HA$–N6 (N6), $pCDNA_3HA$ (H) and $pCDNA_3HA$–DRAGO (D); WT represents wild–type SKOV–3 which were not transfected. N3 and N4 cells expressed the corresponding deleted DRAGO at RNA level. Total RNA, separated on agarose gel (lower part) was transferred onto a nylon filter (upper part). Cells transfected with the vector carrying the full length coding region of DRAGO (lane D) were able to grow in the presence of the neomycin but they did not expressed the protein at the RNA level.

Panel B. Stable clones isolated from transiently expressing N3 and N4 cells did not retain the expression of the corresponding N–deleted mutants at the RNA level.

6.4.3 Activity of peptides

On the basis of the previously reported results, the removal of the last 28 aminoacids from the DRAGO protein, resulted in a truncated protein whose expression was tolerated by the cell. This suggests that the last 28 aminoacids play an important role in the DRAGO growth suppressive activity. To test whether this assumption was reasonable, a peptide corresponding to the 28 aminoacids (DSENSDIQSLLSLTSEEYTDDIPLLKEA) deleted from the C2 mutants has been synthesised. A peptide comprising the 13 aminoacids (EEYTDDIPLLKEA) deleted from the C1 mutants has been also synthesised. Eukaryotic cellular clones stably expressing the C1 mutants were not able to grow. Therefore the deletion of the last 13 aminoacids should not be able to abrogate the growth inhibitory effect that was observed when full length DRAGO is expressed. The activity of the peptides were evaluated against either p53 +/+ or p53 –/– HCT-116 cells which were treated with different concentrations of either the 13 aminoacid or the 28 aminoacid peptide. An unrelated peptide from the human endothelin has been used as a negative control. The cells were treated for 48 hours then washed and stained with crystal violet. The effect of the treatment did not reveal any particular toxic effect on cellular growth related to the tested peptide (Fig. 6.12). Increasing further the concentration of the peptide, a toxic effect was observed, which was, however, not necessarily related to the specific effect of the peptide. In fact, a similar toxic level was found when a DRAGO unrelated peptide was used at a specific concentrations (Fig.6.13).

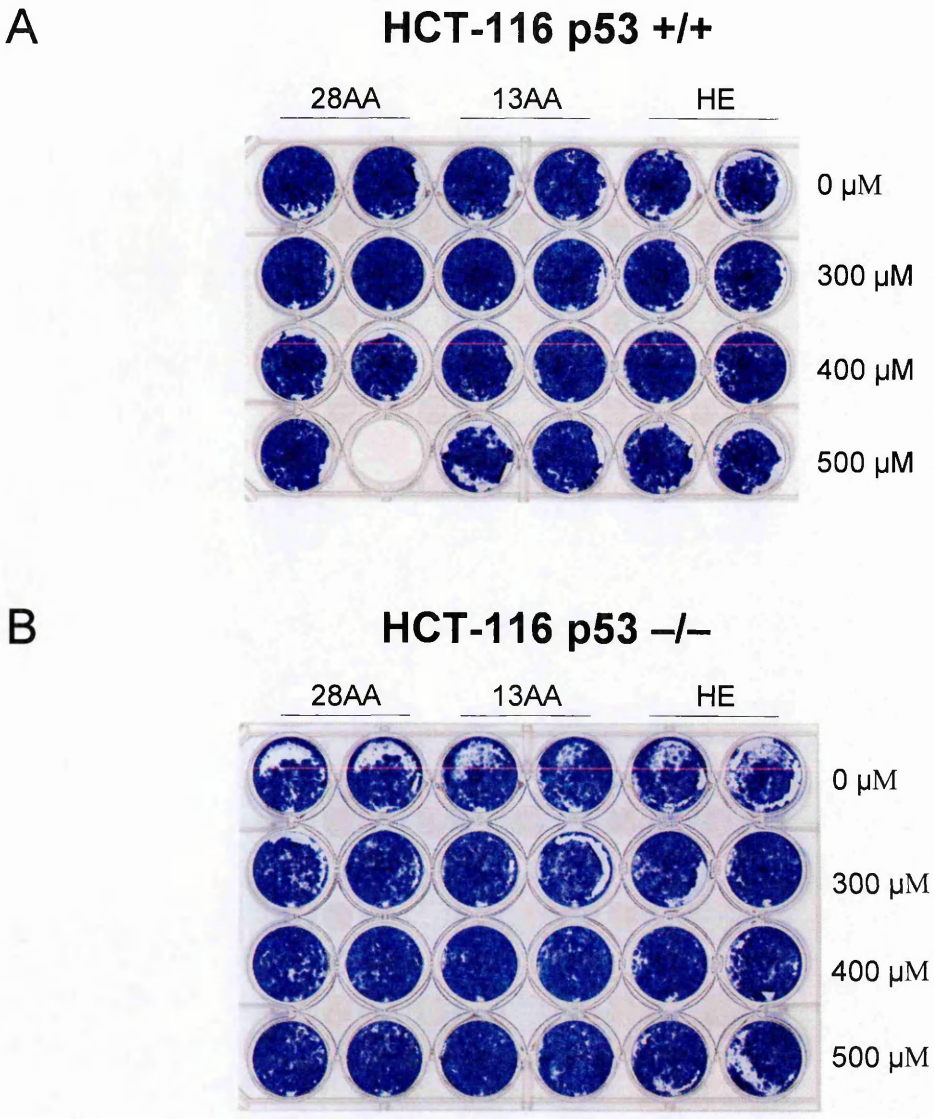

Figure 6.12

Activity of peptides HE, 13 AA and 28 AA against HCT-116 p53 (+/+) (panel A) and HCT-116 p53 (–/–) (panel B). Peptides were added to the cells 24 hours after seeding (at 60,000/ml) at different concentrations as indicated. Cells were stained with crystal violet 72 hours after treatment.

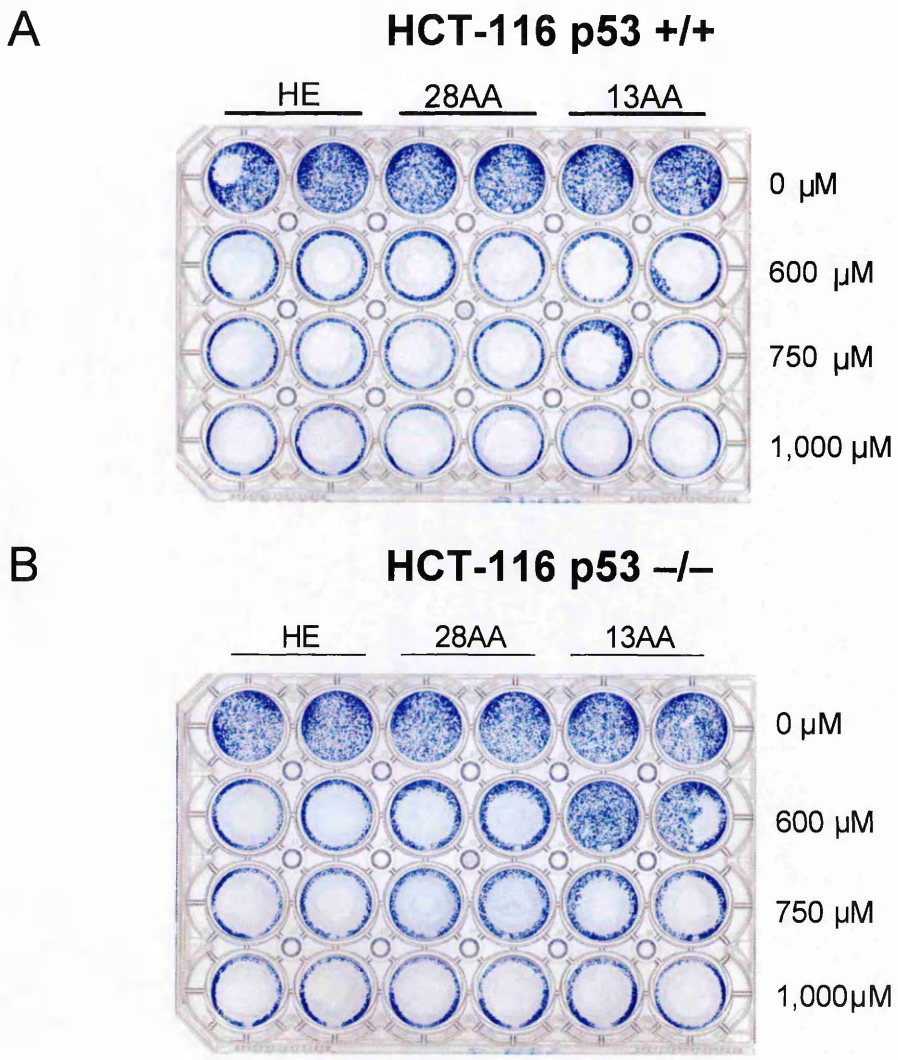

Figure 6.13

Activity of peptides HE, 13 AA and 28 AA against HCT-116 p53 (+/+) (panel A) and HCT-116 p53 (–/–) (panel B). Cells were seeded at 60,000/ml, and treated 24 hours after seeding with the indicated concentrations of peptides and stained 72 hours after treatment with crystal violet.

6.5 Discussion

The results reported in this chapter indicate that when overexpressed, DRAGO has a strong inhibitory effect on cellular growth, preventing any colony formation of stably DRAGO expressing cellular clones. For this reason any experiment aimed at assessing the morphological and biochemical modifications induced by the overexpression of the full length gene had to be carried out in transiently transfected cells. The observation of morphological modifications in contrast phase microscopy evidentiated that the overexpression of the gene caused the formation of many vacuoles in the cytosolic compartment. This morphological effect due to the overexpression of DRAGO was not associated to the activation of any extrinsic or intrinsic apoptotic pathways (see chapter 1.5.3). Nonetheless the mechanisms of death in cells expressing high level of the protein coded by DRAGO gene is discussed in this thesis being the object of still ongoing studies.

The analysis of deletion mutants has been focused to identify possible functional domains of the protein which might be responsible for the growth suppression effects. The analysis has been also extended to bacterial cells in order to purify and isolate the proteins for subsequent studies. Otherwise, any effort of purification from bacteria of the deleted proteins failed. The collected evidences suggest that the exogenous proteins might accumulate in the inclusion body probably due to their hydrophobicity. Another important observation is that bacteria expected to

produce the full length protein retained the ability to overcome the effect of the antibiotic ampicillin used for the selection of positive clones, without producing any protein. This suggests that the full length protein is toxic on cellular growth of prokaryotes as observed in eukaryotic cells. Sometimes, clones transfected with the full length DRAGO were able to grow in the presence of neomycin, but they did not retain the corresponding cDNA expression at RNA level meaning that those clones were able to "skip" the synthesis of the protein which would inhibit their growth. Taken together all the results collected with the deletion mutants expressed in eukaryotic hosts, indicate that the last 28 aminoacids were crucial for the death/grow arrest effects of the entire gene. This evidence was supported by the fact that the SKOV-3 stably expressing the C2 deleted cDNA retained the expression for several passages without any significant morphological change suggesting that the last 28 aminoacids deleted starting from the C–terminus were necessary to the inhibitory effect of the entire gene. Nevertheless, the treatment with the peptides corresponding to the aminoacids deleted in the C2 and C1 constructs did not reveal any suppressive effect on cellular growth. This observation suggests that those peptides, particularly the one with 28 aminoacids, might not have any toxicity per se, but its deletion could interfere with the conformational structure of the protein or its stability, thus compromising its activity. Alternatively, the C–terminus could be important for the interactions with other proteins.

CHAPTER 7

THE COMPUTATIONAL ANALYSIS

OF THE PROTEIN

7.1 Introduction

The aminoacid sequence of the protein coded by DRAGO gene did not resemble any protein with known function. In the following section, the computational prediction of the conformation of the protein has been reported. The theoretical analysis of the primary aminoacid sequence has been then supported by a set of experiments aimed at the determination of the subcellular localisation of the protein itself. To determine the subcellular localisation of the protein two strategies have been undertaken. First, immunofluorescence experiments have been performed on transiently expressing N3 clones, the characterisation of which has been discussed in the chapter 6.4.2. The second strategy was addressed at the use of intrinsically fluorescent protein like the GFP protein fused in frame to one of the deleted mutants which the cell tolerates when it is overexpressed. For this purpose a pEGFPC1-C2 construct has been generated.

7.2 In vitro synthesis of DRAGO protein

As mentioned in introduction chapter (see chapter 1.7), the full length cDNA of DRAGO putatively codes for a protein of 303 aminoacids. The full-length cDNA subcloned in the pBS vector has been used as a template for the in-vitro synthesis of the putative protein coded by the cDNA. A polypeptide was produced with an apparent molecular

weight, calculated by SDS-PAGE, of 25-33 kDa (Fig. 7.1). This molecular weight is consistent with the structure of the polypeptide and with the predicted molecular weight (32 kDa) calculated on the basis of the number (303) of aminoacids and the primary sequence of the protein deducible from the cDNA sequence.

7.3 Conformational prediction of DRAGO protein and computational analysis

The aminoacid sequence has been computationally analysed using bioinformatic tools available from the web in order to identify the similarity with domains of protein with known function. The submission of the primary aminoacid sequence into the CDD database (341) from the NCBI website and into others PROSITE (from the ExPASy website), InterPro, UniProt, Smart or Pfam databases reveals high similarity (about 94%) with the protein region comprised between aminoacids 40 and 104 with the complement control protein (CCP) domain, also known as short consensus repeats (SCRs) or SUSHI repeats. The CCP modules contain approximately 60 amino acid residues and have been identified in several complement and adhesion proteins. By using the TMHMM database (Fig. 7.2A), the presence of putative transmembrane domain, particularly transmembrane helixes, have been predicted to be located between the aminoacid 13 and 35 and between the aminoacids 120 and 142.

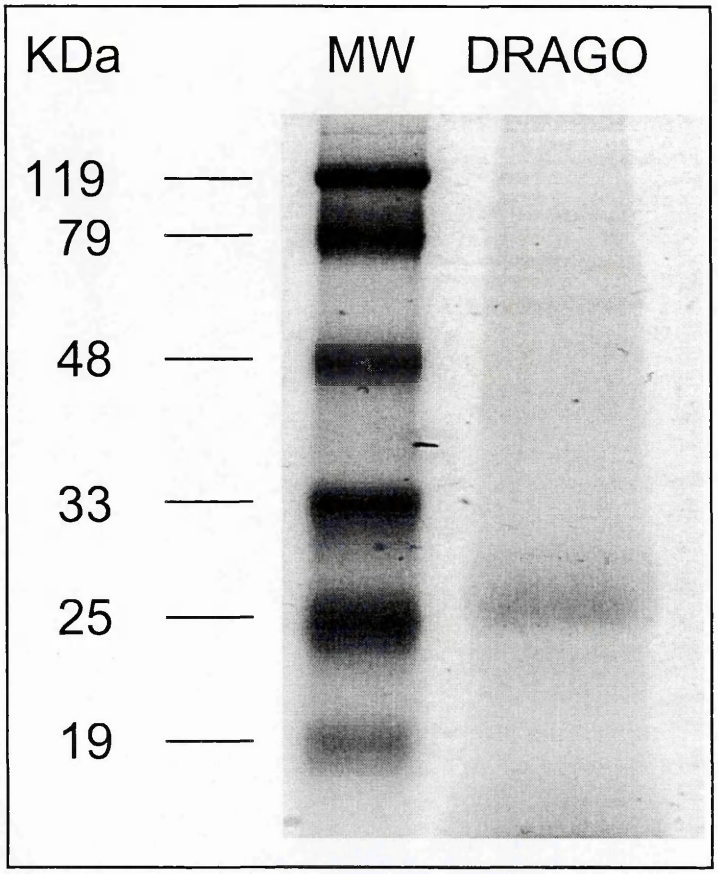

Figure 7.1

SDS–PAGE of protein product synthesised *in vitro* using DRAGO coding sequence as template, as discussed in section 2.11. The apparent molecular weight (MW) around 25–33 kDa of the polypeptide, revealed by Coomassie blue staining, is consistent with the aminoacid sequence of the DRAGO protein.

A

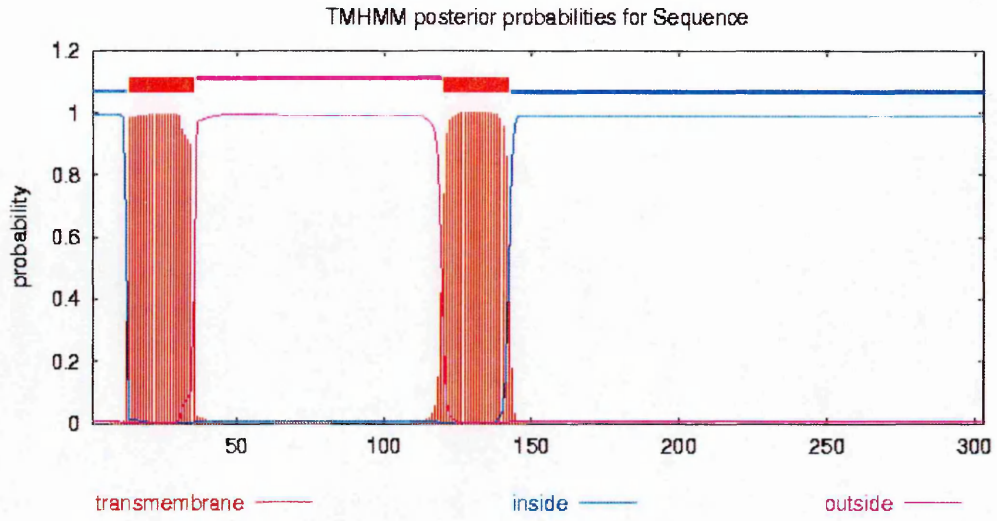

B

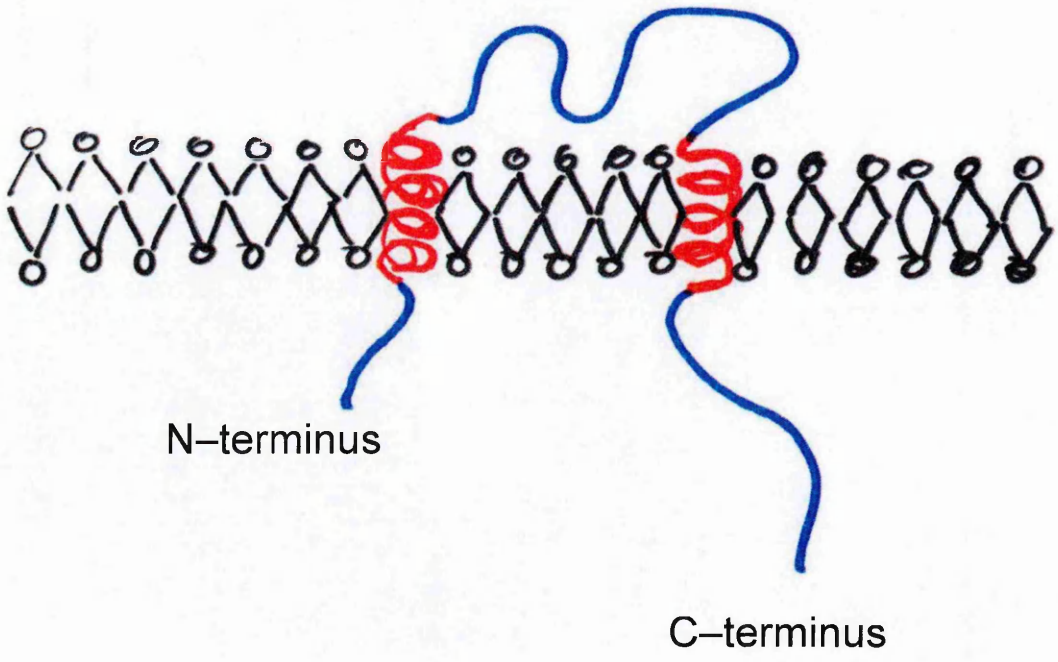

Figure 7.2

Panel A. DRAGO as a membrane–associated protein by informatics modelling. Two transmembrane domains located between the aminoacid 13 and 35 and between the aminoacids 120 and 142 were predicted by TMHMM database.

Panel B. Hypothetic conformational structure of DRAGO protein was derived by computationally prediction

On the basis of this database, the N-terminal region which comprises the aminoacids 1-12 and the C-terminus portion of the protein (aminoacids 143-303) are predicted to be located inside the cellular region that the membrane, where the protein is linked, contains. The remaining protein region (aminoacids 36-119) is predicted to stand in the outside region of the membrane. The prediction of transmembrane domains has been confirmed by other databases, such as prosite and swiss-prot/tremble. Altogether these results have led to draw a hypothetic conformational structure of the protein as shown in figure 7.2B.

7.4 Subcellular localisation of the protein

7.4.1 Immunofluorescence on the N3 clone

The experiments reported in this section were aimed at evaluating the subcellular localisation of the DRAGO protein, by using the immunofluorescence technique taking advantage of the monoclonal antibodies generated against the C–terminus peptide SB of 82 aminoacids. The expression of DRAGO full length protein resulted to be growth suppressive as widely discussed in the previous section. The experiments were performed on SKOV–3 clones transiently expressing N3–deleted DRAGO, the expression of which was characterised and verified by Northern blot (see section 6.4.2, figure 6.11). Immunofluorescence revealed an intracellular localisation of the truncated protein. The fluorescence seemed to localise in correspondence of

membrane structures, supporting the theoretical and computational prediction of the transmembrane domains of the protein. Moreover, whenever the cells were not permeabilised, the signal was absent or homogeneous: this observation suggests that at least the portion of the protein recognised by the antibody is localised intracellularly (Fig. 7.3).

7.4.2 Intracellular localisation of GFP-C2 protein

Another approach aimed at subcellularly localising the protein was to create a fusion protein intrinsically fluorescent such as the GFP. Among the deleted mutants stably expressed by the cells, the C2 is the one which has the smaller deletion, therefore the GFP-C2 fusion protein can be considered as a good tool to get information regarding the intracellular localisation of the wild–type protein with good approximation. With this purpose, the pEGFP–C1 vector which carries the GFP coding region, was used. The coding region of the C2 deletion mutant was subcloned in frame to the C–terminus of the GFP coding region. The C2 deleted was PCR amplified using the construct of pEGFP–C1–DRAGO as a template which was previously generated in the laboratory. To generate the construct, the coding sequence of DRAGO was PCR amplified using as a template the DRAGO cDNA subcloned in the pBS and primers designed to insert the sequence for the *Hind*III and *Kpn*I restriction enzymes respectively at the 5' and 3' end. Once amplified, the PCR product was inserted in the pGEM–T vector, digested with the appropriate enzymes and subcloned in the pEGFP–C1 vector.

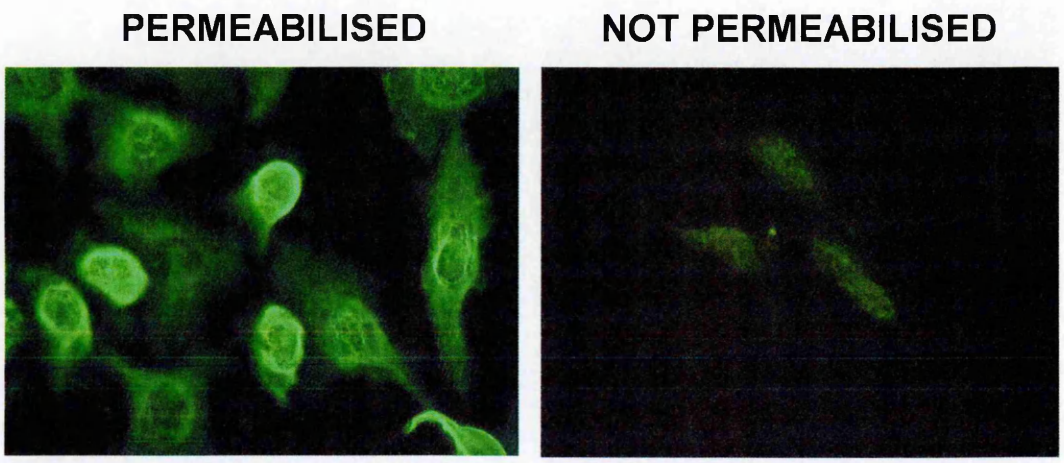

Figure 7.3

Immunofluorescence experiments on SKOV–3 clones transiently expressing the N3-deleted DRAGO. In permeabilised cells, fluorescence localised in correspondence of membrane structures; conversely, if cells were not permeabilised, the signal was absent or barely detectable.

The final construct containing the DRAGO and GFP cDNA was verified by sequencing. For PCR amplification of C2, the upstream primer was the same which had been used for the sucloning of the DRAGO coding region in the same vector. The downstream primer was the same used when the C2 deleted mutant has been generated to be subcloned in the $pCDNA_3HA$ vector and introducing a *Xba*I site at the 3' end of the amplified fragment. The PCR product was inserted in the pGEM–T vector, digested with the appropriate enzymes and subcloned in the pEGFP–C1 vector. The final construct containing the C2 deleted DRAGO and GFP cDNA was verified by sequencing. SKOV–3 cells were transfected with the construct and cellular clones resistant to neomycin were selected and checked for the stable expression of the GFP–C2 construct by Northern blot (Fig. 7.4). This clone was then investigated by fluorescence microscope, revealing and confirming the fluorescent localisation corresponding probably to membrane structures, whereas the cells transfected with the vector alone resulted to be uniformly fluorescent (Fig. 7.5).

7.5 Discussion

The protein coded by the cDNA has been confirmed to be of about 25-33 KDa as that predicted on the basis of the cDNA sequence. The aminoacid sequence of the DRAGO protein, predicted on the basis of the cDNA sequence, did not reveal any particular motif, indicative of possible cellular localisation and function.

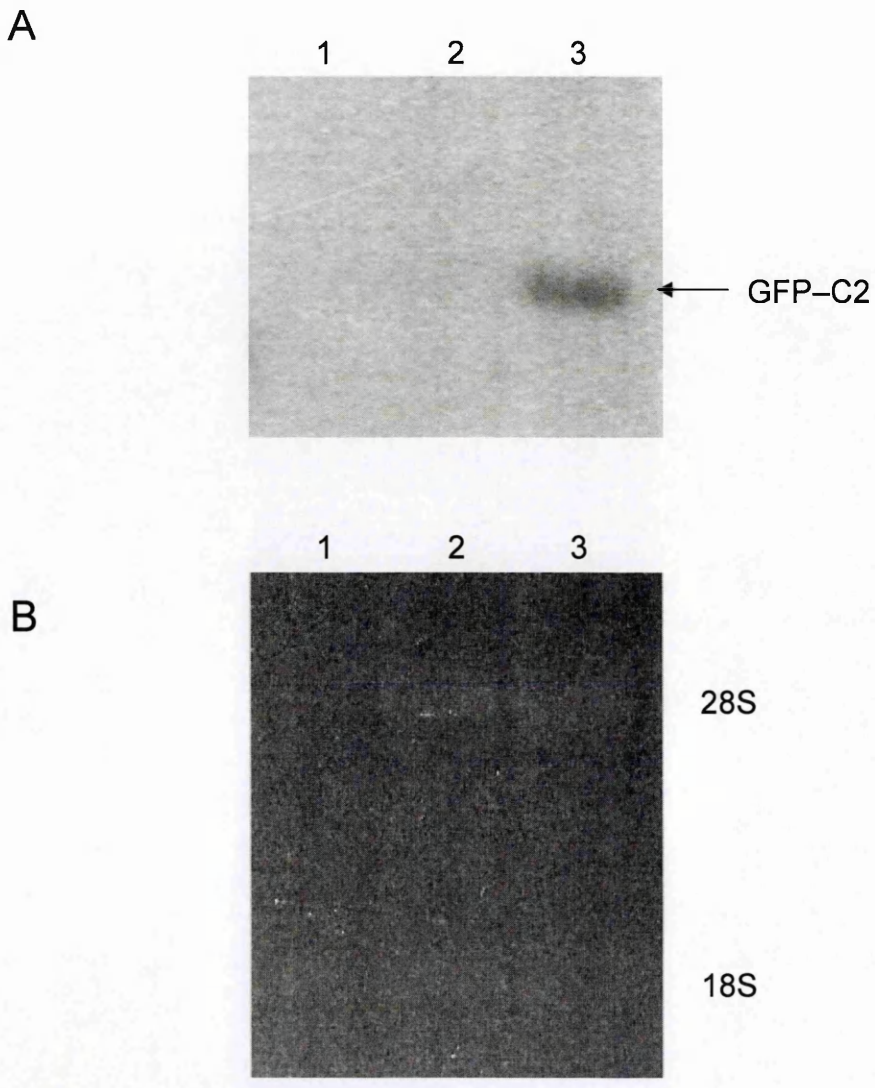

Figure 7.4

Northern Blot showing the expression of the deleted DRAGO mutants C2 (lane 3) in stably transfected SKOV–3 clones. Total RNA was extracted from cells transfected with the vector pEGFP–C1 (lane 1), with pEGFP–C1–DRAGO construct (lane 2) and from pEGFPC1–C2 clone (lane 3). Total RNA was then separated on agarose gel (panel B) and transferred to a nylon filter. The blot was hybridised with the DRAGO exon 3 probe (panel A).

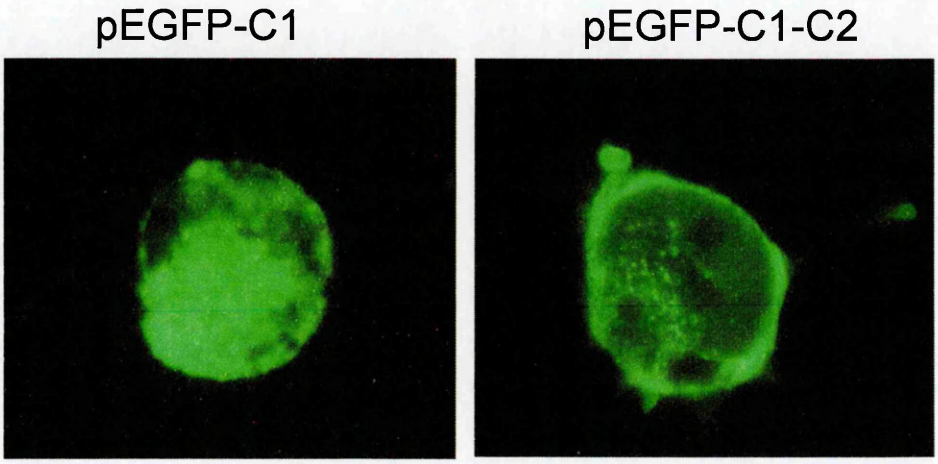

Figure 7.5

Analysis under fluorescence microscope of a SKOV-3 clone stable expressing the GFP–C2 fusion protein. The fluorescence localised in correspondence of membrane structures, whereas the cells transfected with the vector alone (pEGFP–C1, left panel) resulted to be uniformly fluorescent.

However, the bioinformatic analysis of the primary sequence, made it possible to predict that the protein coded by DRAGO gene presumably is a transmembrane protein. The theoretical prediction was then supported the immunofluorescence experiment on N3 transiently expressing clones, showing that the fluorescence seemed to be mostly localised in the membrane. With the immunofluorescence experiments the stably expressing C2 clones were not used since they lacked of the C-terminal portion against which the antibodies were generated. However, the N3 clones used in those experiments expressed the cDNA relative to the deleted mutant as confirmed by Northern blot. To support the results collected so far, the GFP-C2 stably expressing clones were analysed. With this clone the fluorescence was found to be associated to the intracellular membrane. In both cases, the localisation of deleted mutants instead of the wild–type protein was observed. This fact is linked to the strong growth inhibitory effect of the full length protein whether overexpressed by the cell. It has also to be underlined that the N3 deleted mutant which lacks of one of the two theoretical transmembrane domains, seems to retain the membrane-bound localisation.

CHAPTER 8

ANALYSIS OF THE EVOLUTIONARY CONSERVATION OF DRAGO

8.1 Introduction

In the introduction chapter (1.7.2), the isolation of the mouse cDNA coding the murine analogue of DRAGO was reported. The comparison between human and mouse sequences showed a high similarity both at nucleotide and aminoacid level. The striking percentage, more than 80%, of the homology has suggested to investigate the level of conservation of the protein and the corresponding coding region sequences among different organisms. Therefore, the aminoacid sequence of the human DRAGO protein was compared with those available from the sequence databases.

8.2 Search for sequence homology

The search for homologies between the protein sequence of DRAGO and proteins deduced by the available cDNA sequences deposited in the databases was carried out by using the BLASTP program at the NCBI databases. A significant and interestingly high similarity has been found with mammals, such as chimpanzee (*Pan troglodytes*), dog (*Canis familiaris*), mouse (*Mus musculus*), bovines (*Bos taurus*). With those mammals the identity exceeds 85%. In figure 8.1 the alignment between those mammals and DRAGO protein has been reported. In the same region, the proteins aligned were almost identical.

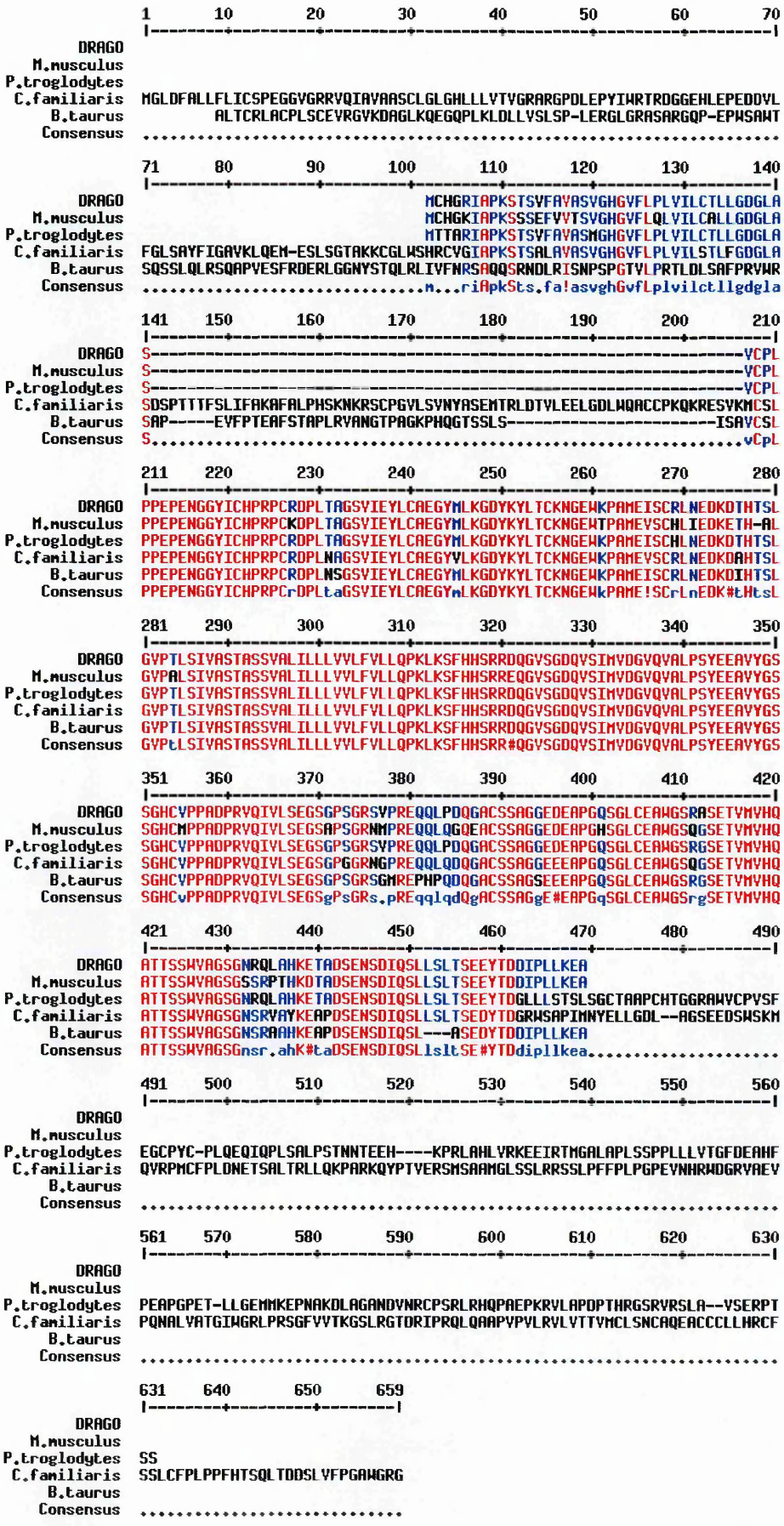
1 10 20 30 40 50 60 70
DRAGO
M.musculus
P.troglodytes
C.familiaris MGLDFALLFLICSPEGGVGRRVQIAVAASCLGLGHLLLVTVGRARGPDLEPYIWRTRDGGEHLEPEDDVL
B.taurus ALTCRLACPLSCEVRGVKDAGLKQEGQPLKLDLLVSLSP-LERGLGRASARGQP-EPWSAWT
Consensus
71 80 90 100 110 120 130 140
DRAGO MCHGRIAPKSTSVFAVASVGHGVFLPLVILCTLLGDGLA
M.musculus MCHGKIAPKSSSEFVVTSVGHGVFLQLVILCALLGDGLA
P.troglodytes MTTARIAPKSTSVFAVASMGHGVFLPLVILCTLLGDGLA
C.familiaris FGLSAYFIGAVKLQEM-ESLSGTAKKCGLWSHRCVGIAPKSTSALAVASVGHGVFLPLVILSTLFGDGLA
B.taurus SQSSLQLRSQAPVESFRDERLGGNYSTQLRLIVFNRSAQQSRNDLRISNPSPGTVLPRTLDLSAFPRVWR
Consensus .....m...riApkSts.fa!asvghGvfLplvilctllgdgla
141 150 160 170 180 190 200 210
DRAGO S---VCPL
M.musculus S---VCPL
P.troglodytes S---VCPL
C.familiaris SDSPTTTFSLIFAKAFALPHSKNKRSCPGVLSVNYASEMTRLDTVLEELGDLWQACCPKQKRESVKMCSL
B.taurus SAP-----EVFPTEAFSTAPLRVANGTPAGKPHQGTSSLS----------ISAVCSL
Consensus S.....vCpL
211 220 230 240 250 260 270 280
DRAGO PPEPENGGYICHPRPCRDPLTAGSVIEYLCAEGYMLKGDYKYLTCKNGEWKPAMEISCRLNEDKDTHTSL
M.musculus PPEPENGGYICHPRPCKDPLTAGSVIEYLCAEGYMLKGDYKYLTCKNGEWTPAMEVSCHLIEDKETH-AL
P.troglodytes PPEPENGGYICHPRPCRDPLTAGSVIEYLCAEGYMLKGDYKYLTCKNGEWKPAMEISCHLNEDKDTHTSL
C.familiaris PPEPENGGYICHPRPCRDPLNAGSVIEYLCAEGYVLKGDYKYLTCKNGEWKPAMEVSCRLNEDKDAHTSL
B.taurus PPEPENGGYICHPRPCRDPLNSGSVIEYLCAEGYMLKGDYKYLTCKNGEWKPAMEISCRLNEDKDIHTSL
Consensus PPEPENGGYICHPRPCrDPLtaGSVIEYLCAEGYmLKGDYKYLTCKNGEWkPAME!SCrLnEDK#tHtsL
281 290 300 310 320 330 340 350
DRAGO GVPTLSIVASTASSVALILLLVVLFVLLQPKLKSFHHSRRDQGVSGDQVSIMVDGVQVALPSYEEAVYGS
M.musculus GVPALSIVASTASSVALILLLVVLFVLLQPKLKSFHHSRREQGVSGDQVSIMVDGVQVALPSYEEAVYGS
P.troglodytes GVPTLSIVASTASSVALILLLVVLFVLLQPKLKSFHHSRRDQGVSGDQVSIMVDGVQVALPSYEEAVYGS
C.familiaris GVPTLSIVASTASSVALILLLVVLFVLLQPKLKSFHHSRRDQGVSGDQVSIMVDGVQVALPSYEEAVYGS
B.taurus GVPTLSIVASTASSVALILLLVVLFVLLQPKLKSFHHSRRDQGVSGDQVSIMVDGVQVALPSYEEAVYGS
Consensus GVPtLSIVASTASSVALILLLVVLFVLLQPKLKSFHHSRR#QGVSGDQVSIMVDGVQVALPSYEEAVYGS
351 360 370 380 390 400 410 420
DRAGO SGHCVPPADPRVQIVLSEGSGPSGRSVPREQQLPDQGACSSAGGEDEAPGQSGLCEAWGSRASETVMVHQ
M.musculus SGHCMPPADPRVQIVLSEGSAPSGRNMPREQQLQGQEACSSAGGEDEAPGHSGLCEAWGSQGSETVMVHQ
P.troglodytes SGHCVPPADPRVQIVLSEGSGPSGRSVPREQQLPDQGACSSAGGEDEAPGQSGLCEAWGSRGSETVMVHQ
C.familiaris SGHCVPPADPRVQIVLSEGSGPGGRNGPREQQLQDQGACSSAGGEEEAPGQSGLCEAWGSQGSETVMVHQ
B.taurus SGHCVPPADPRVQIVLSEGSGPSGRSGMREPHPQDQGACSSAGSEEEAPGQSGLCEAWGSRGSETVMVHQ
Consensus SGHCvPPADPRVQIVLSEGSgPsGRs.pREqqlqdQgACSSAGgE#EAPGqSGLCEAWGSrgSETVMVHQ
421 430 440 450 460 470 480 490
DRAGO ATTSSWVAGSGNRQLAHKETADSENSDIQSLLSLTSEEYTDDIPLLKEA
M.musculus ATTSSWVAGSGSSRPTHKDTADSENSDIQSLLSLTSEEYTDDIPLLKEA
P.troglodytes ATTSSWVAGSGNRQLAHKETADSENSDIQSLLSLTSEEYTDGLLLSTSLSGCTAAPCHTGGRAWVCPVSF
C.familiaris ATTSSWVAGSGNSRVAYKEAPDSENSDIQSLLSLTSEDYTDGRWSAPIMNYELLGDL--AGSEEDSWSKM
B.taurus ATTSSWVAGSGNSRAAHKEAPDSENSDIQSL---ASEDYTDDIPLLKEA
Consensus ATTSSWVAGSGnsr.ahK#taDSENSDIQSLlsltSE#YTDdipllkea.....
491 500 510 520 530 540 550 560
DRAGO
M.musculus
P.troglodytes EGCPYC-PLQEQIQPLSALPSTNNTEEH----KPRLAHLVRKEEIRTMGALAPLSSPPLLLVTGFDEAHF
C.familiaris QVRPMCFPLDNETSALTRLLQKPARKQYPTVERSMSAAMGLSSLRRSSLPFFPLPGPEVNHRWDGRVAEV
B.taurus
Consensus .....
561 570 580 590 600 610 620 630
DRAGO
M.musculus
P.troglodytes PEAPGPET-LLGEMMKEPNAKDLAGANDVNRCPSRLRHQPAEPKRVLAPDPTHRGSRVRSLA--VSERPT
C.familiaris PQNALVATGIWGRLPRSGFVVTKGSLRGTDRIPRQLQAAPVPVLRVLVTTVMCLSNCAQEACCCLLHRCF
B.taurus
Consensus .....
631 640 650 659
DRAGO
M.musculus
P.troglodytes SS
C.familiaris SSLCFPLPPFHTSQLTDDSLVFPGAWGRG
B.taurus
Consensus .....

Figure 8.1

Alignment between the sequence of human DRAGO protein (Homo sapiens) and those from other mammals which exhibited identity higher than 85%. Higher consensus sequences (>90% of identity) are in red colour. Low consensus sequences (>50% of identity) are in blue.

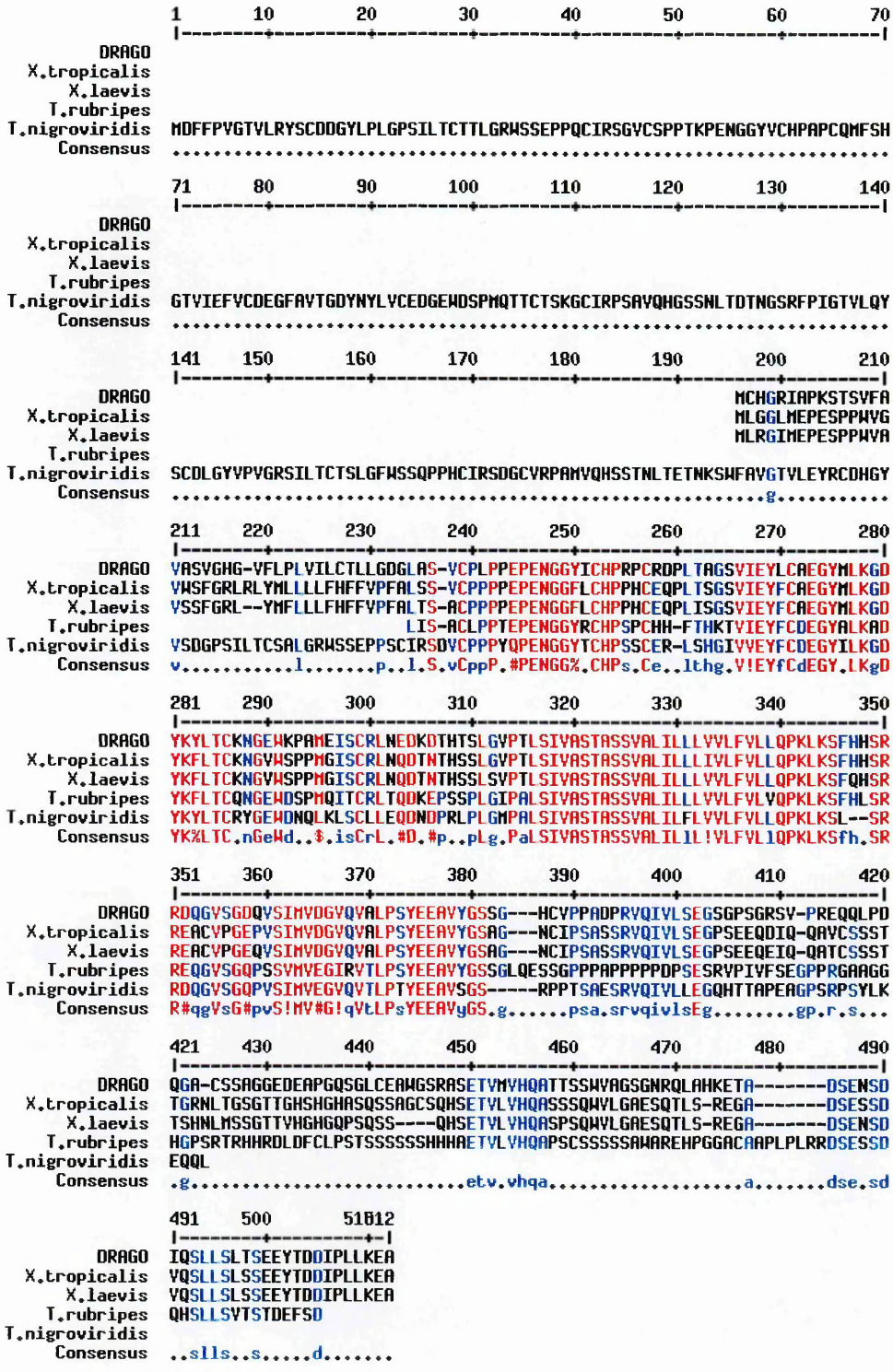

Figure 8.2

Alignment between the sequence of human DRAGO protein (Homo sapiens) and those from vertebrates (zebrafish, puffer and Xenopus). Identity higher than 90% (high consensus)s are indicated in red colour. Low consensus (identity higher than 50%) are in blue.

Similarities has also been found with other mammals such as rats (*Rattus norvegicus*), macaque (*Macaca fascicularis*) orangutan (*Pongo pygmaeus*). Similarities currently extended to all vertebrates for which genomic data is available. Significant similarities, higher than 70% have been found with cocks (*Gallus gallus*) and more than 50% with zebrafish (*Danio rerio*) and *Xenopus leavis.* Similarities have also to be underlined with puffer (*Takifugus rubripes*, *Tetraodon nigroviridis*). In figure 8.2 the alignment with these vertebrates (except for the *Gallus gallus*) is reported showing some identities between the sequences.

8.3 Discussion

In this short section, the attention has been focused on the striking high similarities that DRAGO protein shares with gene products from genomes of mammals. Surprisingly, high levels of similarities have also been found with vertebrates such as cocks and fishes. The similarities found between the human DRAGO protein with proteins of phylogenetically distant organisms revealed an evolutionary conservation of the gene which could suggest an important functional role of the gene. Furthemore, due to the difficulties in generating cellular systems expressing DRAGO, the finding that simple organisms such as zebrafish share significant homologies with humans for DRAGO certainly provide an alternative for investigating the function of DRAGO protein.

CHAPTER 9

GENERATION AND CHARACTERISATION OF DRAGO KO MICE

9.1 Introduction

As mentioned in the Introduction chapter, DRAGO expression is induced upon cytotoxic treatments. In order to investigate the role of DRAGO in determining the response to treatment, and the function of the gene product coding by DRAGO, one of the selected strategy was the development of cellular model systems lacking the gene, which could be morphologically and biologically compared with the isogenic counterparts expressing the wild–type protein. For this purposes, the development of a DRAGO-null mouse line have been conducted in collaboration with Genoway (Lyone–France) in the laboratory directed by Sandrine Millet. The generation of the KO mice lacking DRAGO gene was not carried out by eliminating the ATG site which avoids the risk of expression of truncated form of the protein. The strategy pursued for the generation of the KO mouse line was to delete most of the coding region comprised in exon 3, 4 and 5, to avoid the risk of alternative splicing. This is consistent with two previously reported observations. The first is based on the assumption that the murine gene structure is similar to the human which is supported by the high similarity of the mouse DRAGO cDNA with the human at a nucleotide and aminoacid level. Therefore, consequently to this assumption, it is highly probable the presence of two long introns between the first and second exons and between the second and third exons, containing cryptic ATG which could give rise to isoforms of the protein by alternative splicing. A mouse genomic region comprising most

of the coding region of DRAGO was therefore isolated from a mouse genomic library for the targeting vector construction. Once the KO mice have been generated the MEF cell coltures have been isolated and characterised.

9.2 Isolation of mouse DRAGO genomic sequence

Analogously to human genomic PAC clone, to isolate the genomic clones comprising DRAGO gene from mouse genome, a mouse genomic PAC library spotted in duplicate in seven different filters, obtained through the UK-HGMP-RC was used. These filters contain genomic DNA clones and can be hybridised with different probes derived from the mouse DRAGO cDNA to isolate the genomic sequence of interest.

For the purpose of this study, considering the high similarity between the human and the mouse cDNA, a fragment of the human cDNA, corresponding to the C-terminus deleted cDNA C6 (see chapter 6.4.2) has been used in order to allow the isolation of a genomic region which is likely to contain most of the entire cDNA sequence. On the whole set of seven filters (see figure 9.1 as an example), the use of this cDNA probe led to the identification of four positive clones which, once univocally identified through the coordinates of the filters have been requested to the UK-HGMP-RC. The four positive clones (458-D3, 394-M24, 577-C4, 662-F21) thus obtained were grown in LB media and the DNA was isolated from the overnight culture using the procedures described in the Materials and

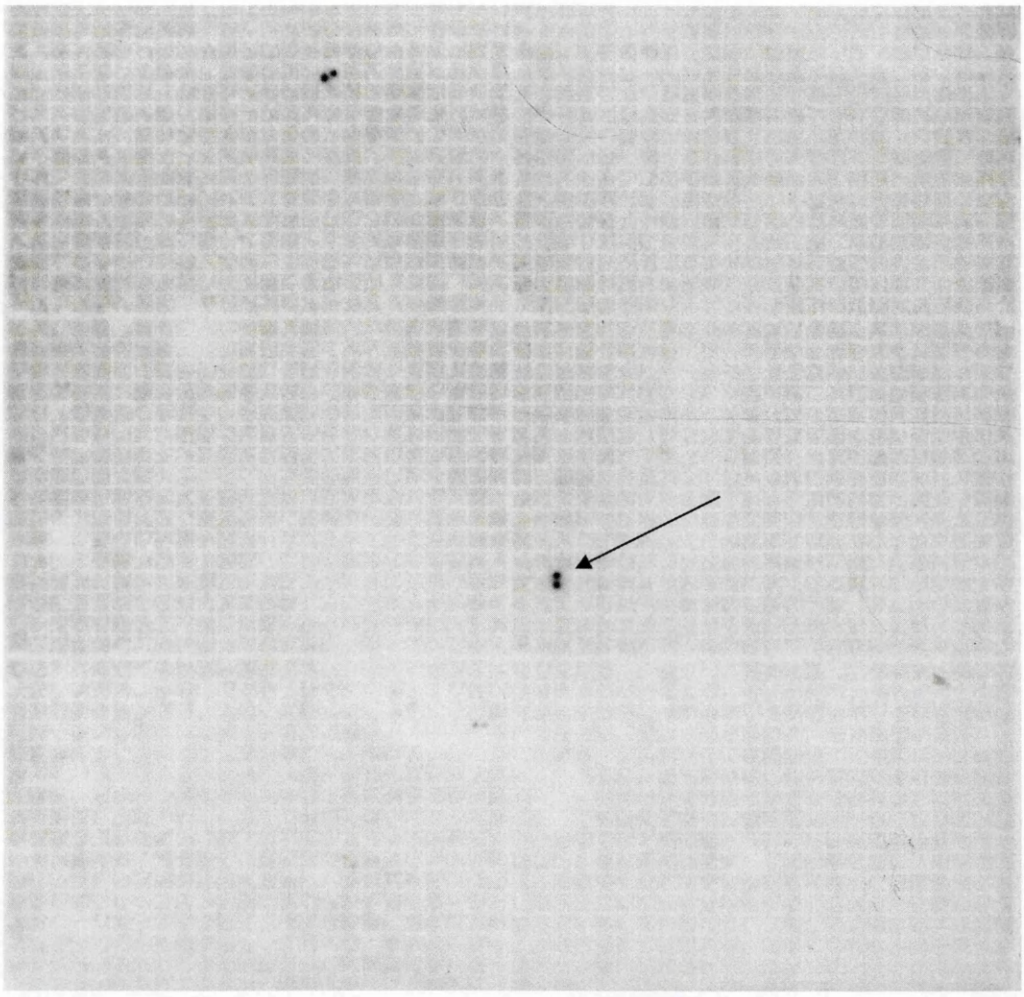

Figure 9.1

Screening of the RPCI mouse genomic PAC library 21.

The figure shows a representative autoradiography obtained from a filter containing the genomic DNA that was probed with a ^{32}P–labelled human DRAGO cDNA C6 fragment. Each clone is spotted in double on the filter. The arrow points the DRAGO positive clone (458–D3) which has been selected based on this screening.

Methods chapter (chapter 2.8). The isolated DNA was then digested with *BamH*I, *EcoR*I and *Hind*III restriction enzymes and half of it loaded on 0.8% agarose gels to separate the fragments of different length. Figure 9.2A, shows fragments of the most representative clone (458-D3) digested with the restriction enzymes. The gel was blotted overnight to nylon filter and hybridised with 3 probes corresponding to the human exon 1, human exon 3 and human exon 5 to identify the restriction fragments of the genomic sequence which presumably contained exon 3, 4 and 5. The results of the hybridisation are shown in figure 9.2B, from which one can deduce that few digested fragments gave positive hybridisation and hence contained the sequence of DRAGO used to hybridise. From these experiments a DNA fragment of approximately 20-23 Kb obtained from clone 458-D3 after digestion with *EcoR*I, which seemed to give positive hybridisation with both exon 3 and 5, was isolated for further characterisation. This DNA fragment was in fact subcloned in the *EcoR*I site contained in the multiple cloning site of the pBS plasmid. The DNA inserted was then sequenced using the primer T7, the sequence of which was upstream the multiple cloning site contained in the plasmid. The obtained sequence (of 696 bp–figure 9.3A) was aligned and matched with the mouse genomic sequences present in the NCBI gene bank database. A complete overlap was found with a genomic sequence located upstream to and partially overlap the exon 3 of DRAGO cDNA sequence (Fig. 9.3B). The mouse PAC fragment isolated presumably contained exon 3, 4 and 5. Therefore the further 10 kb starting from the T7 primer of the 20-23 kb

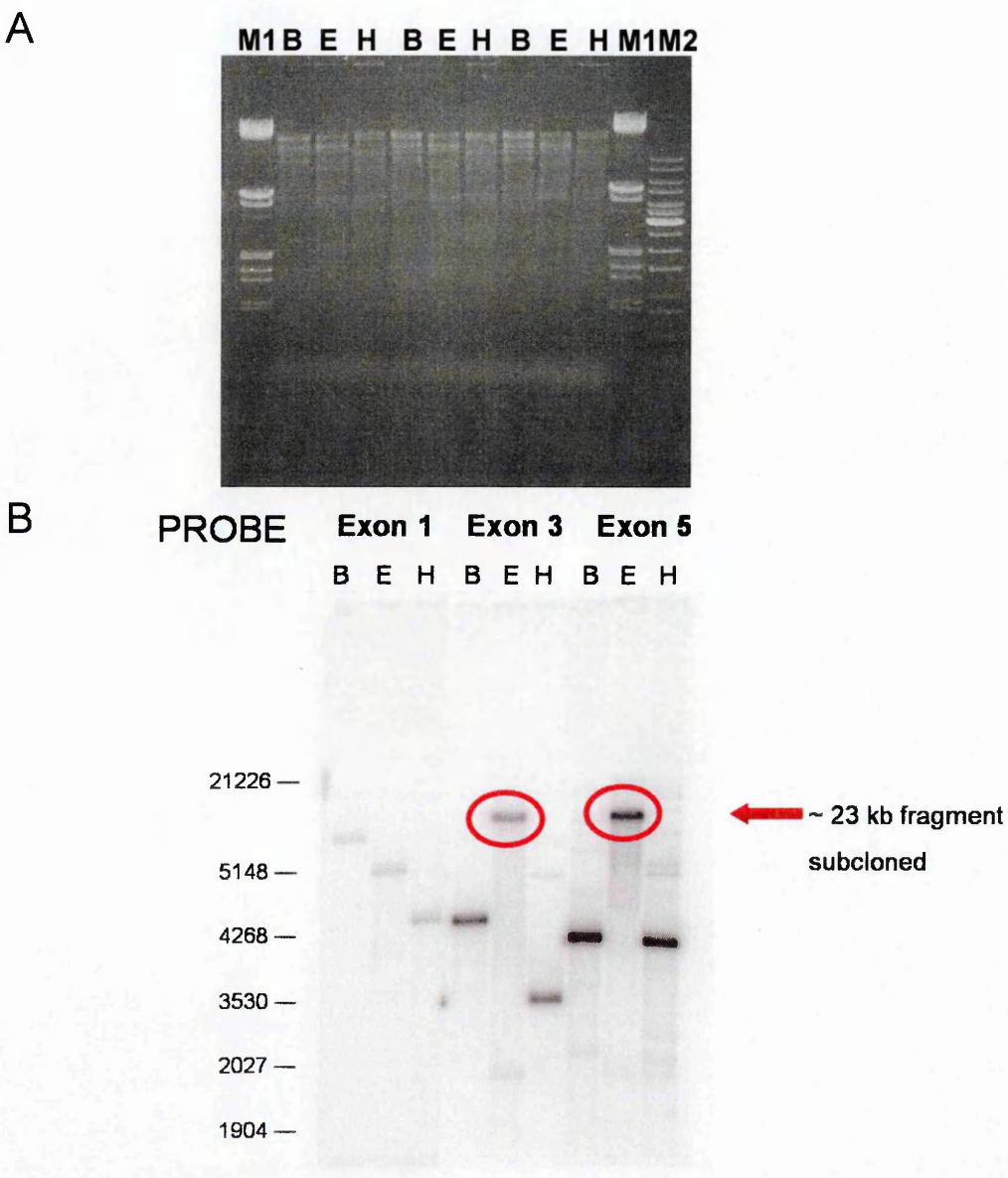

Figure 9.2

Southern Blot from the genomic 458–D3 clone from the RPCI mouse PAC library 21. Panel A. Ethidium bromide staining of the gel. DNA isolated from the clone was digested with *BamH*I (B) *EcoR*I (E) and *Hind*III (H), resolved on agarose gel. M1 is the λ DNA/*Hind*III marker 2, M2 is the 1 Kb DNA molecular weight marker. Panel B. Autoradiography of the gel transferred to a nylon membrane and hybridized with ^{32}P–labelled DRAGO probes containing exons 1, 3 and 5 probes. Numbers on the left are derived from M1 molecular weight markers. The arrow point to the 23–Kb fragment of the DRAGO clone digested with *EcoR*I isolated for further study.

A

>PAC Fragment/pBluescript-T7

GAACGTTCGCGGCNCCCNTNACACNTGCACGGNNTCCANAAGCTNGATATCNAATTCNACACTA
NTTCAGTANGCTTTCCCAANGACGGGTNTATGTCCCTTTGTGANNTGGGGCCNTGCTACTAAGA
CAAGATACCCATTTGAAAGTCTNATTGTAGTACCATCTCCCTCTGTCTTTGCAGTGTGTCCTCT
GCCCCCAGAGCCAGAGAATGGTGGCTACATTTGCCACCCCCGGCCTTGTAAAGACCCCTTGACA
GCAGGCAGTGTCATCGAGTACCTGTGTGCAGAAGGCTACATGTTGAAGGGTGACTACAAATACC
TGACCTGCAAAAATGGCGAGTGGACGCCAGCCATGGAGGTTAGCTGTCATCTCATTGAAGGTCA
GTCTGCAGATAAAAACGGGTGCTGCCTGGGTTCTGCTTTTTCCCTGGCTCCTGGGGAGTAGCAC
ATGCTTTCTCGAGAGCTCTCTTAGGCTGTGTTAAAAGCCATTTGGCCTCTCAGCCTCTGTGGTA
ATTCCATGTCTTGTGGAAGTCCTTGGGTTTGCTGGCGCATGCCATGTTGCATTTACTCTGAACC
ATTGAGGGGCTCTGTTTCTTTATTGANGCATCTGCTTGACTGTGTAAAACTCCTCTGAGGCAAG
GATTTCTGTTTGACTAATCANGTGCTGATACCCCTTAAGCTNGGCTTCTGCTACCG

B

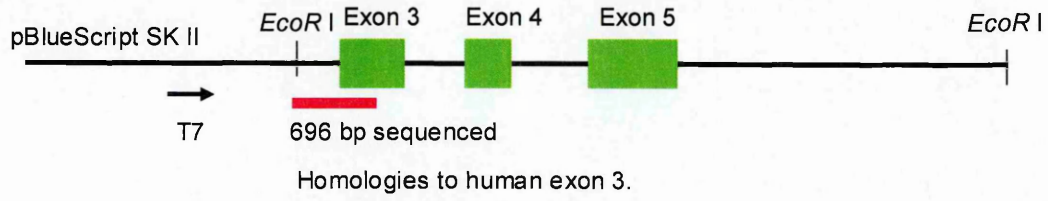

Homologies to human exon 3.

Figure 9.3

Partial sequence of the 23–Kb *EcoR*I fragment isolated from the 458–D3 mouse genomic clone and subcloned in the *EcoR*I site of pBluescript SK II vector. The sequence, obtained using the T7 primer of the plasmid (panel A), partially overlap the exon 3 of DRAGO cDNA sequence as schematically depicted in panel B. Starting from the T7 primer the further 10 Kb of the 23–Kb *EcoR*I fragment were sequenced, revealing to comprise exons 3–5 and to share high level of homology with human exons sequences.

*EcoR*I fragment were sequenced. By sequence alignment, a high level homology to human exons 3, 4 and 5 sequences within the *EcoR*I fragment was found, consistently with previously observation. But the interesting thing was that even the intronic regions were very close between the two species.

9.3 Targeting vector construction

For the construction of the targeting vector for the replacement of the region comprising exon 3 to 5, the first step was the construction of the Neo cassette for selection of the further positive events of recombination. This was performed by inserting the FRT linker at the 3' of the NEO gene and consequently the loxP-FRT linker upstream the NEO-FRT. The loxP and FRT are sites for specific recombinases. The second step was the insertion of the selection cassette in the intronic region upstream the region to delete, that is the intron 2. For this purpose the DNA from mouse PAC genomic clone 458-D3 was digested by several restriction enzymes (*BamH*I, *EcoR*I, *Hind*III, *Kpn*I, *Pst*I, *Sca*I, *Spe*I, *Xba*I and *Xho*I). After Southern blot analysis using the exon 3 probe (Fig. 9.4A), a smaller 2 Kb *Pst*I fragment has been subcloned in pZErO-2 (invitrogen) vector and sequenced, revealing to contain mostly the intronic region upstream the exon 3. The selection cassette was therefore inserted in the unique *Mfe*I site present in intron 2 of the *Pst*I fragment (Fig. 9.4B). The second step was aimed at the insertion of the second LoxP site for specific recombinase in the long homology arm, downstream to the exon 5.

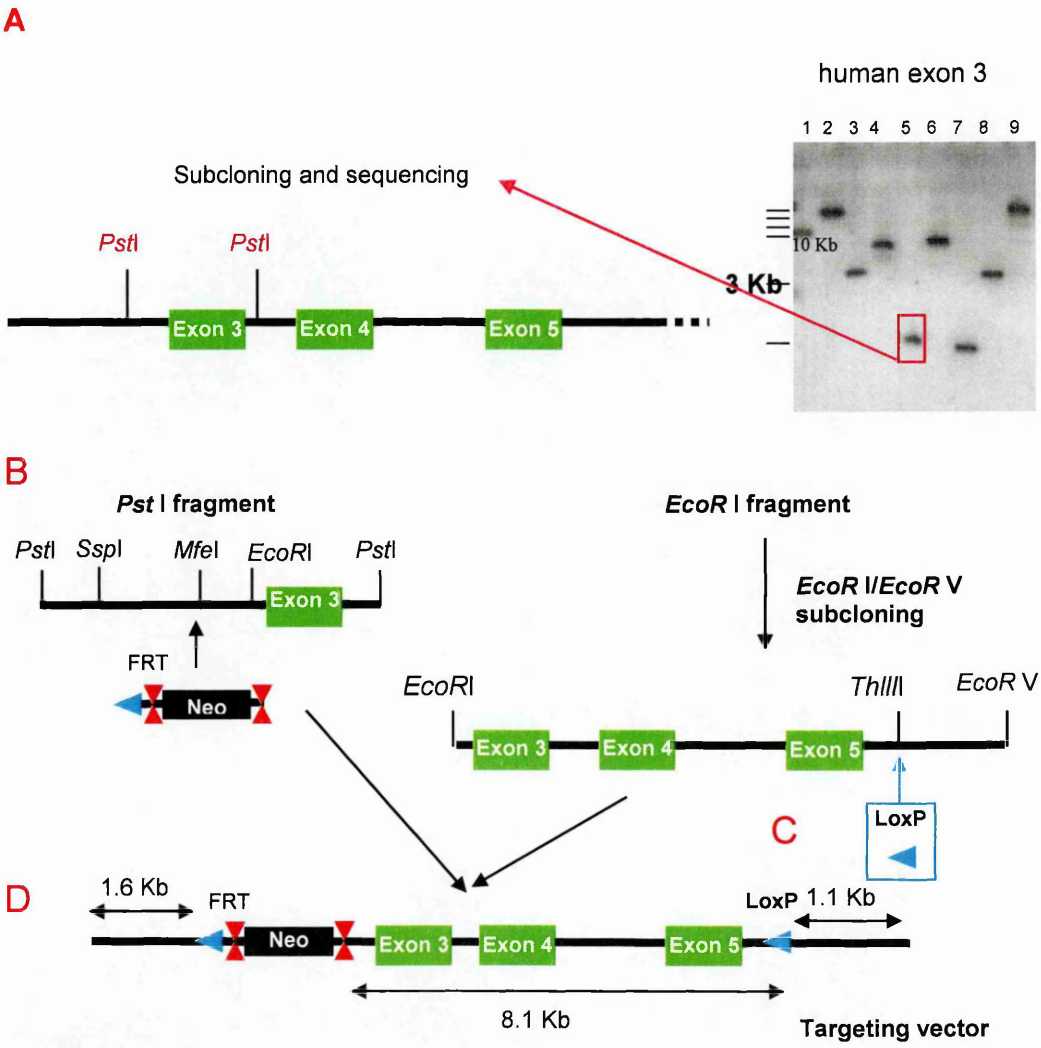

Figure 9.4

Targeting vector construction.

Panel A. Southern blot analysis of the mouse PAC genomic clone 458–D3. DNA extracted from the clone was digested with *BamH*I (lane 1), *EcoR* I (lane 2), *Hind* III (lane 3), *Kpn* I (lane 4), *Pst* I (lane 5), *Sac* I (lane 6), *Spe* I (lane 7), *Xba* I (lane 8) and *Xho* I (lane 9), separated on agarose gel, blotted onto a nylon filter and hybridised with human DRAGO exon 3 fragment. A 2 Kb *Pst* I fragment was isolated and subcloned in pZErO–2 vector. Panel B. the selection cassette was inserted in the unique *Mfe*I site upstream of exon 3 in the *Pst* I fragment. Panel C. the loxP site was inserted in the *ThIII* I site downstream the exon 5. Panel D. the selection cassette was excised from the *Pst*I fragment by *EcoR*I/*Ssp*I digestion and ligated to the *EcoR*I/*EcoR*V fragment to get the targeting vector.

Two loxP sites, oriented in same sense for efficient Cre excision, were inserted in the *Tth111*I site, downstream the exon 5 (Fig. 9.4C). The final construct was confirmed by sequencing.

The final step was the extraction of the selection cassette from the *Pst*I fragment in which it was subcloned by *EcoR*I/*Ssp*I digestion and ligated to the *EcoR*I/*EcoR*V fragment containing the other loxP site. The right orientation of the constructs were checked by DNA sequencing. The resulting targeting vector is represented in figure 9.4D.

9.4 Generation of KO mice

ES cells were then electroporeted with the final construct and positive clones selected were screened for homologous recombination event by PCR and Southern blot. Positive ES cell clones were electroporeted with a Cre-expressing plasmid to carry out an in vitro Cre-mediated deletion of the targeted region. Positive Cre-excision events specifically at the targeted locus were then screened by PCR and Southern blot. This in-vitro Cre-mediated deletion of the targeted region in ES cell clones transiently expressing the Cre recombinase could isolate only one clone which underwent to a complete Cre-mediated excision. This clone was then injected into 42 C57BL/6 blastocysts and reimplanted into 3 CD1 pseudo-pregnant females giving 1 male chimera at 100% and 1 male chimera at 90% chimerism among 12 pups. Those male chimeras were then crossed with 2 wild–type C57BL/6 females each, giving rise to two heterozygous female carrying the floxed allele (with the recombinase specific sites).

These females were bred with a male mouse expressing ubiquitously CRE recombinase under control of CMV promoter. Similarly the male 100% chimera was crossed with 2 female mice expressing ubiquitously CRE recombinase under control of CMV promoter. The F1 generation resulted to be partially Cre-excised DRAGO animals. Among them, the animals with 100% of Cre-mediated excision event were bred with Cre-expressing mice. The second breeding (F2) gave rise to HE DRAGO KO animals, showing a 100% of Cre-mediated deletion of DRAGO targeted region. These were crossed (F3) to generate KO mice. F3 animals were genotyped by PCR and Southern Blotting. Representative results of the screening are shown in figure 9.5.

9.5 DRAGO-null mice status

Homozygously deleted mice are viable and fertile. The male/female ratio is in the expected proportion from breeding of HE mice. Macroscopically they do not present alterations. As an indication of the healthy status of the homozygous (HO) KO mice their weight has been measured and compared to that of WT or HE KO mice and shown in figure 9.6.

9.6 Isolation of MEF and growth rate characterisation

Embryo fibroblast cultures were prepared from 12-15 day embryos derived from either DRAGO HO KO crosses or WT mice crosses. Nine hundred thousand cells were plated in T75 culture flasks and were passaged at

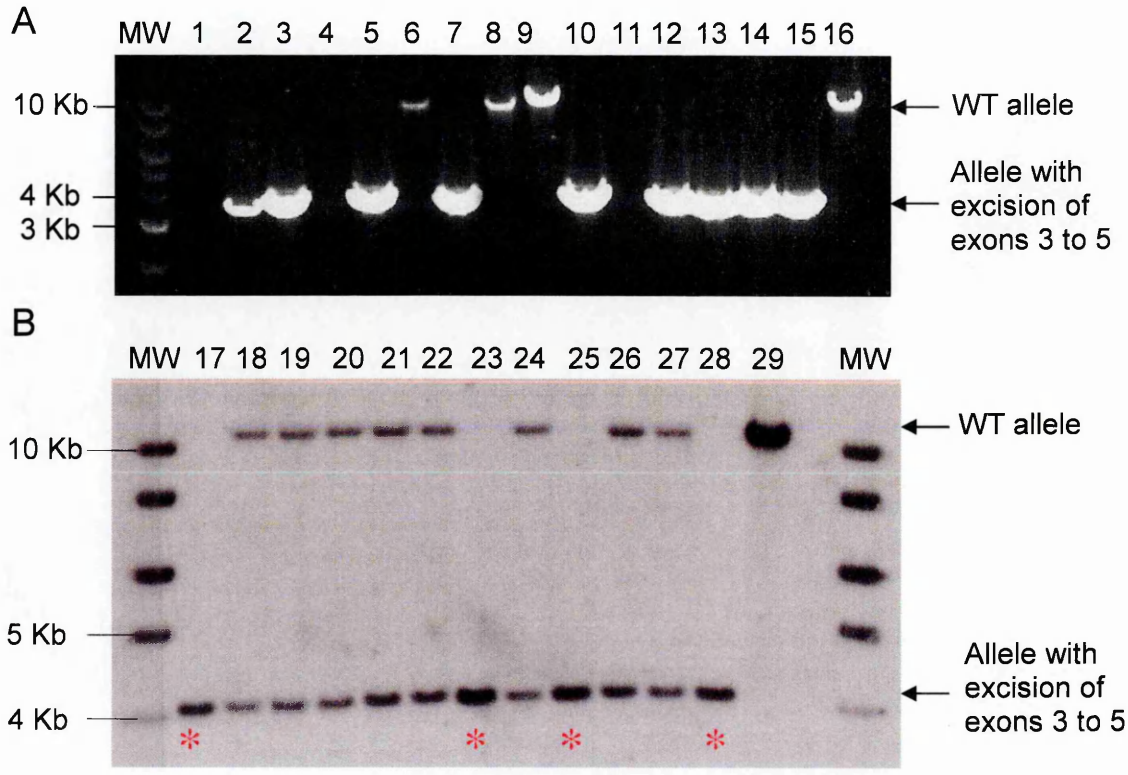

Figure 9.5.

Panel A. Screening by PCR of the animals generated by HE breeding (F3), using GW722/GW723 primers, to identify the allele with the Cre–mediated excision of DRAGO exon 3 to 5. The band 10–Kb corresponding to the wt allele is often absent due to the competition of the more efficient amplification of the 3.6 Kb band. Results obtained are illustrated for 14 animals (lanes 2 to 15). Lanes 1 and 16 are the negative and the positive (wt DNA) controls respectively. The HE versus HO genotyping were obtained by Southern Blotting (Panel B). The genomic DNA digested by *EcoN*I was hybridised with a 3' probe designed by Genoway, in order to screen the wt allele (10.4 Kb band) and the allele with the excision of DRAGO exons 3 to 5 (4.1 K band). Results obtained are illustrated for 12 only animals (lanes 17 to 18). Lane 29 is the wt DNA. MW is the molecular weight. Representative HO animals are highlighted by an asterisk.

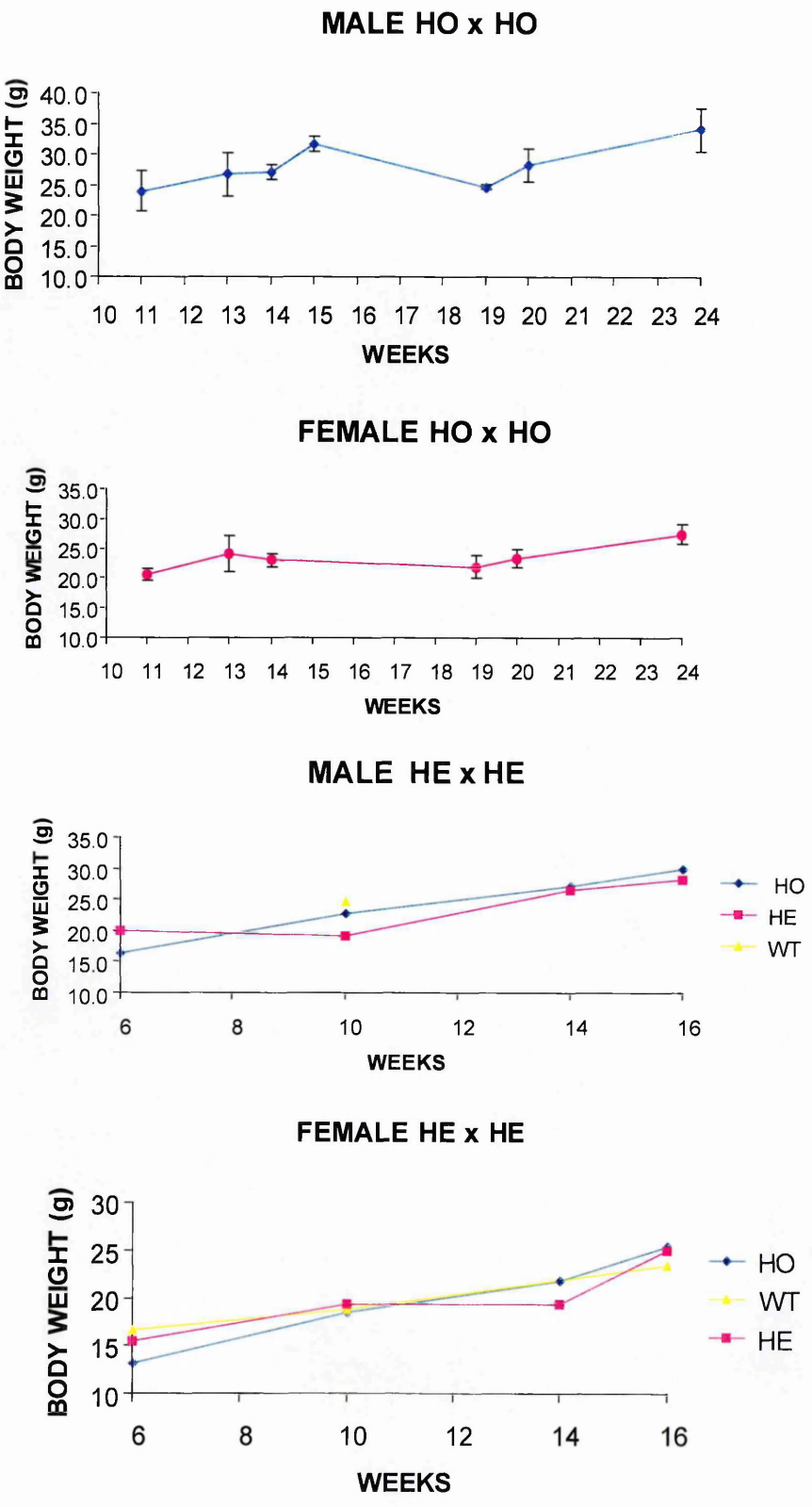

Figure 9.6

Body weight of KO HO male and female mice, generated from HO x HO breeding., and of wild–type, KO HO and HE mice derived from HE x HE breeding.

A

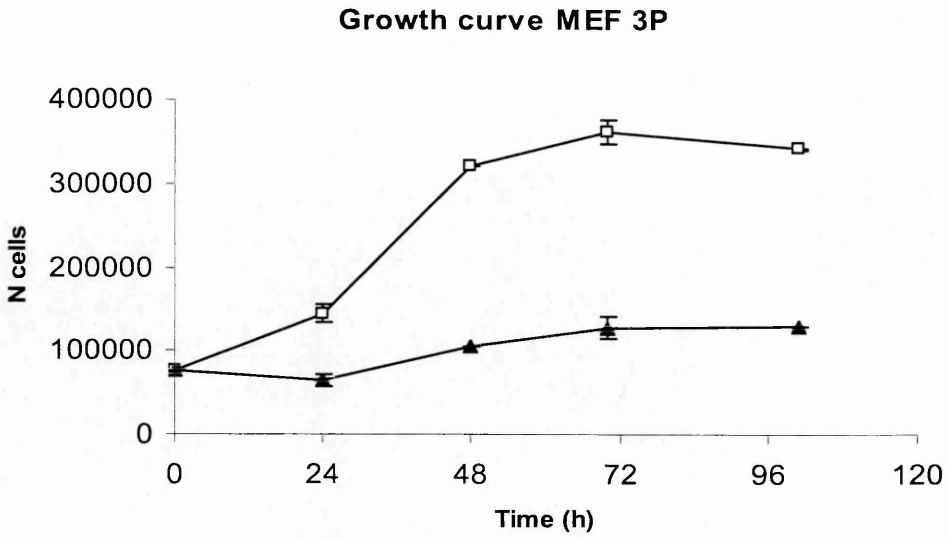

B

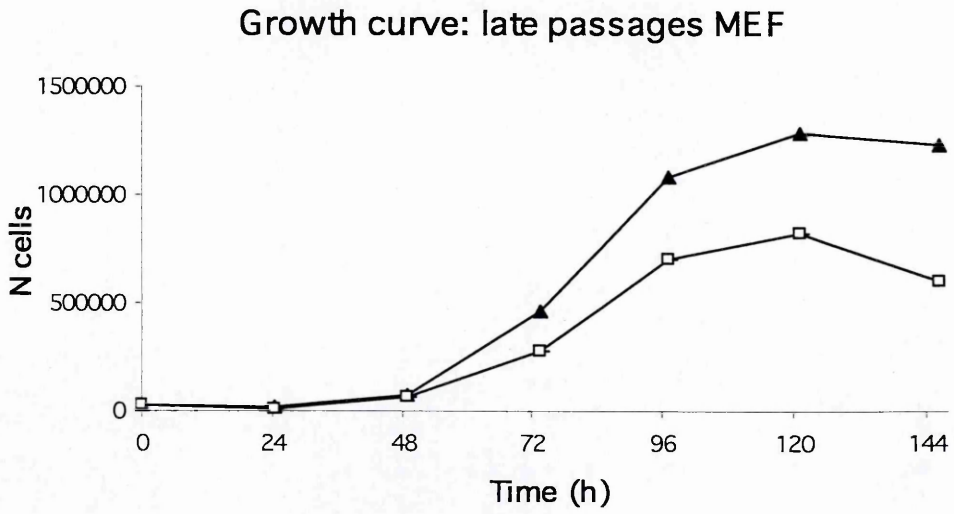

Figure 9.7

Growth curve of DRG–/– and DRG+/+ MEFs cultures at different passages.

Panel A. Growth curve of DRG–/– (□) compared to DRG+/+ (▲) at culturing passage 3. The DRG–/– cells (doubling time 29.43 hours) divided twice and half as rapid as DRG+/+ cells

Panel B. Growth curve of DRG–/– (□) at culturing passage 57 compared to DRG+/+ (▲) at culturing passage 65. At late passages, wild–type and KO HO cells grew similarly with a doubling time around 12 hours.

these densities every 3 days. After the first passage in vitro both DRAGO.HO KO and WT MEF were cryopreserved. For studies of early passage embryo fibroblasts, comparative growth rates was defined with cells at passage 3. The results indicated that DRAGO –/– cells grew more rapidly that DRAGO +/+ cells. The cell doubling times, calculated from early time points of this curve were 29, 43 hours for the DRAGO –/– and 79 hours for the wild–type cells meaning that at early passages, the HO KO MEF divided twice and a half as fast as the WT (Fig. 9.7A). After few passages the growth rate dramatically dropped down till around the passage 20 when both DRAGO –/– and DRAGO +/+ MEF cell lines spontaneously immortalised. At late passages (65P for the WT and 58P for HO KO embryo fibroblast) the WT MEF grew similarly to KO HO cells with a doubling time around 12 hour and 14 hour respectively for WT and HO KO cells (Fig 9.7B).

9.7 Response of MEF to UV and X rays

Both DRAGO –/– and DRAGO +/+, plated on six-well plates were treated with either UV or X rays at different doses. Seventy-two hours after treatment, plates were washed and stained with crystal violet evidencing that both WT and HO KO cells responded to treatments with no differences. The response to UV and X rays have been reported as a growth curve relative to controls (untreated cells) in figure 9.8. These results were confirmed by other experiments conducted with different doses.

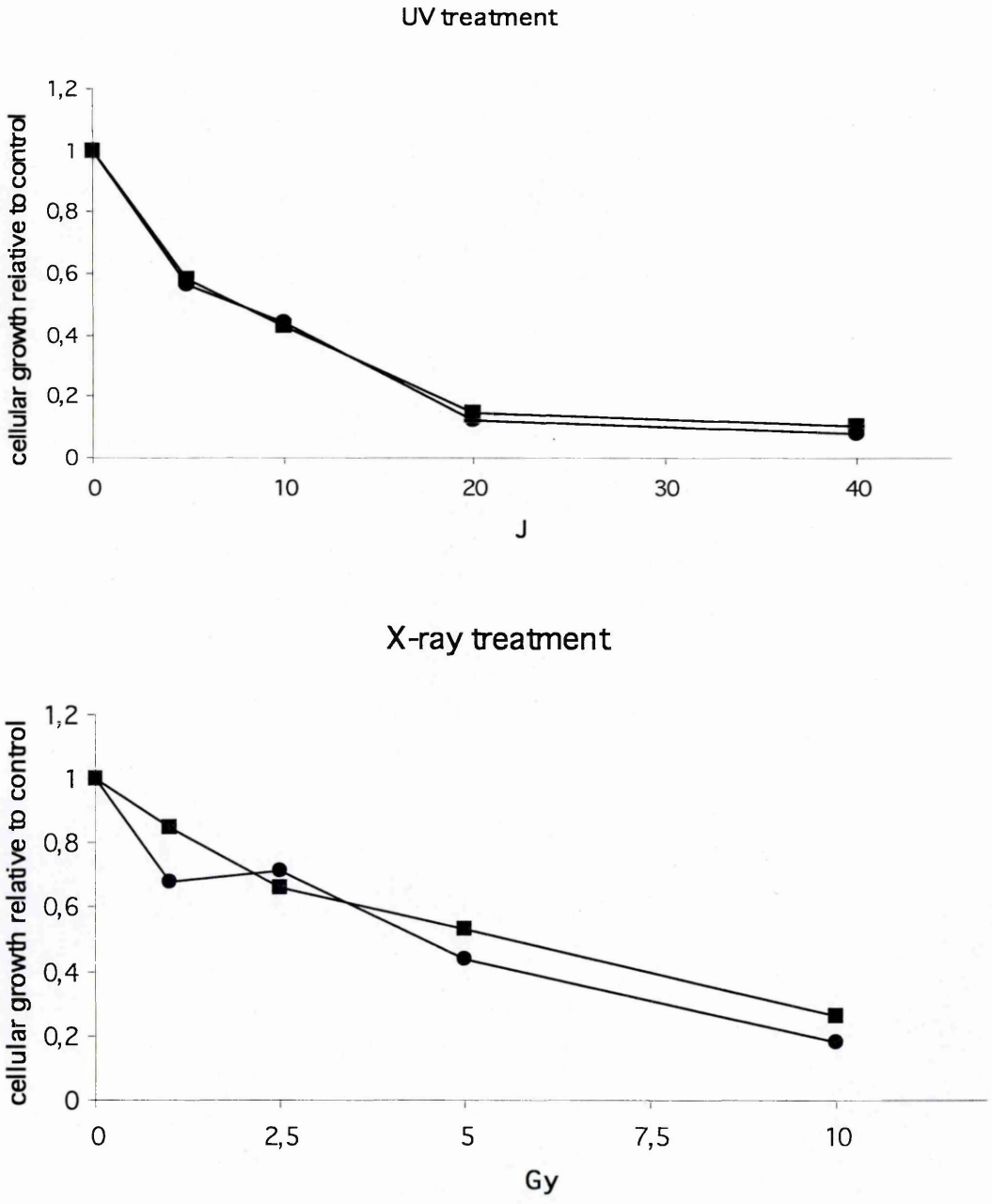

Figure 9.8

UV (upper panel) and X rays (lower panel) treatments. Response of DRG+/+ MEF (●) and DRG–/– MEF (■) has been expressed as cellular growth relative to control (untreated) cells.

9.8 Response of MEF to drug treatment

MEFs were treated with several drugs, most of them were tested on different cells lines showing to induce the increase of DRAGO gene expression. Plated on 24-well plates, both DRAGO –/– and DRAGO +/+ MEFs were treated 24 hours after seeding with 5-FU, CPT, DDP, DX, PS341, taxol and VP-16. Seventy–two hours after treatment, cells were washed and stained with crystal violet. The treatment with DX, DDP, CPT, and etoposide (VP-16) induced a different response in the MEF cultured cells showing that the DRAGO –/– cells were more resistant than the WT MEF to drug treatment as represented in figure 9.9. The other drug treatment determined a similar response in both MEF cultured cell lines. As reported in the introduction chapter, in HCT-116 cell line DRAGO expression is induced by almost strong drug treatment, meaning that the concentrations and time able to induce the gene expression were often higher than the GI50 calculated for each drug used. In particular, 5-FU and taxol determined an increased in the expression of DRAGO in the HCT-116 cell line whether added to the cells at particularly high doses for long time (see table 1.1). Therefore, the observation discussed here are consistent with the real time data reported in the introduction chapter. It is possible that to detect a different response to 5-FU and taxol in WT and HO KO MEFs it is necessary to treat the cells with higher doses tested so far but possibly too toxic for the cells.

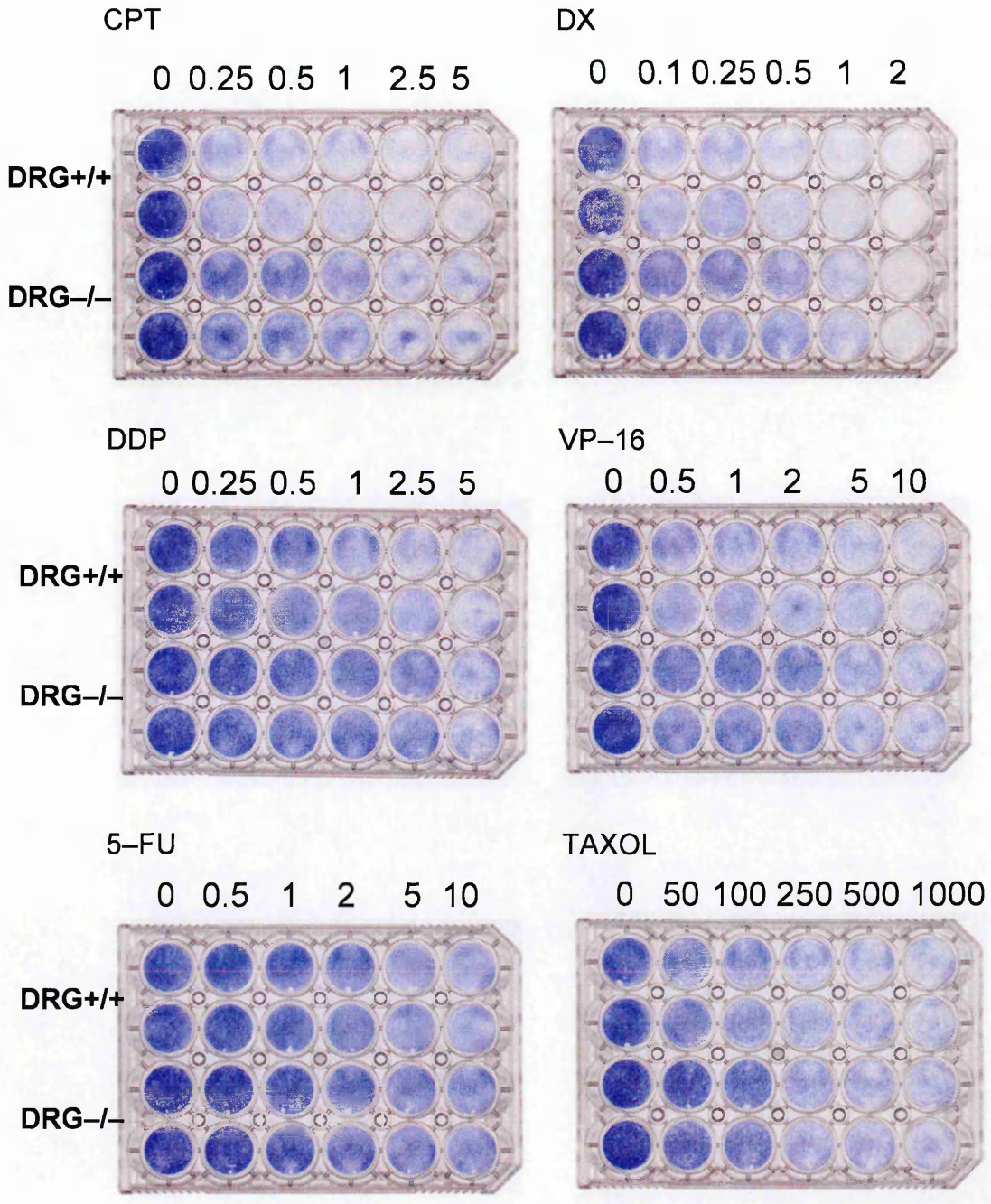

Figure 9.9

MEF response to drug treatments. DRG+/+ (first two rows of each plate) and DRG–/– (last two rows) cells were treated with the indicated concentration of drug for 72 hours. Staining with crystal violet was performed at the end of the treatment.

9.9 Apoptosis of MEF by DAPI/sulphorhodamine staining

In order to understand how the DRAGO-null MEFs are relatively resistant to drug treatment, both DRAGO +/+ and DRAGO –/– nuclei have been stained with DAPI/sulphorhodamine in order to evaluate whether cells underwent to apoptosis following treatment. MEFs cells were then treated with etoposide (VP-16), DX and CPT. Two concentrations were chosen at which in the previously described experiments the highest differences between the two cell lines in response to the treatment were observed. At either 24 or 48 hours of treatment cells were stained and photographed at fluorescence microscope. As represented in figures 9.10–9.11, DRAGO –/– MEFs very rarely showed fragmentation of the nuclei, which is a characterising feature of the apoptotic cells as discussed in the introduction chapter 1.5.3. Conversely, 50% of the nuclei of the DRAGO +/+ cells resulted to be apoptotic. This effect is observable in WT cells after treatment with VP-16 and DX as shown in figures 9.10–9.11. This finding strengthens the hypothesis that DRAGO induced upon drug treatment could drive the cell to respond to stress by activating pathways leading to apoptosis.

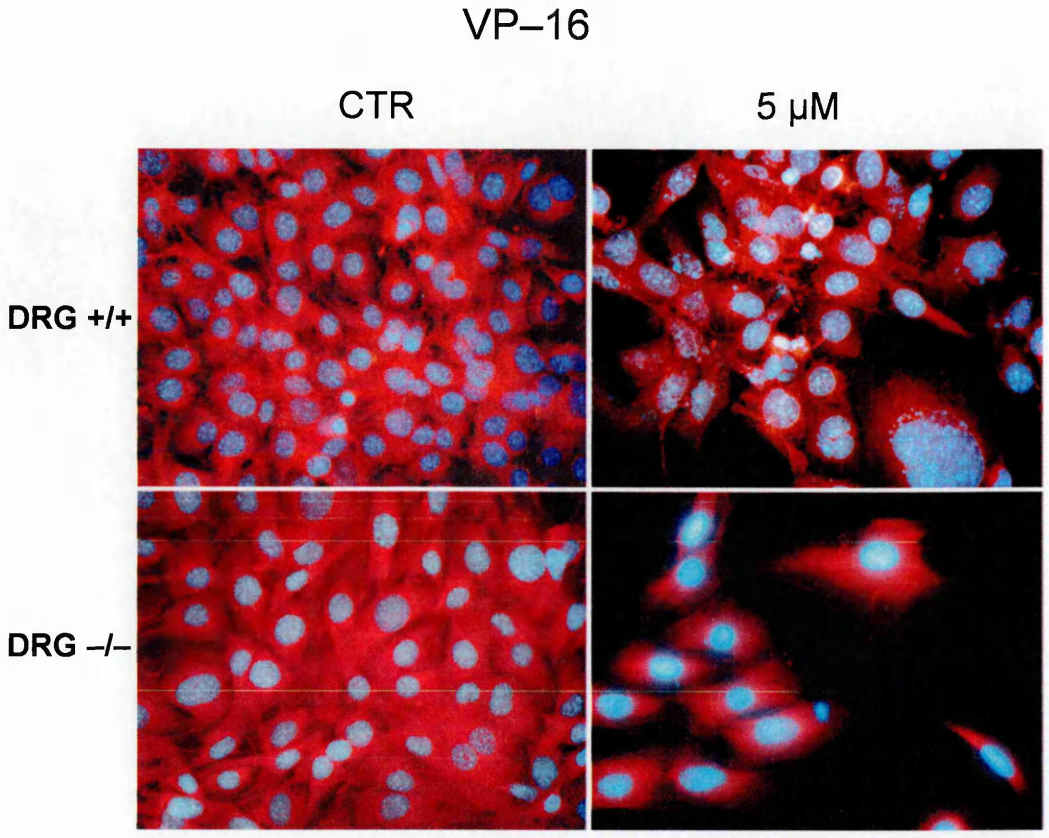

Figure 9.10

DAPI/sulphorhodamine staining of MEF DRG+/+ (upper panel) and DRG–/– (lower panel) after treatment with VP–16 5 µM for 24 hours (left panel) compared to the corresponding untreated cells.

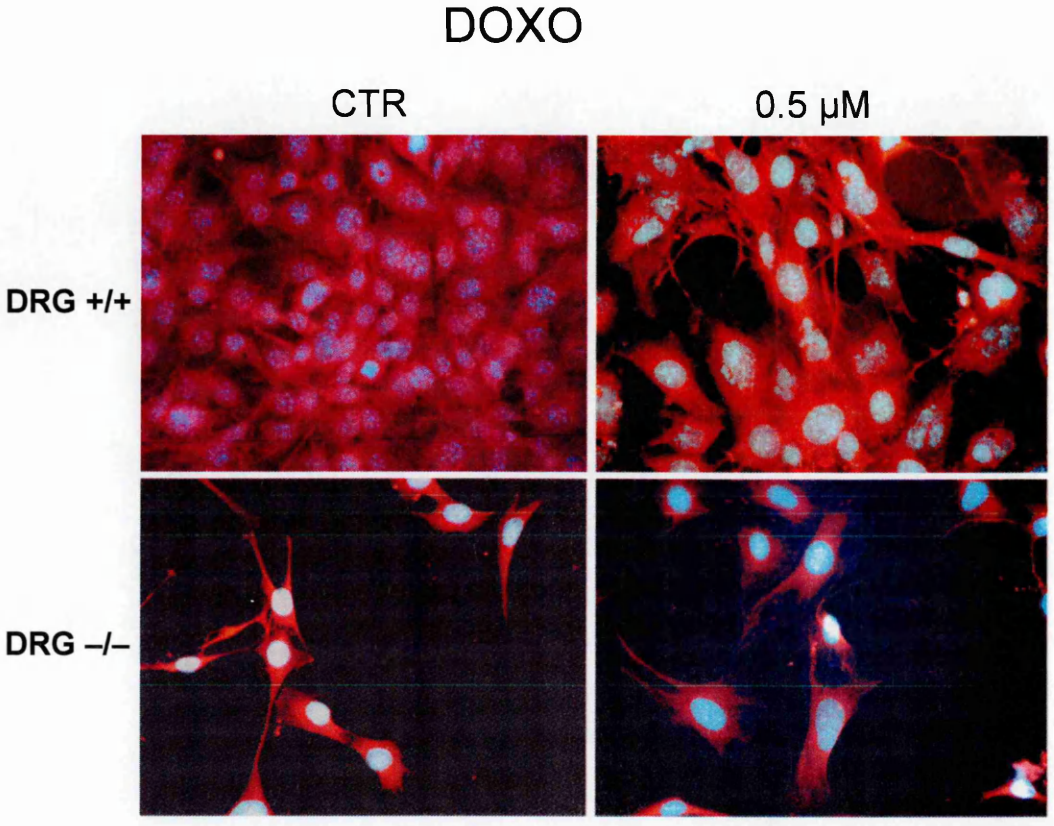

Figure 9.11

DAPI/sulphorhodamine staining of MEF DRG+/+ (upper panel) and DRG–/– (lower panel) after treatment with doxorubicin 0.5 μM for 24 hours (left panel) compared to the corresponding untreated cells.

9.10 Discussion

The determination of the cellular function of DRAGO gene protein product was certainly challenging for the difficulties encountered related to the fact that its expression was associated to a strong growth suppressive effect. With the generation of KO mice, most of the hypothesis derived from previous results could be proven. DRAGO-null mice, generated in collaboration with Genoway, are viable, fertile and do not present any macroscopically evident alteration. No experiments on mice to assess the response to genotoxic insults such as X rays or drug treatment have been conducted as yet although they have been planned to be carried out in the near future.

The experiments for the evaluation of the genotoxic insults, such as X and UV radiation or drug treatment were performed on mouse embryo fibroblast cultured cells isolated from either DRAGO +/+ or DRAGO –/– mice. Those cells show a similar response to UV and X rays treatment. While there was no indications regarding the influence of X rays on DRAGO induction, by real time PCR no increase in the expression level of DRAGO was measured in cells treated with UV radiation (see introduction chapter 1.7.1). Therefore, at least for the UV radiation, MEF response to treatment is consistent with the experimentally collected data reported in the introduction chapter.

Conversely, upon drug treatment DRAGO –/– cells were in general less sensitive than the DRAGO +/+ cells. Moreover, the WT DRAGO MEFs

showed to undergo to apoptosis in contrast to the DRAGO-null cells which less frequently had nuclei fragmentation. This ultimate observation strengthens the hypothesis that DRAGO gene, when induced in cells upon stresses and DNA damage could activate a series of steps ultimately leading to cellular death by apoptosis.

CHAPTER 10

GENERAL DISCUSSION

The overall aim of the present thesis was the characterisation of a new gene named DRAGO (DRugs Activated Gene Overexpressed) identified as a p53-inducible gene by differential expression analysis in cells following genotoxic insults. The hypothesis that DRAGO is a transcriptional target for p53 apoptosis control conferred particular relevance to this work. Being DRAGO a previously uncharacterised gene, the establishment of DRAGO as a mediator of p53–dependent apoptosis could add a novel aspect to the understanding of the mechanism by which p53 physiologically controls cell death, the essential function for its tumor suppressor activity.

The newly identified gene sequenced matched with a cDNA cloned sequence (named KIAA0247) that had been submitted to Genbank databases, but the function of the gene product was unknown. From tissues expression analyses, the gene was found to be ubiquitously expressed at a very low level. From preliminary experimental results collected in my lab, the gene was overexpressed to treatment with DNA damaging agents, at doses and times of treatment were significantly higher than the drugs GI50 established for administered drugs (see table 1.1). Moreover upon stress, the expression of DRAGO was induced after 24 hours following treatment. This evidence suggested that DRAGO could be considered as a late rather than immediate p53–dependent gene activated in response to treatment.

The characterisation of this newly identified gene started with the description of the molecular organisation of the gene. The full cDNA of

5,338 bp had already been isolated and sequenced by colleagues of the Molecular Pharmacology Laboratory of the Department of Oncology at the Mario Negri institute. As reported in chapter 3.2, the 5,338-bp cDNA is the result of the junction of 6 exons. The coding region of the putative 303-aminoacid protein, deduced from the nucleotide sequence, is comprised between exon 2 and the first 26 bases of exon 6. What has to be underlined is the peculiar gene structure, which is characterised by the first two very long introns, about 45-48 kb long, and by the presence of a 4-kb 3'UTR. The unusual length of those regions could imply an involvement in the regulation of the gene at post-transcriptional/translational levels. The 3'UTR-sequence in fact contains several AU and CU-rich regions which are known to be involved in the degradation/stability of mRNA. Moreover, a recently collected observation in my lab, highlights the presence in the same region of sequences which can be specifically bound by at least two miRNAs. As reported in the literature, the miRNAs are small regulatory non–coding RNAs of 19–28 nt in length, which are derived from double–stranded RNA (dsRNA) and can induce gene silencing (post–transcriptional or transcriptional) through specific base–pairing with target molecules in a number of eukaryotes (from nematodes, plant, mammals). It would be interesting, therefore, to evaluate the expression of a reporter gene which is measurable like luciferase, fused to the DRAGO 3'UTR, after treatment with the miRNAs, the specific target regions of which were identified. This experiment, together with the discovery of putative proteins determining the stability of

the mRNA, are some of those planned to be done on the basis of the results of the studies presented here.

As already discussed, in chapter 3.4, the intronic region might contain cryptic ATGs which, by alternative splicing, could give rise to isoforms of the protein. These isoforms could be putatively expressed also in a tissue-specific fashion, therefore the above mentioned intronic region might also include cis-regulatory element together with binding site for tissue-specific transcription factors. It has to be underlined that there is a unique polyadenylation signal, ATTAAA, located at 20 bp upstream of the stop codon. Therefore, the putative isoforms which share the same stop codon, would have another promoter likely comprised in the above mentioned intronic regions. In the chapter 4.2 to 4.7, the analysis of a theoretical promoter region of the gene is reported. The data indicate that p53 transcriptionally controls DRAGO expression, consistently with the results so far collected, even though for the putative promoter regions isolated, p53 only weakly induced the gene. The interesting findings reported here regard p73 and its isoforms, particularly p73β and γ, which induce DRAGO more efficiently than p53. As already discussed, other genes are better activated by p73 than p53. Nevertheless, DRAGO could represent an additional downstream gene of both p73 and p53. The fact that DNp73 acts in a synergising manner with p53 and p73 different isoforms to induce DRAGO expression adds complexity to the numerous mechanisms so far hypothesised to control the expression of the gene. The promoter analysis is not complete and needs to be supported with experimental tests aimed

at defining the DRAGO regulatory regions bound by p53 and p73 isoforms. It is also particularly important to verify whether the sequences tested for promoter activity are really those controlling DRAGO transcription. Therefore the analysis of intronic region should define the binding motif for transcription factors implicated for instance in tissue specific expression of DRAGO, but in particular for p73 isoforms and p53. The search for putative p53, p73 and its isoforms responsive elements should also be address to the 7-Kb sequence, which is located upstream to the 3.8-kb region and is part of the isolated 10,735-bp fragment (see Fig. 4.1). The sequential portions of the 7-Kb region should also be analysed with the luciferase assay.

On the basis of the observed better induction of DRAGO gene by p73 (and its isoforms) than p53, it would be also interesting measuring by real-time PCR the induction of DRAGO at the mRNA level in p73–/– cells after treatments with drugs (i.e 5-FU and Taxol) which are able to induce DRAGO mRNA in p53+/+ and not in p53–/– (as reported in chapter 1.7.1).

As reported in chapter 5.2, DRAGO was not found to be mutated in any of the experimental systems tested, including tumor cell lines sensitive or resistant to anticancer drugs, and clinical human samples. This result is not surprising considering that p53 is frequently mutated in human cancer, thus not necessarily meaning that it requires additional mutations of its downstream effectors. It is also to note that the gene might not be mutated because it can be down-regulated at the mRNA level, as widely discussed above.

In chapter 6, the functional role of the DRAGO gene has been investigated in *in vitro* systems represented by cultured cell lines of different origin (bacterial, human and murine). The data obtained on the effect of ectopic overexpression of DRAGO indicate that the gene has a strong inhibitory effect on cellular growth, preventing the formation of stably expressing cellular clones. At a morphological level, the overexpression of the gene, under the control of a strong viral promoter, induces the formation of a large number of vacuoles to cause the disruption of the membrane leading to the extracellular release of cytosolic material. It is important to stress that whenever overexpressed under the control of a strong constitutive promoter, the level of induction is probably much higher than to the induction level measured by real time PCR following a genotoxic insult. Threfore, the morphological alteration induced by overexpression of the transfected DRAGO might not be modelling the physiological situation. It is important to verify if DRAGO gene product whenever expressed after DNA damage localises in vesicles thus leading to the membrane desruption. Moreover, it has also to be formally proved that the morphological effects observed are really due to the overexpression of the gene by double staining the cells to verify that the plasmid has entered the cells, even if all the results would suggest this. The results reported in chapter 6.4, however, indicate that probably the protein conformation or stability is strictly required for the growth suppressive activity. Cells, in fact, can tolerate the expression of mutant proteins lacking a few aminoacids deleted from the C-terminus. Since the peptides corresponding to those

aminoacids, on the basis of the results reported here, seem not to affect cellular growth, it is possible that the deletion of the same aminoacids could determine a loss of the toxic effect by compromising the stability or the correct folding of the protein. However, to prove that the peptides have no suppressive effects on cells after treatment, it is necessary to show that the peptides have indeed entered the cells, by either doing a fusion peptide with the tat epitope (which is known to favour the entrance of peptides into the cells) or co-transfecting small amounts of FITC fusion peptides to monitor if peptides have entered the cells by fluorescence.

The computational analysis of the aminoacid sequence deduced from the cDNA of the protein (chapter 7) reveals that the DRAGO protein is likely a transmembrane protein. The theoretical prediction has been supported by experimental evidences reported in chapter 7.4 where it has been seen that the protein localises to membrane structures. However it is unclear in which membrane of the cell the protein positions itself. It is to note that the immunofluorescence experiments showing the localisation to membranes of the protein were performed on deleted proteins generated as reported in chapter 6. The deletion mutants were generated by progressive deletions from the N-terminus and C-terminus in order to preserve at least one of the two transmembrane domains to verify the protein can localise at the membrane. However, it is important to detect the wt protein by immunofluorescence, too, in order to support the hypothesis that DRAGO is really a membrane-bound protein.

The generation of DRAGO-null mice would help in answering most of the

unsolved questions identified so far. The fact that KO mice are viable, macroscopically normal and fertile, suggests that DRAGO is unlikely to play a crucial role in development. Embryo fibroblasts cultured cells isolated from KO and WT mice embryos would be important *in vitro* experimental systems. The results reported in chapter 9 finally demonstrated that the absence of the DRAGO gene, as in DRAGO–/– MEFs, renders the cells relatively resistant to several anticancer agents, with different mechanisms of action, by suppressing the ability of the cells to undergo apoptotic death. In contrast, WT MEFs were relatively sensitive to the anticancer agents used to treat KO MEFs, dying by apoptosis (chapters 9.8 and 9.9). These results lead to important conclusions. First, DRAGO is a newly identified p53/p73 target gene involved in the control of growth and apoptosis. These observations are also supported by DNA microarray analyses of p53 target genes involved in apoptosis (342, 343) revealing that KIAA0247/DRAGO was one of the apoptotic genes activated in a p53–dependent fashion.

Second, DRAGO is a gene induced after high doses of anticancer drugs, suggesting that only when cells are subjected to irreparable genotoxic damage is DRAGO induced to execute the suicide of the damaged cells. It is also important to underline the necessity to confirm the direct role of DRAGO on the drug treatment induced apoptosis by knock down of the gene in DRAGO+/+ cells with the use of synthetic siRNA (small–interfering RNA) duplexes against DRAGO, to observe if cells acquire resistance to DNA damage and still undergo apoptosis. Similarly to miRNAs, siRNAs

are regulatory non–coding short RNAs derived from dsRNAs, which, through perfect basepairings with a sequence in the target mRNA, induce the cleavage of the target mRNA, thus silencing the corresponding gene expression at a post–transcriptional level. The isolated DRAGO–/– and DRAGO +/+ MEFs cultured cells would be useful for immunofluorescence experiments aimed at investigating the subcellular localisation of the protein by using a specific staining to distinguished the different cellular compartments. Other experiments planned to be performed on the basis of this work includes the physiological and pathological response to drug and radiation treatments of sensitive tissues, such as thymus, spleen and small intestinal epithelium. With this work the functional role of DRAGO protein has been initiated and further studies identified to explore more fully the specific mechanisms in which DRAGO is involved in the apoptotic response. This important issue remains to be solved with future experiments taking advantage of the DRAGO-null mouse line generated. Nevertheless, DRAGO might be considered a novel potential target for the development of new therapeutic anticancer agents.

CHAPTER 11

REFERENCES

1. Hanahan, D. and Weinberg, R. A. The hallmarks of cancer. Cell, *100:* 57-70, 2000.
2. Evan, G. I. and Vousden, K. H. Proliferation, cell cycle and apoptosis in cancer. Nature, *411:* 342-348, 2001.
3. Vogelstein, B. and Kinzler, K. W. Cancer genes and the pathways they control. Nat Med, *10:* 789-799, 2004.
4. Martin, G. S. The hunting of the Src. Nat Rev Mol Cell Biol, *2:* 467-475, 2001.
5. Yeatman, T. J. A renaissance for SRC. Nat Rev Cancer, *4:* 470-480, 2004.
6. Levine, A. J. p53, the cellular gatekeeper for growth and division. Cell, *88:* 323-331, 1997.
7. Knudson, A. G., Jr. Retinoblastoma: a prototypic hereditary neoplasm. Semin Oncol, *5:* 57-60, 1978.
8. Friend, S. H., Bernards, R., Rogelj, S., Weinberg, R. A., Rapaport, J. M., Albert, D. M., and Dryja, T. P. A human DNA segment with properties of the gene that predisposes to retinoblastoma and osteosarcoma. Nature, *323:* 643-646, 1986.
9. Lee, W. H., Bookstein, R., Hong, F., Young, L. J., Shew, J. Y., and Lee, E. Y. Human retinoblastoma susceptibility gene: cloning, identification, and sequence. Science, *235:* 1394-1399, 1987.
10. Fung, Y. K., Murphree, A. L., T'Ang, A., Qian, J., Hinrichs, S. H., and Benedict, W. F. Structural evidence for the authenticity of the human retinoblastoma gene. Science, *236:* 1657-1661, 1987.
11. Weinberg, R. A. Tumor suppressor genes. Science, *254:* 1138-1146, 1991.
12. Kennedy, B. K., Barbie, D. A., Classon, M., Dyson, N., and Harlow, E. Nuclear organization of DNA replication in primary mammalian cells. Genes Dev, *14:* 2855-2868, 2000.
13. Royzman, I., Austin, R. J., Bosco, G., Bell, S. P., and Orr-Weaver, T. L. ORC localization in Drosophila follicle cells and the effects of mutations in dE2F and dDP. Genes Dev, *13:* 827-840, 1999.

14. Bosco, G., Du, W., and Orr-Weaver, T. L. DNA replication control through interaction of E2F-RB and the origin recognition complex. Nat Cell Biol, *3:* 289-295, 2001.
15. Lipinski, M. M. and Jacks, T. The retinoblastoma gene family in differentiation and development. Oncogene, *18:* 7873-7882, 1999.
16. Hickman, E. S., Moroni, M. C., and Helin, K. The role of p53 and pRB in apoptosis and cancer. Curr Opin Genet Dev, *12:* 60-66, 2002.
17. Ponder, B. A. Cancer genetics. Nature, *411:* 336-341, 2001.
18. Lowe, S. W., Cepero, E., and Evan, G. Intrinsic tumour suppression. Nature, *432:* 307-315, 2004.
19. Hoeijmakers, J. H. Genome maintenance mechanisms for preventing cancer. Nature, *411:* 366-374, 2001.
20. Zhou, B. B. and Elledge, S. J. The DNA damage response: putting checkpoints in perspective. Nature, *408:* 433-439, 2000.
21. Hartwell, L. H. and Weinert, T. A. Checkpoints: controls that ensure the order of cell cycle events. Science, *246:* 629-634, 1989.
22. O'Connor, P. M. Mammalian G1 and G2 phase checkpoints. Cancer Surv, *29:* 151-182, 1997.
23. Melo, J. and Toczyski, D. A unified view of the DNA-damage checkpoint. Curr Opin Cell Biol, *14:* 237-245, 2002.
24. Jackson, S. P. Sensing and repairing DNA double-strand breaks. Carcinogenesis, *23:* 687-696, 2002.
25. Froelich-Ammon, S. J. and Osheroff, N. Topoisomerase poisons: harnessing the dark side of enzyme mechanism. J Biol Chem, *270:* 21429-21432, 1995.
26. Lee, S. E., Moore, J. K., Holmes, A., Umezu, K., Kolodner, R. D., and Haber, J. E. Saccharomyces Ku70, mre11/rad50 and RPA proteins regulate adaptation to G2/M arrest after DNA damage. Cell, *94:* 399-409, 1998.
27. Rich, T., Allen, R. L., and Wyllie, A. H. Defying death after DNA damage. Nature, *407:* 777-783, 2000.

28. Samuels, Y., Wang, Z., Bardelli, A., Silliman, N., Ptak, J., Szabo, S., Yan, H., Gazdar, A., Powell, S. M., Riggins, G. J., Willson, J. K., Markowitz, S., Kinzler, K. W., Vogelstein, B., and Velculescu, V. E. High frequency of mutations of the PIK3CA gene in human cancers. Science, *304:* 554, 2004.
29. Corvera, S. and Czech, M. P. Direct targets of phosphoinositide 3-kinase products in membrane traffic and signal transduction. Trends Cell Biol, *8:* 442-446, 1998.
30. Vivanco, I. and Sawyers, C. L. The phosphatidylinositol 3-Kinase AKT pathway in human cancer. Nat Rev Cancer, *2:* 489-501, 2002.
31. Luo, J., Manning, B. D., and Cantley, L. C. Targeting the PI3K-Akt pathway in human cancer: rationale and promise. Cancer Cell, *4:* 257-262, 2003.
32. Ali, I. U., Schriml, L. M., and Dean, M. Mutational spectra of PTEN/MMAC1 gene: a tumor suppressor with lipid phosphatase activity. J Natl Cancer Inst, *91:* 1922-1932, 1999.
33. Simpson, L. and Parsons, R. PTEN: life as a tumor suppressor. Exp Cell Res, *264:* 29-41, 2001.
34. Shiloh, Y. ATM and related protein kinases: safeguarding genome integrity. Nat Rev Cancer, *3:* 155-168, 2003.
35. Bakkenist, C. J. and Kastan, M. B. DNA damage activates ATM through intermolecular autophosphorylation and dimer dissociation. Nature, *421:* 499-506, 2003.
36. Uziel, T., Lerenthal, Y., Moyal, L., Andegeko, Y., Mittelman, L., and Shiloh, Y. Requirement of the MRN complex for ATM activation by DNA damage. Embo J, *22:* 5612-5621, 2003.
37. Carson, C. T., Schwartz, R. A., Stracker, T. H., Lilley, C. E., Lee, D. V., and Weitzman, M. D. The Mre11 complex is required for ATM activation and the G2/M checkpoint. Embo J, *22:* 6610-6620, 2003.
38. Mochan, T. A., Venere, M., DiTullio, R. A., Jr., and Halazonetis, T. D. 53BP1, an activator of ATM in response to DNA damage. DNA Repair (Amst), *3:* 945-952, 2004.

39. Horejsi, Z., Falck, J., Bakkenist, C. J., Kastan, M. B., Lukas, J., and Bartek, J. Distinct functional domains of Nbs1 modulate the timing and magnitude of ATM activation after low doses of ionizing radiation. Oncogene, *23:* 3122-3127, 2004.

40. Lee, J. H. and Paull, T. T. ATM activation by DNA double-strand breaks through the Mre11-Rad50-Nbs1 complex. Science, *308:* 551-554, 2005.

41. Abraham, R. T. Cell cycle checkpoint signaling through the ATM and ATR kinases. Genes Dev, *15:* 2177-2196, 2001.

42. Brumbaugh, K. M., Otterness, D. M., Geisen, C., Oliveira, V., Brognard, J., Li, X., Lejeune, F., Tibbetts, R. S., Maquat, L. E., and Abraham, R. T. The mRNA surveillance protein hSMG-1 functions in genotoxic stress response pathways in mammalian cells. Mol Cell, *14:* 585-598, 2004.

43. Yannone, S. M., Roy, S., Chan, D. W., Murphy, M. B., Huang, S., Campisi, J., and Chen, D. J. Werner syndrome protein is regulated and phosphorylated by DNA-dependent protein kinase. J Biol Chem, *276:* 38242-38248, 2001.

44. Karmakar, P., Piotrowski, J., Brosh, R. M., Jr., Sommers, J. A., Miller, S. P., Cheng, W. H., Snowden, C. M., Ramsden, D. A., and Bohr, V. A. Werner protein is a target of DNA-dependent protein kinase in vivo and in vitro, and its catalytic activities are regulated by phosphorylation. J Biol Chem, *277:* 18291-18302, 2002.

45. Ma, Y., Pannicke, U., Schwarz, K., and Lieber, M. R. Hairpin opening and overhang processing by an Artemis/DNA-dependent protein kinase complex in nonhomologous end joining and V(D)J recombination. Cell, *108:* 781-794, 2002.

46. Cortez, D., Guntuku, S., Qin, J., and Elledge, S. J. ATR and ATRIP: partners in checkpoint signaling. Science, *294:* 1713-1716, 2001.

47. Zou, L. and Elledge, S. J. Sensing DNA damage through ATRIP recognition of RPA-ssDNA complexes. Science, *300:* 1542-1548, 2003.

48. Unsal-Kacmaz, K. and Sancar, A. Quaternary structure of ATR and effects of ATRIP and replication protein A on its DNA binding and kinase activities. Mol Cell Biol, *24:* 1292-1300, 2004.
49. Osborn, A. J., Elledge, S. J., and Zou, L. Checking on the fork: the DNA-replication stress-response pathway. Trends Cell Biol, *12:* 509-516, 2002.
50. Ellison, V. and Stillman, B. Opening of the clamp: an intimate view of an ATP-driven biological machine. Cell, *106:* 655-660, 2001.
51. Lin, S. Y., Li, K., Stewart, G. S., and Elledge, S. J. Human Claspin works with BRCA1 to both positively and negatively regulate cell proliferation. Proc Natl Acad Sci U S A, *101:* 6484-6489, 2004.
52. Petrini, J. H. and Stracker, T. H. The cellular response to DNA double-strand breaks: defining the sensors and mediators. Trends Cell Biol, *13:* 458-462, 2003.
53. Bartek, J. and Lukas, J. Chk1 and Chk2 kinases in checkpoint control and cancer. Cancer Cell, *3:* 421-429, 2003.
54. Donzelli, M. and Draetta, G. F. Regulating mammalian checkpoints through Cdc25 inactivation. EMBO Rep, *4:* 671-677, 2003.
55. Jenkins, J. R., Rudge, K., and Currie, G. A. Cellular immortalization by a cDNA clone encoding the transformation-associated phosphoprotein p53. Nature, *312:* 651-654, 1984.
56. Eliyahu, D., Raz, A., Gruss, P., Givol, D., and Oren, M. Participation of p53 cellular tumour antigen in transformation of normal embryonic cells. Nature, *312:* 646-649, 1984.
57. Parada, L. F., Land, H., Weinberg, R. A., Wolf, D., and Rotter, V. Cooperation between gene encoding p53 tumour antigen and ras in cellular transformation. Nature, *312:* 649-651, 1984.
58. Finlay, C. A., Hinds, P. W., and Levine, A. J. The p53 proto-oncogene can act as a suppressor of transformation. Cell, *57:* 1083-1093, 1989.

59. Eliyahu, D., Michalovitz, D., Eliyahu, S., Pinhasi-Kimhi, O., and Oren, M. Wild-type p53 can inhibit oncogene-mediated focus formation. Proc Natl Acad Sci U S A, *86:* 8763-8767, 1989.

60. Malkin, D., Li, F. P., Strong, L. C., Fraumeni, J. F., Jr., Nelson, C. E., Kim, D. H., Kassel, J., Gryka, M. A., Bischoff, F. Z., Tainsky, M. A., and et al. Germ line p53 mutations in a familial syndrome of breast cancer, sarcomas, and other neoplasms. Science, *250:* 1233-1238, 1990.

61. Donehower, L. A. The p53-deficient mouse: a model for basic and applied cancer studies. Semin Cancer Biol, *7:* 269-278, 1996.

62. Hollstein, M., Rice, K., Greenblatt, M. S., Soussi, T., Fuchs, R., Sorlie, T., Hovig, E., Smith-Sorensen, B., Montesano, R., and Harris, C. C. Database of p53 gene somatic mutations in human tumors and cell lines. Nucleic Acids Res, *22:* 3551-3555, 1994.

63. Hainaut, P. and Hollstein, M. p53 and human cancer: the first ten thousand mutations. Adv Cancer Res, *77:* 81-137, 2000.

64. Vogelstein, B., Lane, D., and Levine, A. J. Surfing the p53 network. Nature, *408:* 307-310, 2000.

65. Lu, H. and Levine, A. J. Human TAFII31 protein is a transcriptional coactivator of the p53 protein. Proc Natl Acad Sci U S A, *92:* 5154-5158, 1995.

66. Thut, C. J., Chen, J. L., Klemm, R., and Tjian, R. p53 transcriptional activation mediated by coactivators TAFII40 and TAFII60. Science, *267:* 100-104, 1995.

67. Candau, R., Scolnick, D. M., Darpino, P., Ying, C. Y., Halazonetis, T. D., and Berger, S. L. Two tandem and independent sub-activation domains in the amino terminus of p53 require the adaptor complex for activity. Oncogene, *15:* 807-816, 1997.

68. Chen, X., Ko, L. J., Jayaraman, L., and Prives, C. p53 levels, functional domains, and DNA damage determine the extent of the apoptotic response of tumor cells. Genes Dev, *10:* 2438-2451, 1996.

69. Venot, C., Maratrat, M., Sierra, V., Conseiller, E., and Debussche, L. Definition of a p53 transactivation function-deficient mutant and characterization of two independent p53 transactivation subdomains. Oncogene, *18:* 2405-2410, 1999.

70. Zhu, J., Zhou, W., Jiang, J., and Chen, X. Identification of a novel p53 functional domain that is necessary for mediating apoptosis. J Biol Chem, *273:* 13030-13036, 1998.

71. Walker, K. K. and Levine, A. J. Identification of a novel p53 functional domain that is necessary for efficient growth suppression. Proc Natl Acad Sci U S A, *93:* 15335-15340, 1996.

72. Sakamuro, D., Sabbatini, P., White, E., and Prendergast, G. C. The polyproline region of p53 is required to activate apoptosis but not growth arrest. Oncogene, *15:* 887-898, 1997.

73. Venot, C., Maratrat, M., Dureuil, C., Conseiller, E., Bracco, L., and Debussche, L. The requirement for the p53 proline-rich functional domain for mediation of apoptosis is correlated with specific PIG3 gene transactivation and with transcriptional repression. Embo J, *17:* 4668-4679, 1998.

74. Zhu, J., Jiang, J., Zhou, W., Zhu, K., and Chen, X. Differential regulation of cellular target genes by p53 devoid of the PXXP motifs with impaired apoptotic activity. Oncogene, *18:* 2149-2155, 1999.

75. Baptiste, N., Friedlander, P., Chen, X., and Prives, C. The proline-rich domain of p53 is required for cooperation with anti-neoplastic agents to promote apoptosis of tumor cells. Oncogene, *21:* 9-21, 2002.

76. Bargonetti, J., Manfredi, J. J., Chen, X., Marshak, D. R., and Prives, C. A proteolytic fragment from the central region of p53 has marked sequence-specific DNA-binding activity when generated from wild-type but not from oncogenic mutant p53 protein. Genes Dev, *7:* 2565-2574, 1993.

77. Halazonetis, T. D., Davis, L. J., and Kandil, A. N. Wild-type p53 adopts a 'mutant'-like conformation when bound to DNA. Embo J, *12:* 1021-1028, 1993.

78. Wang, Y., Reed, M., Wang, P., Stenger, J. E., Mayr, G., Anderson, M. E., Schwedes, J. F., and Tegtmeyer, P. p53 domains: identification and characterization of two autonomous DNA-binding regions. Genes Dev, *7:* 2575-2586, 1993.

79. Kraiss, S., Quaiser, A., Oren, M., and Montenarh, M. Oligomerization of oncoprotein p53. J Virol, *62:* 4737-4744, 1988.

80. McLure, K. G. and Lee, P. W. How p53 binds DNA as a tetramer. Embo J, *17:* 3342-3350, 1998.

81. McLure, K. G. and Lee, P. W. p53 DNA binding can be modulated by factors that alter the conformational equilibrium. Embo J, *18:* 763-770, 1999.

82. Nicholls, C. D., McLure, K. G., Shields, M. A., and Lee, P. W. Biogenesis of p53 involves cotranslational dimerization of monomers and posttranslational dimerization of dimers. Implications on the dominant negative effect. J Biol Chem, *277:* 12937-12945, 2002.

83. Wolkowicz, R. and Rotter, V. The DNA binding regulatory domain of p53: see the C. Pathol Biol (Paris), *45:* 785-796, 1997.

84. Hupp, T. R., Meek, D. W., Midgley, C. A., and Lane, D. P. Regulation of the specific DNA binding function of p53. Cell, *71:* 875-886, 1992.

85. Bayle, J. H., Elenbaas, B., and Levine, A. J. The carboxyl-terminal domain of the p53 protein regulates sequence-specific DNA binding through its nonspecific nucleic acid-binding activity. Proc Natl Acad Sci U S A, *92:* 5729-5733, 1995.

86. Anderson, M. E., Woelker, B., Reed, M., Wang, P., and Tegtmeyer, P. Reciprocal interference between the sequence-specific core and nonspecific C-terminal DNA binding domains of p53: implications for regulation. Mol Cell Biol, *17:* 6255-6264, 1997.

87. Ayed, A., Mulder, F. A., Yi, G. S., Lu, Y., Kay, L. E., and Arrowsmith, C. H. Latent and active p53 are identical in conformation. Nat Struct Biol, *8:* 756-760, 2001.

88. Ahn, J. and Prives, C. The C-terminus of p53: the more you learn the less you know. Nat Struct Biol, *8:* 730-732, 2001.

89. Giaccia, A. J. and Kastan, M. B. The complexity of p53 modulation: emerging patterns from divergent signals. Genes Dev, *12:* 2973-2983, 1998.

90. el-Deiry, W. S., Kern, S. E., Pietenpol, J. A., Kinzler, K. W., and Vogelstein, B. Definition of a consensus binding site for p53. Nat Genet, *1:* 45-49, 1992.

91. Lohrum, M. A. and Vousden, K. H. Regulation and activation of p53 and its family members. Cell Death Differ, *6:* 1162-1168, 1999.

92. Wu, X., Bayle, J. H., Olson, D., and Levine, A. J. The p53-mdm-2 autoregulatory feedback loop. Genes Dev, *7:* 1126-1132, 1993.

93. Lev Bar-Or, R., Maya, R., Segel, L. A., Alon, U., Levine, A. J., and Oren, M. Generation of oscillations by the p53-Mdm2 feedback loop: a theoretical and experimental study. Proc Natl Acad Sci U S A, *97:* 11250-11255, 2000.

94. Leng, R. P., Lin, Y., Ma, W., Wu, H., Lemmers, B., Chung, S., Parant, J. M., Lozano, G., Hakem, R., and Benchimol, S. Pirh2, a p53-induced ubiquitin-protein ligase, promotes p53 degradation. Cell, *112:* 779-791, 2003.

95. Dornan, D., Wertz, I., Shimizu, H., Arnott, D., Frantz, G. D., Dowd, P., O'Rourke, K., Koeppen, H., and Dixit, V. M. The ubiquitin ligase COP1 is a critical negative regulator of p53. Nature, *429:* 86-92, 2004.

96. Chuikov, S., Kurash, J. K., Wilson, J. R., Xiao, B., Justin, N., Ivanov, G. S., McKinney, K., Tempst, P., Prives, C., Gamblin, S. J., Barlev, N. A., and Reinberg, D. Regulation of p53 activity through lysine methylation. Nature, *432:* 353-360, 2004.

97. Xirodimas, D. P., Saville, M. K., Bourdon, J. C., Hay, R. T., and Lane, D. P. Mdm2-mediated NEDD8 conjugation of p53 inhibits its transcriptional activity. Cell, *118:* 83-97, 2004.

98. Meek, D. W. The p53 response to DNA damage. DNA Repair (Amst), *3:* 1049-1056, 2004.

99. Ashcroft, M., Taya, Y., and Vousden, K. H. Stress signals utilize multiple pathways to stabilize p53. Mol Cell Biol, *20:* 3224-3233, 2000.

100. Saito, S., Yamaguchi, H., Higashimoto, Y., Chao, C., Xu, Y., Fornace, A. J., Jr., Appella, E., and Anderson, C. W. Phosphorylation site interdependence of human p53 post-translational modifications in response to stress. J Biol Chem, *278:* 37536-37544, 2003.

101. Jayaraman, L. and Prives, C. Covalent and noncovalent modifiers of the p53 protein. Cell Mol Life Sci, *55:* 76-87, 1999.

102. Ljungman, M. Dial 9-1-1 for p53: mechanisms of p53 activation by cellular stress. Neoplasia, *2:* 208-225, 2000.

103. Meek, D. W. and Knippschild, U. Posttranslational modification of MDM2. Mol Cancer Res, *1:* 1017-1026, 2003.

104. Katayama, H., Sasai, K., Kawai, H., Yuan, Z. M., Bondaruk, J., Suzuki, F., Fujii, S., Arlinghaus, R. B., Czerniak, B. A., and Sen, S. Phosphorylation by aurora kinase A induces Mdm2-mediated destabilization and inhibition of p53. Nat Genet, *36:* 55-62, 2004.

105. Li, H. H., Li, A. G., Sheppard, H. M., and Liu, X. Phosphorylation on Thr-55 by TAF1 mediates degradation of p53: a role for TAF1 in cell G1 progression. Mol Cell, *13:* 867-878, 2004.

106. Zhang, Y. and Xiong, Y. A p53 amino-terminal nuclear export signal inhibited by DNA damage-induced phosphorylation. Science, *292:* 1910-1915, 2001.

107. Li, M., Luo, J., Brooks, C. L., and Gu, W. Acetylation of p53 inhibits its ubiquitination by Mdm2. J Biol Chem, *277:* 50607-50611, 2002.

108. Gostissa, M., Hengstermann, A., Fogal, V., Sandy, P., Schwarz, S. E., Scheffner, M., and Del Sal, G. Activation of p53 by conjugation to the ubiquitin-like protein SUMO-1. Embo J, *18:* 6462-6471, 1999.

109. Rodriguez, M. S., Desterro, J. M., Lain, S., Midgley, C. A., Lane, D. P., and Hay, R. T. SUMO-1 modification activates the transcriptional response of p53. Embo J, *18:* 6455-6461, 1999.

110. Muller, S., Berger, M., Lehembre, F., Seeler, J. S., Haupt, Y., and Dejean, A. c-Jun and p53 activity is modulated by SUMO-1 modification. J Biol Chem, *275:* 13321-13329, 2000.

111. Yang, X. J. Multisite protein modification and intramolecular signaling. Oncogene, *24:* 1653-1662, 2005.

112. Sims, R. J., 3rd, Nishioka, K., and Reinberg, D. Histone lysine methylation: a signature for chromatin function. Trends Genet, *19:* 629-639, 2003.

113. Freedman, D. A., Wu, L., and Levine, A. J. Functions of the MDM2 oncoprotein. Cell Mol Life Sci, *55:* 96-107, 1999.

114. Blattner, C., Sparks, A., and Lane, D. Transcription factor E2F-1 is upregulated in response to DNA damage in a manner analogous to that of p53. Mol Cell Biol, *19:* 3704-3713, 1999.

115. Zeng, X., Keller, D., Wu, L., and Lu, H. UV but not gamma irradiation accelerates p53-induced apoptosis of teratocarcinoma cells by repressing MDM2 transcription. Cancer Res, *60:* 6184-6188, 2000.

116. Ma, Y., Yuan, R., Meng, Q., Goldberg, I. D., Rosen, E. M., and Fan, S. P53-independent down-regulation of Mdm2 in human cancer cells treated with adriamycin. Mol Cell Biol Res Commun, *3:* 122-128, 2000.

117. Gronroos, E., Terentiev, A. A., Punga, T., and Ericsson, J. YY1 inhibits the activation of the p53 tumor suppressor in response to genotoxic stress. Proc Natl Acad Sci U S A, *101:* 12165-12170, 2004.

118. Sui, G., Affar el, B., Shi, Y., Brignone, C., Wall, N. R., Yin, P., Donohoe, M., Luke, M. P., Calvo, D., and Grossman, S. R. Yin Yang 1 is a negative regulator of p53. Cell, *117:* 859-872, 2004.
119. Li, M., Brooks, C. L., Kon, N., and Gu, W. A dynamic role of HAUSP in the p53-Mdm2 pathway. Mol Cell, *13:* 879-886, 2004.
120. Cummins, J. M., Rago, C., Kohli, M., Kinzler, K. W., Lengauer, C., and Vogelstein, B. Tumour suppression: disruption of HAUSP gene stabilizes p53. Nature, *428:* 1 p following 486, 2004.
121. Hsieh, J. K., Chan, F. S., O'Connor, D. J., Mittnacht, S., Zhong, S., and Lu, X. RB regulates the stability and the apoptotic function of p53 via MDM2. Mol Cell, *3:* 181-193, 1999.
122. Lohrum, M. A., Ludwig, R. L., Kubbutat, M. H., Hanlon, M., and Vousden, K. H. Regulation of HDM2 activity by the ribosomal protein L11. Cancer Cell, *3:* 577-587, 2003.
123. Bhat, K. P., Itahana, K., Jin, A., and Zhang, Y. Essential role of ribosomal protein L11 in mediating growth inhibition-induced p53 activation. Embo J, *23:* 2402-2412, 2004.
124. Zhang, Y., Wolf, G. W., Bhat, K., Jin, A., Allio, T., Burkhart, W. A., and Xiong, Y. Ribosomal protein L11 negatively regulates oncoprotein MDM2 and mediates a p53-dependent ribosomal-stress checkpoint pathway. Mol Cell Biol, *23:* 8902-8912, 2003.
125. Yang, H. Y., Wen, Y. Y., Chen, C. H., Lozano, G., and Lee, M. H. 14-3-3 sigma positively regulates p53 and suppresses tumor growth. Mol Cell Biol, *23:* 7096-7107, 2003.
126. Bernardi, R., Scaglioni, P. P., Bergmann, S., Horn, H. F., Vousden, K. H., and Pandolfi, P. P. PML regulates p53 stability by sequestering Mdm2 to the nucleolus. Nat Cell Biol, *6:* 665-672, 2004.
127. Lane, D. P. Cancer. p53, guardian of the genome. Nature, *358:* 15-16, 1992.

128. Crook, T., Marston, N. J., Sara, E. A., and Vousden, K. H. Transcriptional activation by p53 correlates with suppression of growth but not transformation. Cell, *79:* 817-827, 1994.
129. Pietenpol, J. A., Tokino, T., Thiagalingam, S., el-Deiry, W. S., Kinzler, K. W., and Vogelstein, B. Sequence-specific transcriptional activation is essential for growth suppression by p53. Proc Natl Acad Sci U S A, *91:* 1998-2002, 1994.
130. Chao, C., Saito, S., Kang, J., Anderson, C. W., Appella, E., and Xu, Y. p53 transcriptional activity is essential for p53-dependent apoptosis following DNA damage. Embo J, *19:* 4967-4975, 2000.
131. El-Deiry, W. S. The role of p53 in chemosensitivity and radiosensitivity. Oncogene, *22:* 7486-7495, 2003.
132. Oren, M. Decision making by p53: life, death and cancer. Cell Death Differ, *10:* 431-442, 2003.
133. Mirza, A., Wu, Q., Wang, L., McClanahan, T., Bishop, W. R., Gheyas, F., Ding, W., Hutchins, B., Hockenberry, T., Kirschmeier, P., Greene, J. R., and Liu, S. Global transcriptional program of p53 target genes during the process of apoptosis and cell cycle progression. Oncogene, *22:* 3645-3654, 2003.
134. Kho, P. S., Wang, Z., Zhuang, L., Li, Y., Chew, J. L., Ng, H. H., Liu, E. T., and Yu, Q. p53-regulated transcriptional program associated with genotoxic stress-induced apoptosis. J Biol Chem, *279:* 21183-21192, 2004.
135. Vousden, K. H. and Lu, X. Live or let die: the cell's response to p53. Nat Rev Cancer, *2:* 594-604, 2002.
136. Sionov, R. V. and Haupt, Y. The cellular response to p53: the decision between life and death. Oncogene, *18:* 6145-6157, 1999.
137. Kern, S. E., Kinzler, K. W., Bruskin, A., Jarosz, D., Friedman, P., Prives, C., and Vogelstein, B. Identification of p53 as a sequence-specific DNA-binding protein. Science, *252:* 1708-1711, 1991.

138. Takimoto, R. and El-Deiry, W. S. Wild-type p53 transactivates the KILLER/DR5 gene through an intronic sequence-specific DNA-binding site. Oncogene, *19:* 1735-1743, 2000.
139. Liu, X., Yue, P., Khuri, F. R., and Sun, S. Y. p53 upregulates death receptor 4 expression through an intronic p53 binding site. Cancer Res, *64:* 5078-5083, 2004.
140. Miyashita, T., Harigai, M., Hanada, M., and Reed, J. C. Identification of a p53-dependent negative response element in the bcl-2 gene. Cancer Res, *54:* 3131-3135, 1994.
141. Murphy, M., Hinman, A., and Levine, A. J. Wild-type p53 negatively regulates the expression of a microtubule-associated protein. Genes Dev, *10:* 2971-2980, 1996.
142. Roperch, J. P., Alvaro, V., Prieur, S., Tuynder, M., Nemani, M., Lethrosne, F., Piouffre, L., Gendron, M. C., Israeli, D., Dausset, J., Oren, M., Amson, R., and Telerman, A. Inhibition of presenilin 1 expression is promoted by p53 and p21WAF-1 and results in apoptosis and tumor suppression. Nat Med, *4:* 835-838, 1998.
143. Li, B. and Lee, M. Y. Transcriptional regulation of the human DNA polymerase delta catalytic subunit gene POLD1 by p53 tumor suppressor and Sp1. J Biol Chem, *276:* 29729-29739, 2001.
144. Hoffman, W. H., Biade, S., Zilfou, J. T., Chen, J., and Murphy, M. Transcriptional repression of the anti-apoptotic survivin gene by wild type p53. J Biol Chem, *277:* 3247-3257, 2002.
145. Budhram-Mahadeo, V., Morris, P. J., Smith, M. D., Midgley, C. A., Boxer, L. M., and Latchman, D. S. p53 suppresses the activation of the Bcl-2 promoter by the Brn-3a POU family transcription factor. J Biol Chem, *274:* 15237-15244, 1999.
146. Wu, Y., Mehew, J. W., Heckman, C. A., Arcinas, M., and Boxer, L. M. Negative regulation of bcl-2 expression by p53 in hematopoietic cells. Oncogene, *20:* 240-251, 2001.
147. Seto, E., Usheva, A., Zambetti, G. P., Momand, J., Horikoshi, N., Weinmann, R., Levine, A. J., and Shenk, T. Wild-type p53 binds to

the TATA-binding protein and represses transcription. Proc Natl Acad Sci U S A, *89:* 12028-12032, 1992.

148. Truant, R., Xiao, H., Ingles, C. J., and Greenblatt, J. Direct interaction between the transcriptional activation domain of human p53 and the TATA box-binding protein. J Biol Chem, *268:* 2284-2287, 1993.

149. Horikoshi, N., Usheva, A., Chen, J., Levine, A. J., Weinmann, R., and Shenk, T. Two domains of p53 interact with the TATA-binding protein, and the adenovirus 13S E1A protein disrupts the association, relieving p53-mediated transcriptional repression. Mol Cell Biol, *15:* 227-234, 1995.

150. Farmer, G., Colgan, J., Nakatani, Y., Manley, J. L., and Prives, C. Functional interaction between p53, the TATA-binding protein (TBP), andTBP-associated factors in vivo. Mol Cell Biol, *16:* 4295-4304, 1996.

151. Koumenis, C., Alarcon, R., Hammond, E., Sutphin, P., Hoffman, W., Murphy, M., Derr, J., Taya, Y., Lowe, S. W., Kastan, M., and Giaccia, A. Regulation of p53 by hypoxia: dissociation of transcriptional repression and apoptosis from p53-dependent transactivation. Mol Cell Biol, *21:* 1297-1310, 2001.

152. Murphy, M., Ahn, J., Walker, K. K., Hoffman, W. H., Evans, R. M., Levine, A. J., and George, D. L. Transcriptional repression by wild-type p53 utilizes histone deacetylases, mediated by interaction with mSin3a. Genes Dev, *13:* 2490-2501, 1999.

153. Mirza, A., McGuirk, M., Hockenberry, T. N., Wu, Q., Ashar, H., Black, S., Wen, S. F., Wang, L., Kirschmeier, P., Bishop, W. R., Nielsen, L. L., Pickett, C. B., and Liu, S. Human survivin is negatively regulated by wild-type p53 and participates in p53-dependent apoptotic pathway. Oncogene, *21:* 2613-2622, 2002.

154. Johnson, R. A., Ince, T. A., and Scotto, K. W. Transcriptional repression by p53 through direct binding to a novel DNA element. J Biol Chem, *276:* 27716-27720, 2001.

155. Rouault, J. P., Falette, N., Guehenneux, F., Guillot, C., Rimokh, R., Wang, Q., Berthet, C., Moyret-Lalle, C., Savatier, P., Pain, B., Shaw, P., Berger, R., Samarut, J., Magaud, J. P., Ozturk, M., Samarut, C., and Puisieux, A. Identification of BTG2, an antiproliferative p53-dependent component of the DNA damage cellular response pathway. Nat Genet, *14:* 482-486, 1996.

156. Tirone, F. The gene PC3(TIS21/BTG2), prototype member of the PC3/BTG/TOB family: regulator in control of cell growth, differentiation, and DNA repair? J Cell Physiol, *187:* 155-165, 2001.

157. Goldschneider, D., Million, K., Meiller, A., Haddada, H., Puisieux, A., Benard, J., May, E., and Douc-Rasy, S. The neurogene BTG2TIS21/PC3 is transactivated by DeltaNp73alpha via p53 specifically in neuroblastoma cells. J Cell Sci, *118:* 1245-1253, 2005.

158. Davison, T. S., Vagner, C., Kaghad, M., Ayed, A., Caput, D., and Arrowsmith, C. H. p73 and p63 are homotetramers capable of weak heterotypic interactions with each other but not with p53. J Biol Chem, *274:* 18709-18714, 1999.

159. Polyak, K., Xia, Y., Zweier, J. L., Kinzler, K. W., and Vogelstein, B. A model for p53-induced apoptosis. Nature, *389:* 300-305, 1997.

160. Contente, A., Dittmer, A., Koch, M. C., Roth, J., and Dobbelstein, M. A polymorphic microsatellite that mediates induction of PIG3 by p53. Nat Genet, *30:* 315-320, 2002.

161. Yin, Y., Liu, Y. X., Jin, Y. J., Hall, E. J., and Barrett, J. C. PAC1 phosphatase is a transcription target of p53 in signalling apoptosis and growth suppression. Nature, *422:* 527-531, 2003.

162. el-Deiry, W. S., Tokino, T., Velculescu, V. E., Levy, D. B., Parsons, R., Trent, J. M., Lin, D., Mercer, W. E., Kinzler, K. W., and Vogelstein, B. WAF1, a potential mediator of p53 tumor suppression. Cell, *75:* 817-825, 1993.

163. Brugarolas, J., Chandrasekaran, C., Gordon, J. I., Beach, D., Jacks, T., and Hannon, G. J. Radiation-induced cell cycle arrest compromised by p21 deficiency. Nature, *377:* 552-557, 1995.
164. Harper, J. W., Adami, G. R., Wei, N., Keyomarsi, K., and Elledge, S. J. The p21 Cdk-interacting protein Cip1 is a potent inhibitor of G1 cyclin-dependent kinases. Cell, *75:* 805-816, 1993.
165. Agarwal, M. L., Agarwal, A., Taylor, W. R., and Stark, G. R. p53 controls both the G2/M and the G1 cell cycle checkpoints and mediates reversible growth arrest in human fibroblasts. Proc Natl Acad Sci U S A, *92:* 8493-8497, 1995.
166. Bates, S., Ryan, K. M., Phillips, A. C., and Vousden, K. H. Cell cycle arrest and DNA endoreduplication following p21Waf1/Cip1 expression. Oncogene, *17:* 1691-1703, 1998.
167. Wang, X. W., Zhan, Q., Coursen, J. D., Khan, M. A., Kontny, H. U., Yu, L., Hollander, M. C., O'Connor, P. M., Fornace, A. J., Jr., and Harris, C. C. GADD45 induction of a G2/M cell cycle checkpoint. Proc Natl Acad Sci U S A, *96:* 3706-3711, 1999.
168. Ohki, R., Nemoto, J., Murasawa, H., Oda, E., Inazawa, J., Tanaka, N., and Taniguchi, T. Reprimo, a new candidate mediator of the p53-mediated cell cycle arrest at the G2 phase. J Biol Chem, *275:* 22627-22630, 2000.
169. Cryns, V. and Yuan, J. Proteases to die for. Genes Dev, *12:* 1551-1570, 1998.
170. Ashkenazi, A. and Dixit, V. M. Death receptors: signaling and modulation. Science, *281:* 1305-1308, 1998.
171. Wang, X. The expanding role of mitochondria in apoptosis. Genes Dev, *15:* 2922-2933, 2001.
172. Du, C., Fang, M., Li, Y., Li, L., and Wang, X. Smac, a mitochondrial protein that promotes cytochrome c-dependent caspase activation by eliminating IAP inhibition. Cell, *102:* 33-42, 2000.
173. Verhagen, A. M., Ekert, P. G., Pakusch, M., Silke, J., Connolly, L. M., Reid, G. E., Moritz, R. L., Simpson, R. J., and Vaux, D. L.

Identification of DIABLO, a mammalian protein that promotes apoptosis by binding to and antagonizing IAP proteins. Cell, *102:* 43-53, 2000.

174. Suzuki, Y., Imai, Y., Nakayama, H., Takahashi, K., Takio, K., and Takahashi, R. A serine protease, HtrA2, is released from the mitochondria and interacts with XIAP, inducing cell death. Mol Cell, *8:* 613-621, 2001.
175. Joza, N., Susin, S. A., Daugas, E., Stanford, W. L., Cho, S. K., Li, C. Y., Sasaki, T., Elia, A. J., Cheng, H. Y., Ravagnan, L., Ferri, K. F., Zamzami, N., Wakeham, A., Hakem, R., Yoshida, H., Kong, Y. Y., Mak, T. W., Zuniga-Pflucker, J. C., Kroemer, G., and Penninger, J. M. Essential role of the mitochondrial apoptosis-inducing factor in programmed cell death. Nature, *410:* 549-554, 2001.
176. Wang, X., Yang, C., Chai, J., Shi, Y., and Xue, D. Mechanisms of AIF-mediated apoptotic DNA degradation in Caenorhabditis elegans. Science, *298:* 1587-1592, 2002.
177. Miyashita, T. and Reed, J. C. Tumor suppressor p53 is a direct transcriptional activator of the human bax gene. Cell, *80:* 293-299, 1995.
178. Cory, S. and Adams, J. M. The Bcl2 family: regulators of the cellular life-or-death switch. Nat Rev Cancer, *2:* 647-656, 2002.
179. Kuwana, T., Mackey, M. R., Perkins, G., Ellisman, M. H., Latterich, M., Schneiter, R., Green, D. R., and Newmeyer, D. D. Bid, Bax, and lipids cooperate to form supramolecular openings in the outer mitochondrial membrane. Cell, *111:* 331-342, 2002.
180. Kelekar, A. and Thompson, C. B. Bcl-2-family proteins: the role of the BH3 domain in apoptosis. Trends Cell Biol, *8:* 324-330, 1998.
181. Yu, J., Zhang, L., Hwang, P. M., Kinzler, K. W., and Vogelstein, B. PUMA induces the rapid apoptosis of colorectal cancer cells. Mol Cell, *7:* 673-682, 2001.

182. Bouillet, P. and Strasser, A. BH3-only proteins - evolutionarily conserved proapoptotic Bcl-2 family members essential for initiating programmed cell death. J Cell Sci, *115:* 1567-1574, 2002.
183. Oda, E., Ohki, R., Murasawa, H., Nemoto, J., Shibue, T., Yamashita, T., Tokino, T., Taniguchi, T., and Tanaka, N. Noxa, a BH3-only member of the Bcl-2 family and candidate mediator of p53-induced apoptosis. Science, *288:* 1053-1058, 2000.
184. Nakano, K. and Vousden, K. H. PUMA, a novel proapoptotic gene, is induced by p53. Mol Cell, *7:* 683-694, 2001.
185. Tan, K. O., Tan, K. M., and Yu, V. C. A novel BH3-like domain in BID is required for intramolecular interaction and autoinhibition of pro-apoptotic activity. J Biol Chem, *274:* 23687-23690, 1999.
186. Puthalakath, H. and Strasser, A. Keeping killers on a tight leash: transcriptional and post-translational control of the pro-apoptotic activity of BH3-only proteins. Cell Death Differ, *9:* 505-512, 2002.
187. Yu, J., Wang, Z., Kinzler, K. W., Vogelstein, B., and Zhang, L. PUMA mediates the apoptotic response to p53 in colorectal cancer cells. Proc Natl Acad Sci U S A, *100:* 1931-1936, 2003.
188. Reimertz, C., Kogel, D., Rami, A., Chittenden, T., and Prehn, J. H. Gene expression during ER stress-induced apoptosis in neurons: induction of the BH3-only protein Bbc3/PUMA and activation of the mitochondrial apoptosis pathway. J Cell Biol, *162:* 587-597, 2003.
189. Danial, N. N., Gramm, C. F., Scorrano, L., Zhang, C. Y., Krauss, S., Ranger, A. M., Datta, S. R., Greenberg, M. E., Licklider, L. J., Lowell, B. B., Gygi, S. P., and Korsmeyer, S. J. BAD and glucokinase reside in a mitochondrial complex that integrates glycolysis and apoptosis. Nature, *424:* 952-956, 2003.
190. Yin, X. M., Wang, K., Gross, A., Zhao, Y., Zinkel, S., Klocke, B., Roth, K. A., and Korsmeyer, S. J. Bid-deficient mice are resistant to Fas-induced hepatocellular apoptosis. Nature, *400:* 886-891, 1999.
191. Bouillet, P., Metcalf, D., Huang, D. C., Tarlinton, D. M., Kay, T. W., Kontgen, F., Adams, J. M., and Strasser, A. Proapoptotic Bcl-2

relative Bim required for certain apoptotic responses, leukocyte homeostasis, and to preclude autoimmunity. Science, *286:* 1735-1738, 1999.

192. Cheng, E. H., Wei, M. C., Weiler, S., Flavell, R. A., Mak, T. W., Lindsten, T., and Korsmeyer, S. J. BCL-2, BCL-X(L) sequester BH3 domain-only molecules preventing BAX- and BAK-mediated mitochondrial apoptosis. Mol Cell, *8:* 705-711, 2001.
193. Zong, W. X., Lindsten, T., Ross, A. J., MacGregor, G. R., and Thompson, C. B. BH3-only proteins that bind pro-survival Bcl-2 family members fail to induce apoptosis in the absence of Bax and Bak. Genes Dev, *15:* 1481-1486, 2001.
194. Shangary, S. and Johnson, D. E. Peptides derived from BH3 domains of Bcl-2 family members: a comparative analysis of inhibition of Bcl-2, Bcl-x(L) and Bax oligomerization, induction of cytochrome c release, and activation of cell death. Biochemistry, *41:* 9485-9495, 2002.
195. Letai, A., Bassik, M. C., Walensky, L. D., Sorcinelli, M. D., Weiler, S., and Korsmeyer, S. J. Distinct BH3 domains either sensitize or activate mitochondrial apoptosis, serving as prototype cancer therapeutics. Cancer Cell, *2:* 183-192, 2002.
196. Oda, K., Arakawa, H., Tanaka, T., Matsuda, K., Tanikawa, C., Mori, T., Nishimori, H., Tamai, K., Tokino, T., Nakamura, Y., and Taya, Y. p53AIP1, a potential mediator of p53-dependent apoptosis, and its regulation by Ser-46-phosphorylated p53. Cell, *102:* 849-862, 2000.
197. Donald, S. P., Sun, X. Y., Hu, C. A., Yu, J., Mei, J. M., Valle, D., and Phang, J. M. Proline oxidase, encoded by p53-induced gene-6, catalyzes the generation of proline-dependent reactive oxygen species. Cancer Res, *61:* 1810-1815, 2001.
198. Hwang, P. M., Bunz, F., Yu, J., Rago, C., Chan, T. A., Murphy, M. P., Kelso, G. F., Smith, R. A., Kinzler, K. W., and Vogelstein, B. Ferredoxin reductase affects p53-dependent, 5-fluorouracil-induced apoptosis in colorectal cancer cells. Nat Med, *7:* 1111-1117, 2001.

199. Mihara, M., Erster, S., Zaika, A., Petrenko, O., Chittenden, T., Pancoska, P., and Moll, U. M. p53 has a direct apoptogenic role at the mitochondria. Mol Cell, *11:* 577-590, 2003.
200. Nagata, S. and Golstein, P. The Fas death factor. Science, *267:* 1449-1456, 1995.
201. Muzio, M. Signalling by proteolysis: death receptors induce apoptosis. Int J Clin Lab Res, *28:* 141-147, 1998.
202. Bouvard, V., Zaitchouk, T., Vacher, M., Duthu, A., Canivet, M., Choisy-Rossi, C., Nieruchalski, M., and May, E. Tissue and cell-specific expression of the p53-target genes: bax, fas, mdm2 and waf1/p21, before and following ionising irradiation in mice. Oncogene, *19:* 649-660, 2000.
203. Bennett, M., Macdonald, K., Chan, S. W., Luzio, J. P., Simari, R., and Weissberg, P. Cell surface trafficking of Fas: a rapid mechanism of p53-mediated apoptosis. Science, *282:* 290-293, 1998.
204. Lin, Y., Ma, W., and Benchimol, S. Pidd, a new death-domain-containing protein, is induced by p53 and promotes apoptosis. Nat Genet, *26:* 122-127, 2000.
205. Tinel, A. and Tschopp, J. The PIDDosome, a protein complex implicated in activation of caspase-2 in response to genotoxic stress. Science, *304:* 843-846, 2004.
206. Attardi, L. D., Reczek, E. E., Cosmas, C., Demicco, E. G., McCurrach, M. E., Lowe, S. W., and Jacks, T. PERP, an apoptosis-associated target of p53, is a novel member of the PMP-22/gas3 family. Genes Dev, *14:* 704-718, 2000.
207. Gudkov, A. V. and Komarova, E. A. The role of p53 in determining sensitivity to radiotherapy. Nat Rev Cancer, *3:* 117-129, 2003.
208. De Feudis, P., Vignati, S., Rossi, C., Mincioni, T., Giavazzi, R., D'Incalci, M., and Broggini, M. Driving p53 response to Bax activation greatly enhances sensitivity to taxol by inducing massive apoptosis. Neoplasia, *2:* 202-207, 2000.

209. Vousden, K. H. p53: death star. Cell, *103:* 691-694, 2000.
210. Friedlander, P., Haupt, Y., Prives, C., and Oren, M. A mutant p53 that discriminates between p53-responsive genes cannot induce apoptosis. Mol Cell Biol, *16:* 4961-4971, 1996.
211. Ludwig, R. L., Bates, S., and Vousden, K. H. Differential activation of target cellular promoters by p53 mutants with impaired apoptotic function. Mol Cell Biol, *16:* 4952-4960, 1996.
212. Szak, S. T., Mays, D., and Pietenpol, J. A. Kinetics of p53 binding to promoter sites in vivo. Mol Cell Biol, *21:* 3375-3386, 2001.
213. Kaeser, M. D. and Iggo, R. D. Chromatin immunoprecipitation analysis fails to support the latency model for regulation of p53 DNA binding activity in vivo. Proc Natl Acad Sci U S A, *99:* 95-100, 2002.
214. Shikama, N., Lee, C. W., France, S., Delavaine, L., Lyon, J., Krstic-Demonacos, M., and La Thangue, N. B. A novel cofactor for p300 that regulates the p53 response. Mol Cell, *4:* 365-376, 1999.
215. Samuels-Lev, Y., O'Connor, D. J., Bergamaschi, D., Trigiante, G., Hsieh, J. K., Zhong, S., Campargue, I., Naumovski, L., Crook, T., and Lu, X. ASPP proteins specifically stimulate the apoptotic function of p53. Mol Cell, *8:* 781-794, 2001.
216. Flores, E. R., Tsai, K. Y., Crowley, D., Sengupta, S., Yang, A., McKeon, F., and Jacks, T. p63 and p73 are required for p53-dependent apoptosis in response to DNA damage. Nature, *416:* 560-564, 2002.
217. Hayflick, L. and Moorhead, P. S. The serial cultivation of human diploid cell strains. Exp Cell Res, *25:* 585-621, 1961.
218. Blackburn, E. H. Telomere states and cell fates. Nature, *408:* 53-56, 2000.
219. Harley, C. B., Futcher, A. B., and Greider, C. W. Telomeres shorten during ageing of human fibroblasts. Nature, *345:* 458-460, 1990.
220. de Lange, T. Cell biology. Telomere capping--one strand fits all. Science, *292:* 1075-1076, 2001.

221. Watson, J. D. Origin of concatemeric T7 DNA. Nat New Biol, *239:* 197-201, 1972.
222. Blackburn, E. H. Switching and signaling at the telomere. Cell, *106:* 661-673, 2001.
223. Kim , S., Kaminker, P., and Campisi, J. Telomeres, aging and cancer: in search of a happy ending. Oncogene, *21:* 503-511, 2002.
224. Campisi, J. Cellular senescence as a tumor-suppressor mechanism. Trends Cell Biol, *11:* S27-31, 2001.
225. Dimri, G. P., Testori, A., Acosta, M., and Campisi, J. Replicative senescence, aging and growth-regulatory transcription factors. Biol Signals, *5:* 154-162, 1996.
226. Munoz-Jordan, J. L., Cross, G. A., de Lange, T., and Griffith, J. D. t-loops at trypanosome telomeres. Embo J, *20:* 579-588, 2001.
227. de Lange, T. Protection of mammalian telomeres. Oncogene, *21:* 532-540, 2002.
228. Shay, J. W. and Wright, W. E. Ageing and cancer: the telomere and telomerase connection. Novartis Found Symp, *235:* 116-125; discussion 125-119, 146-119, 2001.
229. Serrano, M., Lin, A. W., McCurrach, M. E., Beach, D., and Lowe, S. W. Oncogenic ras provokes premature cell senescence associated with accumulation of p53 and p16INK4a. Cell, *88:* 593-602, 1997.
230. Serrano, M. and Blasco, M. A. Putting the stress on senescence. Curr Opin Cell Biol, *13:* 748-753, 2001.
231. Lloyd, A. C. Limits to lifespan. Nat Cell Biol, *4:* E25-27, 2002.
232. von Zglinicki, T., Saretzki, G., Docke, W., and Lotze, C. Mild hyperoxia shortens telomeres and inhibits proliferation of fibroblasts: a model for senescence? Exp Cell Res, *220:* 186-193, 1995.
233. Forsyth, N. R., Evans, A. P., Shay, J. W., and Wright, W. E. Developmental differences in the immortalization of lung fibroblasts by telomerase. Aging Cell, *2:* 235-243, 2003.

234. Parrinello, S., Samper, E., Krtolica, A., Goldstein, J., Melov, S., and Campisi, J. Oxygen sensitivity severely limits the replicative lifespan of murine fibroblasts. Nat Cell Biol, *5:* 741-747, 2003.

235. Smogorzewska, A. and de Lange, T. Different telomere damage signaling pathways in human and mouse cells. Embo J, *21:* 4338-4348, 2002.

236. d'Adda di Fagagna, F., Reaper, P. M., Clay-Farrace, L., Fiegler, H., Carr, P., Von Zglinicki, T., Saretzki, G., Carter, N. P., and Jackson, S. P. A DNA damage checkpoint response in telomere-initiated senescence. Nature, *426:* 194-198, 2003.

237. Gire, V., Roux, P., Wynford-Thomas, D., Brondello, J. M., and Dulic, V. DNA damage checkpoint kinase Chk2 triggers replicative senescence. Embo J, *23:* 2554-2563, 2004.

238. Lowe, S. W. and Sherr, C. J. Tumor suppression by Ink4a-Arf: progress and puzzles. Curr Opin Genet Dev, *13:* 77-83, 2003.

239. Ben-Porath, I. and Weinberg, R. A. The signals and pathways activating cellular senescence. Int J Biochem Cell Biol, *37:* 961-976, 2005.

240. Hwang, B. J., Ford, J. M., Hanawalt, P. C., and Chu, G. Expression of the p48 xeroderma pigmentosum gene is p53-dependent and is involved in global genomic repair. Proc Natl Acad Sci U S A, *96:* 424-428, 1999.

241. Adimoolam, S. and Ford, J. M. p53 and DNA damage-inducible expression of the xeroderma pigmentosum group C gene. Proc Natl Acad Sci U S A, *99:* 12985-12990, 2002.

242. Itoh, T., O'Shea, C., and Linn, S. Impaired regulation of tumor suppressor p53 caused by mutations in the xeroderma pigmentosum DDB2 gene: mutual regulatory interactions between p48(DDB2) and p53. Mol Cell Biol, *23:* 7540-7553, 2003.

243. Reardon, J. T., Mu, D., and Sancar, A. Overproduction, purification, and characterization of the XPC subunit of the human DNA repair excision nuclease. J Biol Chem, *271:* 19451-19456, 1996.

244. Rubbi, C. P. and Milner, J. p53 is a chromatin accessibility factor for nucleotide excision repair of DNA damage. Embo J, *22:* 975-986, 2003.

245. Seeberg, E., Eide, L., and Bjoras, M. The base excision repair pathway. Trends Biochem Sci, *20:* 391-397, 1995.

246. Sobol, R. W., Kartalou, M., Almeida, K. H., Joyce, D. F., Engelward, B. P., Horton, J. K., Prasad, R., Samson, L. D., and Wilson, S. H. Base excision repair intermediates induce p53-independent cytotoxic and genotoxic responses. J Biol Chem, *278:* 39951-39959, 2003.

247. Zhou, J., Ahn, J., Wilson, S. H., and Prives, C. A role for p53 in base excision repair. Embo J, *20:* 914-923, 2001.

248. Zurer, I., Hofseth, L. J., Cohen, Y., Xu-Welliver, M., Hussain, S. P., Harris, C. C., and Rotter, V. The role of p53 in base excision repair following genotoxic stress. Carcinogenesis, *25:* 11-19, 2004.

249. Scherer, S. J., Maier, S. M., Seifert, M., Hanselmann, R. G., Zang, K. D., Muller-Hermelink, H. K., Angel, P., Welter, C., and Schartl, M. p53 and c-Jun functionally synergize in the regulation of the DNA repair gene hMSH2 in response to UV. J Biol Chem, *275:* 37469-37473, 2000.

250. Yang, T., Namba, H., Hara, T., Takmura, N., Nagayama, Y., Fukata, S., Ishikawa, N., Kuma, K., Ito, K., and Yamashita, S. p53 induced by ionizing radiation mediates DNA end-jointing activity, but not apoptosis of thyroid cells. Oncogene, *14:* 1511-1519, 1997.

251. Tang, W., Willers, H., and Powell, S. N. p53 directly enhances rejoining of DNA double-strand breaks with cohesive ends in gamma-irradiated mouse fibroblasts. Cancer Res, *59:* 2562-2565, 1999.

252. Bristow, R. G., Hu, Q., Jang, A., Chung, S., Peacock, J., Benchimol, S., and Hill, R. Radioresistant MTp53-expressing rat embryo cell transformants exhibit increased DNA-dsb rejoining during exposure to ionizing radiation. Oncogene, *16:* 1789-1802, 1998.

253. Bill, C. A., Yu, Y., Miselis, N. R., Little, J. B., and Nickoloff, J. A. A role for p53 in DNA end rejoining by human cell extracts. Mutat Res, *385:* 21-29, 1997.

254. Lee, H., Sun, D., Larner, J. M., and Wu, F. S. The tumor suppressor p53 can reduce stable transfection in the presence of irradiation. J Biomed Sci, *6:* 285-292, 1999.

255. Akyuz, N., Boehden, G. S., Susse, S., Rimek, A., Preuss, U., Scheidtmann, K. H., and Wiesmuller, L. DNA substrate dependence of p53-mediated regulation of double-strand break repair. Mol Cell Biol, *22:* 6306-6317, 2002.

256. Okorokov, A. L., Warnock, L., and Milner, J. Effect of wild-type, S15D and R175H p53 proteins on DNA end joining in vitro: potential mechanism of DNA double-strand break repair modulation. Carcinogenesis, *23:* 549-557, 2002.

257. Cromie, G. A., Connelly, J. C., and Leach, D. R. Recombination at double-strand breaks and DNA ends: conserved mechanisms from phage to humans. Mol Cell, *8:* 1163-1174, 2001.

258. Liu, Y. and Kulesz-Martin, M. p53 protein at the hub of cellular DNA damage response pathways through sequence-specific and non-sequence-specific DNA binding. Carcinogenesis, *22:* 851-860, 2001.

259. Liang, F., Han, M., Romanienko, P. J., and Jasin, M. Homology-directed repair is a major double-strand break repair pathway in mammalian cells. Proc Natl Acad Sci U S A, *95:* 5172-5177, 1998.

260. Szostak, J. W., Orr-Weaver, T. L., Rothstein, R. J., and Stahl, F. W. The double-strand-break repair model for recombination. Cell, *33:* 25-35, 1983.

261. Haber, J. E. Partners and pathwaysrepairing a double-strand break. Trends Genet, *16:* 259-264, 2000.

262. Mazin, A. V., Alexeev, A. A., and Kowalczykowski, S. C. A novel function of Rad54 protein. Stabilization of the Rad51 nucleoprotein filament. J Biol Chem, *278:* 14029-14036, 2003.

263. Petukhova, G., Stratton, S., and Sung, P. Catalysis of homologous DNA pairing by yeast Rad51 and Rad54 proteins. Nature, *393:* 91-94, 1998.

264. Bertrand, P., Saintigny, Y., and Lopez, B. S. p53's double life: transactivation-independent repression of homologous recombination. Trends Genet, *20:* 235-243, 2004.

265. Dudenhoffer, C., Rohaly, G., Will, K., Deppert, W., and Wiesmuller, L. Specific mismatch recognition in heteroduplex intermediates by p53 suggests a role in fidelity control of homologous recombination. Mol Cell Biol, *18:* 5332-5342, 1998.

266. Linke, S. P., Sengupta, S., Khabie, N., Jeffries, B. A., Buchhop, S., Miska, S., Henning, W., Pedeux, R., Wang, X. W., Hofseth, L. J., Yang, Q., Garfield, S. H., Sturzbecher, H. W., and Harris, C. C. p53 interacts with hRAD51 and hRAD54, and directly modulates homologous recombination. Cancer Res, *63:* 2596-2605, 2003.

267. Bouffler, S. D., Kemp, C. J., Balmain, A., and Cox, R. Spontaneous and ionizing radiation-induced chromosomal abnormalities in p53-deficient mice. Cancer Res, *55:* 3883-3889, 1995.

268. Fukasawa, K., Choi, T., Kuriyama, R., Rulong, S., and Vande Woude, G. F. Abnormal centrosome amplification in the absence of p53. Science, *271:* 1744-1747, 1996.

269. Cross, S. M., Sanchez, C. A., Morgan, C. A., Schimke, M. K., Ramel, S., Idzerda, R. L., Raskind, W. H., and Reid, B. J. A p53-dependent mouse spindle checkpoint. Science, *267:* 1353-1356, 1995.

270. Hickson, I. D. RecQ helicases: caretakers of the genome. Nat Rev Cancer, *3:* 169-178, 2003.

271. Sengupta, S. and Harris, C. C. p53: traffic cop at the crossroads of DNA repair and recombination. Nat Rev Mol Cell Biol, *6:* 44-55, 2005.

272. Sengupta, S., Linke, S. P., Pedeux, R., Yang, Q., Farnsworth, J., Garfield, S. H., Valerie, K., Shay, J. W., Ellis, N. A., Wasylyk, B.,

and Harris, C. C. BLM helicase-dependent transport of p53 to sites of stalled DNA replication forks modulates homologous recombination. Embo J, *22:* 1210-1222, 2003.

273. Tanaka, H., Arakawa, H., Yamaguchi, T., Shiraishi, K., Fukuda, S., Matsui, K., Takei, Y., and Nakamura, Y. A ribonucleotide reductase gene involved in a p53-dependent cell-cycle checkpoint for DNA damage. Nature, *404:* 42-49, 2000.
274. Dameron, K. M., Volpert, O. V., Tainsky, M. A., and Bouck, N. Control of angiogenesis in fibroblasts by p53 regulation of thrombospondin-1. Science, *265:* 1582-1584, 1994.
275. Weinstat-Saslow, D. L., Zabrenetzky, V. S., VanHoutte, K., Frazier, W. A., Roberts, D. D., and Steeg, P. S. Transfection of thrombospondin 1 complementary DNA into a human breast carcinoma cell line reduces primary tumor growth, metastatic potential, and angiogenesis. Cancer Res, *54:* 6504-6511, 1994.
276. Zabrenetzky, V., Harris, C. C., Steeg, P. S., and Roberts, D. D. Expression of the extracellular matrix molecule thrombospondin inversely correlates with malignant progression in melanoma, lung and breast carcinoma cell lines. Int J Cancer, *59:* 191-195, 1994.
277. Hsu, S. C., Volpert, O. V., Steck, P. A., Mikkelsen, T., Polverini, P. J., Rao, S., Chou, P., and Bouck, N. P. Inhibition of angiogenesis in human glioblastomas by chromosome 10 induction of thrombospondin-1. Cancer Res, *56:* 5684-5691, 1996.
278. Grant, S. W., Kyshtoobayeva, A. S., Kurosaki, T., Jakowatz, J., and Fruehauf, J. P. Mutant p53 correlates with reduced expression of thrombospondin-1, increased angiogenesis, and metastatic progression in melanoma. Cancer Detect Prev, *22:* 185-194, 1998.
279. Nishimori, H., Shiratsuchi, T., Urano, T., Kimura, Y., Kiyono, K., Tatsumi, K., Yoshida, S., Ono, M., Kuwano, M., Nakamura, Y., and Tokino, T. A novel brain-specific p53-target gene, BAI1, containing thrombospondin type 1 repeats inhibits experimental angiogenesis. Oncogene, *15:* 2145-2150, 1997.

280. Mashimo, T., Watabe, M., Hirota, S., Hosobe, S., Miura, K., Tegtmeyer, P. J., Rinker-Shaeffer, C. W., and Watabe, K. The expression of the KAI1 gene, a tumor metastasis suppressor, is directly activated by p53. Proc Natl Acad Sci U S A, *95:* 11307-11311, 1998.

281. Zou, Z., Gao, C., Nagaich, A. K., Connell, T., Saito, S., Moul, J. W., Seth, P., Appella, E., and Srivastava, S. p53 regulates the expression of the tumor suppressor gene maspin. J Biol Chem, *275:* 6051-6054, 2000.

282. Kunz, C., Pebler, S., Otte, J., and von der Ahe, D. Differential regulation of plasminogen activator and inhibitor gene transcription by the tumor suppressor p53. Nucleic Acids Res, *23:* 3710-3717, 1995.

283. Kaghad, M., Bonnet, H., Yang, A., Creancier, L., Biscan, J. C., Valent, A., Minty, A., Chalon, P., Lelias, J. M., Dumont, X., Ferrara, P., McKeon, F., and Caput, D. Monoallelically expressed gene related to p53 at 1p36, a region frequently deleted in neuroblastoma and other human cancers. Cell, *90:* 809-819, 1997.

284. Yang, A., Kaghad, M., Wang, Y., Gillett, E., Fleming, M. D., Dotsch, V., Andrews, N. C., Caput, D., and McKeon, F. p63, a p53 homolog at 3q27-29, encodes multiple products with transactivating, death-inducing, and dominant-negative activities. Mol Cell, *2:* 305-316, 1998.

285. Augustin, M., Bamberger, C., Paul, D., and Schmale, H. Cloning and chromosomal mapping of the human p53-related KET gene to chromosome 3q27 and its murine homolog Ket to mouse chromosome 16. Mamm Genome, *9:* 899-902, 1998.

286. Trink, B., Okami, K., Wu, L., Sriuranpong, V., Jen, J., and Sidransky, D. A new human p53 homologue. Nat Med, *4:* 747-748, 1998.

287. Osada, M., Ohba, M., Kawahara, C., Ishioka, C., Kanamaru, R., Katoh, I., Ikawa, Y., Nimura, Y., Nakagawara, A., Obinata, M., and

Ikawa, S. Cloning and functional analysis of human p51, which structurally and functionally resembles p53. Nat Med, *4:* 839-843, 1998.

288. Senoo, M., Seki, N., Ohira, M., Sugano, S., Watanabe, M., Inuzuka, S., Okamoto, T., Tachibana, M., Tanaka, T., Shinkai, Y., and Kato, H. A second p53-related protein, p73L, with high homology to p73. Biochem Biophys Res Commun, *248:* 603-607, 1998.
289. De Laurenzi, V., Costanzo, A., Barcaroli, D., Terrinoni, A., Falco, M., Annicchiarico-Petruzzelli, M., Levrero, M., and Melino, G. Two new p73 splice variants, gamma and delta, with different transcriptional activity. J Exp Med, *188:* 1763-1768, 1998.
290. Di Como, C. J., Gaiddon, C., and Prives, C. p73 function is inhibited by tumor-derived p53 mutants in mammalian cells. Mol Cell Biol, *19:* 1438-1449, 1999.
291. Courtois, S., Verhaegh, G., North, S., Luciani, M. G., Lassus, P., Hibner, U., Oren, M., and Hainaut, P. DeltaN-p53, a natural isoform of p53 lacking the first transactivation domain, counteracts growth suppression by wild-type p53. Oncogene, *21:* 6722-6728, 2002.
292. Yin, Y., Stephen, C. W., Luciani, M. G., and Fahraeus, R. p53 Stability and activity is regulated by Mdm2-mediated induction of alternative p53 translation products. Nat Cell Biol, *4:* 462-467, 2002.
293. Fillippovich, I., Sorokina, N., Gatei, M., Haupt, Y., Hobson, K., Moallem, E., Spring, K., Mould, M., McGuckin, M. A., Lavin, M. F., and Khanna, K. K. Transactivation-deficient p73alpha (p73Deltaexon2) inhibits apoptosis and competes with p53. Oncogene, *20:* 514-522, 2001.
294. Stiewe, T. and Putzer, B. M. Role of p73 in malignancy: tumor suppressor or oncogene? Cell Death Differ, *9:* 237-245, 2002.
295. Ishimoto, O., Kawahara, C., Enjo, K., Obinata, M., Nukiwa, T., and Ikawa, S. Possible oncogenic potential of DeltaNp73: a newly identified isoform of human p73. Cancer Res, *62:* 636-641, 2002.

296. Stiewe, T., Theseling, C. C., and Putzer, B. M. Transactivation-deficient Delta TA-p73 inhibits p53 by direct competition for DNA binding: implications for tumorigenesis. J Biol Chem, *277:* 14177-14185, 2002.

297. Irwin, M. S. and Kaelin, W. G., Jr. Role of the newer p53 family proteins in malignancy. Apoptosis, *6:* 17-29, 2001.

298. Mills, A. A., Zheng, B., Wang, X. J., Vogel, H., Roop, D. R., and Bradley, A. p63 is a p53 homologue required for limb and epidermal morphogenesis. Nature, *398:* 708-713, 1999.

299. Yang, A., Schweitzer, R., Sun, D., Kaghad, M., Walker, N., Bronson, R. T., Tabin, C., Sharpe, A., Caput, D., Crum, C., and McKeon, F. p63 is essential for regenerative proliferation in limb, craniofacial and epithelial development. Nature, *398:* 714-718, 1999.

300. Yang, A., Walker, N., Bronson, R., Kaghad, M., Oosterwegel, M., Bonnin, J., Vagner, C., Bonnet, H., Dikkes, P., Sharpe, A., McKeon, F., and Caput, D. p73-deficient mice have neurological, pheromonal and inflammatory defects but lack spontaneous tumours. Nature, *404:* 99-103, 2000.

301. Hibi, K., Trink, B., Patturajan, M., Westra, W. H., Caballero, O. L., Hill, D. E., Ratovitski, E. A., Jen, J., and Sidransky, D. AIS is an oncogene amplified in squamous cell carcinoma. Proc Natl Acad Sci U S A, *97:* 5462-5467, 2000.

302. Nozaki, M., Tada, M., Kashiwazaki, H., Hamou, M. F., Diserens, A. C., Shinohe, Y., Sawamura, Y., Iwasaki, Y., de Tribolet, N., and Hegi, M. E. p73 is not mutated in meningiomas as determined with a functional yeast assay but p73 expression increases with tumor grade. Brain Pathol, *11:* 296-305, 2001.

303. Ahomadegbe, J. C., Tourpin, S., Kaghad, M., Zelek, L., Vayssade, M., Mathieu, M. C., Rochard, F., Spielmann, M., Tursz, T., Caput, D., Riou, G., and Benard, J. Loss of heterozygosity, allele silencing and decreased expression of p73 gene in breast cancers:

prevalence of alterations in inflammatory breast cancers. Oncogene, *19:* 5413-5418, 2000.

304. Park, B. J., Lee, S. J., Kim, J. I., Lee, C. H., Chang, S. G., Park, J. H., and Chi, S. G. Frequent alteration of p63 expression in human primary bladder carcinomas. Cancer Res, *60:* 3370-3374, 2000.
305. Koga, F., Kawakami, S., Fujii, Y., Saito, K., Ohtsuka, Y., Iwai, A., Ando, N., Takizawa, T., Kageyama, Y., and Kihara, K. Impaired p63 expression associates with poor prognosis and uroplakin III expression in invasive urothelial carcinoma of the bladder. Clin Cancer Res, *9:* 5501-5507, 2003.
306. Urist, M. J., Di Como, C. J., Lu, M. L., Charytonowicz, E., Verbel, D., Crum, C. P., Ince, T. A., McKeon, F. D., and Cordon-Cardo, C. Loss of p63 expression is associated with tumor progression in bladder cancer. Am J Pathol, *161:* 1199-1206, 2002.
307. Puig, P., Capodieci, P., Drobnjak, M., Verbel, D., Prives, C., Cordon-Cardo, C., and Di Como, C. J. p73 Expression in human normal and tumor tissues: loss of p73alpha expression is associated with tumor progression in bladder cancer. Clin Cancer Res, *9:* 5642-5651, 2003.
308. Park, H. R., Kim, Y. W., Park, J. H., Maeng, Y. H., Nojima, T., Hashimoto, H., and Park, Y. K. Low expression of p63 and p73 in osteosarcoma. Tumori, *90:* 239-243, 2004.
309. Flores, E. R., Sengupta, S., Miller, J. B., Newman, J. J., Bronson, R., Crowley, D., Yang, A., McKeon, F., and Jacks, T. Tumor predisposition in mice mutant for p63 and p73: evidence for broader tumor suppressor functions for the p53 family. Cancer Cell, *7:* 363-373, 2005.
310. Nakagawa, T., Takahashi, M., Ozaki, T., Watanabe Ki, K., Todo, S., Mizuguchi, H., Hayakawa, T., and Nakagawara, A. Autoinhibitory regulation of p73 by Delta Np73 to modulate cell survival and death through a p73-specific target element within the Delta Np73 promoter. Mol Cell Biol, *22:* 2575-2585, 2002.

311. Casciano, I., Ponzoni, M., Lo Cunsolo, C., Tonini, G. P., and Romani, M. Different p73 splicing variants are expressed in distinct tumour areas of a multifocal neuroblastoma. Cell Death Differ, *6:* 391-393, 1999.

312. Casciano, I., Mazzocco, K., Boni, L., Pagnan, G., Banelli, B., Allemanni, G., Ponzoni, M., Tonini, G. P., and Romani, M. Expression of DeltaNp73 is a molecular marker for adverse outcome in neuroblastoma patients. Cell Death Differ, *9:* 246-251, 2002.

313. Concin, N., Becker, K., Slade, N., Erster, S., Mueller-Holzner, E., Ulmer, H., Daxenbichler, G., Zeimet, A., Zeillinger, R., Marth, C., and Moll, U. M. Transdominant DeltaTAp73 isoforms are frequently up-regulated in ovarian cancer. Evidence for their role as epigenetic p53 inhibitors in vivo. Cancer Res, *64:* 2449-2460, 2004.

314. Marabese, M., Marchini, S., Sabatino, M. A., Polato, F., Vikhanskaya, F., Marrazzo, E., Riccardi, E., Scanziani, E., and Broggini, M. Effects of inducible overexpression of DNp73alpha on cancer cell growth and response to treatment in vitro and in vivo. Cell Death Differ, *12:* 805-814, 2005.

315. Kartasheva, N. N., Lenz-Bauer, C., Hartmann, O., Schafer, H., Eilers, M., and Dobbelstein, M. DeltaNp73 can modulate the expression of various genes in a p53-independent fashion. Oncogene, *22:* 8246-8254, 2003.

316. Miro-Mur, F., Meiller, A., Haddada, H., and May, E. p73alpha expression induces both accumulation and activation of wt-p53 independent of the p73alpha transcriptional activity. Oncogene, *22:* 5451-5456, 2003.

317. Goldschneider, D., Blanc, E., Raguenez, G., Barrois, M., Legrand, A., Le Roux, G., Haddada, H., Benard, J., and Douc-Rasy, S. Differential response of p53 target genes to p73 overexpression in SH-SY5Y neuroblastoma cell line. J Cell Sci, *117:* 293-301, 2004.

318. Lu, X. p53: a heavily dictated dictator of life and death. Curr Opin Genet Dev, *15:* 27-33, 2005.

319. Nagase, T., Seki, N., Ishikawa, K., Ohira, M., Kawarabayasi, Y., Ohara, O., Tanaka, A., Kotani, H., Miyajima, N., and Nomura, N. Prediction of the coding sequences of unidentified human genes. VI. The coding sequences of 80 new genes (KIAA0201-KIAA0280) deduced by analysis of cDNA clones from cell line KG-1 and brain. DNA Res, *3:* 321-329, 341-354, 1996.

320. Hurley, L. H. DNA and its associated processes as targets for cancer therapy. Nat Rev Cancer, *2:* 188-200, 2002.

321. Broggini, M., Marchini, S., Fontana, E., Moneta, D., Fowst, C., and Geroni, C. Brostallicin: a new concept in minor groove DNA binder development. Anticancer Drugs, *15:* 1-6, 2004.

322. Marchini, S., Broggini, M., Sessa, C., and D'Incalci, M. Development of distamycin-related DNA binding anticancer drugs. Expert Opin Investig Drugs, *10:* 1703-1714, 2001.

323. Hartmann, J. T. and Lipp, H. P. Camptothecin and Podophyllotoxin Derivatives : Inhibitors of Topoisomerase I and II - Mechanisms of Action, Pharmacokinetics and Toxicity Profile. Drug Saf, *29:* 209-230, 2006.

324. Longley, D. B., Harkin, D. P., and Johnston, P. G. 5-fluorouracil: mechanisms of action and clinical strategies. Nat Rev Cancer, *3:* 330-338, 2003.

325. Mukherjee, A. K., Basu, S., Sarkar, N., and Ghosh, A. C. Advances in cancer therapy with plant based natural products. Curr Med Chem, *8:* 1467-1486, 2001.

326. Brown, R., Clugston, C., Burns, P., Edlin, A., Vasey, P., Vojtesek, B., and Kaye, S. B. Increased accumulation of p53 protein in cisplatin-resistant ovarian cell lines. Int J Cancer, *55:* 678-684, 1993.

327. Giannakakou, P., Sackett, D. L., Kang, Y. K., Zhan, Z., Buters, J. T., Fojo, T., and Poruchynsky, M. S. Paclitaxel-resistant human ovarian

cancer cells have mutant beta-tubulins that exhibit impaired paclitaxel-driven polymerization. J Biol Chem, *272:* 17118-17125, 1997.

328. Danks, M. K., Yalowich, J. C., and Beck, W. T. Atypical multiple drug resistance in a human leukemic cell line selected for resistance to teniposide (VM-26). Cancer Res, *47:* 1297-1301, 1987.
329. Grandi, M., Geroni, C., and Giuliani, F. C. Isolation and characterization of a human colon adenocarcinoma cell line resistant to doxorubicin. Br J Cancer, *54:* 515-518, 1986.
330. Dolfini, E., Dasdia, T., Arancia, G., Molinari, A., Calcabrini, A., Scheper, R. J., Flens, M. J., Gariboldi, M. B., and Monti, E. Characterization of a clonal human colon adenocarcinoma line intrinsically resistant to doxorubicin. Br J Cancer, *76:* 67-76, 1997.
331. Sambrook, J. and Russel, D. W. Molecular cloning:a laboratory manual, 3rd edition. Cold Spring Harbor, NY: Cold Spring Harbor laboratory Press, 2001.
332. Todaro, G. J. and Green, H. Quantitative studies of the growth of mouse embryo cells in culture and their development into established lines. J Cell Biol, *17:* 299-313, 1963.
333. Wilusz, C. J., Wormington, M., and Peltz, S. W. The cap-to-tail guide to mRNA turnover. Nat Rev Mol Cell Biol, *2:* 237-246, 2001.
334. Ueda, Y., Hijikata, M., Takagi, S., Chiba, T., and Shimotohno, K. Transcriptional activities of p73 splicing variants are regulated by inter-variant association. Biochem J, *356:* 859-866, 2001.
335. Blint, E., Phillips, A. C., Kozlov, S., Stewart, C. L., and Vousden, K. H. Induction of p57(KIP2) expression by p73beta. Proc Natl Acad Sci U S A, *99:* 3529-3534, 2002.
336. Tullo, A., Mastropasqua, G., Bourdon, J. C., Centonze, P., Gostissa, M., Costanzo, A., Levrero, M., Del Sal, G., Saccone, C., and Sbisa, E. Adenosine deaminase, a key enzyme in DNA

precursors control, is a new p73 target. Oncogene, *22:* 8738-8748, 2003.

337. Zauberman, A., Flusberg, D., Haupt, Y., Barak, Y., and Oren, M. A functional p53-responsive intronic promoter is contained within the human mdm2 gene. Nucleic Acids Res, *23:* 2584-2592, 1995.
338. Muller, M., Wilder, S., Bannasch, D., Israeli, D., Lehlbach, K., Li-Weber, M., Friedman, S. L., Galle, P. R., Stremmel, W., Oren, M., and Krammer, P. H. p53 activates the CD95 (APO-1/Fas) gene in response to DNA damage by anticancer drugs. J Exp Med, *188:* 2033-2045, 1998.
339. Munsch, D., Watanabe-Fukunaga, R., Bourdon, J. C., Nagata, S., May, E., Yonish-Rouach, E., and Reisdorf, P. Human and mouse Fas (APO-1/CD95) death receptor genes each contain a p53-responsive element that is activated by p53 mutants unable to induce apoptosis. J Biol Chem, *275:* 3867-3872, 2000.
340. Terry, L. A., Boyd, J., Alcorta, D., Lyon, T., Solomon, G., Hannon, G., Berchuck, A., Beach, D., and Barrett, J. C. Mutational analysis of the p21/WAF1/CIP1/SDI1 coding region in human tumor cell lines. Mol Carcinog, *16:* 221-228, 1996.
341. Marchler-Bauer, A. and Bryant, S. H. CD-Search: protein domain annotations on the fly. Nucleic Acids Res, *32:* W327-331, 2004.
342. Kannan, K., Kaminski, N., Rechavi, G., Jakob-Hirsch, J., Amariglio, N., and Givol, D. DNA microarray analysis of genes involved in p53 mediated apoptosis: activation of Apaf-1. Oncogene, *20:* 3449-3455, 2001.
343. Robles, A. I., Bemmels, N. A., Foraker, A. B., and Harris, C. C. APAF-1 is a transcriptional target of p53 in DNA damage-induced apoptosis. Cancer Res, *61:* 6660-6664, 2001.

CHAPTER 12

APPENDICES

12.1 List of abbreviations

3-MeAde	3-methyladenine
53BP1	p53 binding protein 1
5–FU	5–fluorouracil
AD	activator domain
AIF	apoptosis inducing factor
ALL	acute lymphoblastic leukaemia
APAF-1	apoptotic protease-activating factor 1
AT	annealing temperature
ATM	ataxia–telangectasia mutated gene
ATR	ATM–related gene
ATRIP	ATR-interacting protein
AUR K	Aurora kinase
BAI–1	brain-specific angiogenesis inhibitor 1
BER	base-excision repair
bFGF	basic fibroblast growth factor
BH	Bcl-2 homology
BLM	Bloom syndrome protein
bp	base pair
BRCA1	breast cancer 1
CAK	CDK-activating kinase
CDK	cyclin-dependent kinases

CFU	colony forming unit
cIAP1	cellular inhibitor of apoptosis protein 1
CK	casein kinase
CMV	cytomegalo virus
CPT	campthotecin
dam	DNA adenine methylation
DBD	DNA–binding domain
dcm	DNA cytosine methylation
DD	death domain
DDP	cisplatinum
DIABLO	direct IAP-binding protein with low pI
DISC	death-inducing-signalling-complex
DMSO	dimethyl sulfoxide I
DNA	Deoxyribonucleic acid
DNA–PK	DNA–dependent protein kinase
dNTPs	nucleotides
DR	death receptor
DRAGO	DRugs Activated Gene Overexpressed
DSB	double-strand breaks
dsRNA	double–stranded RNA
DX	doxorubicin
EndoG	endonucleases G
ER	endoplasmatic reticulum
GFP	green fluorescent protein

GI50	growth inhibitory concentration by 50%
GST	Glutathione S–transferase
H2AX	Histone-2A family, member X
HAT	histone acetyl-transferase
HAUSP	herpesvirus associated ubiquitin-specific protease
HDAC	histone deacetylase
HE	heterozygous
HEBS	HEPES-Buffered Saline
HH	head-to-head
HJ	Holliday junctions
HO	homozygous
HPV	human papillomavirus
HR	Homologous recombination
HT	head-to-tail
Htr2A	high temperature requirement A2
IAP	inhibitors of apoptosis proteins
IPTG	isopropyl β–D–thiogalactoside
IR	ionizing radiation
JNK	Jun N-terminal kinase
Kb	kilobase pair
KO	knock–out
LB	Luria–Bertani
maspin	mammary serine protease inhibitor
MCS	multiple cloning site

MDC1	mediator of DNA damage chekpoint 1
MDM2	mouse double minute 2
MEF	mouse embryo fibroblasts
MMR	mismatch repair
MPG	3-MeAde DNA-glycosylase gene
mRNA	messanger ribonucleic acid
MSH2	MutS homologue-2
NBS1	Nijmegen breakage syndrome-1
NER	nucleotide-excision repair
NES	nuclear exportation signal
NHEJ	Non-Homologous End-Joining
NLS	nuclear localization signal
NO	nitric oxide
OD	oligomerization domain
P/CAF	p300/CBP-associated HAT
p53BS	p53 binding site
p53RE	p53 responsive element
PAC1	pro-apoptotic phosphate
PAGE	polyacrylamide gel electrophoresis
PAI–1	plasminogen activator inhibitor 1
pBS	pBluescript–SKII+
PBS	phosphatase buffer saline
PCR	polymerase chain reaction
PERP	p53 apoptosis effector related to PMP–22

PI	phosphatidylinositol
PI3K	phosphatidylinositol 3- kinase
PIDD	p53-induced protein with a death domain
PIG	p53-induced gene
PIKK	PI3K-like protein kinases
PIP_2	phosphatidylinositol 4,5-bisphosphate
PIP_3	phosphatidylinositol 3,4,5-triphosphate
PKC	protein casein C
PML	promyelocytic leukaemia
PRD	proline-rich region
PUMA	p53 up-regulated modulator of apoptosis
RNA	ribonucleic acid
ROS	reactive oxygen species
RPA	replication protein A
RTS	Rothmund-Thomson syndrome
SAM domain	sterile alpha motive domain
SCE	sister chromatid exchange
SDS	sodium dodecyl sulphate
Smac	second mitochondria-derived activator of caspases
SMC1	structural maintenance of chromosomes 1
SSCP	single strand conformation polymorphism
ssDNA	single-strand DNA
TA domain	transactivation domain
TAF	TBP-associated factor

TBP	TATA box-binding protein
TD	tetramerization domain
TNF-R	tumor necrosis factor receptor
TRAIL	TNF-related apoptosis-inducing ligand
TSP–1	thrombospondin-1
TT	tail-to-tail
UK-HGMP-RC	UK Human Genome Mapping Project Resource Centre
USP	ubiquitin-specific protease
UTR	untranslated region
UV	ultra violet
UV-DDB	UV-damage DNA-binding proteins
WRN	Werner Syndrome protein
WT	wild–type
XIAP	x-linked inhibitor of apoptosis protein
XPC	xeroderma pigmentosum complementation group C
YY1	Yi Yang 1